Transitioning from batch to continuous systems: enzymatic hydrolysis of a waste pulp into fermentable sugars

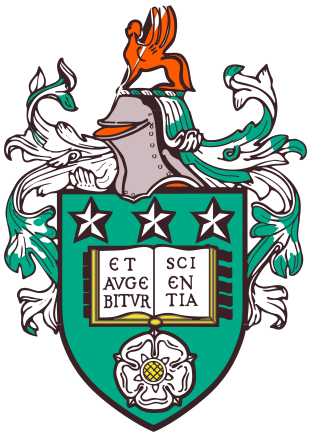

Fernando Climent Barba

School of Chemical and Process Engineering

University of Leeds

Submitted in accordance with the requirements for the integrated degree

Doctor of Philosophy and Master of Science in Bioenergy

July 2021

In loving memory of Bernat Llobet Martí, co-founder and head coach of the Banyoles Rugby Club

Declaration of authorship

The candidate confirms that the work submitted is his own, except where work which has formed part of jointly-authored publications has been included. The contribution of the candidate and the other authors to this work has been explicitly indicated within the text. The candidate confirms that appropriate credit has been given within the thesis where reference has been made to the work of others.

Signed: _____

Date: _____

Acknowledgments

First and foremost, I would like to thank my supervisor Prof. A. John Blacker for his continuous support and guidance through this process. Always with a positive attitude and constructive feedback, whilst finding time to meet me. Secondly to the rest of supervisors, Prof. Richard A. Bourne and Prof. Nikil Kapur, for helping on the areas of process optimisation and reactor design, which were key for the addressing the Thesis aims and goals. Thirdly, I am grateful to Dr. Dhivya J. Puri (Industrial supervisor) for the technical assistance, material supply and technology transfer from Fiberight Limited. Moreover, thanks to the supervision team for let me participate on the grant projects (OPTOMS and the India/UK MSW), that led to further academic and industrial opportunities. These experiences have been amazing for boosting my career profile.

My sincere gratitude to Dr. Will Reynolds and Dr. Micaela Chacón, which inducted me and improve my skills within to closely allied research projects at the University of Leeds. Thanks to them, I could improve my research skills and start publishing in this area. Moreover, I am also grateful to Dr. Jeanine Williams for her constant support on product analysis and instrument maintenance, vital for the obtaining the results of this project. Not to forget James McKay and Emily Bryan-Kinns for supporting me on the management and administration part of the PhD.

A special acknowledgment to the EPSRC Centre for Doctoral Training in Bioenergy for providing the funding and this opportunity, and, Fiberight Ltd. for the additional funding, material supply and transfer knowledge of the company.

I have been very lucky to meet amazing people within the Bioenergy CDT, iPRD and SCAPE, in particular to: Aaron Brown, Andy Price-Allison, Daisy Thomas, Dougie Philips, Jessica Quintana, Jaime Borbolla, Oli Grasham, Lee Roberts, Luke Higgins and Rich Birley. Last but not least, to my family for constantly checking on me from the distance: Mama, Papa and Aitor. A special mention to my grandmother (*Iaia*), and not to forget the rest of relatives from Banyoles and Seville as well as close friends. Thanks to all for the kind support, this could not have been possible without you.

Abstract

Fiberight Ltd. has developed an innovative waste biorefinery system which transforms municipal solid waste (MSW) into recyclables, chemicals and energy. The core technology pivots around the production of an organic MSW-pulp substrate, converted to fermentable sugars via enzymatic hydrolysis. The enzymatic hydrolysis is still not viable due to the high enzyme costs, low productivity rates and intrinsic biological infection of substrates. For the commercialisation of enzymatic hydrolysis, at least 80-100 g L^{-1} of glucose are required for decreasing capital (e.g. smaller equipment) and operational costs (e.g. downstream processing). To achieve this, high-solids loadings (above 15% w/w solids) are necessary, but mass-transfer is limited during mixing due to a highly viscous media, particularly in stirred tanks. In batch, high-solids loadings leads to high power consumption and long residence times, leading to a unprofitable process. Hence, the enzymatic hydrolysis needs redesigning to a more productive approach, e.g. continuous mode.

A multi-disciplinary study was proposed for assessing the batch-to-continuous transition. Firstly, pH/DO monitoring was used as metrics for determining the antimicrobial efficacy of several compounds, where 1,2-benzisothiazolinone (BIT) showed the highest cost-effective. The rheology of MSW-pulp slurries was characterised as Herschel-Bulkley fluids. And, a two-stage viscosity reduction profile (0-4 and 4-24 h) during enzymatic saccharification was shown by *In situ* rheometry. Among compared reactor designs, it was concluded that horizontal bioreactors are more adequate than stirred tanks due to higher energy efficiency and suitability for high-solids operations. By employing rotary drum reactors (RDBs), both maximum high-solids loadings (25%TS) and continuous processing were investigated. Although manual handling, steady-state was achieved for an interval of 4 space-volumes, yielding above 80 g L^{-1} in less than 3 days. From the experimental data, a simple techno-economic assessment was completed with industrial costings. Among investigated configurations, the two-stage (6/48h) continuous hydrolysis system was the preferred option, as resulting to productivity rates and profits 7-fold higher than the reference systems (batch and fed-batch).

Overall, this study provides the proof-of-concept and techno-economic guidelines, for the continuous high-solids enzymatic hydrolysis of MSW-pulp to fermentable sugars. This work supports the demonstration scale-up of current Fiberight Ltd. hydrolysis technology, and, bench-scaling of an alternative continuous process.

List of publications and conferences

Journal articles

- **Climent Barba, F.**, Chacón M.G, Reynolds,W.R., Puri., D.J., Bourne. R.A., Blacker, A.J., 2021. Improved conversion of residual MSW biomass waste to sugars using online process monitoring and integrated contamination control. Bioresour. Technol. Reports
- Ghuram, D.P., Rathi, O., Mule, T.A., **Climent Barba, F**., Khadye, V.S., Chavan, A., Odaneth, A., Thorat, B., 2021. Overview of municipal solid waste (MSW) technologies within the scope of the circular bioeconomy. Biofuels, Bioprod. Bioref. (SUBMITTED)
- None, S., **Climent Barba, F**., Rodríguez-Jasso, R.S., Ruiz H.A., 2021. High-solid loading processing of lignocellulosic biomass to enhance bioconversion under biorefinery concept: Effects of transport phenomena and rheology. Renew. Sustain. Energy Rev. (SUBMITTED)

Conference talks

- **Climent Barba, F.,** Bourne, R.A., Kapur, N., Blacker, A. John., 2018. Rheological analysis of municipal solid waste (MSW) pulp in enzymatic hydrolysis: from bench to pilot-scale. North American Mixing Forum (NAMF). San Juan, Puerto Rico. (ORAL)
- **Climent Barba, F.,** Bourne, R.A., Kapur, N., Blacker, A.J., 2019. Transitioning from batch to continuous systems: the enzymatic hydrolysis of waste pulp into fermentable sugars. 4th Lignocellulosic Biorefineries Network (LBNet) International Conference. Chesire, UK. 2019 (ORAL AND POSTER)
- **Climent Barba, F.,** Bourne, R.A., Kapur, N., Blacker, A. J., 2019. Anti-microbial strategies in the enzymatic hydrolysis of a waste-derived pulp into monomeric sugars. 41^{st} Symposium on Biotechnology for Fuels and Chemicals. Seattle, USA. (ORAL)

Abbreviations

2G	First-generation of biorefineries
2G	Second-generation of biorefineries
AAB	Acetic Acid Bacteria
AD	Anaerobic Digestion
AFEX	Ammonia Fiber Expansion pretreatment
AHP	Alkaline Hydrogen Peroxide
BIT	Benzisothiazolinone
BMSW	Biogenic Municipal Waste
BSA	Bovine Serum Albumin
C5	Carbon five sugars
C6	Carbon six sugars
CAPEX	Capital Expenditures
CBH	Cellobiohydrolase
CBP	Consolidated Bioprocessing
CBU	Cellobiose Unit
CD	Catalytic Domain
CDH	Cellobiose Dehydrogenase
CCF	Central Composite Face-Centred
CEH	Continuous Enzymatic Hydrolysis
CFU	Colony Forming Units
CFD	Computational Fluid Dynamics
CLD	Chord-length Distribution
CSTR	Continuous Stirred Tank Reactor
DM	Dry Matter
DMR	Deacetylated and mill refining pretreatment
DO	Dissolved Oxygen
DOE	Design of Experiments
DT	Down-time
EC	Enzyme Commission
EEDP	Elephant Ear Down-draft
EEUP	Elephant Ear Up-draft
EF	Erlenmeyer Flask
EG	Endoglucanase
EH	Enzymatic hydrolysis
FBRM	Focused Beam Reflectance Measurement
FIS	Fraction of Insoluble Solids
FPU	Filter Paper Unit
FTIR	Fournier Transformed Infra-Red
GAM	Galactan/Manna/Arabinan fraction
GOW	Garden Organic Waste

HPAEC	High-Performance Anion-Exchange Chromatography
HPLC	High-Performance Liquid Chromatography
HSBR	Horizontal Surface Bioreactor
IBUS	Integrated Biomass Utilisation System
IL	Ionic Liquids
LAB	Lactic Acid Bacteria
LPMO	Lytic Polysaccharide Monooxygenases
MIC	Minimum Inhibitory Concentration
M&E	Mass and Energy
MBR	Membrane Bioreactors
MESP	Minimum Ethanol Selling Price
MLR	Multiple Linear Regression
MSW	Municipal Solid Waste
NPV	Normalised Product value
NREL	National Renewable Energy Laboratories
OFMSW	Organic Fraction of Municipal Solid Waste
OPEX	Operational Expenditures
OPW	Orange Peel wastes
OVAT	One-variable-at-a-time
PAD	Pulse Amperometric Detection
PBR	Parallel Bottle Reactors
PBT	Pitched-blade Turbine
PCS	Pretreated Corns Stover
PEG	Polyethylene Glycol
PHS	Post-Hydrolysis Solids
POC	Proof-of-Concept
PSD	Particle Size Distribution
PSW	Paper Scraped Waste
PTI	Peak Tracking Instrument
RBR	Roller Bottle Reactors
RDB	Rotary Drum Bioreactor
ROI	Return on Investment
RSM	Response Surface Methodology
RT	Retention Time
SEM	Scanning Electron Microscope
SHF	Separate Hydrolysis and Fermentation
SSBR	Scraped Surface Bioreactor
SSCF	Simultaneous Saccharification and Co-Fermentation
SSF	Simultaneous Saccharification and Fermentation
STR	Stirred Tank Reactor
TC	Tetracycline
TEA	Techno-economic Assessment
TS	Total Solids
TSS	Total Steady-state time
XRD	X-ray Diffraction

Nomenclature

Parameters

B_c	Clearance between tank wall and baffle, mm
B_t	Thickness of the baffle, mm
B_w	Width of the baffle, mm
C	Concentration of product, g L^{-1}
CrI	Crystallinity index, %
D	Diameter of the vessel, mm
D_f	Adjustment factor (conservative design = 1)
DO_F	Last monitored DO reading (mg/L),
$DO_{f'}$	DO reading prior DO_F (mg/L)
E	Total energy consumption, W h L^{-1}
E_d	Enzyme adsorption, mg protein mL^{-1}
$E{:}S$	Enzyme to substrate ratio (m/m), %
$Enzy$	Amount of dosed enzymes, g
f	Frequency of monitoring, s
F_B	Force on each baffle (N)
I_{002}	Intensity (XRD) at peak at 22.2 °
I_{am}	Intensity (XRD) at peak at 18.4°
K	Consistency flow index, Pa s^n
K_p	Newtonian power draw constant, dimensionless
K_{pn}	Non-Newtonian power draw constant, dimensionless
M	Torque, N cm
m_{dry}	Reaction mass in dry basis, g
m_{in}	Inlet reaction mass in dry basis, g
m_{out}	Outlet reaction mass in dry basis, g
m_{wet}	Reaction mass in wet basis, g
N	Rotational speed, rpm
n	Flow behaviour index, dimensionless
N_P	Power number, dimensionless
P	Power consumption, W
p	Ratio of inner per outer cylinder radius of the vessel, dimensionless
P_1	Reference power demand, kW
P_2	Scaled power demand, kW
P_{Hn}	Power demand of thermostat (heating), kW
P_n	Sum of power per hydrolysis step, kW
P_{Pn}	Sum of the positive cavity pumps (pumping) power, kW
P_{Rn}	Sum of the mixing-related power kW
P_w	Specific power consumption, W L^{-1}

Q	Flow-rate, l h^{-1}
R	Wall thickness of the vessel, mm
R_{in}	Inner cylinder radius, mm
Re	Reynolds number for Newtonian fluids, dimensionless
Re_n	Reynolds number for non-Newtonian fluids, dimensionless
S	Allowed bending stress, N/mm^2)
t	Time of analysis, s
T	Temperature of media, °C
T_0	Room temperature, °C
t_m	Mixing time, s
t_n	Running time, h
t_{yr}	Annual operation time, hr
V	Volume of reactor, l
V_1	Reference reactor volume for scaling-up, l
V_2	Scaled reactor volume, l
W_v	Working volume, l

Greek letters

γ	Shear rate, s^{-1}
γ_{eff}	Effective shear rate, s^{-1}
ϵ	Total energy consumption, kW h
η	Normal viscosity, Pa s
Σ	Sum of factors
σ	Standard deviation
ρ	Density, kg m^m
μ	Viscosity, Pa s)
μ_{app}	Apparent Viscosity, Pa s
μ_{eff}	Effective Viscosity, Pa s
τ	Shear stress, Pa
τ_0	Yield stress, Pa
ω	Angular velocity, rad s^{-1}

Table of Contents

List of Figures

List of Tables

List of Equations

Chapter 1

Introduction

1.1 Current status of lignocellulosic biorefineries

It was not until the 2010s that the decommissioning and operation of industrial cellulosic bioethanol plants become a global reality [1]. During these years, only few companies were capable of producing 25 million gallons per year (MMgy) : *DuPont* (US), *GranBio* (Brazil) and *Enviral* (Slovakia). Others experienced large financial difficulties, e.g *BetaRenewables* (Italy) and *Abengoa* (Spain), declaring bankruptcy only after few years of commercial operation. Or, they were forced to business strategies such as corporate mergers, technology licensing or joint adventures to keep operating. Notwithstanding, current examples of successful cellulosic bioethanol plants using agricultural (corn stover, sugarcane bagasse, wheat straw) and forestry (spruce) can be found worldwide, as revised by Da Silva et al. [2].

A further literature analysis of US and EU initiatives in regards of research and development (R&D), demonstration and commercialisation of lignocellulosic biofuels, was assessed by Balan et al. [3]. In this review, a concise description of biofuel commercialisation activities is provided, split between; thermochemical, biochemical and hybrid (thermochemical + biochemical) of US or EU origin. Apart from bioethanol, other fuels (biobutanol and biogas) and bio-based chemicals are derived through the biochemical pathway - involving biomass pretreatment and enzymatic hydrolysis. Installed capacity vary according of type of technology and scale, e.g. 30 MMgy of bioethanol by *DuPont Biofuels Solution* (US) employing agricultural biomass via NaOH-based pretreatment, enzymatic hydrolysis and *Zymomonas* fermentation. Meanwhile, pilot and demonstration -scale initiatives do not produce more than 0.25 and 3 MMgy, respectively. In the European continent, wheat straw is the chosen feedstock for ethanol fermentation, with *Clariant* (Germany) and *Inbicon* (Denmark) as key players but still operating at demo-scale (approx. 4 MMgy). Another company, *BioGasol*, has industrialised their patented technologies pretreatment (Carbofrac®) and co-fermentation (Pentocrobe®), processing up to 12 tons per hour of woody biomass, without using enzymes: www.biogasol.com/products.

1.2 Production of sugars, key intermediates for biorefining

Sugars are important sources of energy for the human body, an essential additive for food preparations and precursor of commodities. Glucose (or dextrose) is the most common type of sugar, which can be produced from different feedstocks: sugar-crop biomass, starchy biomass, lignocellulosic biomass and marine biomass [4]. These are classified as first (edible), second (lignocellulosic) and third generation (algal) feedstocks. Each type of feedstock is converted to fermentable sugars by following different conversion pathways, as seen in Fig. 1.1.

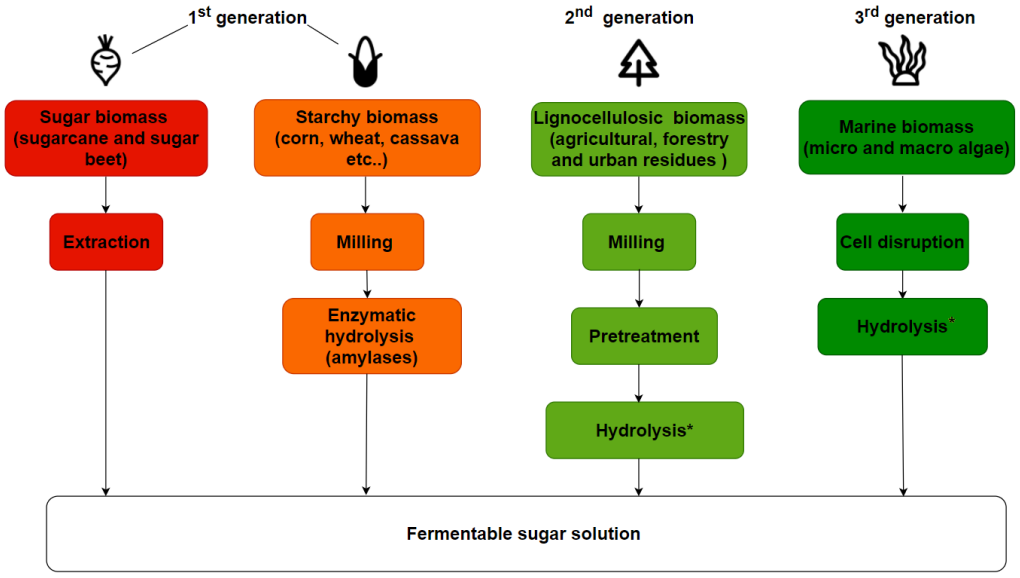

Figure 1.1. Schematic diagram of generations of sugar production

*An hydrolysis reaction can be acid, alkaline or enzymatic

The depolymerisation of hemicellulose, second most abundant polysaccharides, results into the release of carbon five (xylose and arabinose) and six (glucose, mannose, galactose and rhamnose) carbon sugars. Xylose is the main co-product of enzymatic saccharification of biomass, offering a range of possibilities as precursor (Fig.**1.3**). Acid-catalysed dehydration transforms xylose into furfural, a furan-based organic compound which is widely used as building block for solvent, polymer and fuel synthesis. From furfural, a vast array of chemicals, e.g. C_9-C_{16} alkanes or 2-methylfuran for fuel applications. The second option is the fermentation of xylose into xylitol, a dental-care product for avoiding teeth caries. Xylitol is also an important intermediate in the pentose phosphate pathway and glycolysis, incorporated as an extra carbon sources for the ethanol co-fermentation [5].

The rest of the monosaccharides, from galactose to rhamnose, are utilised to a lesser extent as low-calorie sweeteners, although, they can be converted into high-added value chemicals: e.g. mannose to mannitol, a brain and eye pressure reducer [5]. New bio-based products encompassing speciality carbohydrates and glycolipid

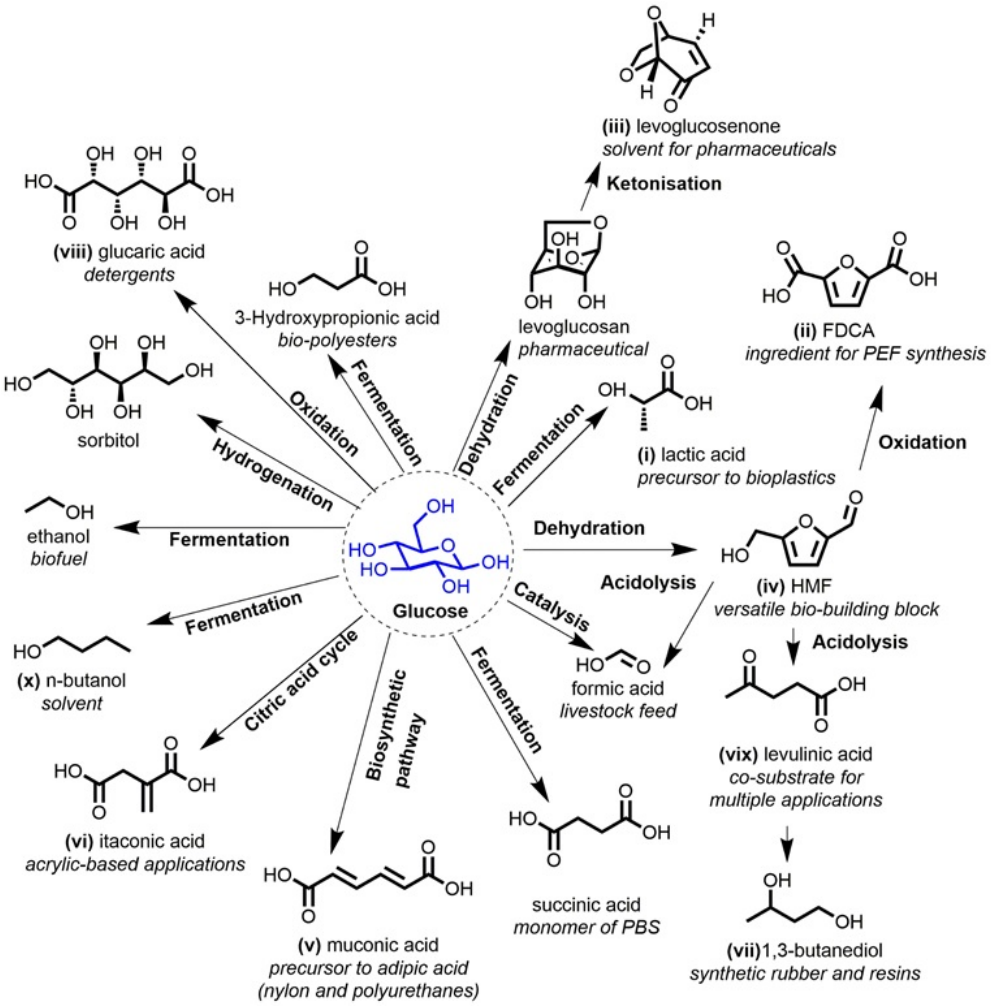

Figure 1.2. Examples of glucose conversion routes and their applications

biosurfactants are being developed via fermentative routes as alternative of food-grade products. Speciality carbohydrates are derived from dairy by-products into oligosaccharides for human milk applications. For example, Inbiose (a spin-out of Ghent University) can produce up to 10000 kilos per year of speciality carbohydrates by microbial processes. The second group of new carbohydrates, glycolipids structured as a lipid with a carbohydrate attached by a glycosidic bond, are gaining interest as biosurfactants. One of these glycolipids, rhamnolipids, is currently being commercialised by *Unilever* as 100% renewable and biorenewable surfactant, providing an efficient cleaning agent as alternative to chemical-based equivalents [6].

Other bio-products that can be synthesised from monosaccharides are binders and insulation materials. Binding of carbohydrates with resins from renewable sources is now a reality. For instance, *Knauf* insulation developed a thermoset resins from lignocellulosic sugars produced by Fiberight Limited [7].

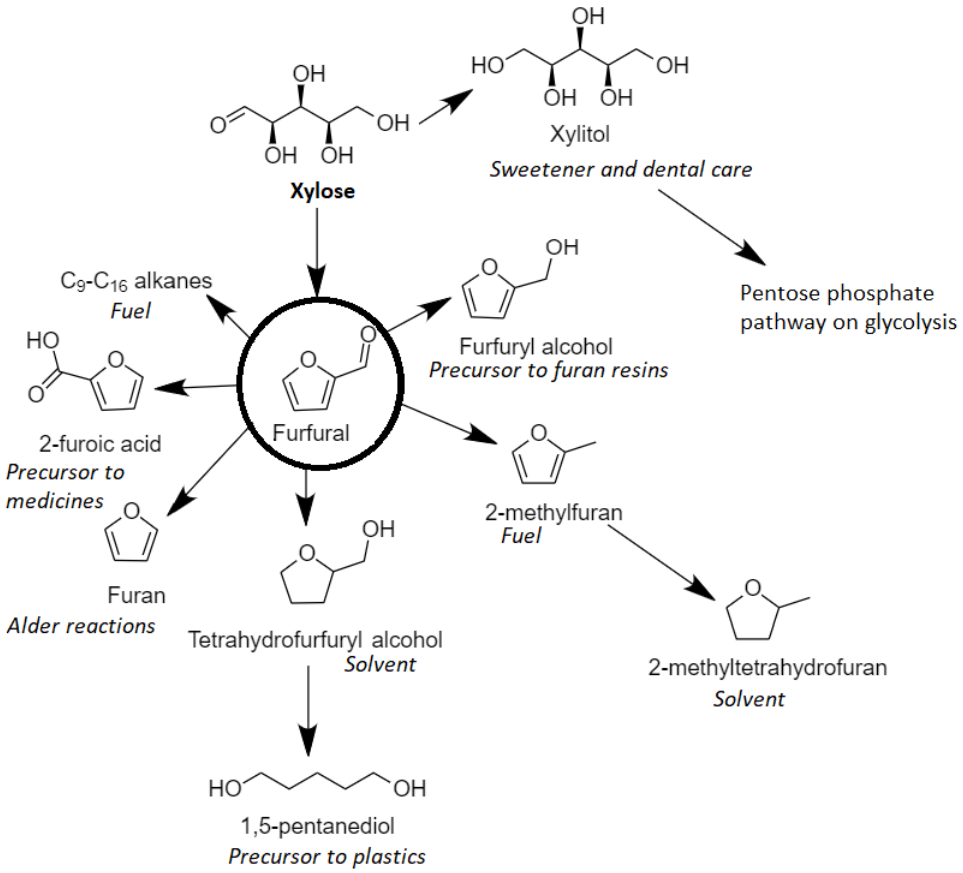

Figure 1.3. Xylose utilisation and derivatives, furfural as bio-building block

1.2.1 Classifications of top-priority biochemicals

It is important to emphasises the important role of glucose, as the main precursor for the synthesis of top-priority biochemicals. In the UK, the a report commissioned by The Lignocellulosic Biorefinery Network (LBNet), a Biotechnology and Biological Sciences Research Council Network in Industrial Biotechnology and Bioenergy (BBSRC-NIBB), identified a list of ten bio-based chemicals according to UK strengths and business opportunities in the long-term [8]. In the UKBioChem10 report, a case-by-case definition of ten bio-based chemicals is envisioned with a commercial reality, involving a combination of academic and business partnerships. All listed chemicals are derived from glucose, directly or indirectly, via several routes of different routes. Table 1.1 shows the list of 10 priority chemicals and the main applications.

Preceding this work,the US Department of Energy (USDOE) published a technical report which included chemicals as potential candidates from sugar and synthesis gas platforms [9]. From an initial screening of 300 bio-building blocks, a first shortlist of 30 candidates was selected, then shortened to 12 sugar-derived chemicals: (1) four carbon 1.4-diacids, (2) 2,5-furan dicarboxylic acid (FDCA), (3) 3-hydroxy propionic acid (3-HPA), (4) aspartic acid, (5) glucaric acid, (6) glutamic

Table 1.1. List of top-priority biochemicals report for the UK industry [8]

Order	Chemical	Uses
1	Lactic acid	Bioplastics
2	2,5-furandicarboxylic acid (FDCA)	Bioplastics precursor
3	Levoglucosenone	Solvents, flavours and fragrances
4	5-Hydromethylfurfural (HMF)	Bioplastic and biofuels precursor
5	Muconic acid	Bioplastic and fibers ingredient
6	Itaconic acid	Ingredient for acrylic acid applications
7	1.3-butanediol (1,3-BDO)	Building blocks for high-value products*
8	Glucaric acid	Ingredient for phosphate-based detergents
9	Levulinic acid	Herbicides and cosmetics
10	N-butanol	Materials, plastics and solvents

*High-value products are pheromones, fragrances, insecticides, antibiotics and synthetic rubber

acid, (7) itaconic acid, (8) levulinic acid, (9) 3-hydroxybutyrolactone, (10) glycerol, (11) sorbitol and (12) xylitol. The first group of chemical, grouped as C4 diacids, includes succinic, fumaric and malic acids. The ranking of the top-12 chemicals was based on feedstock availability, maturity of conversion pathways, market impact and variety of applications. In 2010, Bozell and Petersen et al. [10] updated the 2004 list by following a similar methodology on the selection process, but including new compounds. A clear case-by-case comparison between the two list was conducted by Chandel et al. [11], highlighting the main modifications of the new list. In this, ethanol followed by furans and glycerol were the most important platform chemicals as well as novel molecules such as lactic acid and xylitol. Ethanol fulfilled all 9 proposed criteria, from literature importance to commercial capabilities, and its technology needs were also reported. It is well-known of importance of bioethanol in US economy, mainly driven by supporting the energy security, established supply-chain and large subsidies of corn plantations as starting material [12].

Both at European and International level, glucose-derived products play a key role in the manufacturing of top-value added chemicals [12–14]. Although, no list of top-priority chemicals are proposed as in the UK and US, worldwide, the International Environmental Agency (IEA) leads the public dissemination and consultation of bio-based chemicals, issuing annual reports on biorefinery classifications [12, 14]. Among bio-based chemicals, bioethanol is by far the most abundant and mature commodity, totalling a production of 15800, 7060 and 1415 MMgy for the US, Brazil and EU, respectively. Other glucose-derived products via fermentation such as citric acid and sorbitol are also notable examples of bio-based chemicals. The bio-economy is still driven by glucose due to its high market volume and high versatility as precursor for key building blocks: alcohols, organic acids, lipids and hydrocarbons [**Isikgor2015**]. In addition to fine chemicals such as amino acids, vitamins, antibiotics and enzymes. At European level, the EU Joint Research Centre published the insights of European market for bio-based chemicals, providing factsheets, market indicators, drivers and constraints of various groups of commodities,

e.g. from platform chemicals to man-made fibers [13]. Most of the key products stated by the EU-28 member states are glucose or cellulose-derived, but from first generation of feedstocks. For instance, around 25 kilo tonnes per annum (kt/a) of acetic acid are manufactured from bioethanol. Hence, it is evident of the importance of glucose in the bio-economy [5].

1.3 Research overview

1.3.1 Previous research and gap in knowledge

Previous work on batch-to-continuous conversion of enzymatic hydrolysis of an organic pulp derived from municipal solid waste (MSW), falls into two categories:

- Continuous enzymatic hydrolysis of biomass with membrane-based systems
- Feasibility of MSW-based biorefineries

Continuous processing leads to several processing advantages such as higher productivity, reduction of downtime costs and lower capital and operational investment per unit of product [15]. Conversion from batch to continuous enzymatic biomass saccharification has been investigated since the early 1980s [16], as an efficient intermediate pathway for fermentation processes. Although, continuous enzymatic liquefaction of starchy materials provides some advantages: (i) constant production of high-solids production, (ii) low power input and short residence time, (iii) energy savings in cooking (pretreatment) methods and (iv) decrease in microbial contamination probability [16]. These claims would not be directly applied to lignocellulosic substrates, due to its high recalcitrance/viscosity and complexity of structure [17].

Some efforts on adapting batch to continuous enzymatic hydrolysis of lignocellulosic were pioneered by Ishihara et al. [18]. Continuous enzymatic saccharification of steamed *shirakamanda* wood-chips was evaluated with enzymes recovery at 10-L scale. Further investigations continued after the millennia, by employing a tubular reactor [19] and stirred tank reactors [20] coupled with an ultra-filtration unit for enzyme recycling. Although, it was evident of production improvements of continuous to batch mode. These systems cannot be translated into commercial applications due to low concentrations of sugars were produced [2]. More recently, NREL researchers demonstrated the continuous enzymatic hydrolysis for a continuous period of 1000 hours at 10% w/w with corn stover [21], even integrating the experimental data with kinetic modelling [22]. Despite achieving steady-state for a prolonged operating time, this work used excessive amounts of enzyme [23] and unrealistic particle-sizes of a milled lignocellulose material [24], which are not cost-effective options for the industry.

MSW enzymatic hydrolysis into fermentable sugars has been poorly explored outside the laboratory [25]. The term "MSW" is often referred as the preparation

of artificial (synthetic) mixtures of biological origin in academia, with well-defined proportions and homogeneous sourcing [26]. In reality, MSW has many disadvantages for enzymatic hydrolysis compared to other feedstocks: e.g. higher susceptibility of microbial contamination, heterogeneity and initial viscosity. The decomposition of carbonaceous materials, i.e. carbohydrates, liquefies into "leachate" - a complex mixture of organic compounds [27]. This promotes microbial activity, rapidly consuming remaining sugars and oxygen, therefore, MSW-derived sugars are prone to microbial contamination. Secondly, due to many factors (geographical location, seasonality and human habits), the composition of MSW significantly varies throughout the year. Even between same samples [26]. These fluctuations impact the production of lignocellulosic sugars, and great care is required for guaranteeing the industrial exploitation. In the third place, the addition of corrugated cardboard and scrap paper into MSW mixture increases viscosity of MSW mixture, as being more compacted and recalcitrant fraction than food waste alone [28]. The industry-based manufacturing of recycled streams leads to poor enzyme accessibility to cellulosic fibrils for the efficient release of sugars. In addition, the presence of microplastics and other inerts (e.g. ink) may cause enzyme de-activation, hindering biomass liquefaction. Compared with other lignocellulose feedstocks, mixed MSW bioconversion routes are less investigated and established in the industry.

To avoid using surrogate materials, several authors have investigated the viability of the organic fraction of MSW (OFSMW). Substrates are directly sourced from various landfill site, households or composting sites around: e.g. Spain [29], Greece [30] and Iran [31]. Another group of feedstocks, mixed MSW streams, are also investigated as lignocellulosic wastes which include cardboard and paper in addition to the food waste fraction [28, 32]. Compared with OFMSW, an additional pre-processing step consisting of thermomechanical processes for removing recyclable parts (plastic, metals, glass etc..) is required to obtain a lignocellulosic raw material. To the best of our knowledge, only three companies are working on biochemical conversion of MSW into fuels, chemicals and energy; IMECAL S.A, Fiberight Ltd. and Wilson Bio-chemical. To date, several EU-funded projects under the Horizons 2020 (H2020) and/or Bio-Based Industries Joint Undertaking (BBI-JU) grants framework have been completed; Waste2Bio, PERCAL, and in a city context: WaysTUP!, HOOP and Scalibur. These projects are demonstrating state-of-the-art systems for urban biowaste collection and transformation into high-added value products as pilot-cases, e.g. biosolvents in Athens (Greece). Other projects such as URBIOFIN and VAMOS, among others, are dedicated to the demonstration scale-up, techno-economic (TEA) and life cycle assessment of MSW biorefining. For instance, the *Perseo Bioethanol*® is the core technology of various H2020 projects, developed by Perseo biorefinery®/IMECAL S.A. It is an integrated biorefinery system, structured in three modules: (i) OFMSW to ethylene via simultaneous saccharification and fermentation, (ii) OFMSW to medium chained and short chained PHAs via VFAs and (iii) biogas to biomethane, digestate and acetic acid. The main application, per

bio-based product is: (1) ethylene (fruit ripening), (2) PHAs (agriculture/cosmetic bioplastics) and (3) digestate/acetic acid (fertilisers) [25]. This biorefinery technology has been scaled-up to 10 tonnes per day of MSW biorefinery, currently investigated under the URBIOFIN project. The commercialisation of MSW biorefineries, including the enzymatic hydrolysis route, is mainly spreading around Europe due to more favourable favourable funding streams, waste management policies and supply-chain [25]. These are factors are key for establishment of MSW biorefineries in the market.

1.3.2 Fiberight Ltd. in the context of MSW biorefineries

Fiberight LLC (USA/UK), a small and medium enterprise (SME) waste management company, has developed an innovative system for the valorisation of MSW into high-added value products. By a sequence of processes, house-hold waste is screened until obtaining an organic waste-pulp [33]. Most of the recyclables (metals, glass and plastics) are removed during this process. The fibrous organic pulp is washed for the solubilisation and separation of food waste and unrecyclable mixed fractions from the fiber. The solubilised food is decomposed via anaerobic digestion (AD) for biogas production, which is then upgraded to biomethane or burnt for electricity, heat or both . Whilst, the washed organic fiber is further treated by a thermomechanical pretreatment [34], producing a clean and sterile MSW-derived pulp. During enzymatic hydrolysis, the organic MSW-pulp is converted into monomeric sugars by Cellic® CTec (Novozymes). After the solid/liquid separation, the lignin-rich residue known as post hydrolysis solids (PHS) is burnt for on-site electricity generation. More details of Fiberight biorefinery system can be found in various technical reports [34, 35], and summarised at: www.fiberight.com.

Previous academic work on the enzymatic hydrolysis of MSW-derived pulp was assessed by Puri [36], demonstrating the process advantages of a two-stage hydrolysis step instead of single-phasic [32]. Other investigations were carried out at the University of Southampton, in regards to reducing the contamination risk and improving yields during the production of MSW-derived sugars [37]. In the University of Leeds, two Innovate UK grants were completed, summarised as follows with the main aims.

- **Driving down the cost of waste derived sugar – CelluPAT (45031-305142):** conceptualisation and optimisation of enzymatic saccharification of cellulosic-rich fiber from MSW
- **Optimising the production of thermoset resins from MSW-derived sugars – OPTOMS (TS/S003177/1,104391):** pilot-scaling of enzymatic saccharification of MSW-derived pulp

Three Fiberight plant sites (pilot, demonstration and commercial) were commissioned and operated from 2010 to date, the latter excluding the enzymatic hydrolysis step. At pilot-scale, early stage development and fundamental research was conducted at kilo-scale, with full integration the whole Fiberight process. This site is located at Southampton (UK), and has been a part of both Cellupat and OPTOMS projects. In the US (Lawrenceville, West Virginia), Fiberight logged over 10,000 hours of plant operation with enzymatic hydrolysis campaign. This industrial site is a 1/10 version of the new commercial plant, located at Hampden (Maine, US), which is capable of processing MSW from 116 communities around the region [38].

Currently, Fiberight Ltd. is collaborating with various partners within BBI-JU VAMOS project for the production and valorisation of MSW-derived sugars into lactic acid at demonstration scale. Further screening of bio-based products such as thermo-set resins and polylactic acid (PLA) and PLA/Fibre polymers will also take part. The residual solids generated during the enzymatic saccharification process will be converted into energy and materials (e.g. adhesives). The whole VAMOS process will be evaluated by TEA and LCA studies. Overall, this projects aims to deliver high-added value products from low-cost feedstocks whilst enabling a zero waste and circular economy concept.

1.3.3 Aims and objectives

In batch, the enzymatic hydrolysis of MSW-derived pulp lacks commercial viability due to several technical barriers: prolonged reaction time, high enzyme costs and low solids loadings. Working under industrial conditions restricts the amount of enzymes and chemicals used, as these have a great impact on process economics, particularly the enzymes. MSW-derived feedstocks have an intrinsic biological contamination from urban residues, which is more accentuated than other lignocellulosic feedstocks. Tackling microbial contamination is of great importance to preserve the final product (monomeric sugars), ideally with a cost-effective option to increase the viability of the process. Identifying the most affordable but effective antimicrobial agent and its concentrations is of great importance for preserve the produced lignocellulosic sugars. Therefore the first question is :

1. Which antimicrobial strategy is more cost-effective ?

Currently, the enzymatic hydrolysis of biomass is operated in stirred tank reactors, at 8-10% (w/w/) solids loadings in batch. At least 80 g L^{-1} glucose content is required for achieving the commercial readiness of enzymatic hydrolysis of biomasses, decreasing the capital and operational expenditures per volume of product [2]. The operation needs to achieve solids loadings above 15% w/w, as increasing carbohydrates (re-agents) would lead to increasing monomeric sugars (products). This raises the second question, posed when operating at high-solid loading:

2. What is the maximum percentage of solids loading and which reactor configuration are suitable ?

During enzymatic hydrolysis, MSW-derived pulp converts from *paper maché* into a muddy-like slurry. Higher solids loadings result in slower liquefaction rates, understood as the time for achieving a "pumpable" substrate. Understanding the liquefaction rate is vital for designing more efficient systems and operations. This leads to the third research question:

3. What information does the rheology study provide regarding the process/reactor design ?

Switching from batch to continuous operation provides an alternative opportunity to enhance productivity and decrease the manufacturing costs. A full continuous enzymatic hydrolysis is not yet feasible due to high complexity and associated costs at laboratory-scale. Nevertheless, an experimental approach can be pursued to determine potential designs which are subsequently modelled for defining scale-up. This lead to the fourth research question:

4. Which reactor configuration is viable for mimicking continuous processing ?

From the experimental data, continuous processing can be modelled alongside other modes of operation. Coupling process engineering with economic evaluation, a basic but empirical techno-economic assessment can be performed. This leads to the last question.

5. What techno-economic advantages does continuous processing bring over reference cases ? What are the financial implications at commercial-scale ?

To address above-mentioned aims and research questions, we propose the following objectives:

- Determine the limits of solid loadings and suitable reactor configuration
- Identify an efficient antimicrobial strategy and integrate of bespoke application of automated reaction control and monitoring
- Understand biomass liquefaction and characterisation of Non-Newtonian rheology of MSW slurries
- Conduct a pseudo-flow enzymatic hydrolysis at laboratory-scale as predecessor of continuous bioprocessing
- Establish a mass/energy balances of various modes for the techno-economic evaluation at pilot and commercial scale

The combination of individual aims facilitate the process design of proof-of-concept (POC) continuous hydrolysis within Fiberight technology at high-solids loadings. The work the provides the guidelines for:

- A prototype a bench-scale continuous hydrolysis system
- A detailed techno-economic and life cycle assessments

1.3.4 Scope and outline of thesis

The thesis is structured as seven chapters (Fig. 1.4), with four "results" chapters (3-6). Firstly, the current status of lignocellulosic biorefineries with the sugar-platform (enzymatic hydrolysis) and commercial examples are explained. Chapter 1 also contains a brief overview of previous R&D projects related to MSW biorefineries, role of Fiberight Limited and gap in knowledge. Chapter 2 then provides whole research methodology, from materials characterisation to design of experiments, passing through employed reactor configuration and monitoring techniques for enzymatic saccharification of the MSW-derived pulp.

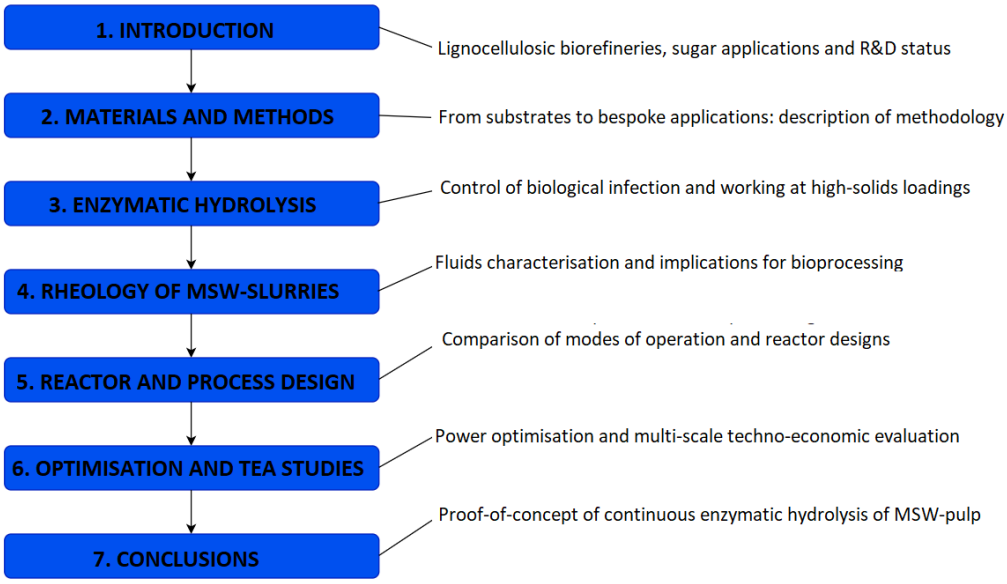

Figure 1.4. Schematic diagram of PhD Thesis structure and milestones

TEA is techno-economic assessment

From Chapter 3 to 6, a short literature review of each research area is included per chapter prior presentation and discussion of results. Chapter 3 focuses exclusively on overcoming biological infection by means of process analytical techniques coupled with bespoke applications, and, working under the high-solids loadings regime. The investigation of automated contamination control and screening of antimicrobial compounds is published as part of paper I. The following Chapter 4 studies the rheological profile of MSW-derived slurries as Non-Newtonian fluids. The

rheological implications into of bioreactor design, optimisation on mixing-related energy requirements and other bioprocessing (e.g. pumping) activities are also described. In Chapter 5, several reactor designs and modes of operation are compared by experimentation and literature analysis. Based on the main findings of Chapter 3 and 4, a pseudo-flow hydrolysis experiment is designed and tested for mocking continuous processing. Chapter 6 provides a basic techno-economic assessment of different systems in accordance of optimisation and kinetic studies. The modelling work is scaled-up from pilot (30 L) to industrial (50 m^3) as well. Lastly, Chapter 7 summarises research work and fulfilment milestones per chapter, providing the basic guidelines as proof-of-concept for transitioning from batch into continuous enzymatic saccharification of MSW-derived pulp. The Thesis also includes some case studies done in collaboration in form of R&D projects with the sponsor (Fiberight Ltd.) and the University of Leeds. The Thesis is finalised with the description of future opportunities that can arise from this work.

Chapter 2

Materials and Methods

2.1 Substrates, re-agents and enzymes

Two types of MSW-derived pulps were supplied by Fiberight Ltd. (UK-USA) from its demonstration plant (Lawrenceville, West Virginia, USA) and commercial plant (Hampden, Maine, USA). Incoming house-hold waste was treated in the following step-wise manner: (i) de-bagging, (ii) sieving and (iii) screening. Once plastics and metals are removed, the waste stream contains mainly paper, card and food-waste. This organic fraction was then washed to solubilise the food-waste and remove any remaining unrecyclable materials [33]. The resulting MSW pulp is a cellulose rich material suitable for enzymatic hydrolysis. More information of the Fiberight's technology can be found in: www.fiberight.com.

The lignocellulosic composition of the MSW pulp obtained from Lawrenceville and Hampden is described in Table 2.1. The compositional variability between both sources can be attributed to the difference in geography, local economy, and social factors [39].

A commercial enzymatic cocktail (Cellic® CTec3 EU) containing cellulases, β-glucosidases and hemicellulases, was kindly donated by Novozymes (Copenhagen, Denmark). All other chemicals and re-agents were purchased from Sigma Aldrich (Dorset, UK) or Fisher Scientific (Loughborough, UK) unless stated otherwise.

Table 2.1. Key compositional parameters of Fiberight's MSW pulps

Parameters	Lawrenceville pulp	Hampden pulp
Lignocellulosic content		
Glucan, %	55	53
Xylan, %	12	7
Mannan/Araban/Galactan, %	6	5
Lignin, %	24	13
Ash, %	3	7
Extractives, %	-	5
Dry matter content, %	52	38
Moisture content, %	48	62

2.2 Sample preparation

2.2.1 Physical analysis

For some of the physical analysis (e.g. crystallinity index or compositional analysis), particle-size reduction (< 4000 μm) and homogenization was required. Prior to particle reduction, materials were dried at 50 °C for minimum 2 days in a drying oven. Three types of particle reduction methods were conducted depending on the degree of homogeneity and particle size: shredding, milling and cryo-milling. Table 2.2 summarises the pre-processing techniques, instruments used and aim of technique upon the required volume. Processed materials were filtered through soil sampling sieves placed on a vibratory sieve shaker AS200 (Retsch, Germany) or manually, to obtain samples within a particular size range, e.g. 1000 < x < 2000 μm.

Table 2.2. Particle reduction techniques employed in MSW pulps

Technique	Instrument	Aim
Grinding	Blender (Nutribullet)	Size reduction of small sample volumes ($\sim$ 20 g)
Shredding	Jaw Crusher model BB200	Size reduction of large sample volumes ($\sim$ 1 kg per batch)
Milling	Planetary Ball Mill PM100	Fine milling of small sample volumes ($\sim$ 100 grams per batch)
Cryo-milling	Mixer Mill MM400	Pulverisation of tiny sample volumes ($\sim$ grams per batch)

Retsch (Germany) is the main manufacturer of all stated machinery, apart from the Nutribullet blender

2.3 Reactor configurations and designs

In this study, a number of reactor vessels and configurations were assayed for the enzymatic hydrolysis of MSW-pulp to monomerics sugars. Table 2.3 summarises their dimensions, type of agitation as well as other details (e.g. heating system).

2.3.1 Shake flasks experiments

Hydrolysis experiments (80 % working volume) were carried out in 150 or 250 ml Erlenmeyer flasks (EFs), fitted into an orbital shaker incubators (e.g. Kuhner Shaker Inc., Basel, Switzerland), at 200-250 rpm and 55 °C. EFs were covered with aluminium foil and/or cotton plugs to minimize evaporation during the given hydrolysis time course. Experiments were run in either duplicate or triplicate.

Table 2.3. Reactor configurations used for the enzymatic hydrolysis of MSW pulp into fermentable sugars

Configuration	Volume (L)	Diameter (cm	Height/ Length (cm)	Agitation	Rotational speed (rpm)	Material	Heating	Design
Stirred tank reactor	1	10	15	Impeller	0-1000	Borosilicate	Jacketed-vessel	Scientific UK
	1.5	10	20					
Erlenmeyer flasks	0.250	7	7	Shaking	0-250	Borosilicate	Incubator	Cole-Parmer
	0.125	8	8					
Drum rotatory reactors[1]	2	11.9	24.4	Rolling	0-80	HDPE	Incubator	Thermo Fischer
	0.5	7.3	16.8			PPC		
	0.05	0.3	1.15			PP		
	Multiple	0.025/0.04	5-25			PVC	Home-made[3]	
Scraped surface bioreactor	8	13.9	58.5	Scraped blades[2]	0-10	Borosilicate	Heating chamber[2]	Home-made[2]
	7	15	40	Paddle blades[3]	0-30	PVC	Coiled tubing[3]	Home-made [3]

[1] Drum rotatory reactors are bottles or tubes that rotate in the mini-roller (model MR-03UA, Crystal Inc., USA)

[2] All items are included in the home-made design by Dasari *et al* [40], further description can be found in the corresponding subsection

[3] All items are included in the home-made design by Climent Barba *et al* (PhD Thesis), further description can be found in the corresponding subsection

2.3.2 Stirred tank reactor

Both 1 and 1.5 L volume stirred tank reactors (STRs) were employed for enzymatic hydrolysis, operating at 80 % of the working volume. The temperature was maintained using a Huber ministat CC thermostat batch circulating 55 °C silicon oil through the jacketed vessel. Stirring was applied with a PTFE 4-blade impeller (Caframo Limited, Ontario, Canada) - 40 mm diameter and 45 ° pitched blades. To drive the impeller, mechanical or digital overhead stirrers (IKA, UK) were coupled to the shaft. A multi-flange lid was used to enable the attachment of various monitoring probes (section 2.5.1). The whole reactor set-up was placed in a home-made protection cage (Fig. 2.1).

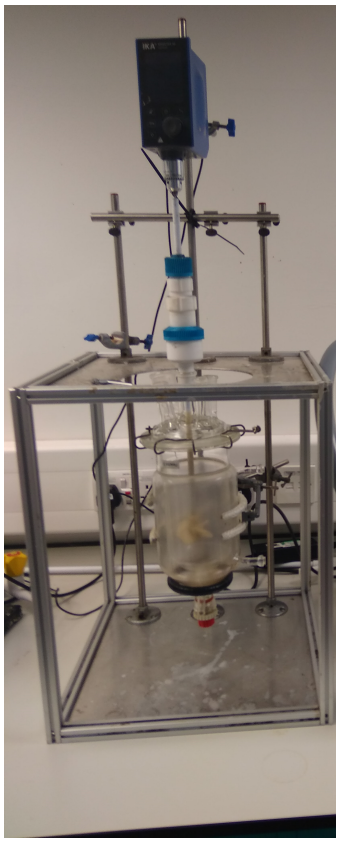

Figure 2.1. Experimental set-up of 1.5 L stirred tank reactor

2.3.3 Scraped surface bioreactors

2.3.3.1 Dasari's design, University of Louisville (USA)

A 8 L scraped surface bioreactor (SSBR) was tested during a placement stage at Louisville University (Kentucky, USA), designed by Dasari and co-workers [40–42], used at 50 % working volume. The SSBR was a 58.5 cm long and 13.9 cm diameter borosilicate cylinder, encapsulated with aluminum lids and resting in a stand. The stainless steel impeller was structured as three scraping blades (placed 120° from each other) welded on a shaft, which divides the vessel in three compartments.

Scraped blade dimensions were 18.5 cm length, 3.2 cm width and a 0.8 cm thickness. Across each blade, a 5 mm polystyrene rubber strip is attached to facilitate scraping on the interior wall of the vessel. Three sampling ports are placed along the reactor; left and right with a diameter of 1.7 cm and a centrally located port which doubles as a feeding port as well (7.62 x 5.08 cm square).

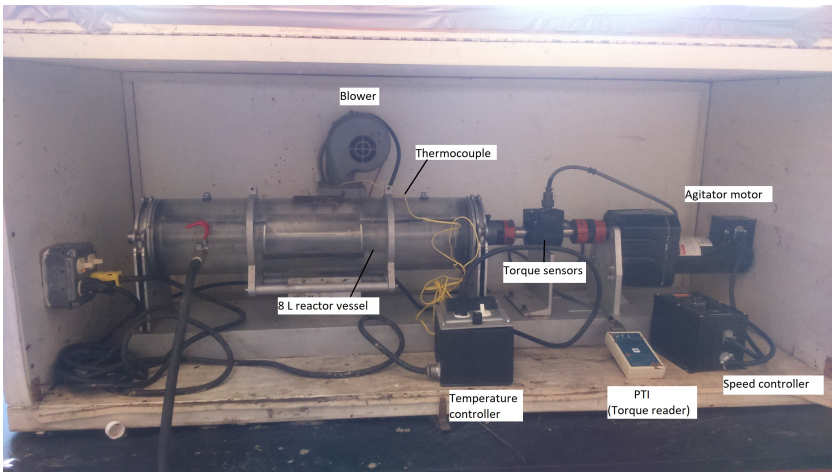

Figure 2.2. Experimental set-up of Dasari's scraped surface bioreactor (SSBR) [40]

Agitation was driven throughout the shaft by an electrical DC motor, set at 8-10 rpm. Torque measurements were recorded by a rotating torque sensor (Sensor Developing Inc, USA), which is coupled between the DC motor and the reactor shaft. Torque readings were displayed by a portable peak tracking instrument (PTI), so readings were taken manually. Temperature was kept constant at 55 °C by blowing hot air with a blower fan, and controlled with thermo-couples inserted into the reactor. The whole reactor set-up was placed inside a home-made heating chamber, a 2 × 1 m box as seen in Fig. 2.2.

Unless otherwise stated, MSW pulp was shredded for enhancing the mixing process, except for the 1^{st} run. In runs 2 and 4, fed-batch feeding strategy consisted on adding 50% of working volume at time 0, followed by filling of remaining volume at time 8. In contrast, in batch no. 3, reactor was gradually fed by 33% of working volume at times 0, 8 and 24 hours of hydrolysis. These time-lines were selected to enable sufficient reduction in the system viscosity.

2.3.3.2 Home-made SSBR design

A 7 L SSBR was designed and commissioned, consisting of a 50 x 15 cm PVC cylinder (Plastic Pipe Shop, UK) enclosed with two PVC end-caps and coupled with a scraped impeller. Three types of stainless steel scraped blades were built by technicians in the School of Mechanical Engineering (University of Leeds), to the following designs: flat-paddles, angled-wing and large paddles (Fig. 2.3). Paddles/scraped blades were welded in shaft (50 cm long and 12 cm diameter), and their dimensions

are 9 x 6.6 cm (flat-paddles), 12 x 6.8 cm (angled-wings) and 14 x 12 cm (large paddles), respectively. To enhance the support of the mixing element, flanges bearings (RS components, UK) were installed in the centre of each end-cap. Three sampling ports of 1.2 cm diameter were included per side: two at $\sim$ 60% working volume (probes port) and one at the top of vessel (sampling port) and sampling (top of vessel). In addition, a 5 cm radius feeding port was found in the center of the vessel, which can be tightly closed with a home-made end-cap during experimentation.

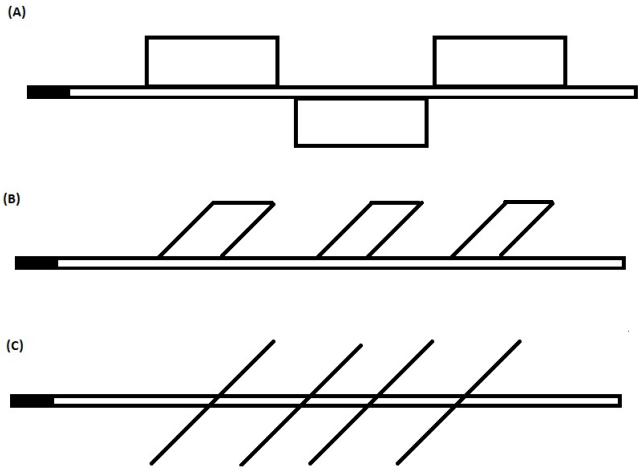

Figure 2.3. Scraped blades impeller configuration of the home-made SSBR: (a) flat, (b) winged and (c) large paddles

Agitation was provided by a horizontally placed overhead stirrer maintained between 30-60 rpms. To maintain the internal temperature of the vessel, hot water (from a water-bath) was pumped by a peristaltic pump (323Du model, Watson Marlow, UK) through silicon tubing which is coiled around the reactor vessel. Swagelok fittings were positioned between silicon and Masterflex® tubing to ensure efficient pumping and avoid potential leakages. By operating the peristaltic pump at $\sim$ 200 rpm and covering the water-bath (maintained at 70 °C), the temperature within the vessel was kept around 50-55 °C during the course of hydrolysis. The whole reactor set-up is shown in Fig. 2.4.

2.3.4 Rotary drum reactor

Rotary drum reactors (RDBs) can be set as falcon tubes placed in between two rollers. The mini-roller apparatus (model MR-02UA, Crystal Industries, US) was fitted inside a large incubator (Fig. 2.5). The drum vessels used varied in size, including the: 2L Nalgene® and 500 ml bottles, 50 ml falcon tubes and home-made tubes. Home-made tubes (Plastic Pipe Shop, UK) have a similar design to the SSBR described in section 2.4, except for the absence of an internal impeller and holding a smaller volume.

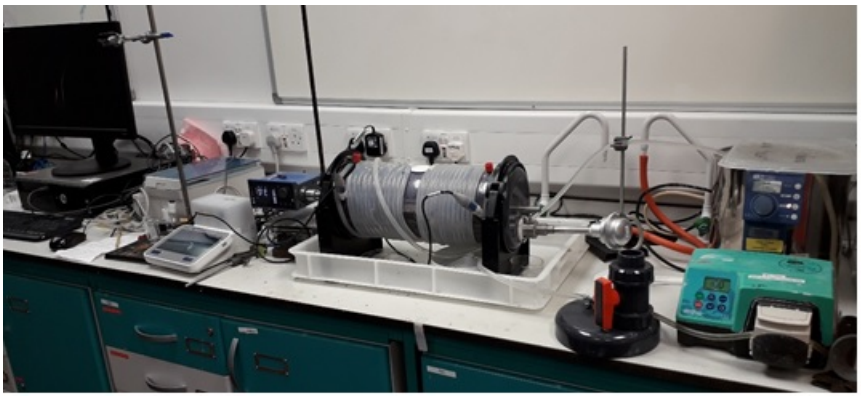

Figure 2.4. Experimental set-up of the home-made SSBR with coiled tubing and process monitoring components

Figure 2.5. Miniroller apparatus as means of RDBs set-up

2.3.4.1 Design of baffles: drum and tube reactors

Baffles were installed in the 2 L rotary drum reactors. For the 2 L vessels, the width of baffle was of 4 cm which is 30 % of reactor diameter and is a reference value used for designing solid-state fermentation drum reactors [43]. Four main baffled reactors (one to four baffles) were built using stainless steel sheets, fixed equidistantly from each other. For the rotatory drum reactors, the baffle width was determined as one-tenth (D/10) of vessel diameter, a standard design used in stirred tank reactors [44].

Further design of baffle thickness was pursued by following the methodology as described below. The minimum baffle thickness can be calculated from the fluid forces acting on the baffle, and the allowable bending stress for the baffle material of construction. One method shown below assumes that the baffles will have to absorb the total force supplied by the mixer torque. By the given expression (Eq. 2.1), absorbed torque is determined:

$$M = \frac{9550 \times P}{N} \tag{2.1}$$

Where M is the torque (N m), P the power consumption (W), N the rotational

speed (rpm) and 9550 is a conversion constant for using rpms in the torque calculation. Torque is converted into an applied force int the baffles and divided by the number of baffles (Eq. 2.2. The adjustment factor (Df) is used to take into account the distribution of forces along the baffle length. But for a conservative design this can be set to 1, assuming that all of the force imparted by the mixer is focused towards a single point level with the impeller.

$$F_B = \frac{m \times D_f 1000}{N_B \times [(D/2) - (B_w/2) - B_c} \tag{2.2}$$

Where F_B the force on each baffle (N), D_f equal to 1 (conservative design), N_B the number of baffles, D is the vessel diameter (mm), B_w the baffle width (mm) and B_c the baffle off wall clearance (mm). By fitting F_b, the baffle thickness is calculated taking into account the bending stress (34 or 600 N/mm^2 for steel or stainless steel, respectively) and mounting arrangements, assuming that the force is applied half way between two baffle supports (Eq. 2.3).

$$B_t = \sqrt{\frac{3 \times F_B \times W}{2 \times B_w \times S}} \tag{2.3}$$

Where B_t the baffle thickness (mm), W the space gap between baffles (mm) and S the allowable bending stress (N/mm^2). Thickness of baffles for the home-made tube reactors is summarised (Table **??**), depending on the number of baffles and sizing of each reactors, previously described above.

	Thickness (mm)			
Configurations	**1 Baffle**	**2 Baffles**	**3 Baffles**	**4 Baffles**
2.5 cm diameter				
L/D = 2	2.0	1.8	0.9	0.7
L/D = 4	1.8	1.7	0.9	0.8
L/D = 6	1.0	0.9	0.5	0.4
L/D = 8	1.2	1.2	0.6	0.6
L/D = 10	0.7	0.7	0.4	0.3
5 cm diameter				
L/D = 2	1.2	1.1	0.5	0.5
L/D = 4	1.1	1.1	0.6	0.5

2.4 Enzymatic hydrolysis assays

MSW pulps were sterilized via autoclaving at 121 °C for 1 hour prior to being stored at -20 °C. Before use, the MSW pulp was removed from -20 °C storage and thawed overnight at room temperature. Once thawed, the pulp was manually mixed to roughly homogenize fragment size. Hydrolysis reaction were carried out between

50-55 °C and pH 4.75- 5.25, and consisted of: MSW pulp, Cellic® CTec3 enzyme cocktail (Novozymes, Denmark), and an antimicrobial agent in water. The ratio of the assay components varied depending on a given experimental design. The following is an example of such an assay: 52 % dry matter (DM) MSW pulp at 5 % total solids (TS) content, 2 % enzyme- to-substrate (E:S) loading and 0.01 % (w/w dry substrate) anti-microbial agent in 1000 ml working volume (W_v). Under these conditions, the reaction mass consisted of: 50 g dry pulp (m_{dry}), 96 g wet pulp (m_{wet}), 904 g water (H_2O), 0.8 ml enzymes (enz) and 5.0 mg of anti-microbial agent (biocide). The calculation of enzymatic hydrolysis "ingredients" (all in mass units, except for enzyme loading) is derived from Eqs. 2.4 to 2.8:

$$m_{dry} = W_D \times (TS/100) \tag{2.4}$$

$$m_{wet} = m_{dry} \times (DM/100) \tag{2.5}$$

$$H_2O = W_D - m_{wet} \tag{2.6}$$

$$Enzy = \frac{m_{dry \times (E:S/100)}}{1.2} \tag{2.7}$$

$$Biocide = m_{dry} \times (biocide\%/100) \tag{2.8}$$

Where the density (g/ml) of Cellic Ctec® enzyme cocktail (Novozymes, Denmark) is 1.2. Prior to enzyme addition, the pH of the slurry was adjusted to between 4.75-5.35 with 6 % (w/w) H_3PO_4, and incubated at 50-55 °C in the selected reactor configuration. Pre-conditioning was carried out for a minimum of 30 minutes to ensure an even distribution of the antimicrobial agent (e.g. benzisothiazolinone , BIT).

2.4.1 Pseudo-flow hydrolysis set-up

Automated continuous hydrolysis with membranes and enzyme recycling was not possible to set-up, due to budget limitations and the particularity of the feedstock (coarse size) [21]. Hence, a manual continuous system was designed - termed as

pseudo-flow hydrolysis- using the drum rotary reactor configuration described in section 2.3. The reactor set-up consisted of a 2L pre-conditioning vessel a primary hydrolysis reactor and a secondary hydrolysis reactor (Fig. 2.6), operational parameters also included.

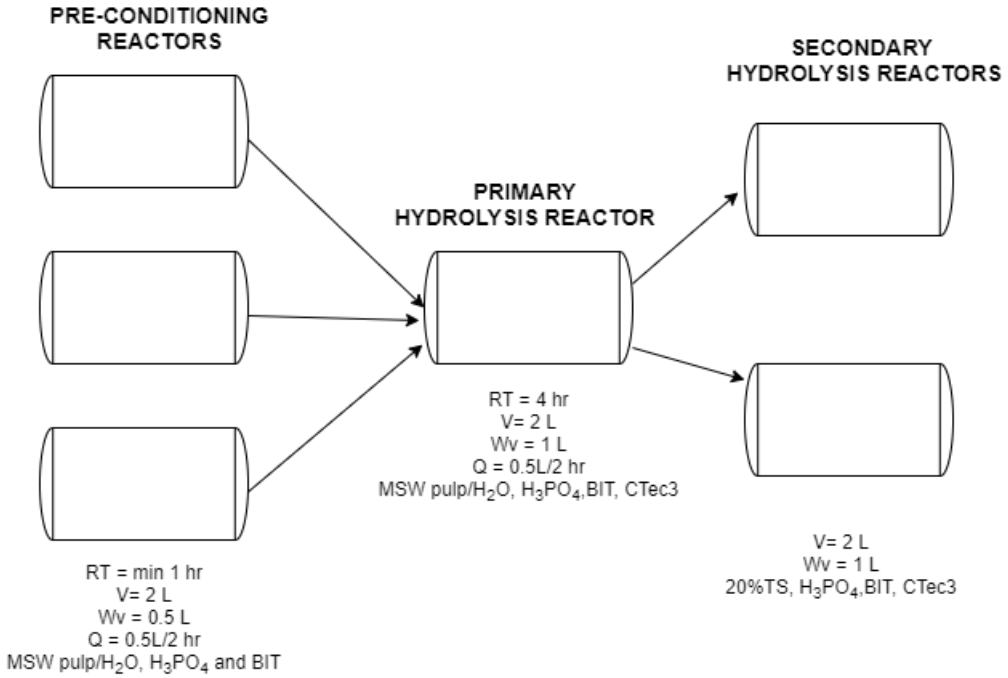

Figure 2.6. Pseudo-flow hydrolysis process design using 2L drum reactors

RT is residence time, V is volume, W_V is working volume, Q is flow-rate and the rest depict the present components (e.g. no enzymes in pre-conditioning reactors)

MSW slurries (Hampden pulp) were prepared in the three pre-conditioning vessels (working volume of 0.5 L) and the primary hydrolysis reactor (working volume of 1 L) at 20 % solids loadings. The four vessels were incubated over-night (pH-adjusted to 5), rolling at 10 rpm at 55 °C. The following morning, the slurry within the primary reactor was innoculated with 0.02% (w/w dry substrate) BIT and mixed at 10 rpm for an additional 30 min before the addition of 2% (w/w) enzyme, marking the start of hydrolysis. After 4 hours, the 500 ml of slurry was purged from the primary hydrolysis vessel, with 250 ml added to each of the secondary hydrolysis vessels. The removed 500 ml from the primary hydrolysis vessel was replaced with 500 ml from one of the pre-conditioning vessels, with appropriate addition of antimicrobial agent and pH adjustment.

In parallel to the primary and secondary hydrolysis, additional premix reactions were rolling as feeding preparations for the *pseudo-flow* hydrolysis. This "purging/loading" sequence was repeated every two hours (250 ml/hr), totalling 4 space-volumes, which is equivalent of filling each of the secondary hydrolysis to 1L working volume. Slurry samples were taken approximately every two hours for analysis. All experiments were conducted in duplicates. The time-lines and reactor conditions

are included in Fig. 2.6.

2.5 Process monitoring techniques

Process monitoring encompasses the use of techniques for the in-line readings of parameters throughout the course of enzymatic hydrolysis. Process monitoring was only carried out bioreactors (STRs and SSBRs) which allowed the attachment of probes or devices. The basis of process monitoring is the continuous reading of parameters by specific probes or devices, which convert a signal into the desired factor (e.g.[H^+] to pH as pH = - log [H^+]), and transferred it to a PC unit by commercial or bespoke software. The files generated were exported into manageable files (e.g. *Excel*) for data-processing and graphical analysis. In this section, the process monitoring of several parameters (e.g. pH and power consumption) is covered, some of which are grouped as the "slurry-media quality". For each parameter a description of particular instrumentation, methodology and calibration is included.

2.5.1 Slurry-media quality

To control the optimum performance of the enzymatic hydrolysis (section 2.4), a number of laboratory-probes can be inserted in the reactor configuration for on-line monitoring of corresponding parameters: pH, dissolved oxygen (DO), conductivity and temperature. These probes are based on the InLab® technology, automatic sensor recognition for data-logging, and are integrated with a thermocouple. Either pH and DO are used as metrics for studying the microbial contamination (further discussed in chapter 3). A third probe was also available, the conductivity probe InLabInLab® 741-5m for mixing-time analysis (section 2.8.2. All probes were fitted into a modular multi-channel bench-top meter (*SevenExcellence*), allowing the data-logging with a commercial software known as Easydirect pH^{TM} - Mettler Toledo (USA). Lab-grade probes are periodically calibrated with vendor or custom-made* standards:

- **pH**: 4.01, 7 and 9.21 technical buffers. A "corroboration" standard of pH 10 was used as well
- **DO***: zero oxygen tablets (0 %) and ambient air (100 %)
- **Conductivity**: 1413 μS cm^{-1} technical buffer

*DO can also be calibrated by analysis of a water media stirred in a round-bottom flask, which is saturated with nitrogen (0 % DO) or air (100 % DO).

2.5.2 Power consumption

The power consumption is directly calculated from the torque and rotational speed (Eq. 2.9). To measure the torque, the force caused by rotating an object in an axis, a

sensor is coupled with the motor unit. A IKA ministar 40 (IKA, UK) stirrer with an integrated torque-meter was used (section 2.3), allowing torque measurements up to 40 N cm. The instrument was calibrated following the manufacturer's instructions; torque-recording at the highest speed (1000 rpm) with the absence of impeller and air as media. During the hydrolysis reaction, automatic control and torque data-logging was set via a bespoke software, coded by Matthew Buckley (electronic technician, University of Leeds), in LabVIEW (NI Instruments, UK). In-line torque and rotational speed was transferred into a PC unit by USB cable at a desired interval, creating a *.xlsx* file. Fig. 2.7 shows the mentioned features, others are described in the subsection 2.6.2.

$$P = 2\pi NM \tag{2.9}$$

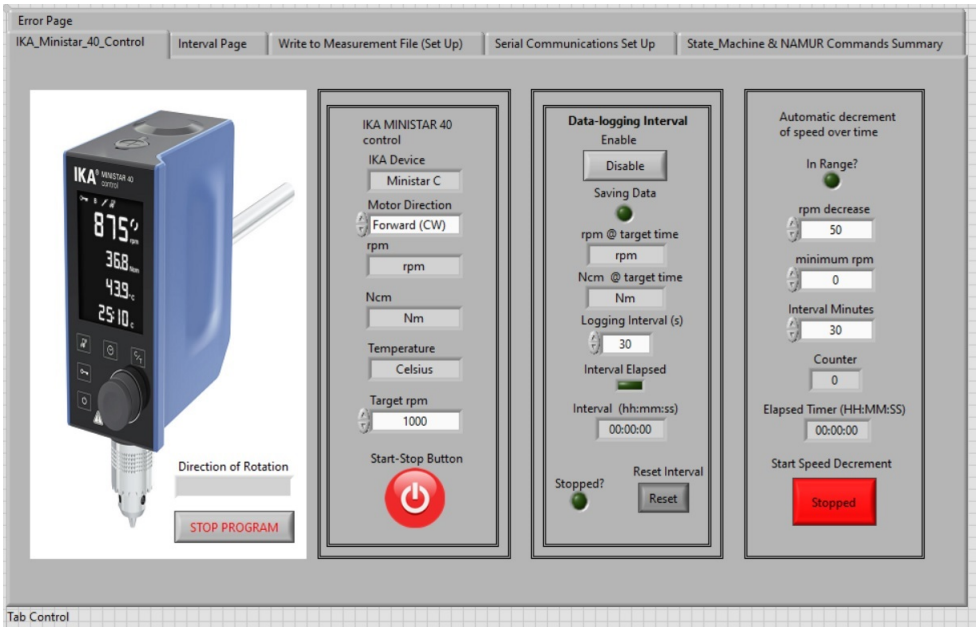

Figure 2.7. Interface of integrated power-control system known as *IKA Ministar 40 State*

For the SSBR, a 0.5 HP AC motor controlled by a single phase drive inverter (TEC, UK) was coupled with a torque sensor (FYO1 model, Forsentek, China) and load cell indicator. This configuration offers the possibility of combining the motor-sensor system with a modified version of the *IKA Ministat 40 State* (Fig. 2.7) for in-line monitoring and process optimisation.

2.5.3 Viscosity

In-line viscosity measurements were made by a QVis viscometer (model 01/o, Fluconcon Gmbh, Germany), constructed as a probe and compact electronic unit (Fig 2.8a). Viscosity determination is based on the quartz technology, a method developed by W.P Mason [45]. The working principle is that particles are distorted by the quartz

(piezoelectric) crystal, creating an electrical field that causes a torsional oscillation back to the quartz crystal (Fig. 2.8b). The high shearing frequency (s^{-1}) and pressure (Pa) of the torsional oscillation is translated into the viscosity of the fluid (Pa s).

(a)

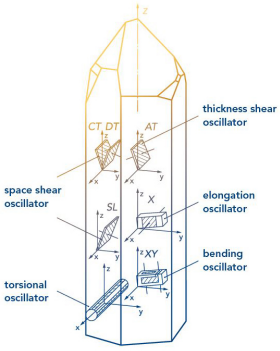

(b)

Figure 2.8. Process viscosimeter QVis 01/o: (a) probe and (b) fundamentals of quartz viscosimetry

The instrument is calibrated using a general purpose viscosity standard (Type S3, Paragon Scientific, UK) with a viscosity of 3.291 mPa s. In-line viscosity measurements were carried out using the home-made SSBR (Fig. 2.4), as an adapted lid was installed for adequate probe fitting. Data was read by the electronic unit and transferred into the QVis software by a RS232 cable, with continuous measurements were recorded every 10 seconds. Monitored data is then exported as *CSV*. file for further data-processing.

2.5.4 FBRM: in-line particle size analysis

Focus beam reflectance measurement (FBRM) is an in-line technique that provides real time measurement of dimensions (0.5 to 1000 μm, as cord length equivalents) and number of particles. A relation between chord-length distributions (CLD) and particle-size distribution (PSD) could be established by following the finding of Wynn [46], allowing thereafter the comparison with the laser-diffraction technique. For this analysis, a FBRM instrument (model S400A PI 8/91, Mettler Toledo, USA) structured as a electronic unit and a stainless steel probe (Fig. 2.9). Prior inserting the FBRM probe in the MSW slurry-media, a baseline calibration is run with air as background. In-line measurements were taken every 5 minutes during the course of hydrolysis, where data was acquired by the instrument software (Lasentec, Mettler

toledo). The conversion of CLD to PSD was computed with MATLAB (Mathworks, UK) coding software from exported files, programmed by James Daglish (PhD student).

Figure 2.9. Lasentec FBRM 400A system, showing the electronic unit and probe

2.5.5 FTIR: real-time analysis of sugars

In-line sugar analysis was performed by in-situ FTIR using a MB3000 FTIR instrument (ABB, Switzerland), seen in Fig. 2.10. As glucose has an absorption peak at a wavelength of 1035 cm^{-1}, a calibration curve was created by plotting absorbance at 1035 cm^{-1} against glucose standards ranging from 0 to 100 g/L. After calibration, the probe was inserted into stirred tank reactors during the enzymatic saccharification, absorbance (at 1035 cm^{-1}) readings taken every 120 s by averaging 3 scans. The calibration curve was used to convert FTIR values to g L^{-1} of glucose.

Figure 2.10. ABB MB330 FTIR instrument, probe not included

2.6 Bespoke software applications

The bespoke software described here are developments of specific applications for custom-made necessities. For instance, LabVIEW (NI instruments, UK) or Arduino (Italy) are used to code the integration of process monitoring for data-logging, feedback control and self-control. These bespoke software are described in the corresponding sub-sections.

2.6.1 Integrated control system

To prevent the growth of microorganisms in the sugar-rich reaction mass, an integrated control system was designed with three main sub-systems: (1) process monitoring, (2) operating system, (3) automatic dosing system. A schematic of this set up is shown in Fig. 2.11. During enzymatic hydrolysis, the pH and DO were measured with the corresponding sensors: InLaB® probes (previously calibrated with vendor standards) installed in the SevenExcellence^{TM} multi-parameter kit. Continuous recordings (1 minute frequency) were automatically transferred to, Labx direct pH 3.3 (Mettler Toledo, USA) monitoring software, generating *.txt* files. A bespoke operating system, named "glucose bioreactor model", was programmed using LabVIEW (National Instruments, UK). This incorporates the recorded (in-line) data and commands the automatic dosing of anti-microbial agents by a syringe-pump unit (model 11, Harvard apparatus UK) according to pre-defined settings whereby a DO gradient threshold (Δ) is set as an "alarm" for triggering the sterilising product: Δ < - 0.028 mg L^{-1} s^{-1}. The algorithm determines the DO gradient according to the equation shown below (Eq. 2.10). A full description of the glucose bioreactor model can be found in [47].

$$\Delta DO = \frac{DO_F - DO_{f'}}{f} \tag{2.10}$$

Where: DO_F is the last monitored DO reading (mg L^{-1}), $DO_{f'}$ the value prior DO_F (mg L^{-1}) and f is the frequency of monitoring (in s, e.g. 10 s).

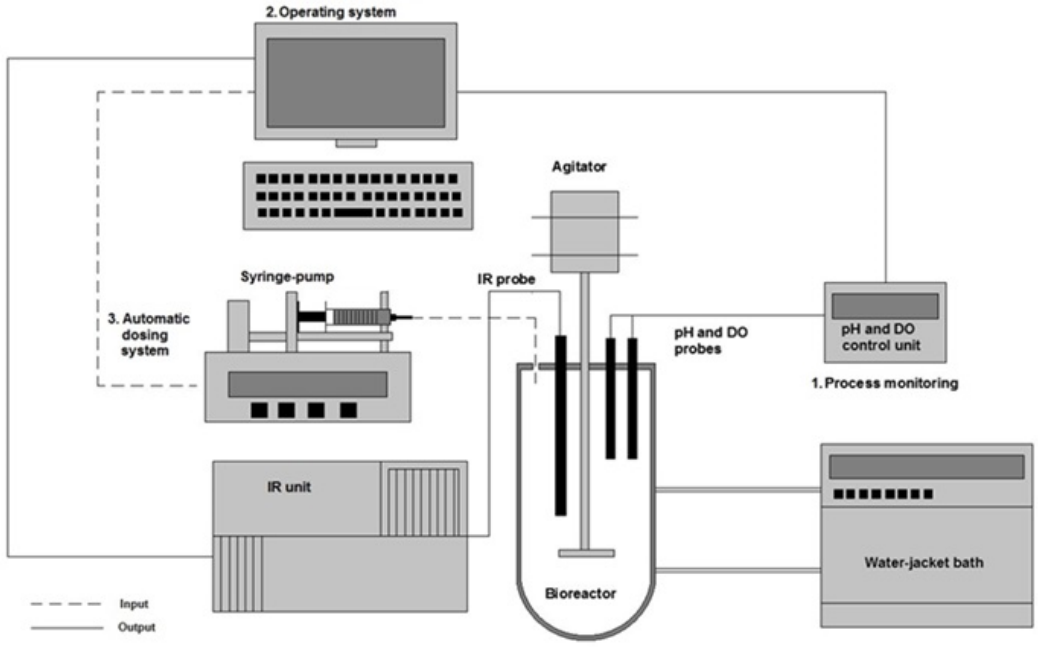

Figure 2.11. Experimental set-up of the integrated control system

2.6.2 Integrated power-control system

Remote start-up and automatic data-logging are features of the bespoke application, known as *integrated power-control system*. In addition to this, the operating system was further developed for an automated decrease stirring speed over time. For example, the rotational speed is reduced from 700 to 600 rpm over 2 hours. An additional function is available for changing the rotational direction, clock -wise to counter clockwise, which helps to prevent the formation of dead zones (unmixed) during mixing. All features are illustrated in Fig. 2.7.

2.7 Rheological analysis

The rheology of MSW hydrolysates was analysed by a Discovery HR-2 Hybrid rheometer (TA instruments, USA), equipped with Peltier concentric cylinder and vane-in-cup geometry (Fig. 2.12). The vane dimensions were 53 mm long, 30 mm of diameter and a thickness of 1 mm, whilst, the cup is of 40 ml volume (Fig. 2.12b). The instrument was controlled with an associated software (TRIOS, TA instruments), also providing data-acquisition and other features. Before analysis, the instrument was calibrated without and with the vane-in-cup geometry, adjusted at a zero-gap of 4000 μm (clearance reference). This configuration requires at least 38 ml for experimentation. However, for smaller samples, the parallel plate-plate geometry (8-10 mm of diameter) is the preferred option (Fig. 2.12c). All samples were covered with fitted lids to avoid potential evaporation or leakage.

Unless otherwise stated, the vane-in-cup was the chosen geometry for the two main methods were employed: flow sweeps and *in situ* rheology. A wide range of other techniques (low-torque, creep recovery and oscillatory sweeps etc..) were less commonly investigated, so are included in the corresponding sections.

Flow sweeps consisted of measuring the apparent viscosity at controlled shear rate, starting of 0.1 and going up logarithmically to 100 s^{-1}. Slurries were pre-sheared at 170 s^{-1} for 10 min for ensuring steady-state viscosity readings, i.e. no particle settling [48]. This procedure was conducted in duplicate, with a 10 min relaxation time (no agitation) between flow sweeps. In some cases, a descending flow sweep (100 to 0.1 s^{-1}) is also included after the ascending step (0.1 to 100 s^{-1}), with replicates performed as required.

In situ rheology involves the monitoring of rheological parameters (e.g. viscosity and shear stress) during the course of hydrolysis at fixed rotational speed. MSW slurries are prepared as described in section 2.4 but for a 40 ml volume. Prior enzyme addition, samples were pre-heated for 10-min. Temperature was maintained during the course of hydrolysis at 50 °C. pH was adjusted to $\sim$ 5 with 6 % H_3PO_4. Hydrolysis conditions were typically 5% TS, 2% E:S and 0.01% anti-microbial agent for at least 4 hours at 600 rpm (10 s^{-1}). Rheological measurements were taken every taken every 30 seconds and whole reactions were conducted at least in duplicates.

Figure 2.12. Rheometer instrumentation: Discovery Hybrid Rheometer HR-2 apparatus (a), vane-in-cup geometry (b) and parallel plate-plate geometry (c)

2.7.1 Determination of non-Newtonian properties

Flow sweeps (mainly viscosity and shear determination over a shear rate spectrum) are used to determine rheological parameters that are specific to reactor configuration and operational conditions. Due to the Non-Newtonian behaviour (further explained in chapter 4), two main models can be fitted: Power-law and Herschel-Bulkley model. By fitting a power-law model (Eq. 2.11), as a $y = ax^b$ curve, the following parameters are determined: flow consistency (K, in N s/m^2) and flow behaviour index (n, dimensionless).

$$y = ax^b = \mu_{app} \longrightarrow kK{\gamma_{eff}}^{n-1} \tag{2.11}$$

Where μ_{app} is apparent viscosity (Pa s) and γ_{eff} is effective shear rate (s^{-1}). Metzner and Otto [49] formulated Eq. 2.12, a correlation of γ_{eff} as function of shear impeller constant (k) and rotational speed (N, in s^{-1}). More recently, Bakker et al [50] determined the impeller constant (k) upon impeller geometry, e.g. k is equal to 11 for a pitched-blade impeller (our case). By combining both expressions, the apparent viscosity (μ_{app}) can be computed at given reaction conditions (Eq. 2.13).

$$\gamma_{eff} = kN \tag{2.12}$$

$$\mu_{app} = K(kN)^{n-1} \tag{2.13}$$

Likewise, a Herschel-Bulkley model (Eq. 2.14) is fitted in flow sweeps that include shear stress (τ, in Pa) as function of shear rate (γ, in s^{-1}). In the below expression, an additional parameter known as yield stress (τ_0) is included which is the minimum amount of pressure to start the fluid motion. Yield stress was calculated by curve-extrapolation at zero γ. Model fitting of Non-Newtonian models,

and statistical analysis such as the coefficient of regression (r^2), are performed by the graphical software OriginPro (OriginLab, USA).

$$\tau = \tau_o + K\gamma^n \tag{2.14}$$

2.8 Agitation and Mixing

Characterisation of power consumption and typology of fluid regime are key experimental factors for the optimising the design of reactors and impeller geometries in accordance with the application. These two factors are typically expressed as two dimensionless parameters known as Power (N_p) and Reynolds (R_e), determined by Eq. 2.15 and 2.16, respectively.

$$N_P = \frac{P}{\rho N^3 D^5} \tag{2.15}$$

$$R_e = \frac{\rho N D^2}{\mu} \tag{2.16}$$

Where ρ is fluid density (kg m^{-3}) and D is impeller diameter (m). For Non-Newtonian fluids, a modified expression of Reynolds number (R_e) is elaborated by integrating the power-law model (Eq.2.17).

$$R_e^n = \frac{\rho N D^2}{\mu_{app}} = \frac{\rho N^{2-n} D^2}{K(k)^{n-1}} \tag{2.17}$$

2.8.1 Power curve test

In the laminar regime, the product of N_p and R_e is a specific constant (K_p) to the reactor and impeller configuration (Eq. 2.18). As μ is the ratio of τ and γ, μ is inversely proportional to the R_e numerator (ρND^2) for Newtonian fluids (e.g. water and glycerol). A modified version for Non-Newtonian fluids (K_p^n) equal to $N_p \times R_e^n$, can be calculated with the previous determination of power-law properties (Eq. 2.13).

$$K_p = N_P \times N_{Re} \; or \; \frac{P}{\rho N^3 D^5} \times K_p = N_P = \frac{P}{\rho N^3 D^5} \times \frac{\rho N^3 D^5}{\mu} = \frac{P}{\mu N^2 D^3} \tag{2.18}$$

In both cases, the associated power constant, is determined by conducting a power-curve (also known as power-draw) analysis. This method is based on recording power consumption as function of rotational speed during the agitation of fluids in either STRs and SSBRs configurations. Hereby, the integrated power-curve system (section 2.6.2) was performed to automatically reduce the rotational speed whilst recording torque measurements, e.g from 900 to 200 rpm. No torque was detected at lower speeds. A wide range of materials of both Newtonian (water, silicon oil and glycerol) and Non-Newtonian (Xantham gum, cellulose methyl carbonate) fluids were available for experimentation. Power-curve analysis was also performed in initial (no enzyme) and final (enzymes deactivated with NaCl) hydrolysate slurries, taken into account as Non-Newtonian fluids. Once the N_p and R_e (or R_e^n) plot was constructed, it was necessary to define the Reynolds number where the fluid turns from laminar to transient, and from transient to turbulent. In theory, the slope of the power-curve is -1 and 0 in the laminar and turbulent "section", respectively [51]. So the lower (laminar) and upper (turbulent) Reynolds threshold is derived as the crossover point to the transient regime slope ($-1 < m < 0$). Tangential curves are fitted into the experimental data via linear processing of OriginPro (OriginLab, USA).

2.8.2 Mixing time

Due to the lack of resources and opacity of waste slurries, only four methods were considered for determining mixing-time: conductometry, thermometry and pH-metry. In all cases, a $\sim 0.01\%$ tracer (v/v), which mimicked the enzyme-to-total volume ratio, was injected into the opposite side of the installed probe in the bioreactors.

The methodology for conductometry, thermometry and pH-metry was based on using the corresponding probes installed in the SevenExcellence multi-parameter unit (Mettler Toledo, USA) - all with integral thermocouples. A 10 % NaCl (w/w DI water) aliquot is prepared, sonicated for 10 minutes to ensure complete mixing of particles, before loading, conductivity of aliquot was measured as reference. The reagent was pre-heated at 70 °C, and injected in the reactor where conductivity and temperature were mixed until stabilisation of values (mixing time). Similarly, pH-metry was performed but with two probes, locate on opposite sides (top to bottom or left to right). By using InLab^{TM} probe models, all monitored data was transferred into the Easydirect pH sofware (Mettler Toledo, USA) for further data-processing.

2.9 Analytical methods

2.9.1 Dry matter analysis

Dry matter (DM) content - also known as total solids in the NREL method [52] - was assayed by the "oven-drying method" which is based on the weight difference after overnight drying at 105 °C of wet samples. A variant of this method is to determine the moisture content (MC), by a moisture analyser (model HX204, Mettler

Toledo, USA). This device works as an oven with an integrated scale, that calculates the amounts of evaporated moisture instead of remaining solids. DM was determined by difference of total weight minus moisture content, thus providing similar results than the first method. Experiments were performed in triplicates with at least 20 g of representative samples, which were previously sub-sampled by the coning-quartering method, sample preparation method for obtaining a representative analyte [53].

2.9.2 Lignocellulosic compositional analysis

Lignocellulosic content was analysed by the so-called "two-stage acid hydrolysis", a standardised method by NREL [54]. Structural carbohydrates (glucan and xylan) and Klason Lignin were determined as the amounts of release monosaccharides and lignin fractions, respectively, after acid digestion of biomass. 0.3 g of substrate, previously dried at 40-45 °C and sieved at $2000 < x < 1000$ μm for 2 days, was hydrolysed with 3 ml of 72% (w/w) acid sulphuric in pressure tubes (Ace Glass Inc. USA) in a water-bath at 30 °C for 1-hour. The substrate was stirred every 5-10 minutes to ensure homogeneous mixing. A second acid hydrolysis was carried out by diluting the acid solution with 83 ml of DI water (yielding 4% (w/w) H_2S_4) and then sterilised at 110 °C for 1-hour. Following this, autoclaved hydrolysis solutions were vacuum-filtered through a filtering crucible. A portion of the filtrate was then used for acid soluble lignin and structural carbohydrates analysis. Acid soluble lignin was analysed by a UV-Vis spectrophotometer at a wavelength of 240-320 nm, whilst structural carbohydrates were quantified by HPLC (subsection 2.9.3). The sugar analyte was neutralised to pH 6-7 with $CaCO_3$ and supernatants filtered with 0.2 μm syringe filters. The remaining solids residue after filtration was dried at 105 °C for approximately 4 hours (moisture content), and ashed at 550 °C for two hours (ash content). Lignin (insoluble) content was determined by subtracting the previously calculated moisture content and ash content of the hydrolysed biomass, totalling as Klason lignin with the addition of acid soluble lignin. To take into account the amounts of loss sugars after acid hydrolysis, high-purity carbohydrates (glucose, xylose, mannose, arabinose and galactose) were autoclaved as before with 4 % (w/w) H_2SO_4 - recovery standards. The whole experimentation was carried out in duplicates and can be visualised in Fig. 2.13.

2.9.3 High-performance Liquid Chromatography

Hydrolysates were collected periodically during enzymatic hydrolysis and boiled-off at 90 °C for 10 min to deactivate the enzymatic activity. Samples were centrifuged at 4000 rpm for 10 minutes in a Megafuge 16R centrifuge (Thermo Scientific, UK). Supernatants were passed through 0.45 μm syringe filter (Sartorius, Germany); analyte vials were prepared as a 10-fold dilution from neat aliquot and stored in a freezer at -20 °C until analysis. Monomeric sugar and acid concentrations were quantified

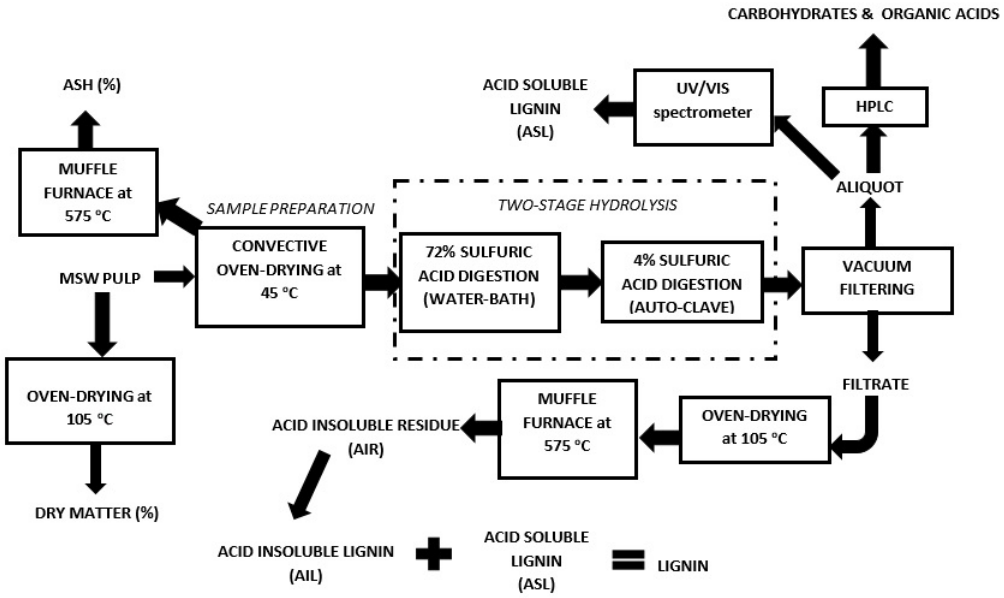

Figure 2.13. Schematic diagram of the lignocellulosic compositional analysis in biomass

by HPLC (Shimadzu, Japan). Monosaccharides (D-glucose and D-xylose) and organic acids (L-Lactic acid and Acetic acid) were analysed simultaneously by HPLC fitted with an Ultimate^{TM} Dionex 3000, UK column. A 10 μL sample was injected and separated by a Supelcogel^{TM} C-610H (6% Crosslinked) column with a deashing guard column, operating at 30 °C with 0.1 wt% phosphoric acid at a flow rate of 0.5 ml min^{-1} as mobile phase. Monosaccharides and organic acids were detected respectively by a Shodex RI-101 refractive index and a diode array detector (Thermo Scientific, UK). High-purity analytical standards were used for external calibrations in the linear range of 0.5 to 20 g L^{-1} and 0.125 to 2 g L^{-1} for monosaccharides and organic acids, respectively. All chromatograms were processed by Chromoleon^{TM} software (Thermo Scientific, UK).

2.9.4 High-performance anion-exchange chromatography with pulse amperometric detection

Analyte vials were prepared as described above for the HPLC method, except the supernatant was filtered through a 0.2 μm syringe filter (Sartorius, Germany) and 100-fold diluted. A wide range of cellulose-derived products (monosaccharides, disaccharides, aldonic acids and oligosaccharides) were determined by HPAEC-PAD Dionex ICS-5000 instrument (Thermo Scientific), using the method described by Basumallick and Rohrere [55]. A 10 μL sample was injected and separated by PA20 3 x 150 mm column, protected with a guard-column PA20 30 $\times$ 30 mm (Dionex, Thermo Scientific), operating at 30 °C and flow-rate of 0.4 ml min^{-1}. A 60-min gradient program was run whereby ratio of the three eluents (DI water (A), 200 mM NaOH (B), and 100 mM NaOAc (C)) were alternated (Table 2.4). Molecules were detected with

a pulsed amperometric detector, made of a gold working and silver reference electrodes. Sample composition was elucidated and quantified using previously prepared standard curves (ranging from 0.01 to 10 mg L^{-1}) for monosaccharides (glucose and xylose), disaccharides (cellobiose and sucrose), aldonic acids (gluconic and cellobionic acid) and oligosacharides (cellotriose, cellotetraose, cellopentaose and cellohexaose). Oligosaccharides were purchased from Megazyme Ltd. (Ireland) and the cellobionic acid was synthesised according to the Wing and Freer method [56]. Chromatograms were processed by the Chromoleon^{TM} software (Thermo Scientific, UK).

Table 2.4. Step-wise gradient program in HPAEC-PAD analysis

Time (min)	Eluent A (%)	Eluent B (%)	Eluent C (%)
0.0	98.8	1.2	0
18.0	98.8	1.2	0
20.0	50	50	0
30.0	50	50	0
30.1	0	0	100
46.0	0	0	100
46.1	0	100	0
50.0	0	100	0
50.1	98.8	1.2	0
60.0	98.8	1.2	0

2.9.5 Protein content

Protein concentration was determined using the Bradford Method [57], with bovine serum albumin (Sigma-Aldrich, USA) used as protein standard. Using a 2:7 dilution of Bradford reagent (BioRad, UK) a standard curve ranging from 0-100 μg BSA/ml DI water was used for sample quantification. Dilutions of hydrolysate samples were prepared in dH_2O. Absorbance of standards and samples were read at 595 nm using a spectrophotometer (Perker Elmer, USA).

2.9.5.1 Enzyme adsorption

Adsorption of cellulase enzymes onto the substrate surface, enzyme adsorption (E_d), were determined by difference of fresh (neat) and free (hydrolysate) enzyme concentration in equivalent protein units. The calculation of enzyme adsorption was performed in consideration of dilution factor of UV-based and hydrolysis assays, with an initial reference of 150 mg BSA/ml of Cellic® CTec3.

2.9.6 Particle size distribution

The particle size distribution (PSD) of MSW hydrolysates ($\sim$ 1 ml) was measured by a Mastersizer 2000E (Malvern Instruments Ltd, United Kingdom). This instrument is based on the laser diffraction theory. A laser beam is passed through a particle,

scattering an angle of light that is directly proportional to the particle size. A sample dispersion unit (Hydro SM), also from Malvern, was used to incorporate the samples with deionised water (dispersant) at a pump speed of 1700 rpm. Resulting angles were detected and analysed by using a software, provided by the Mastersizer 2000E. Refractive index and absorption coefficient were set at 1.5 and 1.0, respectively [58]. This experiment was conducted in triplicate, obtaining results with an average residual smaller than 0.5%. Two main parameters were extracted from the PSD analysis: surface weighted mean diameter ($D_{3,2}$), volume weighted mean diameter ($D_{4,3}$). Acquired data can also be translated into other parameters such as fiber length or number of particles by the instrument's software.

2.9.7 Crystallinity index (CrI)

Crystallinity index (CrI, %) of various samples was determined by powder x-ray diffraction (XRD). Samples were oven-dried at 105 °C during the night and kept in hermetic containers until analysis. XRD analysis was carried out by Bruker X8 single crystal diffractometer with a Cu Kα radiation, operating at voltage of 30 kV and a current of 10 mA. Scans were taken from 5° to 50° of 2θ. The intensity spectrum was recorded, and, crystallinity index (CrI, Eq. 2.19) calculated according to the Segal method [59], where I_{002} is the peak intensity at 22.2 ° and I_{am} is the peak intensity at 18.4° (Fig. 2.14).

$$CrI(\%) = \frac{I_{002} - I_{am}}{I_{002}} 100\% \tag{2.19}$$

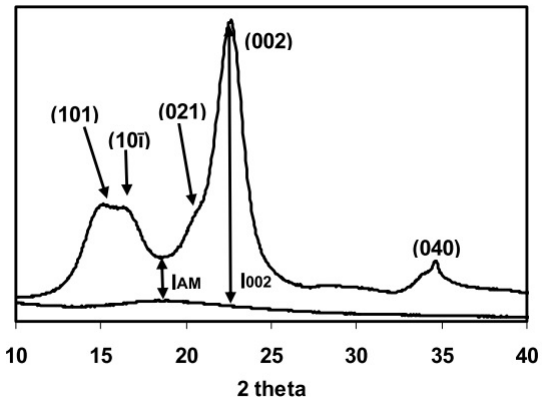

Figure 2.14. Example of XRD diagram for the determination of the crystallinity index

2.9.8 Scanning electron microscope

SEM imaging of raw and blended MSW pulp was performed by a Hitachi TM3030 bench-top microscope, applying a voltage of 15 kV. Prior to analysis, samples were

oven-dried at 105 °C overnight and mounted on a thin layer of gold using an EMS 550 sputter coater. SEM was carried out at vacuum-conditions and imaging was taken at 10,000x magnifications.

2.10 Mass and Energy balances

Governing equation of mass balances of any system (batch, fed-batch or continuous), including each term in mass units, is depicted in Eq. 2.20:

(mass accumulation rate) = (mass flux in) - (mass flux out) + (net rate of chemical production)

$$\frac{dm}{dt} = m_{in} - m_{out} + m_{rxn} \tag{2.20}$$

Accumulation rate ($\frac{dm}{dt}$)

$$\frac{dm}{dt} = \frac{\Delta m}{\Delta t} \rightarrow m = CV \rightarrow \frac{VdC}{dt} \tag{2.21}$$

Where V is working volume (L), C is concentration of product (g L^{-1}) and t is process time (hr).

Mass fluxes (m_j)

$$m_j = Q_j C_j \tag{2.22}$$

Where $_j$ depicts inlet (in) or outlet (out) stream to reactor and Q is flow-rate (l/hr).

Net rate of production (m_{rxn})

Since the enzymatic hydrolysis of biomasses into monomeric sugars have been identified as first-order kinetics [60–62], m_{rxn} adopts the following equation:

$$m_{rxn} = kVC \tag{2.23}$$

Where k is catalytic rate or rate constant (h^{-1}). Processes can be mainly operated in three modes: batch, fed-batch and continuous. Fig. 2.15 illustrates the mass energy components for each system, which are used to construct mass balances and model the determination of product concentration at discrete times.

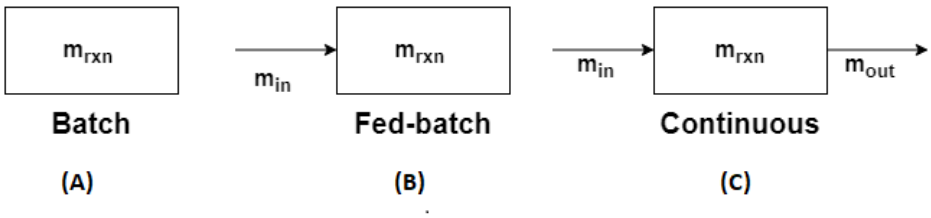

Figure 2.15. Schematic diagram showing mass balances upon mode of operation: batch, fed-batch and continuous

2.10.1 Batch mode

Assuming a well-mixed batch reaction with no inlets or outlets, the only mass component is the reaction mass that was loaded at once (Fig. 2.15a). Therefore, the rate of changing mass is proportional to the rate of product formation (Eq. 2.24). From that, product concentration at given time (t) can be computed as Eq.2.25.

$$\frac{dm_r}{dt} = m_r xn = kVC \tag{2.24}$$

$$C(t) = C_0 e^{kt} \tag{2.25}$$

2.10.2 Fed-batch mode

A fed-batch is an hybrid mode between batch and continuous, whereby slurry is periodically and discretely fed into an initial reaction slurry mass via an inlet stream (Fig. 2.15b). In a well-mixed system, the product formation (at a given time) is equivalent of the entering mass plus the reaction mass (Eq. 2.26). Concentration of product is determined by Eq. 2.27, where V_t is working volume at given time (t).

$$\frac{dm_r}{dt} = Q_{in}C + m_r xn \tag{2.26}$$

$$C(t) = \frac{Q}{V_t}(C - C_0) + C_0 e^{kt} \tag{2.27}$$

2.10.3 Continuous mode

In the continuous mode, all entering and exiting streams are taken into consideration when modeling the mass-balances. As seen in Fig. 2.15c, there is one inlet and one outlet stream as well as reaction mass in the system. In steady-state, there are few

considerations to be made: Q_{in}= Q_{out} = Q and C_{out} = C_{rxn} = C. Hereby, mass-balance is formulated as Eq. 2.28 and product concentration can be isolated (Eq. 2.29).

$$\frac{dm_r}{dt} = QC_{in} - QC + kVC \tag{2.28}$$

In this work, the initial concentration is considered 0 so the differential equation is solved for product concentration at given time.

$$C_t = C_0 \cdot e^{-(\frac{Q}{V}+k)t} \tag{2.29}$$

Other parameters that can be calculated in continuous processing are: steady-state concentration (C) and time to reach X% of its conversion (t_{ss}). Eq. 2.30 and Eq. 2.31 are included below:

$$C = \frac{m_{out} - m_{in}}{kV} \tag{2.30}$$

$$t = \frac{lnX/100}{\frac{Q}{V} + k} \tag{2.31}$$

2.11 Design of Experiments

Design of experiments (DoE) is an alternative experimental design tool to one variable at at time (OVAT), which optimises a process/reaction with fewer required experiments and more statistical evidence [63]. Designs and statistical analysis were performed in the software MODDE Pro 12.1 (Umetrics AB, Sweden). Two main groups of models were employed: (i) screening and (ii) response surface modelling (RSM).

As a primary step in DoE study, it is essential to identify the interaction and importance of factors of responses with investigated variables. For this, a screening approach as the full-factorial (two-levels, 2^k) was run, as the primary option as suggested for the software. The computation of number of experiments is equal to equal to 2^k, where k is the number of factors. These designs have two levels, coded as -1 and +1, and variables can have a quantitative (e.g. rotational speed) or qualitative nature (e.g. type of enzyme cocktail). The experimental matrix is summarised in Table 2.5, for a 2^3 factorial design. Here, a matrix is constructed for all combinations of three factors, reporting their minimum and maximum values as -1 and +1 respectively. Same procedure can be used to build any type of full-factorial design, for k number of variables.

Table 2.5. Experimental matrix of a 2^3 full-factorial design

Factor A (Y1)	Factor B (Y2)	Factor C (Y3)
-1	-1	-1
+1	-1	-1
-1	+1	-1
+1	+1	-1
-1	-1	+1
+1	-1	+1
-1	+1	+1
+1	+1	+1

Table 2.6. Experimental matrix of 2^2 central composite face-centred (CCF) design

Factor A (Y1)	Factor B (Y2)
-1	-1
+1	-1
-1	+1
+1	+1
-1	0
+1	0
0	-1
0	+1
0	0

After screening, RSM designs can be used to define and predicted the response of factors with further precision. RSM models are constructed as full-factorial, except introducing the 0 code, an intermediate point between minimum-maximum range. Table 2.6 depicts the simplest central composite design known as face-centred (CCF).

From a geometric point of view, 2^3 full-factorial and CCF design can be visualised as Fig. 2.16a-b. The 2^3full-factorial is shaped like a cube, three variables (Y1, Y2 and Y3) in two levels (-1 or +1). Then, central composite face-centred (two variables, Y1 and Y2) is a square with three levels (-1, 0 and +1). Unless stated otherwise, full-factorial (two to 4 variables) and central composite face-centred (two variables) are the chosen designs. Other models used were modifications of above-mentioned designs. Each study that included a DoE is reported accordingly with its variables, responses and statistical analysis.

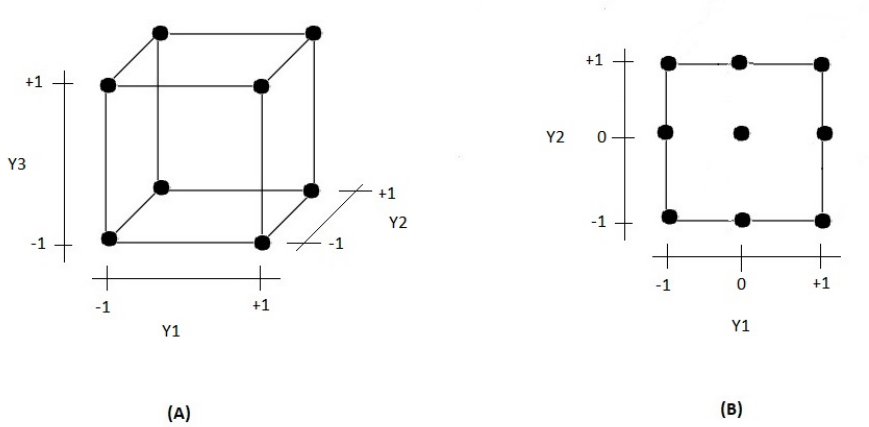

Figure 2.16. Graphical representations of employed DoE designs: (a) 2^3 full-factorial full-factorial and (b) 2^2 CCF

Chapter 3

Enzymatic hydrolysis of MSW-derived pulp: limitations and challenges

3.1 Introduction

The growth in worldwide population and industrialisation generates vast amounts of waste which emit potent greenhouse gases [64]. Renewable technologies such as incineration and AD valorise surges as option for waste valorisation, providing energy products and some chemicals, but not commodities. Whilst, biorefinery systems convert lignocellulosic biomass into multiple products such as fuels, chemicals and materials [4]. In contrast to oil refineries, biorefineries manufacture various product streams form one feedstock, in this case lignocellulosic biomass [64]. Lignocellulosic biomass is a broad group which includes residues from the agricultural (e.g. wheat), forestry (e.g. poplar) and urban (e.g. food waste) sector [39]. They offer a series of advantages compared to their predecessors (edible crops): avoidance of food versus fuel debate, constant supply and valorisation of wastes [65]. However, processing lignocellulosic biomass is less effective than food-based feedstocks due to the recalcitrant structure, composed as a lignin-hemicellulose-cellulose complex. To process this, severe pre-treatments methods are applied to disrupt the feedstock morphology and liberate the lignin-bonded polysaccharides, increasing the associated costs and process yields [66]. Once the feedstock structure is modified, enzymatic hydrolysis (or saccharification) is undergone by cellulolytic enzymes (cellulases) to release fermentable sugars from the structural carbohydrates fraction of biomass. A mix of sugars, organic acids and phenolics known as hydrolysate broth is commonly fermented into ethanol, a potential gasoline substitute, and carbon dioxide by yeast or bacteria. Although many other commodities can be derived from monosaccharides.

3.2 Literature review

3.2.1 Enzyme mechanisms of cellulases

Cellulases are a group of enzymes secreted by fungi, bacteria and protozoans for the biocatalysis of cellulosic substrates into intermediate and monomeric compounds. For commercial purposes, they are produced by *Trichoderma ressei* and *Aspergillus niger* culturing due to their efficiency, thermostability and versatility of using various carbon sources [67]. In the enzymatic hydrolysis, at least three types of enzymes are required to enzymatically degrade lignocellulosic biomass, listed by the enzyme commission (EC) number; endoglucanases (EC 3.2.14), exoglucanases or cellobiohydrolases (EC. 3.2.1.91) and β-glucosidases (EC. 3.2.1.21) [68]. Structure of cellulase enzymes consist on a catalytic domain (CD) and carbon-binding module (CBM) joined with a peptide linker to either catalyst the enzymatic mechanism and adsorb to the substrate, respectively. It has been demonstrated that cellulases takes around 10-15 min to strongly adsorb to the substrate [24]. Enzymatic mechanisms of each cellulases are describe below:

1. **Endogluconases:** Cleavage of internal bonds, β-1,4 glucosidase linkages in the amorphous region of cellulose to generate reducing and non-reducing ends
2. **Cellobiohydrolyases:** Hydrolysis of β-glycosidic bonds in crystalline region of cellulose (cellobiohydrolases, CBH). Two types of CBH, CBHI and CBHII, cleavage reducing and non-reducing end-terminals of polymeric chain, respectively, generating cellobiose units
3. $\beta-$**glucosidases**: Hydrolysis of short-chain oligo and disaccharides by cleaving internal linkages (β-glycosidic bonds) to generate monomeric glucose units

More recently, a new group of enzymes known lytic polysaccharide monooxygenases (LPMOs) have exhibited potential to deconstruct crystalline cellulose. In the 1990s, researchers identified the first fungus that secreted polysaccharide monooxygenases (PMOs) and shown a positive outcome in the degradation of cellulosic substrates [69]. These enzymes can be produced by either bacteria or fungus domains. LPMOs break-down the cellulose chain by oxidative cleavage, not by hydrolytic means as other cellulases. It is inconclusive of which is the source of oxygen. Bissaro et al. [70] reported that H_2O_2 is the preferred electron donor, as showing further improvements on enzymatic saccharification than supplied oxygen sources. However, it is vital to optimise their biocatalytic activity as it can lead to over-oxidation of glucose to gluconic acid, [24], putting at risk the produced glucose titres. A schematic diagram of synergistic mechanisms associated with the enzymatic degradation of cellulosic biomass by cellulases can be seen in Fig. 3.1.

Several enzyme mixtures containing cellulases and LPMOs, among other auxiliary enzymes (e.g. hemicellulases and mannases), are formulated for commercialisation. From an academic viewpoint, main cellulase complexes used are: Cellic®

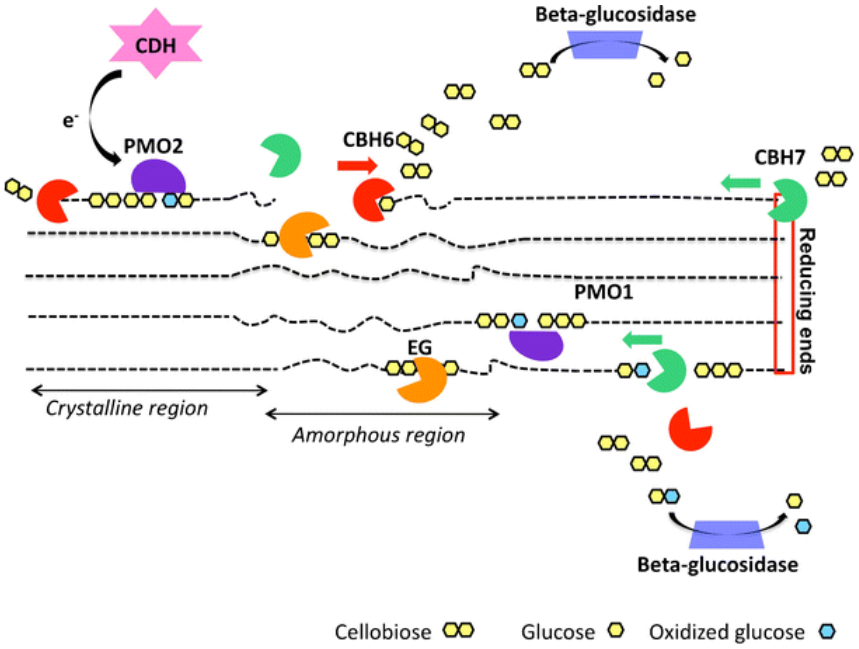

Figure 3.1. Schematic diagram of the synergistic mechanisms of cellulases in enzymatic hydrolysis [71]

Legend: EG is endogluconases, CBH6/CBH7 are cellobiohydrolase (non-reducing and reducing ends, respectively), CDH is a cellobiose dehyrogenase (an electron acceptor) and PMO2 and PMO1 are two types of LPMOs

XL CTec2 and 3 (Novozymes, Denmark) and ® XL 1500 (Dupont, USA) [68]. Further supplementation of β-glucosidases, produced commercially as Spezyme CP (Novozymes), was explored with pure cellulases (e.g. Celluclast® XL 1.5L). Other biorefining studies used alternatives cocktails such as AlternaFuel AF100L, AlternaFuel A200L (Dyadic, Canada) [72] and Zylase^R (Abengoa, Spain) [73–75], containing a blend of cellulases, xylases and β-glucosidases without LPMOs. It still unknown about the exact proportion of individual enzymes in commercial blends, but Jorgensen and Pinelo [24] provide an approximate composition of 36, 13, 9 and 1.5% for cellobiohydrolases, endogluconases, β-glucosidases and LPMOs, respectively, based on proteomic analysis by Chundawatt et al. 2011 [76].

Further developments in enzyme engineering and formulation are necessary to bring down enzyme costs to competitive values [77]. In particular, LPMOS needs to increase their thermostability and reactivity towards recalcitrant cellulose for improving its formulation in celluloytic mixtures. Therefore, it might be possible to tackle the major bottlenecks of bottleneck of commercial enzymatic hydrolysis of lignocellulosic biomass, in particular at high-solids loadings, leading to better commercialisation [17].

3.2.2 Municipal solid waste as feedstock for biorefining

There is interest in the utilisation of MSW as lignocellulosic feedstock for enzymatic hydrolysis, as alternative to agricultural and forestry residues [26]. MSW is a heterogeneous, abundant and affordable resource, mainly composed of an organic (food waste, paper, cardboard) and inorganic (metals, plastics , glass) fraction [78]. Depending on the source, the biodegradable (organic) fraction of municipal solid waste (BMSW) is around 60%. Just in the UK, 7.4 million tpa were produced, which are mainly constituted of carbohydrate. The conversion to monomeric equivalents by enzymatic or acid hydrolysis [79], and further utilisation faces many technological difficulties (eg. segregation, heterogeneity, stability, contamination) [80]. BMSW, also known as the organic fraction of MSW (OFMSW) is commonly processed via composting or AD processes, but not through enzymatic hydrolysis [81]. In the literature, MSW is investigated under the umbrella of various feedstocks, from single-stream to synthetic materials or unsorted MSW. Table 3.1 summarises different studies about bioconversion of each mentioned group; including the origin of feedstock, processed technology and lignocellulosic composition.

3.2.3 High-solids loadings

Enzymatic hydrolysis using solids loadings above 15% (w/w) fits a new paradigm known as "high-solids loadings enzymatic hydrolysis". Between 12 to 15 % (w/w) solids loadings, slurry mixing in stirred tank reactors is challenging due to its high-initial viscosity [42]. The absence of free water turns the feedstock to a thick paste, hindering mass-transfer phenomena and diminishing the enzymatic performance. To solve mass-transfer limitations, impeller rotational speeds can be increased up to 700 rpm consequently spending large sums of mixing energy. Another drawback of such high agitation is the shearing of cellulases, causing protein denaturation and deactivation [91]. To balance the decrease of conversion rates, additional enzymes can be loaded which increases the associated costs. Operating at high-solids loadings has several technical drawbacks: poor mixing, higher enzyme usage, higher inhibitory effect and long residence times (> 4 days) [92]. Despite this, high-solids loadings enzymatic hydrolysis can boost overall yields and process economics since more feedstock, therefore more product can be obtained per batch. Hence, it is possible to reduce the size of equipment (biorefining and downstream processing) and energy consumption in the distillation of highly-concentrated sugar syrups, significantly decreasing the capital (CAPEX) and operational (OPEX) expenditures [93]. Further description of suitable bioreactor designs for operation at high-solids loading is included in section 5.2.5 of Chapter 5.

3.2.4 Potential sources of contamination

Sugar monomers are versatile molecules for the synthesis of high-added value chemicals either through chemical and biological routes [94]. This strength is also a

Table 3.1. Summary of municipal solid waste (MSW) enzymatic hydrolysis studies

	Lignocellulosic composition ($\overline{x} \pm \sigma$)[1]				
Raw materials - source (origin)	**Cellulose (%)**	**Hemicellulose (%)**	**Lignin (%)**	**Ash (%)**	**Reference(s)**
Modelled (synthetic) wastes					
Individual food, paper and garden items - Denmark reference	40 ± 0.2	8.0 ± 0.9	14 ± 3.1	11 ± 1.2	Jensen *et al.* [82]
Glossy/non-glossy paper and cardboard	56 ± 5.0	10 ± 1.4	12 ± 0.3	11 ± 1.3	Sun *et al.* [79]
Carrot and potato peelings (KOW)	54	NA	9.1	NA	Li *et al.* [83]
Garden wastes (GOW)	43	NA	9.1	NA	Li *et al.* [83]
Newspaper and scrap paper (PSW)	61	NA	0.2	NA	Li *et al.* [83]
$\sum$ KOW + GOW + PSW[1]	54	NA	6.2	NA	Li *et al.* [81, 83, 84]
Individual food and kitchen residues - Washington State reference	~ 66	~ 13	18	3.1	Schmitt *et al.* [85]
Unsorted MSW					
OFMSW[2] - landfill site (Isfahan, Iran)	5.6 ± 0.5	1.7 ± 0.2	8.5 ± 0.4	1.40 ± 0.1	Mahmoodi *et al.* [78]
OFMSW[2] - Wilson Biochemical technology (UK)	44 ± 5.0	4.0 ± 1.0	50 ± 5		Meng *et al.* [86]
OFMSW[2] - Wilson Biochemical technology (UK)	28 ± 0.1	15 ± 0.07	18 ± 0.05	NA	Abdullah *et al.* [87]
OFMSW[2] - Fiberight technology (Lawrenceville, US)	55 ± 0.4	12 ± 0.1	26 ± 0.7	1.8 ± 0.0	Puri *et al.* [32, 36]

Table 1.1: Continued

Raw materials - source (origin)	Lignocellulosic composition ($\overline{x} \pm \sigma$)				Reference(s)
	Cellulose (%)	**Hemicellulose (%)**	**Lignin (%)**	**Ash (%)**	
OFMSW[2] - local composting plant EPELE (Gipuzkoa, Spain)		$\sim 49^{*}$		34	Izaguirre *et al.*[29]
OFMSW[2] - compost plant (Isfahan, Iran)	31 ± 0.4	21 ± 0.1	26 ± 0.3	12 ± 0.2	Ghanavati *et al.* [31]
House-hold food waste (HFW) - Kerbside collection (Athens, Greece)	12 ± 0.7	5.6 ± 0.6	3.8 ± 0.2	3.2 ± 0.20	Loizidou *et al.* [30]
Single-stream waste					
Lower grade paper - Tacoma recycling facility (USA)	~ 74	~ 14	0.6	6.9	Schmitt *et al.* [85]
Mixed office paper - University of Florida (USA)	~ 80	~ 10	~ 10		Brooks and Ingram [88]
Newspaper - Northwest Arkansas Morning News (USA)	55	30	14	1.0	Rivers and Emert [89]
Corrugated cardboard - Container Corporation of America (USA)	74	14	12	1.0	Rivers and Emert[89]
Old corrugated cardboard - Mzymes Oy (Finland)	56 ± 0.8	14 ± 0.2	15 ± 0.6	13 ± 0.1	Sotaniemi *et al.* [90]

[1] Unless otherwise stated, lignocellulosic composition was determined by the so-called NREL two-stage method [52]

*The fiber-detergent method was undertaken adapted for the ANKOM system, where fiber content is the sum of cellulose, hemicellulose and lignin fractions

[2] OFMSW is derived from MSW landfill sites, removing all recyclables such as plastics and glass, constituted with paper, cardboard, newspaper, food waste, kitchen tissues, yard waste, textiles etc..

NA is Not Analysed

weakness since they can be easily degraded into undesirable compounds via side-reactions such as isomerization or dehydration. The carbohydrates released from the lignocellulosic structure are prone to decomposition by chemical and biological means, turning into enzyme-related inhibitors. Without tackling the contamination, the economic viability of the process is at risk as overall yields are likely to decrease. Before introducing realistic strategies for overcoming the contamination in the system, it is important to identify the origin of such pollution. Herein, the main inhibitors are grouped by direct (lignocellulosic deconstruction) and indirect (biological infection) sources of contamination. In Fig. 3.2, the lignocellulosic structure of biomass is illustrated, highlighting the main sources of contamination by lignocellulosic deconstruction and biological infection. This subsection aims to describe each source of contamination, whilst reviewing potential mitigation strategies.

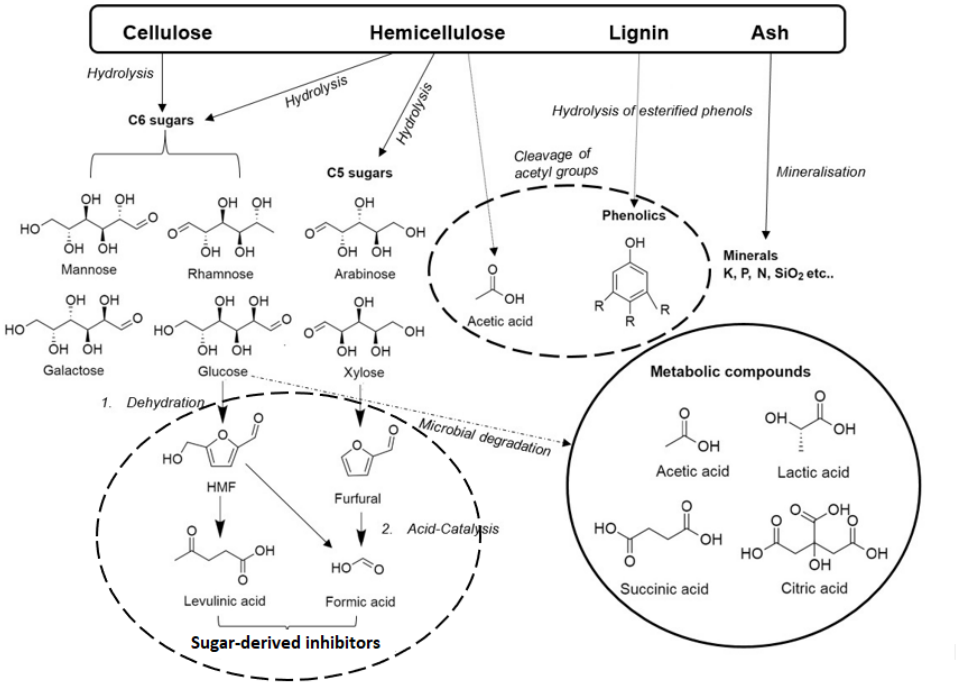

Figure 3.2. Schematic diagram of product inhibition by lignocellulosic and biological sources

3.2.4.1 Lignocellulosic deconstruction

Apart from hexoses and pentoses, other products are yielded as potential inhibitors during the biomass pretreatment and enzymatic hydrolysis steps [95] from the lignocellulosic matrix: small acids, furans and phenolics. The furanoic compounds such as hydroxymethyl furfural (HMF) and furfural are synthesised via dehydration of C-6 and C-5 sugars, respectively. At acidic conditions, further catalysis is promoted: (i) HMF to levulinic and formic acid and (2) furfural to formic acid [96]. Another weak acid, acetic acid, is released from the hemicellulosic fraction of biomass via

hydrolyis of acetyl groups [97]. The third group of inhibitors include a wide range of aromatic compounds derived from the lignin and extractive part of the biomass, known of phenolics. They are released by the hydrolysis of esterified phenols; ferulic and coumaric acid, vanillin and syringealdehyde are some examples of phenolic molecules. Less commonly though, small concentrations of uronic acid (e.g. glucuronic acid), aliphatic aldehydes and benzoquinoes are also present. The concentration of inhibitor is dictated by several factors: biomass composition, temperature, pressure and type of pretreatment [98]. Hence, it is crucial to find the optimum pretreatment conditions [99], to either minimise the formation of inhibitors whilst deconstructing the biomass structure. Fig. 3.2 illustrates part of the commented molecules and associated chemical routes, grouped as lignocellulosic-derived inhibitors.

The toxic effects of inhibitors in the lignocellulosic hydrolysates are various: decrease of pH-media, damage of cellular membranes, decrease of ATP and inhibits DNA synthesis/repair, among others [95]. Consequently, posing a detrimental impact on the effectiveness to release lignocellulosic sugars. More acidic conditions promote the sugar degradation to furanoic compounds and these weak acids are undesirable in the saccharified broth. Besides, the acidification of media leads to enzyme inhibition as optimum pH-range is not maintained, e.g. 4.75-5.25 for commercial enzyme cocktails. For example, it is well-known that Cellic CTec3 cocktail from Novozymes (a mixture of celulases, hemicellulases and LPMOs) loses more than 20% its enzymatic activity at pH < 4.5 [100]. Complications of this nature would accentuate the enzyme de-activation/inhibition. Hereby, it is crucial to control the pH of media during the saccharification assay, especially when buffer solutions are not used.

The minimisation of inhibitory effects during enzymatic hydrolysis is a key aspect of the biochemical processing of lignocellulosic biomass. Jønsson et al. [99, 101] reviewed a wide range of detoxification techniques, grouped as: chemical, enzymatic, thermal, microbial as well as liquid-liquid and liquid-solid extractions. The addition of chemical additives, alkali and reducing agents, is a mature and cost-effective option for *in situ* mitigation of inhibitors (e.g. NaOH or dithionite). The main considerations for introducing new molecules into the lignocellulosic slurry are: (i) use of additional chemicals and (ii) potential difficulties in the downstream processing such as enzyme recycling or end-user sugar application. These issues can hamper the profitability of the enzymatic saccharification, even specific strategies have been proven (e.g. sulfite to furfural). More recently, Jønsson L.J et al. [99] summarised the range of strategies to alleviate the potential release of lignocellulose-derived inhibitors, including their approaches and potential drawbacks. Some niche technologies are based on disciplines such as feedstock or genetic engineering. However, it is beyond the scope of this study to review these techniques to alleviate lignocellulosic-derived inhibitors.

3.2.4.2 Biological infection

Amongst the carbohydrates, glucose is the main source of carbon for bacteria. Glucose is converted to pyruvate via four different pathways: Embden-Meyerhof-Parnas (EMP), hexose monophosphate, Entner-Doudoroff and Phosphoketolase [102]. The EMP pathway, also referred as glycolysis, involves the anaerobic degradation of glucose to lactate via pyruvate synthesis by microorganisms (Fig. 3.3). For instance, *Lactobacilli* are homofermentative microorganisms, capable of completing the cycle by converting any remaining pyruvate to lactate. Other fermentative bacteria can utilise alternative hydrogen acceptors (acetaldehyde or carbon dioxide) for the metabolisation into acetic acid or ethanol. The primary 5-carbon sugar, xylose, also plays a role as auxiliary carbon source in the glucose metabolism, the so-called *Pentose Phosphoketolase Pathway*. Minor sugar monomers are also involved in the metabolic pathway of glucose: mannose [103], galactose [104], rhamnose [105], arabinose [106] and ribose [102].

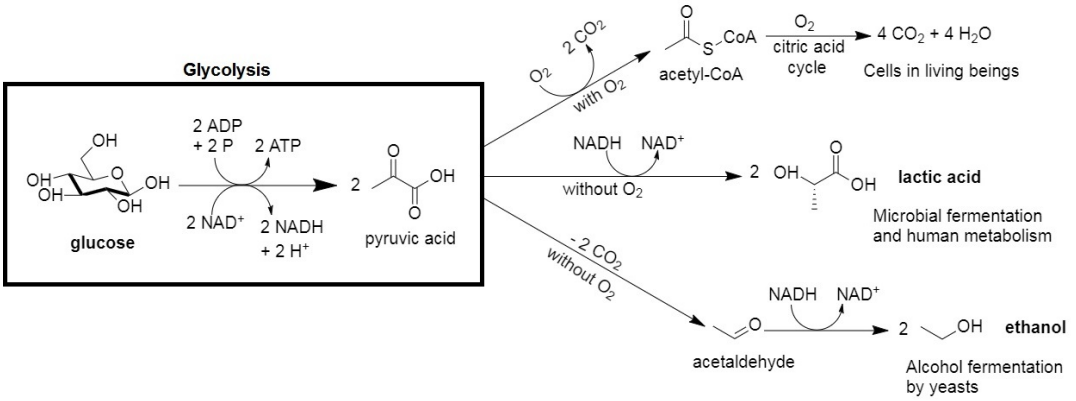

Figure 3.3. Metabolic pathways options after glycolysis [102]

Some of the microorganisms (e.g. *Escherichia coli* and *Lactobacillus*) are found in residual streams, which convert glucose into inhibitory compounds [27]. Lignocellulosic substrates inherently contain bacteria, therefore, newly produced carbohydrates are prone to decomposition,e.g. glucose to lactic acid. A large and varied population of microorganisms (e.g. yeast and fungi, bacterial spores and faecal forms etc..) have been found in municipal solid wastes [27]. Although it is notorious that these type of feedstocks contain microbes, not much bacterial characterisation has been carried out on the enzymatic hydrolysis compared to ethanol fermentation [107]. Rich et al [108] sequenced around 768 isolates from different site locations, mostly lactic acid bacteria (LAB), obligate and facultative homofermentative systems. Without exception, the liquefaction and saccharification steps contain the largest amounts of contaminant species (by analogy of enzymatic hydrolysis), followed by the yeast propagation tank. To confirm the origin of inhibitors, Skinner K. and Leathers T. [109] investigated the bacterial contamination associated to *Lactobacillus sp.*, which produces the an unwanted main product (lactic acid). This paper

provided a detailed analysis of the organic acids associated with the identification of bacterial communities. Microbial characterisation was conducted by using an analytical profile index (API) and biological (phenotypic analysis of microbes) under sterile conditions. Moreover, Muthaiyan et al. [107] identified that wild yeast is another source of contamination, surging as mutation of fermentation yeast (e.g. *Saccharomyces cerevisae* and cannot be alleviated by antibiotics and acid treatments. Wild yeast are those microbial strains not intentionally added in the fermentation broth, which not enhance the ethanol production, in contrast, spoil the final product. These are well-reported but cannot be mitigated by antibiotics, so other treatment are applied (e.g. change yeast population in fermentor) [110]. Notwithstanding, wild yeast contamination does not occur in the enzymatic hydrolysis, as structural carbohydrates are purely hydrolysed into monomeric sugars by enzymes.

Unhygienic conditions are the main reason of contamination, as the proliferation of undesirable microbial communities grow exponentially in the presence of dirt, containing key nutrients as nitrogen, phosphorus and potassium. Biochemical processes are vulnerable to different sources of contamination, direct (e.g. lignocellulosic substrate) or indirect (e.g. pumped water). It is challenging to identify the specific source of contamination, as normally it is a mix of both. Only at laboratory-scale, pure sterile conditions can be achieved by auto-claving of reagents/equipment and working under a laminar fume hood. . However, these scrupulous measures are impractical and unrealistic at larger scales, as being laborious and uneconomical. At industrial scale, the sterilisation of bioprocessing equipment is done with steam or dilute caustic, however the nature of the MSW process makes it impractical due to high energy costs of auto-claving. Also, working on a semi-open space avoids sterility of reagents and other materials. With this in mind, simple precautions such as ethanol-washing of the tank and adequate storage (freezer and fridge, for substrate/samples and enzymes, respectively) are only adopted.

To overcome bacterial contamination, two groups of compounds are added into the fermentation broth: antibiotics or chemical additives. Among antibiotics, penicillin was the prevalent option in food-based ethanol fermentations for decades, prior the discovery of virginiamycin. This is a more attractive option due to its effectiveness at low pH [109]. The abuse of antibiotics, however, posses several techno-economic hurdles: (1) persistence in co-products (e.g dried distillers grain with solubles, DDGS) and (2) building of antibiotic resistance by microorganisms [111]. On the other hand, chemical additives are also administrated *in* or *ex situ* the fermentation step; where the common options are: acid, sulphur, hydrogen or chlorine dioxides. Some are strain-specific, e.g. SO_2 to *Acetobacter* or H_2O_2 and ClO_2 to *Lactobacillus*, respectively. Likewise, remaining chemical additives would need additional washing (acids) or enzyme additions (catalases to degrade (H_2O_2). It is vital to understand the mode of administration as well as minimum inhibitory concentration (MIC) per antimicrobial strategy in order to find out the most efficient

method.

In the enzymatic hydrolysis (saccharification) field, antimicrobial strategies were adopted from the ethanol industry to preserve the sugar-rich hydrolysate without interference to enzyme activities. NREL published a standard procedure for conducting the enzymatic hydrolysis of biomass at laboratory scale, including three antimicrobial agents: tetracycline, cycloheximide and sodium azide [112]. The first one, tetracycline, is an antibiotic agent that surged as replacement to penicillin and virginiamycin in alcohol fermentation of sugarcane molasses [113]. Despite there is no evidence of cycloheximide and sodium azide as antimicrobial for fermentation processes, they are recommended options for the enzymatic saccharification. Within enzymatic hydrolysis of biomass, many publications followed NREL guidelines using tetracycline [42, 48, 114, 115], cycloheximide [42, 48] or sodium azide [23, 114, 116, 117].

Other antimicrobial agents that can be used for biorefining options are: chlorine dioxide, hydrogen peroxide and benzisothiazolinone (Table 3.2). The first two are adapted from ethanol fermentation, for instance chlorine dioxide is commercialised under the trademark - Fermasure ® (DuPont, US). Since they are also bleaching agents of the kraft pulp mill industry [118, 119], several authors tested their efficiency as biomass pretreatment "ingredients" for the dismantling of recalcitrant structure to facilitate the release of fermentable sugars with enzymes [119–122]. Ho et al. [123] extensively reviewed the reaction mechanisms of alkaline hydrogen peroxide (AHP), compared it with other oxidising agents as well as applicability in a range of pretreatment methods. Recently though, interest in H_2O_2 has increased due to its importance as electron donor for the newly discovered LPMOs [70, 124–127]. Moreover, benzisothiazolinone (BIT), a cheap commodity used as protease/lipase inhibitor in the biomedicinal [128, 129] and preservative in the paint industry [130, 131], respectively. BIT is a biocide residue in wastewater treatments as well [132, 133], removed by ozonation. Its mode of action is to inhibit the glucose transportation between the cells of bacteria. Fuller et al. [134] tested the efficiency of BIT in *Staphylococcus aureus* with great success. Herein, we have present a series of compounds which can be applied in enzymatic saccharification of biomass, describing its modes of activation and literature analysis. Table 3.2 summarises a list of antimicrobial agents with their advantages and disadvantages, bulk-price and main publications in regards of biochemical conversion of biomasses.

3.3 Results and discussion

3.3.1 High-solids loadings

Objective: To investigate the maximum threshold of solids loadings and efficacy of antimicrobial agents in the enzymatic hydrolysis of MSW-pulp

Table 3.2. Overview of anti-microbial agents for biomass conversion

Compound	Advantages	Disadvantages	Price[a]	Examples
Antibiotics				
Tetracycline	Proven-track in EtOH industry Standard choice for biorefining Versatile bacterial	Antibiotic resistance Co-product persistence High cost Thermodynamically unstable	\$70/kg	[107, 135]
Virginiamycin	Proven-track in EtOH industry Low-concentration efficacy LAB specific	Antibiotic resistance Co-product persistence	\$0.5/kg	[136–138]
Chemicals				
BIT	Biorefining Low-concentration efficacy Thermodynamically stable	Health and safety Little biorefining history Low solubility	\$10/kg	[47]
Sodium azide	Standard choice for hydrolysis Low concentrations	Yeast inhibition Health and safety issues Gram-positive bacteriostat	\$10/kg	[135, 139]
Chlorine dioxide	Proven-track in EtOH industry Easy removal	Flammable Poor stability	\$1.15/kg	[140–142]
Hydrogen peroxide	LPMO booster Pretreatment use Cheap Gram-positive specific	Thermodynamically unstable High-concentration Foaming tendency Glucose oxidation	\$0.07/kg**	[110, 143, 144]

[a] All prices are taken from www.alibaba.com and selected for high-purity commodities (> 90 %)
*Hydrogen peroxide prices are for a 50 % solution since higher concentrations were not found

3.3.1.1 From medium to high-solids loadings

At high-solids loadings (15-22.5 %TS), preliminary tests were carried out in 2L drum reactors, with determination of monomeric sugars and lactic acid concentrations (Fig. 3.4). At 72 hours, glucose concentrations increased in proportion of solids contents: 52.8, 48.8, 40.5 and 39.2 g L^{-1} glucose for 22.5, 20, 17.5 and 15 %TS, respectively. Interestingly, no great differences in glucose yields (40.5 and 39.2 g L^{-1}) were observed in 17.5 and 15 %TS runs, respectively. Kristensen [145] concluded that the decrease of conversion rates as increasing solid contents is a general effect on enzymatic hydrolysis, based on a compilation of several publications. This could explain why the 17.5 and 15 %TS yielded glucose concentrations in the same range, as the first assay experienced lower cellulose conversion. This phenomenon has been widely observed and frequently reported in the academic community [92, 93]. Although, most of these publications focused the comparison (conversion rates vs solid loadings) at the end of reaction. Others have shown the evolution of glucose concentrations/ cellulose conversion during enzymatic hydrolysis [145–148], indirectly illustrating the reaction rates. For instance, Tengborg [148] reported similar results in cellulose conversion for 2-10% TS at 140 hours. Since each study calculates conversion rates differently, case-by-case comparisons are hard to achieve. So, it is recommended to use other parameters, e.g. sugar concentrations. Roche et al. [146] compared sugar monomers (glucose and xylose) and cellobiose concentrations after 7 days of enzymatic saccharification of pretreated corn stover in accordance of solids

contents. In this case, a substantial difference on final titers was observed: 100, 120 and 170 g L^{-1} of glucose for 15, 20 and 30 % TS, respectively. There is still uncertainty about the correlation between conversion rates and solid loadings, regarding MSW-derived pulps. Hence, further investigations are described in the following sections, increasing the number of replicates to achieve better repeatibility as well as better reaction control.

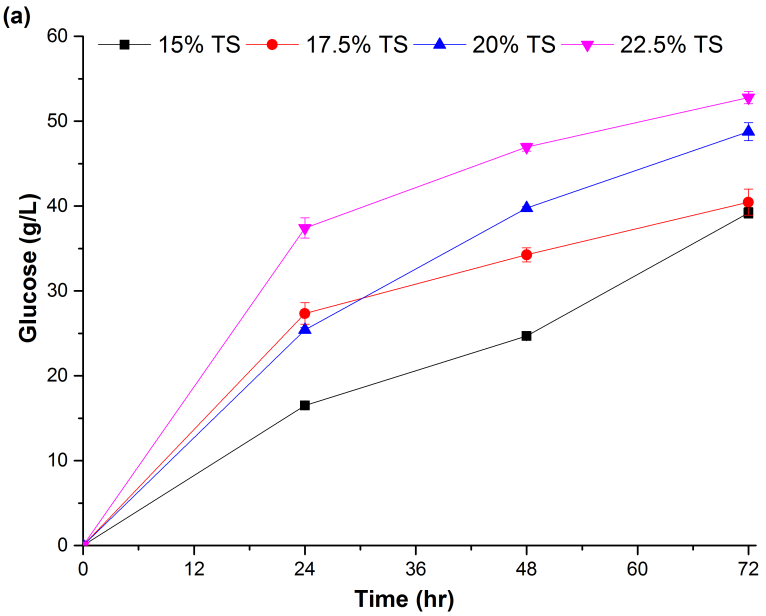

Figure 3.4. Testing high-solid enzymatic hydrolysis (15-22.5 %TS) in 2L drum reactors

Reaction conditions: 15-22.5 %TS, 2 % E:S, 0.01 % (w/w dry substrate), 60 rpm and 80 % V
Error bars represent standard deviation of triplicate measurements for each sampling point

3.3.1.2 Improving the repeatability of high-solids loadings

To improve the repeatability of high-solids loadings assays, duplicate hydrolysis experiments were performed at solids loadings of 20, 22.5 and 25 %TS in 500 ml drum reactors (Fig.3.5). The reaction conditions were unchanged (section 3.3.1.1), apart from the filled volume (25%V) rotational speed (30 rpm). Due to high-initial viscosity, controlling of the pH was very challenging during first two hours of reaction, oscillating outside the optimum range (4.75-5.25) for Cellic CTec3 enzymes [100]. The lignocellulosic slurry behaves as a solid prior to biomass liquefaction, visualised after 8 hours of reaction. Therefore, accurate pH measurements were only achieved after this period. As the slurry viscosity decreased very slowly as well, certain technical difficulties were experienced during sampling. Approximately 50 ml were withdrawn per aliquot, otherwise, insufficient liquid was collected for product analysis. These technical limitations have been previously described on a review article by Koppram [149], during high-gravity conditions in a stirred tank reactor, which also occurred in the horizontal configuration. Inefficient mixing separates the solid

and liquid part, resulting into technical problems in sampling and pH/temperature adjustment. The use of syringes for sampling is inappropriate, resulting in unrepresentative samples and misleading estimation of the solid fraction. Unreliable pH measurements and slow pH adjustment could be occurring as solids precipitates until recording. The experimental set-up was enclosed within laboratory incubator, poor mass and heat transfer could be experienced as well. A heterogeneous temperature profile within the slurry, would lead to suboptimal conditions for cellulases.

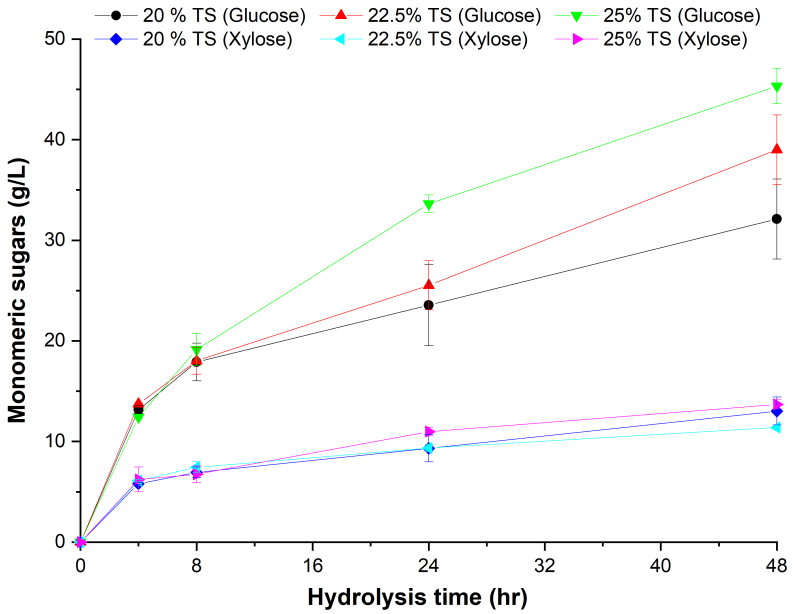

Figure 3.5. High-solids loadings (20, 22.5 and 25 %TS) enzymatic hydrolysis of MSW pulp in 500 ml drum reactors: glucose and xylose yields

Reaction conditions: 20-25 %TS, 2 % enzyme loading, 0.01 % (w/w dry substrate), 30 rpm and 25 % V Error bars represent standard deviation of duplicate experiments

Between 80-100 g L^{-1} glucose is required for commercialisation of lignocellulosic sugars [2], as leads to a 4% w/w ethanol fermentaiton with lower expenses on distillation. As observed in other studies, these "industrialisation glucose levels" are achieved after a week of enzymatic hydrolysis at 20-30%TS [146]. In Fig. 3.5, it can be seen that glucose and xylose concentrations independent of the solid loadings only at 4-8 hours of hydrolysis. As the enzymatic hydrolysis progresses, a clear difference between the glucose yields for the highest solids contents (25%TS) is seen, surpassing the 30 g L^{-1} levels. Surprisingly, little distinction was observed for the 20-22.5%TS hydrolysis after one-day of reaction. A similar behaviour occurred with the xylose yields during the experimentation, with measurements in the range 12.6 $\pm$ 0.6 g L^{-1} for all runs. At 48 hours, the glucose titers increased: 32.1 $\pm$ 3.97, 39.2 $\pm$ 3.46 and 45.3 $\pm$ 1.76 g L^{-1} for solids loadings of 20, 22.5 and 25 %TS, respectively. This study evolved from previous section 3.3.1.1, demonstrating the success of working at higher solids loadings (25 %TS). Although, high standard deviations

were determined, in particular for 20 and 25%TS assays, indicating great variability of results. In addition, the relative standard deviation (RSD = 100 X σ /$\hat{x}$) of each data-points was around of 10%. The "Horwitz trumpet" function determines for analyte concentrations in the range of 1-50 g L^{-1} [150]. This indicates adequate repeatibility between assays, mainly attributed to good reaction control and quality on sampling. To the best of our knowledge, we can recommend the following strategies to alleviate the above-mentioned issues (a) attachment of on-line pH measurements, (b) whole slurry sampling with pre-mixing and (c) conducting a third replicate run. These recommendations are in agreement of technical challenges addressed by Koppram [149], but glucose titers still low due to end-product inhibition, reaction control and reliable sampling.

3.3.1.3 Pushing the limits in the high-solids regime

As part of a DoE study to investigate the limits of high-solids regime in MSW-derived pulps, several hydrolysis experiments were carried out in the range of 15-30 %TS. Herein, two runs (15 and 30%TS) were included with discrete analysis of monomeric sugars (Fig.3.6), enabling direct comparison with a previous study (3.5) as reaction conditions were kept constant: filled volume (50%V), rotational speed (80 rpm), enzyme loading (2%) and antimicrobial usage (0.01% BIT). As described in the literature [17, 145], the release of glucose is not proportional to the solids loadings, which also occurred in this case: 25 and 65 g L^{-1} of glucose for 15 and 30%TS, respectively, at 48 hours of reaction. The same disproportional relationship was observed for xylose: 13 g L^{-1} (15% TS) and 23 g L^{-1} (30 %TS). Interestingly, in the 15%TS run, the sugar monomer concentrations experienced the so-called "plateau effect" at 24-48 hours, which could indicate complete enzymatic saccharification due end-product inhibition [92]. With the high-initial viscosity of 30%TS, further glucose titers were released after 24 hours of hydrolysis, associated with slurry liquefaction (visually observed). As commented earlier with 25%TS (section 3.3.1.2), a low viscosity reduction (24-hours) is a common behaviour seen in the range of 25-30%TS, leading to technical limitations on reaction control and sampling [149]. In this case, pH adjustment and sampling was more laborious than experienced before (section 3.3.1.2), disabling any reliable measurements and withdrawal of aliquots after one-day of reaction. Even operating with more severe mixing strategies (80 rpm), the addition of 2% (w/w) enzymes was not sufficient with little free water accessible for adsorption due to high-surface area and entanglement of lignocellulosic fibrils [149]. Few studies have reported successful enzymatic hydrolyis above 30%TS [2], unless they employed more severe pretreatment methods (organosolv or steam explosion) used in non-MSW feedstocks: e.g. wheat straw [93], agave bagasse [151] or beechwood [152]. This shows the difficulties of efficient bioprocessing in these regimes, even when raw materials are milled to 1 mm prior pretreatment [151]. Without increasing the severity of the pretreatment conditions or increasing enzymatic doses, saccharification of MSW-derived pulps is not recommended at 30%TS due to poor

reaction control, low viscosity reduction and resulting monomeric sugars per gram of substrate.

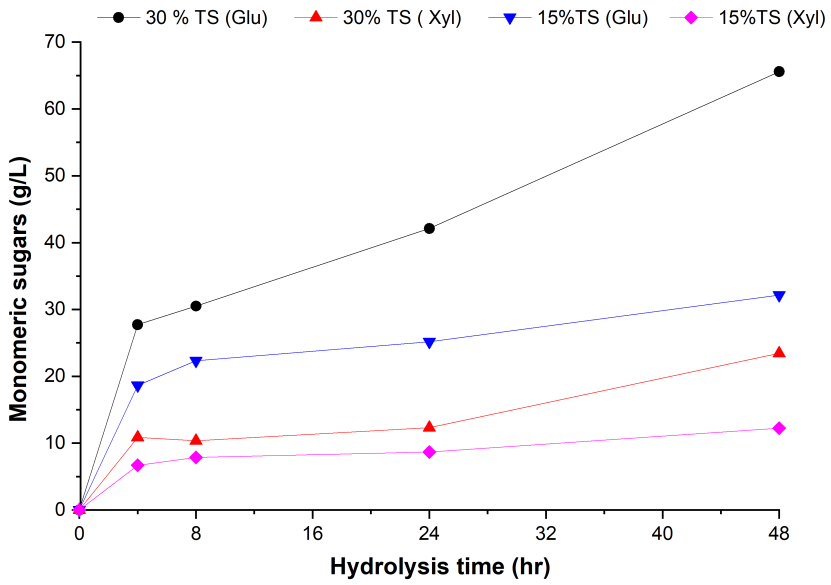

Figure 3.6. High-solids (15 and 30 %TS) enzymatic hydrolysis assays as part of DoE study in 2L drum reactors: glucose (a), xylose and lactic acid (b) yields

Reaction conditions: 15 and 30 %TS, 2 % E:S, 0.01 % (w/w dry substrate), 80 rpm and 50 % V

Part of a DoE study included the investigation of centre-points (22.5 %TS), and settings of other operational parameters such as filled volume (25% V) and rotational speed (40 rpm). The enzymatic saccharification of MSW-derived pulp was carried out in triplicates runs with periodic withdrawal of sugar aliquot for analysis (Fig.3.7). Adequate reaction control and low variability of results was achieved in this study. Only 24 hours were necessary to yield 52 and 17 g L^{-1} of glucose and xylose (on average), which looks promising considering the low enzyme loading (2 % E:S). A low volume filling could promote mass-transfer and enzyme adsorption at moderate agitation rates [93], resulting to efficient lignocellulosic deconstruction to fermentable sugars. Taking into account a reference of 120-200 filter paper units (FPU) per ml of CTec3 [32, 153, 154], a 2% enzyme loadings is translated into 2-3.5 FPU/g dry substrate. According to Humbird et al. [147], 8.8 FPU per g substrate is the maximum enzyme dose for the commercialisation of corn stover into ethanol. Although, direct comparison are difficult to make, our study demonstrates the efficient bioprocessing of highly-recalcitrant substrates with low-enzyme usages. And moves towards the target of 80-120 g L^{-1} threshold [2], the minimum requirement for the commercial viability of lignocellulosic sugars, if the reactions is carried out for longer residence time.

Overall, up to 25%TS solids loadings were used successfully in the MSW hydrolysis using low enzyme doses (2 % or 2-3.5 FPU/g dry substrate). Drum reactors, further discussed in section 5.2, are an optimal reactor configuration for the efficient

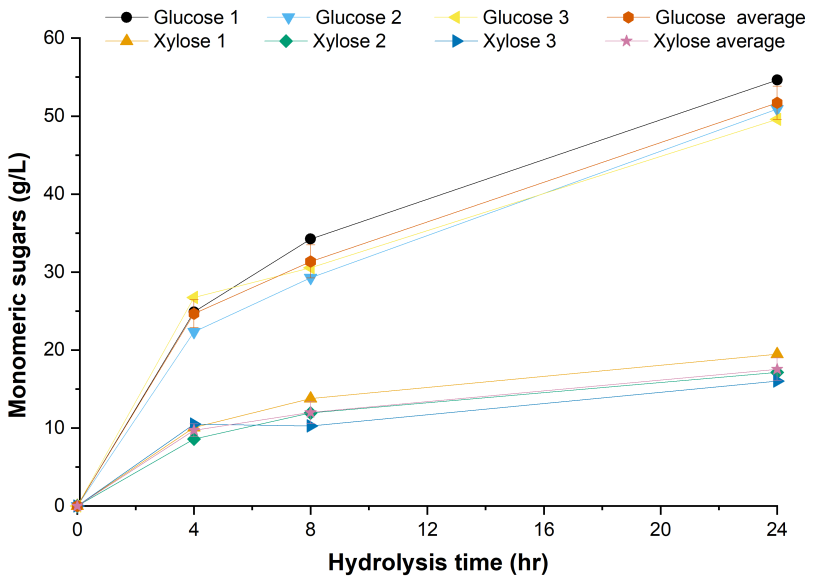

Figure 3.7. Enzymatic hydrolysis of centre-points of a DoE study (22.5% TS) in 2L drum reactors: glucose (a), xylose and lactic acid (b) yields

Reaction conditions: 22.5 %TS, 2 % enzyme loading, 0.01 % (w/w dry substrate), 40 rpm and 25 % V

hydrolysis at high-solids loading. However, at 30 %TS, the biomass slurry is not manipulable for adequate sampling and pH-adjustment as well as low enzymatic digestibility, which hampers the pumpability of the slurry. Fig. 3.8 illustrates a range of MSW-derived pulp slurries from low (5%TS) to high (30%TS) for the visualisation of slurry viscosity/appearance. Although, all MSW-derived slurries are prepared at a constant volume of 40-ml, a vast difference in bulk density is seen, in particular in the range of 20-30%TS. Based on previous experimentation, high-solids enzymatic hydrolysis of MSW-derived pulp is not recommended above 25% due to technical limitations in processing: reaction control, sampling and viscosity reduction. Therefore, 25 %TS is set as upper limit on high-solids enzymatic saccharification, which will be further investigated in terms of process optimisation and techno-economic assessments (Chapter 6).

3.3.2 Investigating the antimicrobial efficacy of various compounds

3.3.2.1 Screening of anti-microbial agents

A short enzymatic hydrolysis (Fig. 3.9) was performed to screen the potential use of alternative options (BIT, H_2O_2 and Fermasure ® XL), over NaN_3 and tetracycline as anti-microbial agents - previously reviewed and summarised in Table 3.2. A control assay (no compound addition) was included as reference. Identical concentrations (0.1 % w/w dry substrate) of anti-microbial compound were loaded prior enzymatic hydrolysis of 8 % MSW pulp and 5 % enzyme loadings, carried out in 250-ml EFs in an orbital incubator shaker at 250 rpm. After 8 hours of hydrolysis, around 12.5

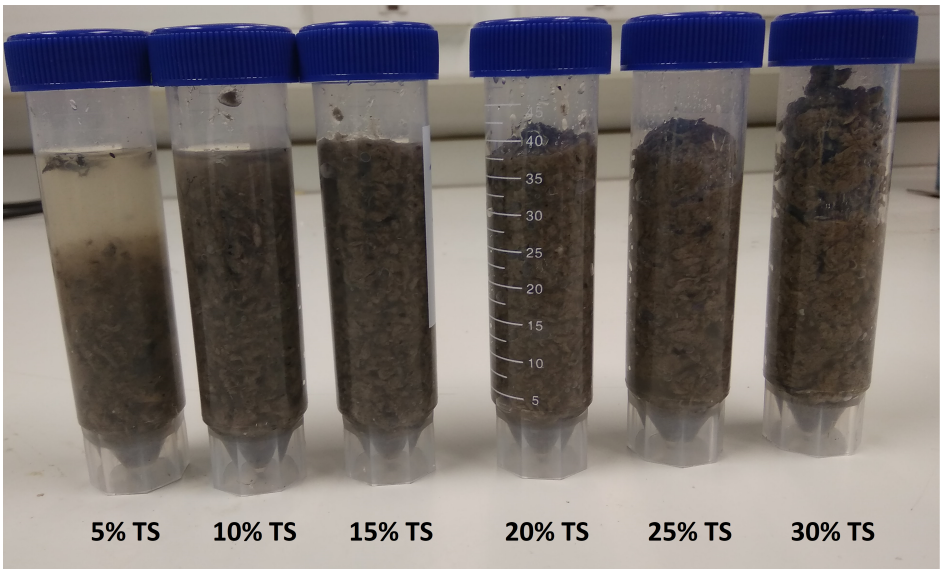

Figure 3.8. MSW-derived slurry preparations in the 5-30%TS range

g L^{-1} of glucose were released by the addition of three main agents (tetracycline, BIT, NaN_3 and Fermasure ® XL), whilst, up to 15 g L^{-1} were generated in the H_2O_2 case. Except for the control assays (less than 10 g L^{-1}), the final hexose concentration was independent of selected anti-microbial agents. Few studies are available on the use of alternative compounds to NaN_3 and tetracycline , differentiating from the standard choices for enzymatic saccharfication of biomass [135]. For instance, a DuPont patent [140] describes the microbial alleviation in carbohydrate feedstocks by Fermasure ® XL, but vague details are given for using it during enzymatic hydrolysis of biomass. The rest of the compounds have been employed in ethanol fermentations [107], biomass pretreatment [122, 123] or as "LPMO-promoters" [124]. This short investigation validates that coherent choice of non-standard disinfectants in the enzymatic hydrolysis of MSW pulp, showing higher glucose titers when hydrogen peroxide was added. But, further investigations are necessary to reduce the concentration of the antimicrobial agent, and study the effect at the end of enzymatic hydrolysis.

3.3.2.2 Effect of anti-microbial concentration

Sodium azide and tetracycline (also cycloheximide) are commonly employed as antibacterial agents in enzymatic saccharification studies [114, 116, 155], however, there is a lack of criteria for how much reagent should be supplied *in situ*. Also, each publication also uses different working units, e.g. w/v or mM, making difficult straightforward comparisons. The NREL recommended the addition of 0.001, 0.0015 and 0.002 % (w/w dry substrate) for sodium azide, cycloheximide and tetracycline, respectively, for low-solids (1% w/w) enzymatic loadings of pretreated agricultural feedstocks [135, 156]. Despite being useful guidelines, these protocols are based

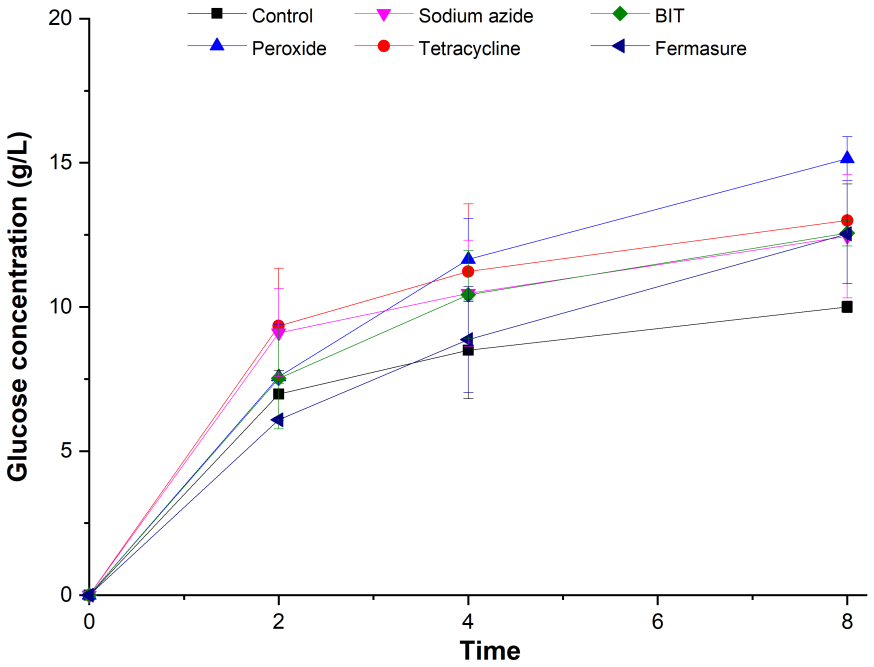

Figure 3.9. Glucose yields during short enzymatic hydrolysis upon anti-microbial screening in EFs

Reaction conditions: 8 % TS, 5 % enzyme loading with 0.1 % (w/w dry substrate) in 250 ml flasks (200 ml working mass, 80 % V) at 50 °C, pH 5-5.25 and 200 rpm
Error bars represent standard deviation (σ) of triplicate runs

on carrying out the hydrolysis reaction under advantageous conditions, e.g. high-sterility (auto-claved flasks and consumables). In industrial environments, the enzymatic saccharification is not conducted in such flawless circumstances. Hereby, it is necessary to test a general approach to calculate the amounts of antimicrobic compounds (including the alternative ones) in the enzymatic hydrolysis of MSW pulp.

In these regards, the exponential dose (0.01, 0.05 and 0.1 % w/w dry substrate) of five compounds (as studied in Fig. 3.9) were added in triplicate into the enzymatic hydrolysis of MSW pulp in 250-ml EFs at pH 5 (50 mM Na-citrate buffer), Figs. 3.10-3.15. A standard buffer (50 mM Na-citrate) solution was used for controlling the pH at optimum conditions (pH 5). During the the hydrolysis, pH was kept at the optimum value for the Cellic CTec3 enzymatic cocktail [100], which is also that for the lactic and acetic acid bacteria: 5.5 to 5.8 and 5.4-6.3, respectively [157]. To ensure that microbial contamination was the only reason of sugar degradation, it was necessary to exclude other acidification mechanisms. For instance, sugar dehydration by acidification of media, leading to the levulinic acid formation from glucose. The results are part of an investigation that Climent Barba contributed to [47], included as supplementary information.

Without anti-microbial addition, the carbohydrates titres plateau after 8 hours

reaction as the formation of lactic and acetic acid rose to 200 and 150 mg L^{-1}, respectively (Fig. 3.10). In contrast, the glucose and xylose yielded only 6.5 and 2 g L^{-1}, respectively. It was expected to find acetic acid in the initial stages of enzymatic saccharification, as acetyl groups from hemicellulose fraction hydrolyse producing acetic acid [101]. However, if acetic acid concentrations does not evolve with the xylose, it may imply that the system is microbially contaminated. Interestingly, no lactic acid was formed during the first two-hours of hydrolysis, as requires sminimum levels of glucose and oxygen depletion for metabolising by microbial communities [158].

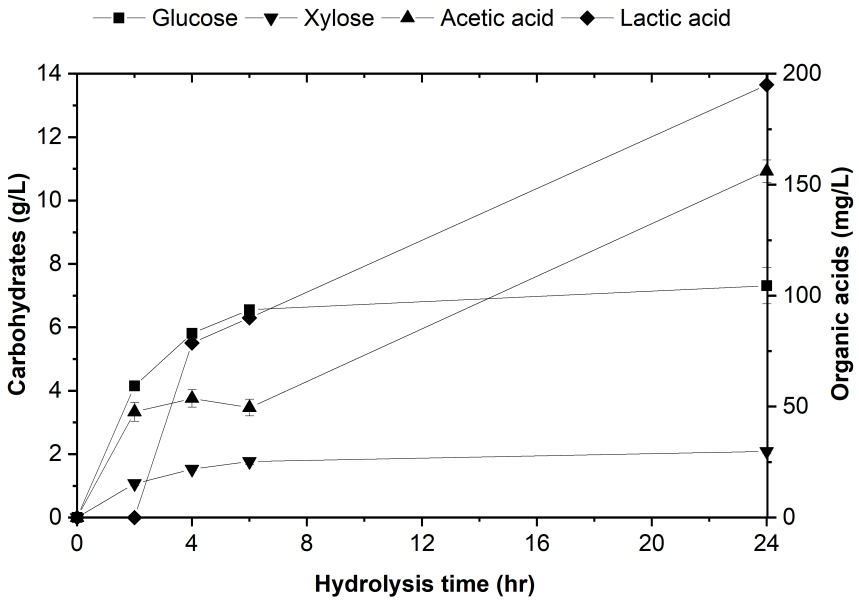

Figure 3.10. Hydrolysate analysis during waste saccharification of the control assay in 250-ml Erlenmeyer flasks (50 mM Na-citrate buffer)

Reactions conditions: 8% TS, 2% E:S, 200 rpm, pH 5 and 50 °C.
Error bars represent standard deviations of triplicate runs

Sodium azide (NaN_3) is a common antimicrobic compound used as a biocide in multiple areas: biochemistry, biomedicine [159] and agriculture [160]. It inhibits the growth of gram-negative and gram-positive bacteria such as LAB and acetic acid bacteria (AAB) [161]. In Fig. 3.11, the release of glucose yields ($\sim$ 6 g L^{-1}) are independent of dosed amounts of NaN_3 (0.01 to 0.1 %w/w), during the first 6 hours of hydrolysis. The final production of acetic acid for 0.01 % NaN_3 is 4-fold higher than other doses (100 to 25 mg L^{-1}). The sudden increase of acetic acid provokes a slight reduction in glucose content (9.1 g L^{-1}) compared to 0.05 (10.5 g L^{-1}) and 0.1% NaN_3 (11.2 g L^{-1}). Herein, we demonstrate the efficient use of NaN_3 with only 0.05 % (w/w dry substrate), a 20-fold dose reduction in comparison with the enzymatic saccharification of rice husk/straw [123]. Even reporting slightly higher glucose yields at 0.1%, antimicrobial usage would result to a 10-fold decrease than enzymatic saccharification of rice-type feedstocks.

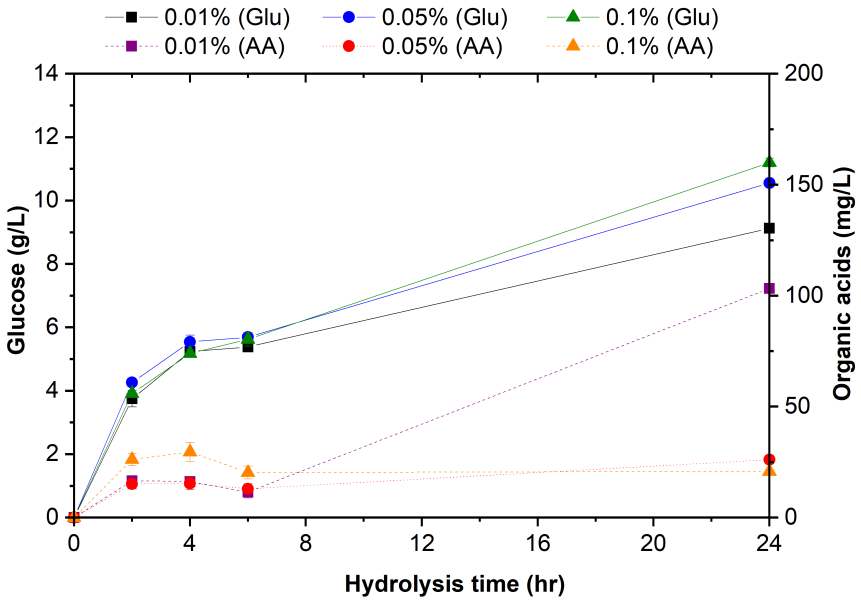

Figure 3.11. Hydrolysate analysis during waste saccharification with incremental dosage (0.01, 0.05, 0.1% w/w of dry substrate) of sodium azide in 250-ml Erlenmeyer flasks (50 mM Na-citrate buffer)

Legend: Glu is Glucose and AA is acetic acid.
Reactions conditions: 8% TS, 2% E:S, 200 rpm, pH 5 and 50 °C. Error bars represent standard deviations of triplicate runs.

In Fig.3.12, the effect of BIT concentration during the enzymatic hydrolysis of MSW pulp was studied. Higher glucose concentrations were found at an intermediate dose (0.05 %) of BIT, 10.3 g L^{-1}, followed by 0.01% (10.2 g L^{-1}) and 0.1% (9.3 g L^{-1}). Interestingly, approximately same glucose titers were seen at lower doses (0.01 and 0.05%), suggesting that BIT is a cost-effective antimicrobial strategy. Similar to antibiotics, the ratio of antimicrobial agent to enzymes is a key factor for enhancing the synergy whilst protecting protein interactions [162]. This may be occurring as higher glucose concentrations are found 0.01% BIT doses. The BIT presents significant efficacy towards certain type of LAB, e.g. *Staphylococcus sp.* by deactivating transport and oxidation of glucose [134]. Little information is available the effect of BIT in enzymatic saccharification [47]. It is noticed acetic acid titers halved at higher than lower BIT doses: 25 mg L^{-1} (0.1 %) to 50 mg L^{-1} (0.01 and 0.05 %). No lactic acid was detected in all runs, demonstrating the good efficiency of BIT as promising agent for enzymatic saccharification.

Another type of chemical additive, H_2O_2, was tested in the enzymatic hydrolysis of MSW pulp (Fig. 3.13). H_2O_2, is an oxidiser, commonly used bleaching and antiseptic agents [163]. It is a versatile molecule which is gaining interest through the enzymatic saccharification field; as an alkaline pretreatment method [120] and molecular donor for boosting the LPMOs activity [127]. Moreover, we wanted to evaluate its "potential" antimicrobial properties as in comparison to other compounds. The amounts of dosed H_2O_2 are independent (considering the standard deviation) of

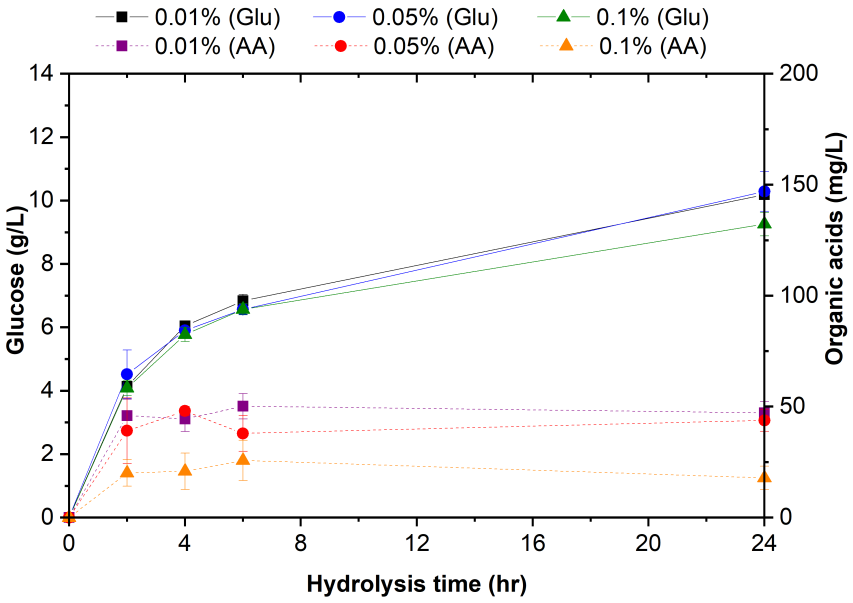

Figure 3.12. Hydrolysate analysis during waste saccharification with incremental dosage (0.01, 0.05, 0.1% w/w of dry substrate) of BIT in 250-ml Erlenmeyer flasks (50 mM Na-citrate buffer)

Legend: Glu is Glucose and AA is acetic acid.
Reactions conditions: 8% TS, 2% E:S, 200 rpm, pH 5 and 50 °C. Error bars represent standard deviations of triplicate runs.

either the release of glucose and acetic acid, with final concentrations of approximately in 9 g L^{-1} and 110 mg L^{-1}, respectively (Fig. 3.13). Interestingly, no acetic acid was detected during 6 hours of hydrolysis. Since H_2O_2 is unstable and prone to decompose by light exposure (parameter not control), it may explain why acetic acid was kept at negligible levels prior becoming thermodynamically unstable.

Moreover, tetracycline (TC) was chosen as the standard antibiotic option for biomass conversion [107, 135], with an alternative nature (antibiotic) than the rest of compounds. The mode of action of tetracycline is the blockage of microbial ribosomes, stopping the synthesis of proteins in a wide range of microorganisms [164]. At same doses, the effect of TC concentration was studied during the enzymatic saccharification of MSW-derived pulp (Fig. 3.14). Increasing the concentration of TC resulted into lower acetic and acetic acid yields, but not in higher glucose yields. Surprisingly, same glucose titers were reported for 0.1 and 0.01% doses (12.7 g L^{-1}), even with a 10-fold.difference in antimicrobial dose. In addition, similar glucose concentrations were yielded for 0.01 and 0.05% in acetic acid (68 mg L^{-1}) and lactic acid (25 mg L^{-1}). Considering the low presence of inhibitors on hydrolysate broth, 0.01-0.05% doses are recommended for the enzymatic hydrolysis of MSW-derived pulp. Compared to other studies, forestry-based feedstocks [165] and cashed apple bagasse [166], two different conclusions can be drawn. On the one side, Li et al. [165] added only 0.003% TC in lignocellulosic slurries, 3-fold less than the lowest dose used in our study (0.01%). The minimal use of TC could be attributed to the

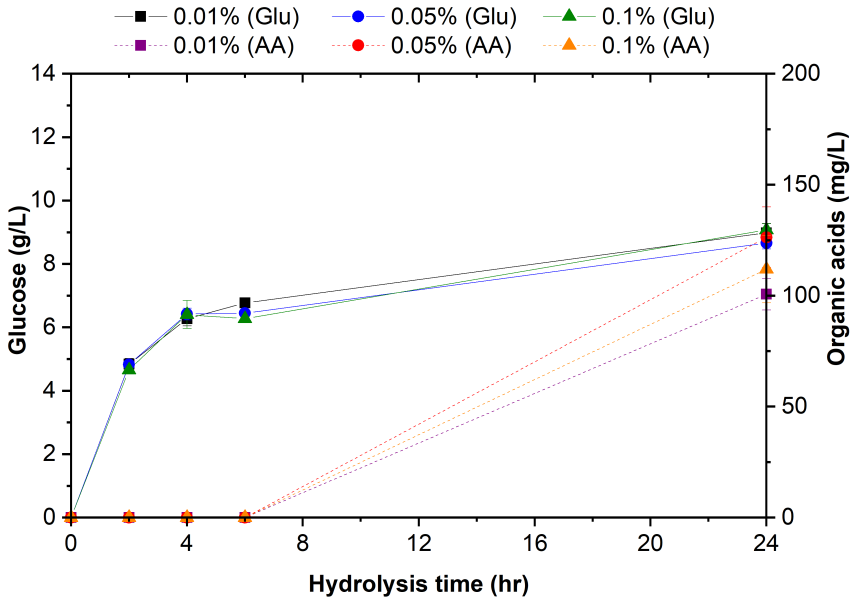

Figure 3.13. Hydrolysate analysis during waste saccharification with incremental dosage (0.01, 0.05, 0.1% w/w of dry substrate) of H_2O_2 in 250-ml Erlenmeyer flasks (50 mM Na-citrate buffer)

Legend: Glu is Glucose and AA is acetic acid.
Reactions conditions: 8% TS, 2% E:S, 200 rpm, pH 5 and 50 °C. Error bars represent standard deviations of triplicate runs.

high oxidation effect of the pretreatment, alkaline hydrogen peroxide coupled with copper(II) 2,20-bipyridine complex, with great antimicrobic properties. On the other hand, daCosta Correia et al. [166] dosed 0.4% of TC in solution with 70% v/v ethanol prior enzymatic hydrolysis of cashew apple bagasse. To increase the solubility, TC is diluted with ethanol, which can pose an inhibitory effect to the enzymes at mili-scale. Even at the highest TC concentrations of our study (0.1%), daCosta Correia et al. [166] used a 4-fold concentration of TC as taken into reference the NREL standard procedure [156].

The last compound used to evaluate its antimicrobial effectiveness during the enzymatic hydrolysis of MSW-derived pulp was Fermasure® XL (Fig. 3.15), a mixture of stabilised chlorine dioxide. It is commercialised under this trademark name by DuPont [142] as carbohydrate preservative against microbial spoilage [140]. For decades, ClO_2-based formulations have been used in the ethanol industry [107, 141] with promising results as alternatives to antibiotics. Some evidence of using ClO_2 as a pretreatment reagent [122] can be found, yet not as antimicrobial compound for enzymatic saccharification. Considering the "bleachability" properties and success in ethanol fermentation, Fermasure® XL was tested therefor. Surprisingly, an increased concentration of Fermasure® XL resulted to an inverse release of lignocellulosic sugars: 8.9 (0.01%), 8.6 (0.05%) and 9.4 g L^{-1}), and, higher concentrations of acetic acid as well: 118 (0.01%), 147 (0.05%) and 146 (0.1%) mg L^{-1}. This demonstrates Fermasure® XL as a cost-effective antimicrobial agent, showing good efficacy

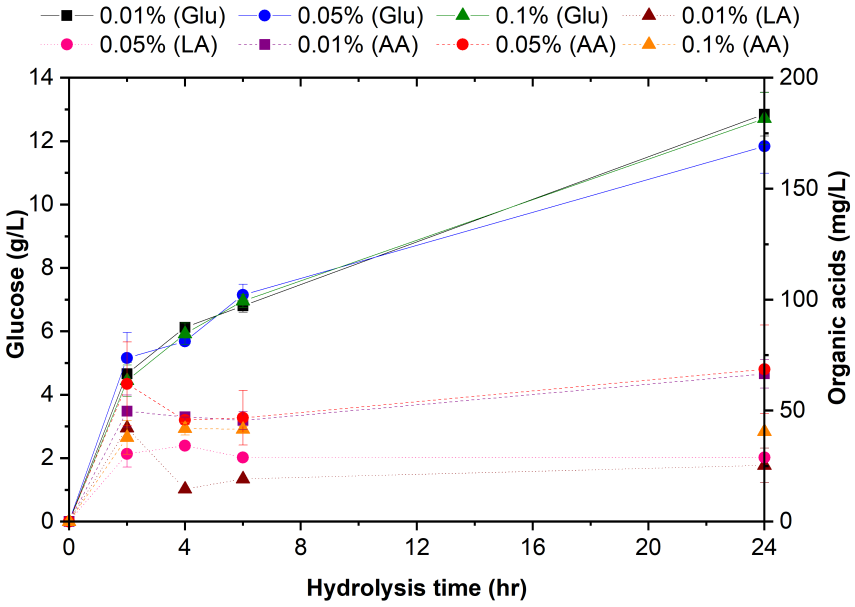

Figure 3.14. Hydrolysate analysis during waste saccharification with incremental dosage (0.01, 0.05, 0.1% w/w of dry substrate) of tetracycline in 250-ml Erlenmeyer flasks (50 mM Na-citrate buffer)

Legend: Glu is glucose, LA is lactic acid and AA is acetic acid.
Reactions conditions: 8% TS, 2% E:S, 200 rpm, pH 5 and 50 °C. Error bars represent standard deviations of triplicate runs.

at low doses. Compared to autoclave biomass pretreatments, the cost of the ClO_2-based compound was reduced around between 9 to 22-fold, if the highest doses was taken as reference (0.1%) [122]. The doses investigated during enzymatic saccharification of MSW-derived pulp (0.01, 0.05 and 0.01%) are in accordance with the concentrations by DuPont (0.01 to 10%) [140]. Although, a further decrease on antimicrobial concentration demonstrated that microbial contamination can be tackled with only 0.01% of Fermasure® XL. As stated by Dupont, Fermasure® XL inhibits the growth of bacterial contamination, such as *L.brevis* and *L.plantarum*, in diluted molasses.

Generally, the concentration of anti-microbial agent is independent of the substrate loading, in the range of 0.01-0.1 % w/w with the same release of carbohydrates and organic acids. Amongst the compounds tested, BIT stands out as the preferred antimicrobial agent, since it deals effectively with microbial contamination (lowest acetic and lactic acid concentrations) whilst yielding the second largest amounts of sugars (after tetracycline) using only a 0.01% dose. Based on the optimised results (i.e. maximum carbohydrates but lower organic acid yields), the five compounds are listed as follows in a decreasing order of efficacy: BIT > NaN_3 > Tetracycline > Fermasure ® XL and H_2O_2 > control. Although tetracycline results in higher sugars concentrations than BIT, its high costs (£58 kg^{-1}) and lower efficiency towards bacteria (higher acetic and lactic acid titers) hinders its choice as preferred antimicrobial. Furthermore, the prolonged use of tetracycline with: (i) persistence in co-products

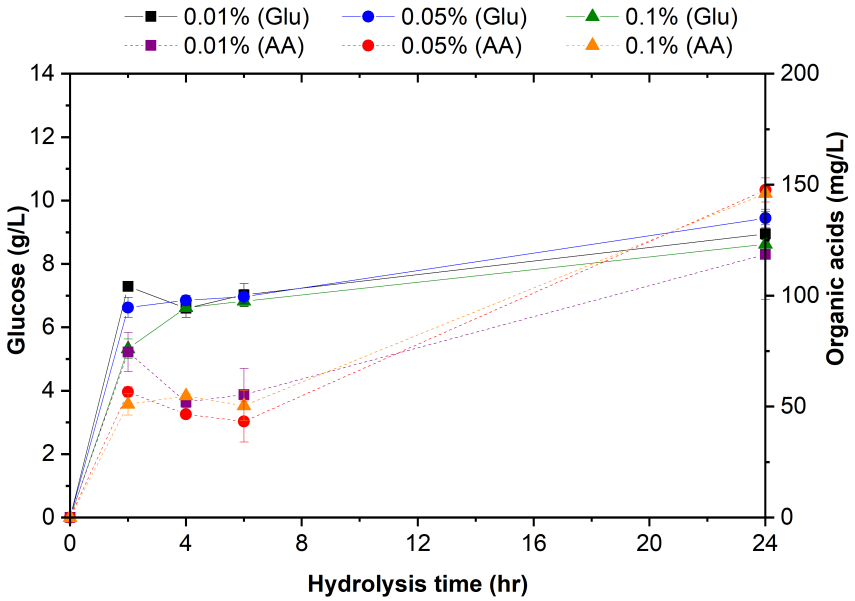

Figure 3.15. Hydrolysate analysis during waste saccharification with incremental dosage (0.01, 0.05, 0.1% w/w of dry substrate) of Fermasure® XL in 250-ml Erlenmeyer flasks (50 mM Na-citrate buffer)

Legend: Glu is glucose, LA is lactic acid and AA is acetic acid.
Reactions conditions: 8% TS, 2% E:S, 200 rpm, pH 5 and 50 °C. Error bars represent standard deviations of triplicate runs.

and (ii) bacteria resistance. It is also worth mentioning that BIT is a more affordable commodity (£8.3 kg^{-1}) than tetracycline (£58 kg^{-1}), but still more expensive than the rest of tested compounds, e.g. £0.07/kg for hydrogen peroxide.

3.3.2.3 Increasing hydrogen peroxide and enzyme concentrations

Since there is a growing interest in the usage of H_2O_2 as an "LPMO booster" [70, 124, 127], additional experiments were carried out (Fig. 3.16) by screening H_2O_2 doses ranging from 0 to 0.8 % (w/w dry substrate). Compared to the previous study (section 3.3.2.2), same reactor geometry was used (EFs) but two variables were changed: enzyme-to-substrate ratio and pH adjustment with 6 % (w/w) H_3PO_4. An intermediate dose (0.4%) was also included in the study, resulting into higher amounts of hexoses after 8 hours of hydrolysis (17.5 g L^{-1}). Doubling the amount of H_2O_2 (0.8 %) only increases glucose yields during first two hours of hydrolysis in comparison without H_2O_2 supplementation (12.5 to 10 g L^{-1}), but these improvements were not maintained thereafter. A 0.2 % H_2O_2 exhibited poorer yields than even when no H_2O_2 was added (15 to 16 g L^{-1}, respectively). If we compare Fig. 3.16 with Fig. 3.10, no clear conclusions in terms of glucose improvements can be made as different conditions were tested: H_2O_2 concentrations, slurry media and enzyme loadings. H_2O_2 helps to improve the enzymatic saccharification as documented in

the literature [70, 124, 127], but does not efficiently tackle the anti-microbial contamination and the "optimum dose" is still unknown. Further glucose oxidation has been reported by dosing of H_2O_2 [167], assessed by an alternative analytical method to HPLC (HPAEC-PAD), which avoids peak co-elution of glucose to gluconic acid [168].

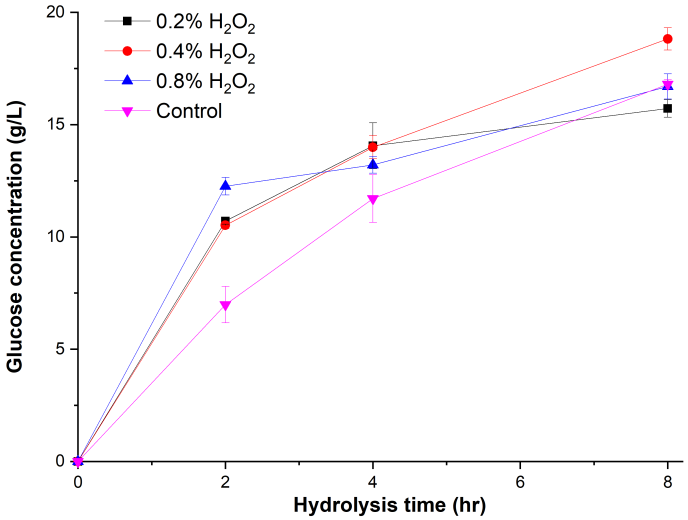

Figure 3.16. Enzymatic hydrolysis of MSW pulp with incremental dose of H_2O_2 in 250-ml Erlenmeyer flasks: 0 % (control), 0.2 %, 0.4 % and 0.8 (w/w dry substrate)

Reaction conditions: 8 %TS, 5 % E:S, pH 5 and 50 °C and 200 rpm. Error bars represent standard deviation of duplicate runs

3.3.2.4 pH/DO monitoring as metrics for evaluating the antimicrobial efficacy of compounds

Enzymatic hydrolyses were carried out individually in 1.5 L STRs with the initial dosing (before enzymes addition) of five anti-microbial agents (Fig. 3.17-3.22). During the course of hydrolysis, pH/DO were monitored with discrete analysis of carbohydrates and organic acids analysis. Both pH and DO are commonly monitored and controlled during microbial fermentations to optimize growth and productivity [169–171]. They are rarely used as quality metrics during enzymatic hydrolysis [124], despite this being typical practice in fermentation processes. We hypothesised that the evolution of pH and DO is correlated to the formation of organic acids related to the microbial activity. Therefore, they could be use as diagnosis tools of biological infection. If pH is not controlled, the media acidifies due to an increment of $[H^+]$ by the proliferation of acidic species (e.g. acetic acid), either from physico-chemical and

biological means. While, oxygen is metabolically consumed by aerobes, e.g. germination of spores. Non-alleviation of microbial communities leads to completed oxygen depletion (anoxia), promoting the anaerobic metabolism of bacillus-like thermotolerant species that use glucose as main source of carbon [172]. Elimination of sporadic forms is not an easy task, implying severe auto-claving and ensuring total sterile conditions in the reaction set-up [173]. By combining both techniques (pH/DO monitoring and HPLC analysis) with the initial dosing of anti-microbial agents, we aim to : (i) correlate physico-chemical parameter monitoring with the production of organic acids, (ii) study most-efficient antimicrobial compound in terms of reaction control and higher carbohydrates yields (and non or minimal organic acids formation) and (iii) validate that pH/DO monitoring as useful tool to prevent biological infection.

To verify the use of pH/DO as metrics for evaluating the microbial contamination, firstly, a control reaction was performed without addition of antimicrobial agent (Fig. 3.17). Initially, the pH and DO values fluctuated due to the viscosity break (first 2 hours) - where a thick mass is converted into a muddy-like substrate by enzymatic catalysis. The starting material was mass-transfer limited, disabling the constant measurements by the attached probes. Biomass liquefaction releases entrained oxygen from the lignocellulosic matrix [124], observed as a sudden increase of DO to 5 mg L^{-1} after two hours. Slurry liquefaction improves mixing as viscosity levels decreases, which enhances species diffusion and conversion rates. Uncontrolled pH-media provokes a substantial drop in pH just after two hours due to proliferation of acetic acid species (Fig. 3.17b). After 4-hours of hydrolysis, pH and DO are no longer in their optimum ranges: pH 4.75-5.25 and DO of 5 mg L^{-1} - illustrated as a purple line in Fig. 3.17a. Once the slurry media shifts towards more anaerobic conditions (0 mg L^{-1}), microbes are prone to convert glucose to lactic acid (50 mg L^{-1} spike), accumulating up to 135 mg L^{-1} (Fig 3.17b). A similar behaviour was observed for acetic acid at 24 hours, yielding > 150 mg L^{-1}. Increasing production of acetic and lactic acid after 8 hours could be associated with oxygen depletion of media, promoting the microbial anaerobic metabolisms. The rise in organic acids is linked to the "plateau effect" of carbohydrates yields, where no sugar yields over the last 16 hours (7.7 and 2.1 g L^{-1} for glucose and xylose, respectively).

By addition of NaN_3, pH and DO measurements stabilise after the "viscosity break" period, finalising the reaction with values of pH 4.25 and DO of $\sim$ 5 mg L^{-1} (Fig. 3.18a). There is a sudden decrease in pH at 2 hours, which can be associated to the release of acetic acid (Fig. 3.18d), as both stabilised thereafter. In Fig. 3.18b, the initial addition of NaN_3 resulted into carbohydrates, 10.3 and 2.5 g L^{-1}, and acetic acid levels of 33 mg L^{-1}. Biological infection was tackled as: (a) no extra acetic acid was produced after hydrolysis of acetyl groups (4 hours) and (b) lactic acid was not found. As acetic acid is released from acetyl group of hemicellulose fraction as xylose [99]. A similar evolution of xylose and acetic acid kinetics could be attributed to no microbial infection as acetic acid was exclusively released from the hemicellulose

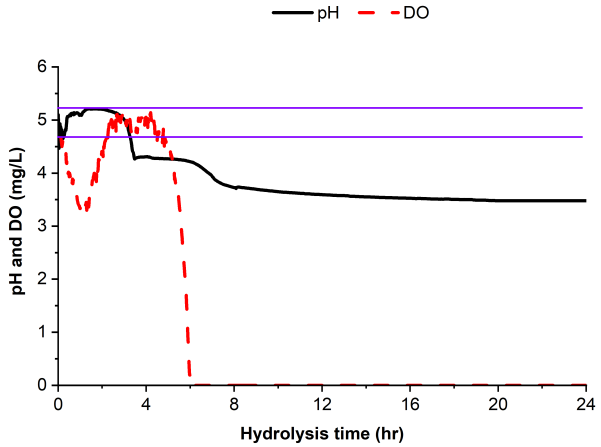

(a)

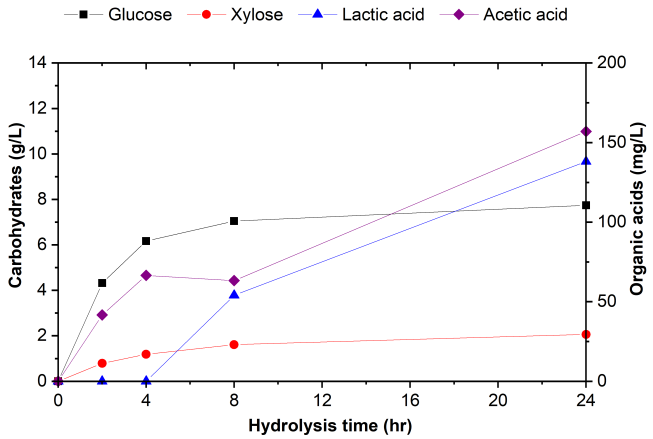

(b)

Figure 3.17. Enzymatic hydrolysis of MSW pulp of control assay (no agent) : process monitoring (a) and product analysis (b)

Reaction conditions: 7 % TS, 2 % E:S, 50 °C and 600 rpm - 1.5L STR. Purple lines represent the optimal pH-range (4.75-5.25) for Cellic CTec3 enzymes [100]

matrix. Meanwhile, high amounts of DO oxygen decreases the activities of some LAB (homofermentative and heterofermentative) as having strict anaerobic facultative metabolism. Without microbial characterisation, it is challenging to determine which microbe is responsible for the acetic and lactic acid production, but as suggested from previous studies of lignocellulosic fermentation, this may be from LAB and acetic acid bacteria (AAB) [109]. Other microbes such as *Salmonella* or *Streptococci* are also contained in MSW-derived feedstocks [27] but producing other types of organic acids. As a bacteriostat, NaN_3 is capable of stopping both aerobic and anaerobic microbial metabolic pathways, being an useful tool for avoiding sugar spoilage [158, 174, 175], but without microbial eradication. Hence, it is not surprising that NaN_3 is selected as one of the standard choices of antimicrobial agents during enzymatic saccharification of biomasses [135, 156].

As seen in Fig. 3.19, the addition of 0.1 % BIT had similar results to NaN_3 in the

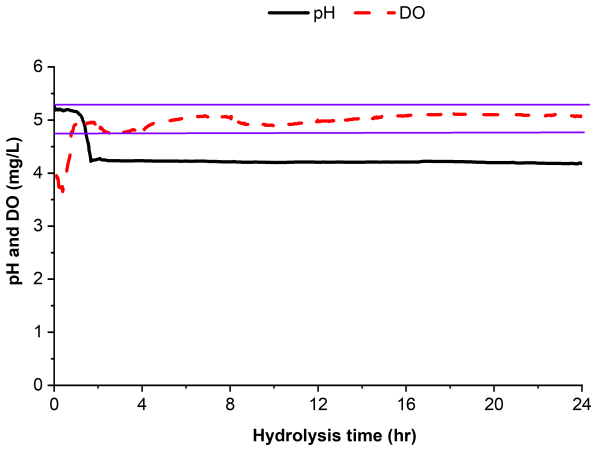

(a)

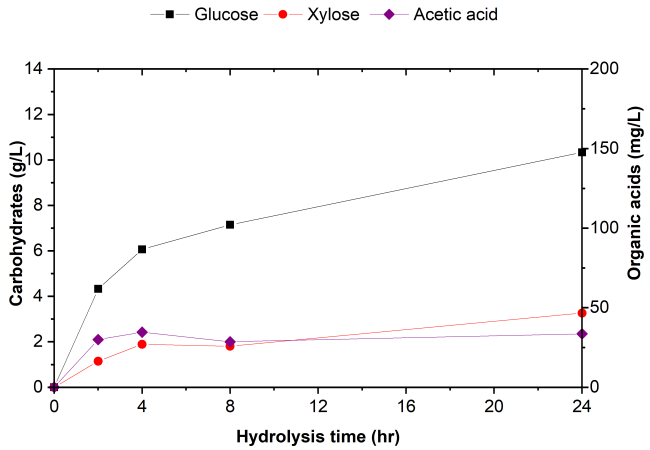

(b)

Figure 3.18. Enzymatic hydrolysis of MSW pulp with initial dosing of 0.1% (w/w dry substrate) NaN_3: process monitoring (a) and product analysis (b)

Reaction conditions: 7 % TS, 2 % E:S, 50 °C and 600 rpm - 1.5L STR. Purple lines represent the optimal pH-range (4.75-5.25) for Cellic CTec3 enzymes [100]

enzymatic hydrolysis . The pH of media decreases from 5 to 4.5 in 4 hours, keeping constant until end of enzymatic hydrolysis. In contrast, the DO measurements fluctuate during first 4 hours of hydrolysis, the so-called "viscosity break" period. By comparing pH/DO monitoring of BIT (Fig. 3.19a) and NaN_3 (Fig. 3.18c), a slight delay in the evolution of pH/DO was observed for BIT. It can be stated that the pH and DO behave differently, even finalising with similar records (pH = $\sim$ 4.25 and DO = 5 mg L^{-1}. In the case of products, carbohydrates and acetic acid yields with BIT addition resulted alike the NaN_3 case (Fig. 3.19b). However, in the BIT run; more glucose (12 g L^{-1}), xylose (4.0 g L^{-1}), acetic acid (34 mg L^{-1}) and no lactic acid were detected as well. BIT is a widely used preservative for the formulation of home-cleaning and personal care products, among other applications [130, 176]. It has shown high efficacy as antimicrobial compound as DO levels were kept higher for longer and less sugar was spoiled, which could be attributed to its different mode

of action compared to NaN_3 (microbiocide and fungicide to bacteriostat). In theory, BIT is also capable of eliminating bacterial spores and render any microbial activity, however, further experimentation is needed in these regards (e.g. optical density or RNA sequencing).

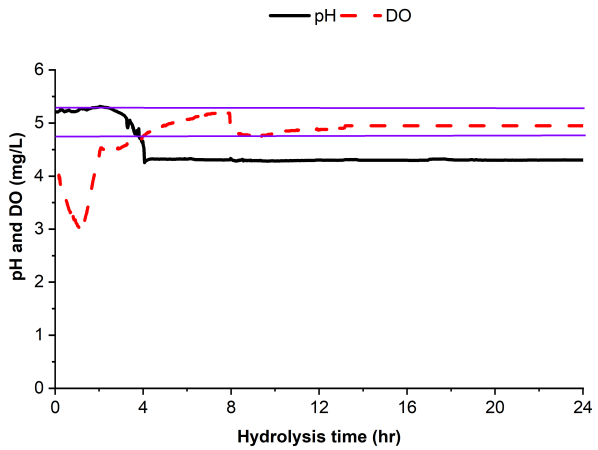

(a)

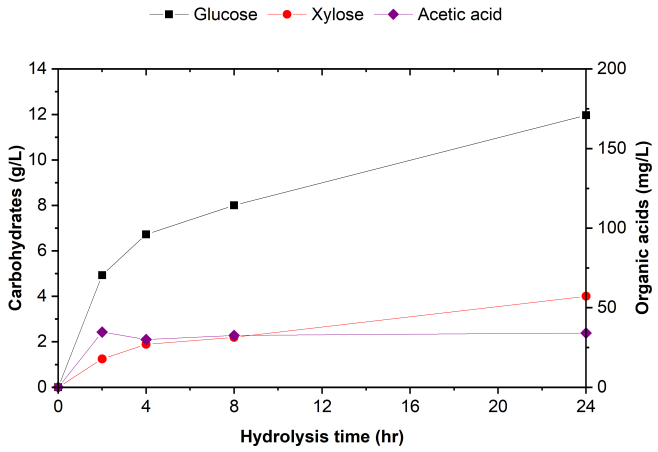

(b)

Figure 3.19. Enzymatic hydrolysis of MSW pulp with initial dosing of 0.1% (w/w dry substrate) BIT: process monitoring (a) and product analysis (b)

Reaction conditions: 7 % TS, 2 % E:S, 50 °C and 600 rpm - 1.5L STR. Purple lines represent the optimal pH-range (4.75-5.25) for Cellic CTec3 enzymes [100]

The effect of H_2O_2 addition in the pH/DO monitoring and hydrolysate analysis of enzymatic hydrolysis of MSW-derived pulp is included in Fig. 3.20. In this case, microbial contamination was not tackled as neither pH/DO nor product analysis evolved as a control assay. An even pH was kept within the optimum range (4.75-5.25) for the first two hours, a major drop was observed afterwards. At the end of reaction, pH was found to be lower than 4, too acidic for Cellic CTec3 enzymes [100]. Meanwhile, DO measurements reached anaerobic conditions, once slurry liquefaction, in 5.25 hours of hydrolysis. The sudden increase in DO increase after the fourth hour, could be explain as some biomass was left unreacted due to formation of dead

zones (heterogeneous mixing). For the product analysis (Fig. 3.20b), unfavourable results of carbohydrates and organic acid metabolites were found for: glucose (9.80 g L^{-1}), xylose (2.4 g L^{-1}), lactic acid (41 mg L^{-1}) and acetic acid (181 mg L^{-1}). As acetic acid, lactic acid stabilised from 8 to 24 hours. The uncontrolled pH-media would hamper the optimum microbial conditions of lactic-fermentative bacteria as opposed of H_2O_2 efficiency as antimicrobial. This effect was not seen in acetic acid titres as measurements soared to > 175 mg L^{-1}. The substantial increase of organic acids (except for lactic acid) inhibit the further enzymatic saccharification, resulting into the plateau effect of carbohydrate values before 24-hours [72]. Herein, it is shown that H_2O_2 is not a useful compound to tackle microbial contamination for a 24-hour reaction, due to poor thermodynamically stability and short half-life (> 8 hours). As recommended [70, 124], periodic dose of H_2O_2 could be more effective instead of a single and initial infusion, which demonstrated vast improvements in LPMO-based studies.

In Fig. 3.21, parameter monitoring and product analysis are shown during the enzymatic hydrolysis of MSW with initial dosing of 0.1 % Fermasure® XL. Prior biological infection (app. 6^{th} hour), pH of media was well maintained at 4.75-5.25, but a strong acidification of media was observed thereafter until 24-hours (pH 4). At the same time, DO measurements behaved similarly to the control assay, achieving anaerobic conditions at 6 hours. Again, and validating our hypothesis, there is a correlation between the drop in pH and DO with an uprise in the concentrations of organic acids (lactic and acetic acid) after 4 hours of hydrolysis (Fig. 3.21b). At aerobic conditions, no lactic acid was found, and acetic acid yielded by following xylose kinetics, which suggest no bacterial contamination. In anaerobic conditions, some microorganism are likely to increase their metabolisms, which could explain the increase in acetic and lactic acid titers (approx. 100 mg L^{-1}) at 24 hours of hydrolysis. On the other hand, glucose and xylose yielded 9.3 and 3.4 g L^{-1}, respectively, which are moderate yields compared with the rest of studies. The use of Fermasure® XL, as other chlorine dioxide-based compounds, resolves bacterial contamination in fermentation broths [109], but this success does not translate well in enhancing the enzymatic saccharification. The different characteristics of enzymatic hydrolysis (pH, temperature and feedstock) to fermentation, including more severe agitation system, could undermine Fermasure® XL shelf-life - only active prior 8 hours of reaction [140].

The tetracycline antibiotic was tested in a similar manner to previous hydrolysis assays, with its effect on pH/DO monitored along with the hydrolysate analysis (Fig. 3.22a,l). Dark conditions were not maintained, tetracycline tends to be photo-oxidised by light exposure, implying a loss of some anti-microbial activity [177, 178]. In Fig. 3.22b, the tetracycline was effective for almost 14 hours : (i) pH around 4.75 and (ii) DO > 4 mg L^{-1}. Even the pH did not decrease as much as with NaN_3 and BIT at these time-frames. However, the incoming biological infection (12 hours) leads to decrease to pH $\sim$ 4 and DO of 0 mg L^{-1}. Completed anoxic media boosts lactic

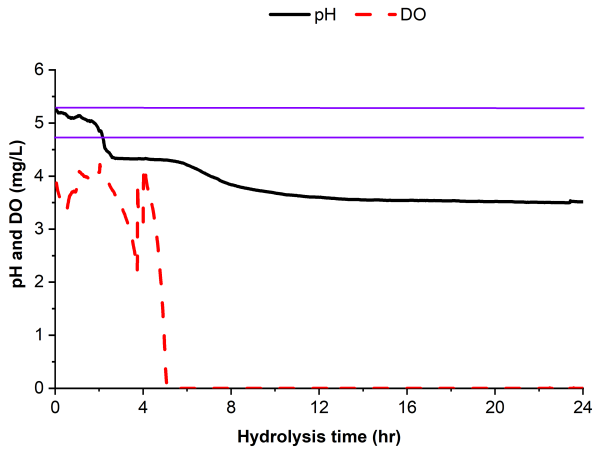

(a)

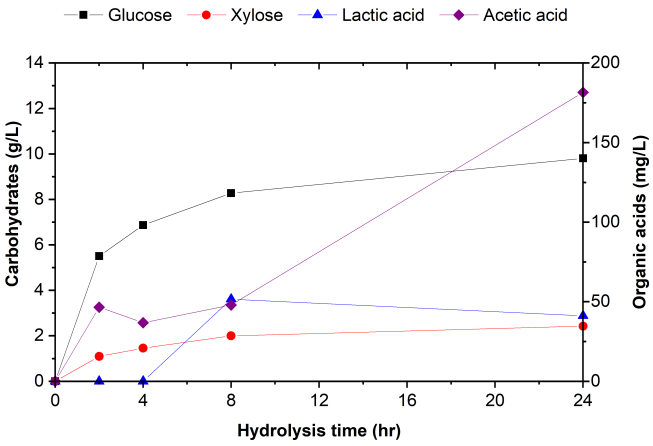

(b)

Figure 3.20. Enzymatic hydrolysis of MSW pulp with initial dosing of 0.1% (w/w dry substrate) H_2O_2: process monitoring (a) and product analysis (b)

Reaction conditions: 7 % TS, 2 % E:S, 50 °C and 600 rpm - 1.5L STR. Purple lines represent the optimal pH-range (4.75-5.25) for Cellic CTec3 enzymes [100]

and acetic acid concentrations 0 to 50 and 28 to 77 mg L^{-1}, respectively, compared with the previous sample (8 hours). In contrast, glucose and xylose only increase by 1-2 g L^{-1} in 16 hours: 8 to 9.7 and 2.4 to 3.4 g L^{-1}, respectively. Tetracycline looks a promising anti-microbial agent for a short time period (> 12 hours), but not thereafter, as higher concentrations of organic acids and lower carbohydrates rates were found. This could be attribute to its low thermostability and photo-sensitivity, in addition, to gained bacterial resistance throughout the reaction. Its effect on the sugar yield was also assessed throughout the enzymatic hydrolysis, showing the its limited applicability on MSW-feedstocks [156].

In summary, the efficiency of five antimicrobial agents has been studied (plus the control assay) and these can be ranked against the analysed the parameters (pH, DO, glucose, xylose, acetic acid and lactic acid). The costs associated with each compound is also another factor to consider, summarised in Table 3.2. Other factors

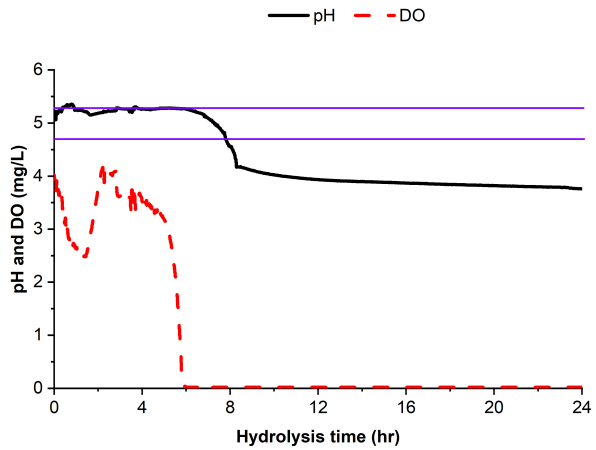

(a)

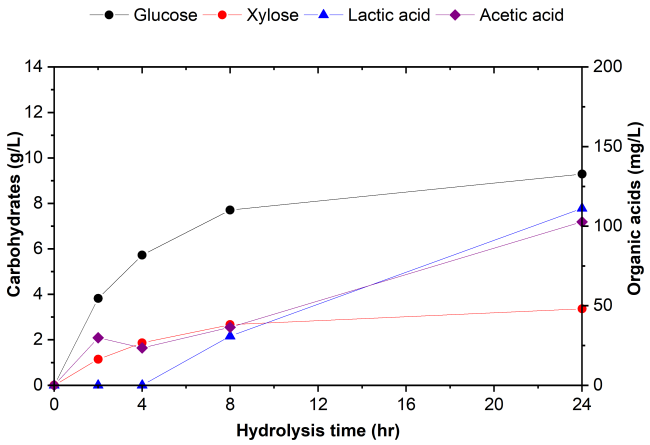

(b)

Figure 3.21. Enzymatic hydrolysis of MSW pulp with initial dosing of 0.1% (w/w dry substrate) Fermasure® XL: process monitoring (a) and product analysis (b)

Reaction conditions: 7 % TS, 2 % E:S, 50 °C and 600 rpm - 1.5L STR. Purple lines represent the optimal pH-range (4.75-5.25) for Cellic CTec3 enzymes [100]

such the effects on downstream processing of the lignocellulosic hydrolysate in the presence of antimicrobial compounds are also important, but not investigated in this study. Uncontrolled (no pH adjustment over time) reactions show that antimicrobial agents are incapable of maintaining pH at the optimum conditions without acid/base addition. Even though, some pH stabilisation was achieved: 4.25 (NaN_3 and BIT), 4 (Fermasure ® XL and Tetracycline) and 3.5 (H_2O_2 and control. The acidification of media is an unavoidable issues as intrinsic acetic acid is released form the hemicellulose fraction. Therefore, automatic or periodic pH control with acids/bases is a must if buffer solutions are not used. In contrast, aerobic conditions (DO $\sim$ 5 mg L^{-1}) were kept for a certain period of time depending on used compound: NaN_3 and BIT (24 hours), tetracycline (13.5 hours), Fermasure ® XL and control (6 hours) as well as H_2O_2 (< 5 hours). The rapid consumption of oxygen is accentuated by the addition of H_2O_2 as molecular oxygen and hydrogen work as

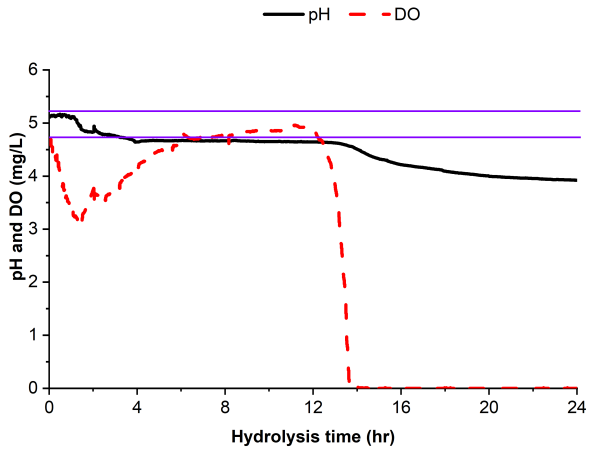

(a)

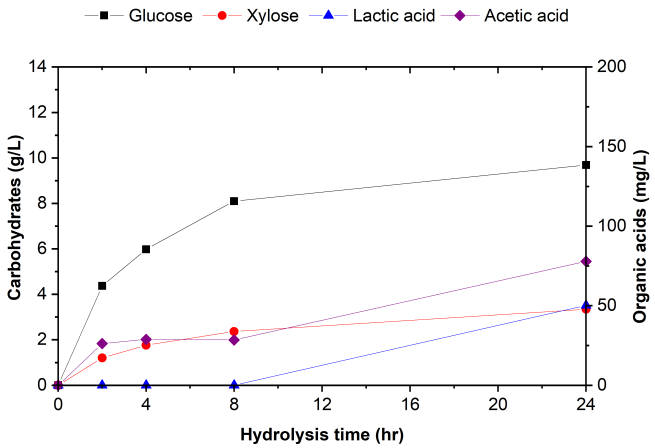

(b)

Figure 3.22. Enzymatic hydrolysis of MSW pulp with initial dosing of 0.1% (w/w dry substrate) tetracycline: process monitoring (a) and product analysis (b)

Reaction conditions: 7 % TS, 2 % E:S, 50 °C and 600 rpm - 1.5L STR. Purple lines represent the optimal pH-range (4.75-5.25) for Cellic CTec3 enzymes [100]

electron acceptor and donor, respectively, boosting the LPMO activity [127]. Peciultye et al.[124] investigated the oxygen concentration (in %) during three rounds of enzymatic incubation of pretreated wheat straw by DO monitoring. A similar trend (DO drop after 6 hours) in a 10 % TS slurry, however, they associated it to abiotic reactions (such as decarboxylation) of biomass decomposition in symbiosis with transition metals, instead of microbial activity (e.g. growth of spores). pH is a well-known parameter in these processes, however, little attention has been given to DO.

The final concentrations of carbohydrates and organic acids were also compared depending the choice of antimicrobial. In the case of glucose, the highest yields were found in the decreasing order: BIT (12.0 g L^{-1}) > NaN_3 (10.3 g L^{-1}) > H_2O_2 (9.80 g L^{-1}) > Tetracycline (9.70 g L^{-1}) > Fermasure® XL (9.30 g L^{-1}) and control (7.80 g L^{-1}). The highest carbohydrates yields were inversely proportional to the

formation of organic acids, as result of glucose (mainly) degradation by metabolic routes [101]. In addition, none or minor pH and DO control during the hydrolysis would results in elevated concentrations of acetic and lactic acid: 157 and 138 mg L^{-1}, 102 and 111 mg L^{-1}, 77.9 and 50.1 mg L^{-1} as well as 181 and 41.1 mg L^{-1} for the control, Fermasure ® XL, tetracycline and $H2O_2$ assays, respectively. Process monitoring of pH/DO with discrete analysis of carbohydrates and organic acids has demonstrated that, initial dose of either NaN_3 or BIT are best options for tackling the microbial contamination during enzymatic saccharification.

3.4 Chapter summary

In this chapter, the basics of enzymatic hydrolysis were covered, with MSW as the main feedstock, high-solids loadings and potential sources of contamination. The latter two sections were investigated with the corresponding experimentation, evaluating:

- High-solids loadings (> 15 % TS): optimum and maximum ranges and associated limitations
- Effectiveness of antimicrobial compounds and concentrations
- Monitoring of pH/DO as metrics for predicting microbial contamination with initial dosing of antimicrobial agents

In the first case:

- MSW saccharification can be pursued at high-solids loading $\leq$ to 25 % TS as effective enzyme adsorption, biomass liquefaction and high-concentrated sugar syrups are achieved (> 80 g L^{-1})
- At more than 25 % TS, no free water is accessible so enzyme diffusion and adsorption in the biomass slurry is ineffective, therefore, poor hydrolysis is observed. Other technical limitations are associated to inaccuracy pH-adjustment and unrepresentative sampling due to the building of dead zones.

A key finding for Chapter 5 (Reactor design and operation), is that high-solids loading experiments have shown that drum reactors are an optimal configuration as these enable operation in these regimes at low rotational speeds and high volume capacity. Other features are commented on the corresponding section.

Secondly, the study related of tackling microbial contamination led to following findings:

- Addition of some antimicrobial compound is a requirement for avoiding sugar spoilage

- BIT surges a good alternative to conventional antimicrobial compounds due to its high effectiveness and attractive costs, but further downstream processing studies are required for evaluating its effect on subsequent bioprocessing.
- Antimicrobial agents (at 0.1 % (w/w)) do not maintain optimum pH levels without addition of acid or bases
- Decreasing antimicrobial doses from 0.1 to 0.01% showed similar efficacy and considerable drop in operational costs

Finally, the monitoring of pH/DO during enzymatic hydrolysis demonstrated that:

- Continuous pH/DO measurements coupled with discrete product analysis (carbohydrates and organic acids) showed a correlation between pH/DO levels with microbial contamination
- pH/DO monitoring is diagnosis tool for examining early stage contamination in well-mixed reactor systems

This latter approach was further investigated with manual (when DO reached 0 mg L^{-1}) and automatic operation (section 2.6.1) dose of the six studied antimicrobial strategies. The corresponding methodology, results and discussion and conclusions can be found in the publication entitled as: "*Improved conversion of residual MSW biomass waste to sugars using online process monitoring and integrated contamination control*" in the Journal of Bioresource Technology Reports [47].

Chapter 4

Rheology of MSW-pulp slurries

4.1 Introduction

Rheology is a branch of physics that studies the deformation of materials that flow. The term rheology was coined by Eugene C. Bingham as the aphorism of Simplicius, *panta rhei*, meaning 'everything flows' in ancient Greek. But earlier, Sir Isaac Newton originated the concept of viscosity (μ, Pa· s), as the ratio between shear stress (τ, N/m^2) and shear rate (γ, s^{-1}): $\mu = \tau/\gamma$. Thus, fluids are classified as Newtonian or non-Newtonian. Most of the fluids are non-Newtonian, where the dynamic viscosity (μ, Pa· s) is strain-rate-dependent, i.e. shear stress (τ, N/m^2) has a disproportional relationship to shear rate (γ, s^{-1}). Otherwise, the fluid is Newtonian, the viscosity only changes due to external factors (e.g. temperature). In addition, four non-Newtonian fluids can be observed in Fig 4.1: Bingham, Plastic/ Hershel-Bulkley, Dilatant/shear thickening and Pseudoplastic/shear thinning. The last two types of fluids follow a power-law model where shear stress (Eq. 2.12) and apparent viscosity (μ_{app}, Eq. 2.13), calculated by the given expressions:

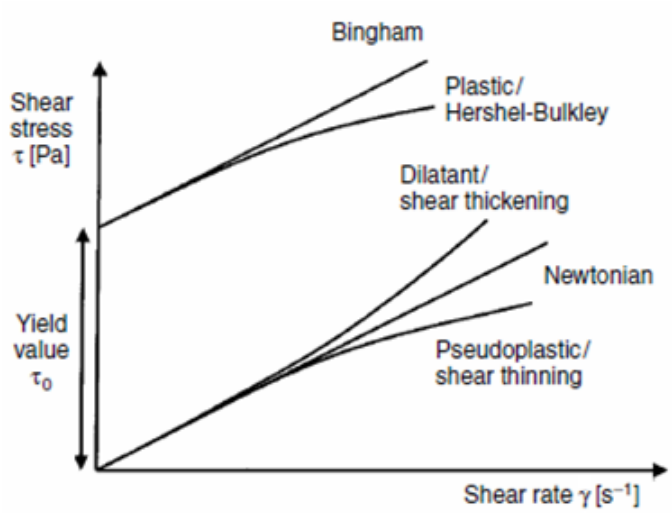

Figure 4.1. Classification of fluids upon τ and γ evolution, adapted from [44]

The n index value determines whether a fluid is Newtonian (n = 1) or non-Newtonian (n $\neq$ 1), and shear-thinning (n < 1) and shear-thickening (n > 1) if non-Newtonian. In shear-thickening fluids the τ increases by increasing γ and μ_{app} decreases by arising the shear rate, and viceversa for shear-thinning (Fig. 4.1. Other non-Newtonian fluids observed in Fig. 4.1 are Bingham (n =1) and Plastic/Hershel-Bulkley (n < 1). In both fluids, a yield value (τ_o, in Pa) also known as yield stress, is defined as the minimum pressure needed for agitation, mixing or pumping purposes. Skelland [179] classified the non-Newtonian fluids into three main categories: time-independent fluids properties, time-dependent fluids properties and viscoelastic. The majority of time-independent are shear-thinning (pseudoplastic), even the fluids found in Fig. 4.1 are also considered in this group. Table 4.1 summarises the non-Newtonian fluids by the McGlash classification, including their definition and some examples [180].

Table 4.1. Overview of non-Newtonian fluids characteristics [180]

Type of non-Newtonian behaviour	Property	Definition	Examples
Time-independent fluid	Shear-thickening (dilatant)	τ increases with increasing γ	Corn starch diluted in water
	Shear-thinning (pseudoplastic)	μ_{app} decreases with increasing γ	Ketchup or molasses
Time-dependent fluid	Rheopecty	μ_{app} increases with duration of τ	Ink or gypsum
	Thixotropic	μ_{app} decreases with duration of τ	Yogurt, peanut butter and xanthan gum
Viscoelastic	Kelvin and Maxwell materials	Combination of elastic and viscous effects	Lubricants or whipped cream

4.2 Literature review

4.2.1 Lignocellulosic biomass as non-Newtonian fluids

Rheology has gained importance in lignocellulosic bioprocessing as useful tool to study fluid characteristics for reactor design and operation. Determination of parameters such as viscosity or yield stress leads to the study of mixing and handling limitations of lignocellulosic substrates, e.g. pumping pressure. Therefore, by understanding the rheology of lignocellulosic biomass, more accurate bioreactors and operations can be designed, e.g. achieving better mass-heat transfer and lower power consumption [181]. Within the type of fluids, lignocellulosic slurries are classified as non-Newtonian fluids, i.e viscosity is independent of shear stress, usually described with different models as Power-law, Casson, Herschel-Bulkley and Wildemuth-Williams [92]. Commonly, they have a tendency to decrease viscosity whilst increasing stirring speed (shear-thinning) with/without tendency to deform (yield stress).

As rheological analyses are performed by distinct instruments, employing different geometries and techniques, it is challenging to achieve absolute viscosity measurements per feedstock/study [182, 183]. High heterogeneity in biomass composition and variability in pretreatment methods, add an extra layer of complexity. Despite this, the suspension is considered "pumpable" when its yield stress is lower than 10 Pa – which is equivalent of 10% insoluble solids - as "rule of thumb" for pretreated corn stover (PCS) slurries. Determination of yield stress was extensively investigated via a vast array of techniques in PCS [182, 183]. Knutsen and Liberatore [182] employed a combination a four rheology-based techniques (torsional, squeeze, shear and oscillatory flows) either in parallel-plate or vane-in-cup geometries to determine yield stresses of PCS at 5-17 fraction of insoluble solids (FIS, in %). A power-law model was fitted for yield stresses ranging from 0.5-5000 Pa upon solids loadings, formulated as: τ_0 = 7.7 x 10^7 $FIS^{6.0}$, showing a great dependence of FIS as yield stress scales to the seventh exponent. At higher values, 20-35 % FIS, accurate yield stress measurements were only achieved by the "squeeze flow" methodology. Similarly, Stickel et al. [183] compared the analysis of yield stresses of PCS in the range of 5-30 wt % by using a parallel plate, vane and torque rheometer, indicating the viscoelastic and shear-thinning behaviours of those slurries as well as concentration-dependent yield stress. Interestingly, no drastic differences were observed in the inter-laboratory analysis of yields stresses even though the differences between the set of methodologies and instruments used, resulting into a 1-2000 Pa. Plotting of yield stress over insoluble solids displays a power-law dependence, resulting into the following expression: τ_0 = a Cm^b; where a is curve slope and Cm is concentration mass (%). For systems working with acid-hydrolysed corn stover, the b exponent ranges from 4 to 5.6 [182, 184, 185] depending on the particle-reduction size and concentration range of each study. Other substrates as wood fibres presented lower power-law exponents in the range of 2-4 [186] with less variability between assays, as consequence of using materials with more constant physical properties (morphology and fiber length).

In Fig. 4.2, a list of publications using a single methodology for the determination of rheology-based parameters, plotting yield stress (Fig. 4.2a) and viscosity (Fig. 4.2b) as function of solid loadings. PCS investigations [146, 187, 188] presented yield stress values (1 to 2000 Pa) in the range of previous studies [182, 183], with different pretreatment conditions, methodologies and rheology analysis. In its raw conditions, untreated biomass (Viamajala et al. [187] and Samaniuk et al. [188]), yield stresses can exceed 10000 Pa at solids loadings > 20%, incapacitating the use of vertically-orientated bioreactors as shake flasks and stirred tanks [146]. Chen et al. 2019 [189] evaluated the yield stress of deacetylated 18-33% dry matter corn stover with disk refined (DDR) and mechanical refined (DMR) of solids loadings ranging from 5-20 %. Differences in dryness did not result into significant changes in yield stress when operating above 15% solids concentrations. Both milling techniques

plus deacetlyation hydrolysed the hemicellulose fraction of corn stover, led to loosing the recalcitrant lignin part as well. A non-biomass study (TiO_2), investigating yield stress as function of 40-70% w/w solids loadings, was carried out by Nguyen et al. [190] and included in Fig. 4.2a as reference. The Newtonian behaviour of the metal oxides displayed a linear relationship between yield stress and solid loadings, but interestingly τ_0 values did not overpass 100 Pa despite the elevated proportion of the insoluble fraction. Compared with corn stover, the rheology of both slurries is completely different due typology of fluid and yield stress upon solid loading. Many reasons are behind the rheological characteristics of lignocellulosic slurries, particularly at high-solids loadings (water scarcity, coarse and fibrous particles, composition etc..), being unique and challenging materials for bioprocessing [2].

Viscosity is the other main rheological parameter, as indication of "thickness" at given rate, measured for a range of solids loadings on lignocellulosic biomass (Fig. 4.2b). Differing to yield stress, viscosity has been determined at fixed rate (γ, s^{-1}) in alternative feedstocks to corn stover such as switchgrass and sawdust. Previous work by Viamajala et al. [187] included also viscosity measurements as function of solid loadings using sieved (0.841 and 0.177 mm) corn stover pretreated with sulfuric acid at room, 170 and 190 °C temperatures. Surprisingly, pretreating temperature does not affect slurry viscosity in particle-size of 0.841 mm (20 mesh size) but it does in 0.177 mm (80 mesh size), particularly at above 20% w/w. It is well-known that particle-size as well as morphology and crystallinity of fibers can greatly affect the viscosity of lignocellulosic slurries[40]. It is also appreciated that viscosity values grow linearly upon solid concentrations but flatter when reaching above 20% w/w. Similar results were found by Berson et al. [192], which used NREL corn stover pretreated under different conditions. Other lignocellulosic feedstocks (switch grass and pine sawdust) were evaluated by following similar methodologies [191, 193]. Cruz et al. 2013 [191] recorded the viscosity of switchgrass slurries (5 to 50% w/w) pretreated by ionic liquids (IL), at fixed rate of 1 s^{-1} using a plate-plate geometry. IL biomasses displayed an exponential relationship between viscosity and solids loadings, reaching almost 1000 Pa s at 50% w/w. Entangling of fibrils and high lignin content (37.4%) of switchgrass are potential reasons of such high-initial viscosity, despite of being sieved through a 40 mesh size and severe pretreatment: [C2min][OAc] at 160 °C for 3 hours. For pinewood sawdust (untreated and hydrothermal-carbonised), shear viscosity measurements were directly proportional to solid loadings, exhibiting maximum values of 1.5 Pa s [193]. The rapid shear rate (102 s^{-1}) translated to lower viscosity measurements than rest of studies, which were analysed at least $\gamma > 5$ s^{-1}. To provide an exact feedstock-to-feedstock comparison as function of solid concentrations, the rheology analysis should be performed with identical instrumentation and running conditions as viscosity measurements are greatly affected by shear rate: $\mu = \tau/\gamma$. Therefore, lowering the denominator (shear stress) provokes an increment in viscosity measurement as impeding the efficient and homogeneous mixing in the system.

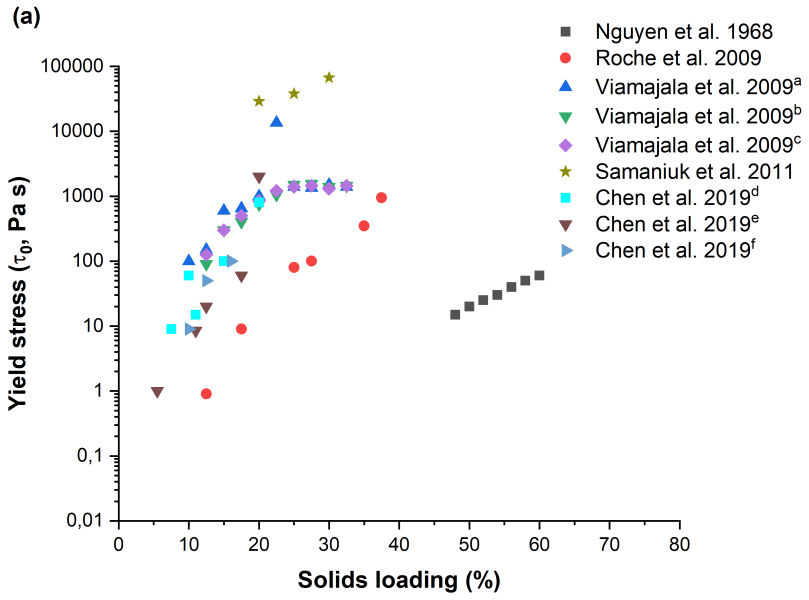

(a)

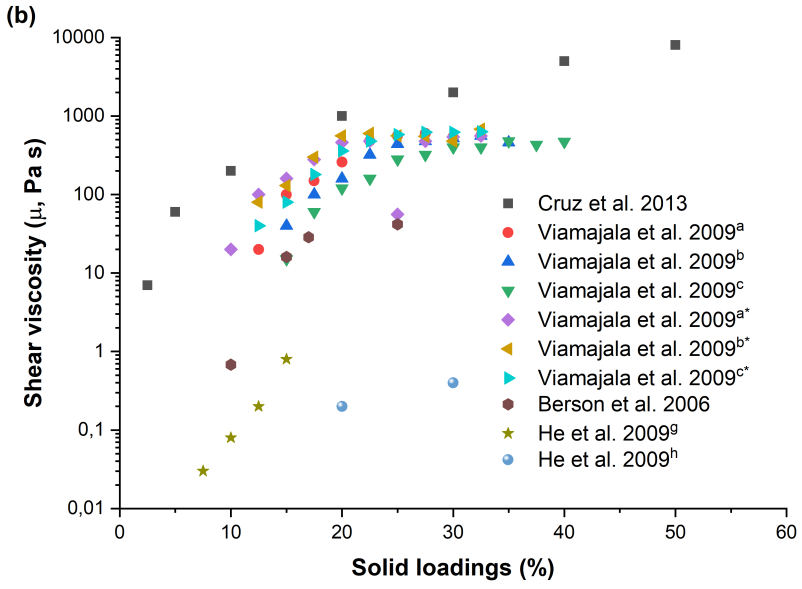

(b)

[a]Untreated, [a]170 °C C, [b]190 °C,[c]deacetylated and disk refined, [d]deacetylated and mechanically refined, [e]dilute acid pretreatment, [f]untreated wood, [g]hydrothermal-preatreated wood and *PCS was sieved at 80 mesh size

Figure 4.2. Literature of rheological parameters as function of solid loadings at pretreatment stage: yield stress (a) and shear viscosity (b)

In Figure: Nguyen et al. [190] used 0.2 μm TiO_2 particles, Roche et al. [146] used 100 μm NREL PCS, Viamajala et al. [187] used NREL PCS^{abc}, Samaniuk et al. [188] used 1 mm switchgrass and Chen et al. [189] used 19 mm CS^{def}. In Fig.4.2b: Cruz et al. 2013[191] used 0.255-0.451 mm IL switchgrass, Viamajala et al. [187] used 0.841^{abc} and 0.177^{a*b*c*} mm NREL PCS, Berson et al. [192] used NREL PCS and He et al.[193] used 0.150 mm Pine wood sawdust.

During enzymatic hydrolysis, the slurry rheology changes due to depolymerisation of lignocellulosic biomass by cellulases and release of fermentable sugars. The slurry viscosity changes upon various factors such as solids contents, enzyme loadings, feedstock and shear rate. Several studies calculated μ_{app} (in mPa s) using different impeller configurations [194], reactor orientations [195] and rotational speeds [196] throughout enzymatic hydrolysis of various lignocellulosic residues (Fig. 4.3). Correa et al. 2016 [194] worked with four different combinations of dual-impellers; Rushton turbines (DIC1), Rushton and elephant-ear (downdraft) turbines (DIC2), Rushton and elephant-ear (updraft) turbines (DIC3), and elephant-ear (dowdraft and updraft) turbines on 10% w/w of steam-exploded sugarcane bagasse at 10 FPU/g biomass. Apparent viscosities, calculated at 470 rpm, highlighted the improving mass-transfer effect of DIC4 dual-impeller geometry as viscosity decrease faster than rest of combinations whilst converting further monomeric sugars. An individual hydrolysis reaction using 13% w/w red-oak sawdust in shake flasks, reported a steep viscosity reduction (> 300 to app. 75 mPa s) inversely correlated to glucose yields (2 to 13 g/L) in eight hours of reaction [40]. Depending on nature of feedstock and applied pretreatment, rheological analysis cannot be pursued at high-solids regimes due to risk of damaging the instrumentation. Although, few studies have successfully determined μ_{app} in lignocellulosic systems above 15% w/w [195, 196], requiring severe particle-size reduction. Palmqvist et al. 2016 [196] compared the fluid properties of 20% w/w SO_2-pretreated spruce chip hydrolysates as function of impeller speed (30, 60 and 120 rpm), in a demonstration-scale (4 m^3) equipped with a pitched-blade impeller. In this study, it was demonstrated that increased rotational speed (120 rpm) has a positive effect in biomass liquefaction as presenting faster viscosity reduction and values after 72 hours of hydrolysis. At 30 rpm, mass-transfer was very limited as no substantial difference between initial and final viscosity values were observed. Other investigations determined apparent viscosities of 25% w/w steam-pretreated corn stover hydrolysed in either horizontal rotating and helical ribbon reactors at 7 FPU/g DM [195]. Hydrolysates were not analysed prior 15 hours due to elevated slurry viscosity, apparent viscosities (fixed shear rate at 4.8 s^{-1}) were 4-fold higher in the vertical than the horizontal rotating configuration – 3500 to 100 mPa s, respectively. Increasing enzymes doses up to 3 FPU/g DM translated into a quicker liquefaction (2500 to 1500 mPa s) than reference conditions in the horizontal geometry.

Off-line analysis of K-values, indicator of viscosity, were plotted throughout 168 hours of PCS enzymatic hydrolysis [41, 48] in either SSBRs and shake flasks in a solids concentration range of 10 to 25 % (Fig.4.3b). At same insoluble concentrations of PCS (10 and 25%), SSBR reflected a greater and faster viscosity decline than SKs, due to the promotion of heat and transfer rates by the scraping blades [41]. Further hydrolysis reactions (10-25%) were incubated at 250 rpm using PCS as substrate, where collected hydrolysates and subjected to "flow sweep" analysis [48]. In

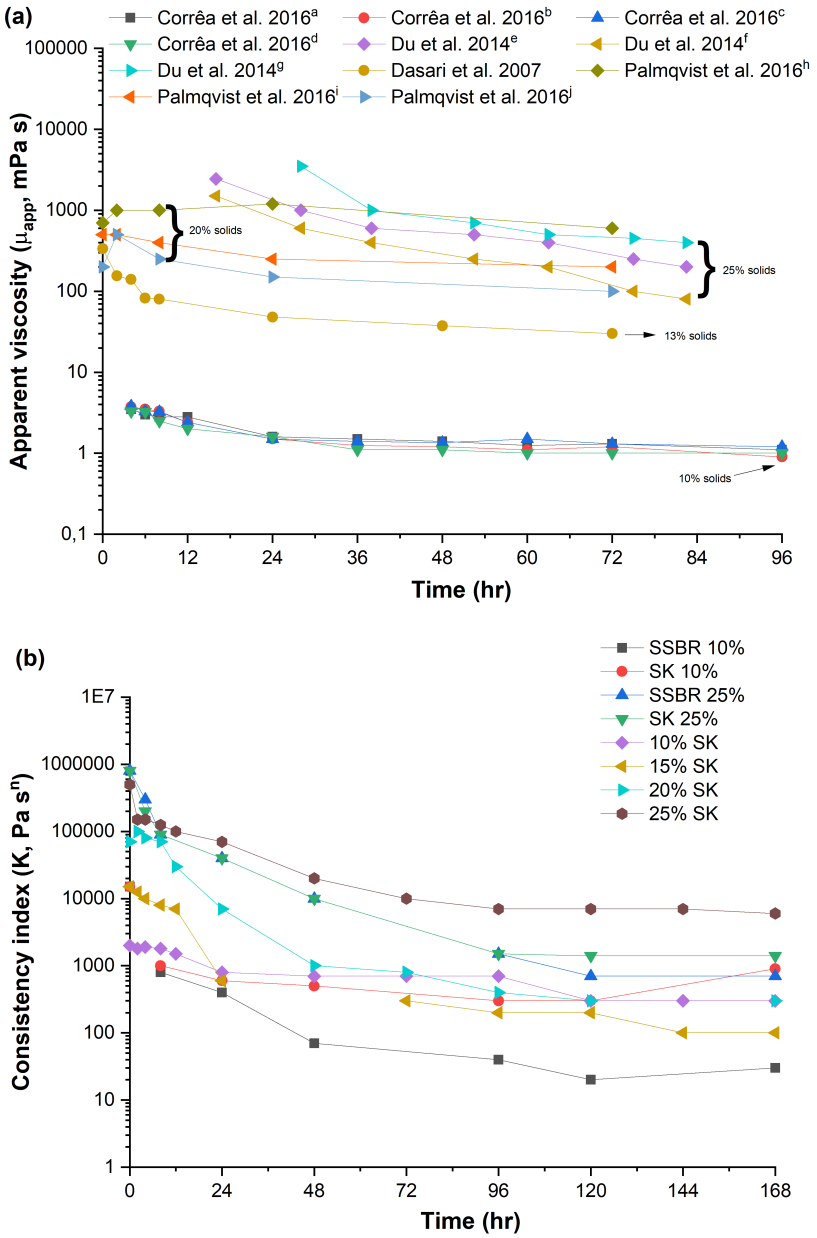

[a]RT-RT, [b]EEDP-RT, [c]RT-EEUP,[d]EEDP-EEUP, [e]7 FPU/g DM in horizontal bottle reactor, [f]10 FPU/g DM in horizontal bottle reactor, [g]pitched-blade at 30 rpm, [h]pitched-blade at 60 rpm and [i]pitched-blade at 120 rpm
Legend: SSBR is scraped surface bioreactor, SK is shake flask, RT is Rushton turbine, EEDP is Elephant Ear Downdraft Pitched, EEUP is Elephant Ear Updraft Pitched, FPU is Filter Paper Unit and DM is Dry Matter

Figure 4.3. Literature of viscosity and K-values during high-solids enzymatic hydrolysis of biomasses

In Figure, Correa et al. 2016 [194] used steam-exploded sugarcane bagasse, Du et al. 2014 [195] used sulfuric acid-steam pretreated corn stover, Dasari et al. 2007 [40] used 33 μm < x < 75 μm red-oak sawdust and Palmqvist et al. 2016 [196] used 2-10 mm SO_2-pretreated spruce chips. The arrows represent solids loading within same study. In Fig4.3b, data is obtained for SSBR/SK 10-25% and 10-25% SK from Dasari 2008 [41] and Dunaway et al. 2012 [48], respectively, using NREL PCS.

this case, 15 and 20% insoluble concentration displayed adequate biomass liquefaction as viscosity decreases substantially after one-day of reaction. We observed that enzymatic hydrolysis presents a two-step kinetics in rheological terms: (i) rapid hydrolysis of amorphous cellulose by cellobiohydrolases and (ii) slow hydrolysis of crystalline cellulose by endogluconases [41]. The rate of liquefaction is determined through rheology-based measurements and depends upon multiple factors such as used feedstock, enzyme dosage, reactor configuration and operation etc.[92].

In-line monitoring of viscosity during the enzymatic hydrolysis of biomass is less well reported in the literature, despite of being a useful approach for real-time analysis with minimal sampling [40, 197]. With this technique, it is possible to characterise the reduction in viscosity, also known as liquefaction rate, upon: enzyme dosages, reactor geometries and solids contents. In situ or continuous rheometry can be investigated by various instruments: viscometer, rheometer or torque-metry. The most common instrumentation are viscometer/rheometers, where the enzymatic saccharification is run *in situ*.. In the case of a viscometer, it is essential to protect the hydrolysis media and ensure a controlled temperature profile as reaction are commonly placed in beakers. The structure of a rheometer normally includes an environmental chamber with steady-state heating and cup container to successfully conduct the experiments. Despite this, viscosity calculations in both devices are based on mechanical parameters and depend upon the impeller geometry, assuming that the fluid is Newtonian. Some authors have used these devices for the in situ rheometry of pretreated Norway spruce with addition of CTec3 and auxiliary enzymes [197] and sawdust [40]. Due to technical considerations (e.g. wall-slip or fracture), hydrolysis assays are not run continuously for more than 12 hours. More recently, Coffman et al. 2018 [198] proposed an alternative rheological method for *in situ* determination of physical properties during high-solids loadings of ionic liquid pretreated switchgrass and Avicel, coupling the monitoring of phase angle and discrete oligosaccharide analysis. Continuous oscillation over the hydrolysis reaction allows the determination of elastic and viscous modules, and ratio (degree of angle). In theory, a phase angle > 45 $^{\circ}$ translates to a liquid-like fluid, so the transition point is equivalent to the liquefaction rate. Other researchers have designed home-made systems (attached torque-sensor into stirred tank reactor), measuring viscosity of low-lignin substrates [199, 200] supported with evident agitation and mixing theory (e.g. "power-curve" for non-Newtonian fluids). For this methodology, the impeller configuration was calibrated by several Newtonian and non-Newtonian fluids in order to determine Power as function of Reynolds number, therefore, deriving viscosity measurements. Diverging from torque-based approaches, in-line rheological measurements were conducted with a non-invasive technique of magnetic resonance imaging (MRI) and close-loop recycling [201, 202]. Yield stress were measured during fed-batch hydrolysis of two grades of powdered cellulose (Solka-floc 200EZ and C100) at 8-30% w/w for a period of time of 12 hours [202]. Incremental addition of substrate with enzymes mitigated the increasing yield stress of the system

compared when only enzymes were added at the beginning.

4.3 Experimental methodology

The whole rheological experimentation follows the research methodology described in section 2.7, and differences in sample pretreatment and gap length (impeller clearance level) are described for each assay.

4.3.1 Parallel bottle reactor

Following the methodology of section 2.3.4, PBRs hydrolysis reactions were conducted in duplicate, using a 50-ml falcon tube for each hydrolysis time: 0.5, 1, 2, 4, 8 and 24 hours. From the whole slurry, a homogenised sample was pipetted (2 ml) out for product analysis, whilst, the rest was subjected to rheological analysis as described in section 2.7. Collected samples were centrifuged at 15000 min^{-1} and filtered with 0.2 μm nylon filters. Supernatants were 10-fold diluted with DI water and frozen until analysis. A blood glucose-meter (Onetouch Verio, UK) was used for glucose analysis. Measurements were validated with high-purity glucose standards (0.5 to 5 g/L) and Onetouch control solutions. All samples were run analysed in triplicate.

Due the lack of impeller constants for rotating drum reactors, only for stirred tanks, μ_{app} was calculated according to a modified shear rate formulae defined by Zhong et al. 1994 [203]. The calculation of shear rate (γ) was proposed for cell cultivation as described by Eq. 4.1:

$$\gamma = (\frac{R_{in}}{R})^{(2/n)}[\frac{2\omega}{1-\frac{1}{\rho^2}}] \tag{4.1}$$

where R_{in} is inner cylinder radius, R is distance between inner and outer cylinder radius (i.e. wall thickness), n is flow behaviour index of fluid, ω is rotational speed (s^{-1}), p is ratio of inner cylinder radius per outer cylinder radius. Dimensions of 50-ml Falcon tubes are taken from vendor's website and a schematic diagram can be found in the Appendix A.

4.3.2 Fed-batch hydrolysis assay at Fiberight's demonstration plant

A fed-batch hydrolysis of MSW-derived pulp was conducted in a 6000 liters stirred tank reactor, located at Fiberight's demonstration plant (Lawrenceville, West Virginia, US). Hydrolysate samples were withdrawn by Fiberight employees during the trial, discharging a 40-ml aliquot from a recycling pipe-line. The *Lawrenceville* batch details are summarised in Table 4.2, filtered as five main intervals with their feeding characteristics. The reactor temperature was held at 50 °C. Other conditions and reactor designs are disclosed in internal reports, available upon approval of Fiberight Limited.

Table 4.2. Feeding strategy details of demonstration-scale fed-batch hydrolysis (Fiberight Limited, Lawrenceville, USA)

Intervals (hours)	Feeding (hours): pulp, enzymes, acid phosphoric and Fermasure®
1 - 6	Pulp (1-6), Acid Phosphoric (5), Enzymes (6) and Fermasure® (6)
7 - 12	Acid Phosphoric (9) and Fermasure® (10)
13 - 24	Pulp (13-14), Enzymes (14) and Fermasure® (16, 18 and 20)
25 - 30	Pulp (25-27), Enzymes (27) and Fermasure ®(26, 27 and 30)
31 - 45	Pulp (31-32), Enzymes (32) and Fermasure® (36, 40 and 45)

4.3.3 Rheometry during Louisville placement stage

Part of the PhD placement stage at Louisville University involved carrying out continuous viscosity measurements during the enzymatic saccharification of MSW-derived slurries as carried out by Dasari [41]. An Anton Parr modular compact rheometer was used for rheological analysis, with a vane-in-cup (40 ml) geometry equipped on a Peltier chamber. The vane geometry was a six-blade vane of 1.6 cm long, 0.9 cm wide and 1 mm thick. Continuous viscosity measurements were run with and 30 ml of working volume at 50 °C as optimum conditions for enzymatic hydrolysis. To enable the comparison with previous studies on same rheometer [40, 41], 10 s^{-1} was selected as fixed shear rate throughout the experimentation. Viscosity was recorded every minute, but average per hour

4.3.4 Torque to viscosity correlation within OPTOMS project

A fed-batch enzymatic hydrolysis was carried out by one of Fiberight employees (Southampton, UK) in a 10-L stirred tank reactor (Radleys, UK), equipped with a dual-hydrofoil impeller. 50 ml samples were withdrawn at discrete time points for the rheological analysis, stored at - 18 °C and shipped to Leeds in ice-packs. Reaction conditions were of 15 %TS, 2 % enzymes and 0.03 % BIT (w/w wet substrate) at 500 rpm. Other reaction details such as feeding strategy, used enzymatic cocktail and torque monitoring is confidential and subject to availability upon Fiberight's approval. Two enzymatic cocktails (CTec3 and CTec5), the latter privately manufactured for Fiberight, were loaded for the fed-batch hydrolysis runs (B79 and B80, respectively). The viscosity measurements (*in situ* and *ex situ*) were conducted based on torque measurements/power constant and power-law properties, respectively. In the laminar regime (Re < 40), the product between Power number ($P/\rho N^3D^5$) and Reynolds number ($\rho ND^2/\mu$) is a constant equal to 49 for the hydrofoil impeller. Once power consumption is calculated from torque measurements, μ can be derived as: P/KpN^2D^3. In contrast, *ex situ* viscosity was calculated from power-law properties and Metzner-Otto concept for non-Newtonian fluids as described in section 2.7. Other conditions and reactor design are disclosed in internal reports, available upon approval of Fiberight Limited.

4.4 Results and discussion

This section is structured into four areas: raw slurries, off-line viscosity monitoring, *in situ* rheology and case studies. Each part preambles with the nature of the samples and the motivation behind the studies.

Objective: To investigate the rheological characteristics of MSW-derived pulp slurries and compare within lignocellulosic materials

4.4.1 Rheological profile of untreated materials

This part covers the rheological studies of unhydrolysed (pre-hydrolysis) waste-pulp slurries at different solids loadings and compares the rheological and physical properties of Fiberight substrates (Lawrenceville and Hampden MSW pulps). Studying the rheological properties of the raw materials, we aim to elucidate the effect of solids loadings for the reactor operability, whilst, identifying possible rheological differences in geographical location of the produced MSW-pulps.

4.4.1.1 Effect of total solids on Herschel-Bulkley properties

A wide range of MSW-pulp dilutions were investigated, plotting yield stress and consistency index as function of solid loadings (Fig. 4.4). To ensure the safe experimentation and integrity of instrument, i.e. axial forces > 50 N, MSW-derived pulps were cryo-milled and sieved at x > 2000 μm as described in the methodology chapter (section 2.2.1). Appendix A includes pre-conditioning and flow sweep of individual hydrolysates (A.3). It is noted that either yield stress and consistency indexes (Herschel-Bulkley properties) increase as increasing solids loadings in the range of 5-15%TS. At higher solid regimes than 12.5%TS, Herschel-Bulkley properties do not grow exponentially, remaining the range of 50 Pa and 100 K Pas$n$ for τ_0 and K, respectively. In contrast, low-solids slurries (5%TS) posses a liquid-like nature, enhancing mixing and pumping processes due minimal yield stress (τ_0 = 1.2 Pa). Once reaching 7.5% TS, the yield stress increments nearly 10 times more than the lowest case (5 % TS), 11 to 1.20 Pa, respectively. Just a 50% increment on solids loadings (7.5 % TS) is responsible for such a difference. The yield stress has a non-linear relationship with solid loadings; 10% TS (23 Pa), 12.5% TS (76 Pa) and 15% TS (101 Pa). Similar results were found for yield stress measurements of several dilute acid-pretreated corn stover as function of solids loadings [92]. The authors grouped several rheological studies within the investigation, providing a general view-point: 5-20 [182], 20-30 [185], 20-35 [185] and 25-35 %TS [185]. Interestingly, the yield stress of high-solids loadings (20-25 %TS) decreases by increasing the pretreatment temperature due to further substrate depolymerisation [185]. Among these works, Knutsen and Liberatore [182] presented yield-stress values of 3 (5% TS) to 1000 Pa (20 %TS) of pretreated corn slurries, determined in the vane-in-cup using the "transient-flow" method. In this, slow (1 rpm) rotational speed are set during a

certain period of time whilst torque monitoring, recorded torque is then extrapolated into yield stress [204].

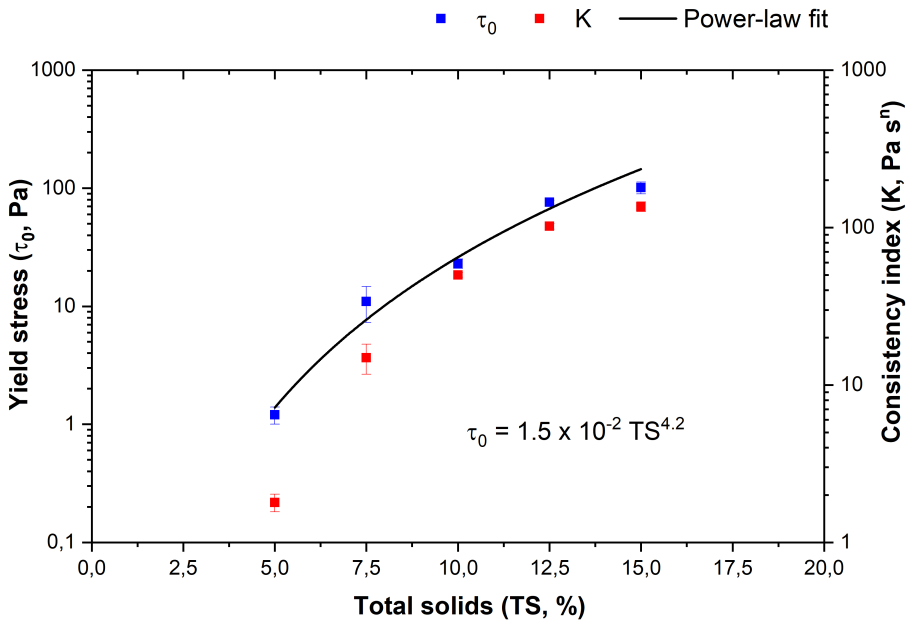

Figure 4.4. Correlation of Herschel-Bulkley parameters as function of solid loadings in milled MSW-pulp slurries (Lawrenceville)

τ_0 values were calculated from data-extrapolation to $\gamma_{eff} = 0$ on fitting the Herschel-Bulkley model for each TS flow sweep. A general power-law model was fitted to τ_0 as function of TS. Error bars represent standard deviations within measurements

The flow consistency index (K) is a useful indicator of viscosity, which also depends on biomass slurry concentrations [204]. In both cases, τ_0 and K became independent at solids loadings higher than 15 %TS, due to the lack of free water and strong contact between fibres [187]. At these regimes, the so-called "high-solids effect" provokes a decrease in agitation efficiency and consequently enzyme adsorption to substrate [92]. Compared to other materials though, MSW-derived slurries presented elevated yield stresses and viscosities even considering the severe pre-processing. The choice of pretreatment has a significant impact in rheology, showing great differences with raw materials. Although not being reported here (Fig. SI A.3), n parameters were also determined, with non-Newtonian model fitting of $r^2 > 0.99$. As shear-thinning indicator, n values were > 1 in all cases, in particular ranging from 0.08 to 0.12: 0.20 ± 0.03, 0.12 ± 0.04, 0.1 ± 0.01, 0.08 ± 0.02 and 0.1 ± 0.01 for 5, 7.5, 10, 12.5 and 15% TS, respectively. In accordance to Wiman et al. [205], n indexes are not proportional to solids loadings as other factors (e.g. morphology) influence pulp suspension, therefore, affecting the shear-thinning behaviour. Compared with other studies, the behaviour indexes of processed MSW-derived slurries are in agreement for 10%TS solids loadings, e.g. n = 0.1 for corn stover suspensions [184].

A power-law correlation between yield stress and solid concentrations can be

formulated as the following expression: τ_0 = a C_m^b, where C_m is concentration of insoluble solids, *a* and *b* empirical parameters [185]. Other curve equations have been proposed including fibre-related and rheological factors by researchers of the Pulp and Paper industry, [186]. In order to facilitate the comparison with biorefinery publications, the above expression would be used, determined as 1.5×10^{-2} $TS^{4.2}$ (r^2 of 0.995) by power-law fitting. Both a and b parameters lie within the range for lignocellulosic suspensions, 1×10^{-4} and 2.45-6.55, respectively. Among literature values, Lavenson et al. 2011 [201] reported similar results (a = 1.9×10^{-3} and b= 4) on a 7-15 % TS range of pretreated corn stover suspensions to the MSW-pulp slurries (a = 1.5×10^{-2} and b = 4.2). Despite using different feedstocks and pretreatments and alternative yield-stress methods (MRI); either fibre length (>2000 μm) and moisture content ($\sim$ 55 %) present similar values. It is suggested that fiber length has a greater effect on the value of a, while several factors would affect the b coefficient. For instance, solids loadings could be contributing to this, as higher values are found (b = 5-6) in studies that ranged from 5-30 %TS [182, 183] in PCS. In non-biomass suspensions as TiO_2 [204], it is shown that lower a values are due lower fiber lengths (2×10^{-4}), whilst, higher b values due higher solids concentration ranges (50-70 %). In addition, these correlations are useful to predict yield stresses out of the studied range, which supports the choice of suitable bioengineering components (e.g. pump) [183].

From the determination of K and n indexes, apparent viscosities (μ_{app}) were calculated per rotational speed (100-600 rpm). The impeller constant (k) of such geometry is 10, and its selection is due to conventional use in enzymatic hydrolysis of MSW-derived pulps. For other impellers (e.g. helical ribbon), higher apparent viscosity of slurries would result as higher impeller constant (k = 29.4) are set. μ_{app} were plotted as function of TS per rotational speed, fitted with power-law curves (Fig. 4.5). Curve-fitting ($y = ax^b$) is highly significant ($r^2 > 0.95$) for each set, therefore, it could be used for data-extrapolation. As the yield stress, μ_{app} increases as increasing solid concentrations, interestingly though, the rotational speed dictates the shape of the curve (exponential or linear). From 100 to 200 rpm, the relationship between μ_{app} and TS is clearly exponential with maximum values of 10 and 5.8 Pa s, respectively, at 15 %TS. The stirring speed vastly affects μ_{app}, in particular in solid concentration below 8 %TS as mass-transfer limitations are not occurring. In the literature, most of the viscosity comparisons in regards of solids loadings are conducted by measurement of steady-state (shear) viscosity at fixed rotation speed. In these measurements, the rheometer assumes a Newtonian behaviour of lignocellulosic fluids, hindering rheological comparison with our study. For instance, Viamajala et al. [187] conducted an extensive set of experiments, 12-34 %TS, using six types of pretreated corn stover: 20 (0.841 mm) and 80 (0.175 mm) mesh-size at room, 170 and 190 °C. At 4.78 s^{-1} ($\sim$ 300 rpm) shear rate, a 12 %TS yields 40 Pa s, 10-fold increase compared to a MSW-derived slurries at 15 % TS. The effect of rotational speed on μ_{app} was studied at initial hydrolysis conditions for pitched-blade and anchor geometries (laboratory and demonstration scale) by varying impeller speed (30-120 rpm) by Palmqvist and

co-workers [196]. It is noted in each reactor scale, the relationship between N and μ_{app} for pitched-blade impeller is different : μ_{app} increases as increasing N and oppositely. At laboratory-scale, elevated stirring speed correspond to lower viscosity for the anchor-type geometry. In another context, Du et al. [116] reported a negative effect in cellulose conversion on increasing impeller speed and solid concentrations, during the enzymatic saccharification of delignified corncob residues. High-solids loadings (20% TS) showed a difference of more than 30 % conversion rates when Erlenmeyer flasks shaked at 150 (55 %) than 10 rpm (10 %). A two-fold decrease (75 rpm) also results in lower cellulose conversions, approx. 30 %. It is well-known that conversion rates decrease by increasing solid concentrations [206], but not due low mixing speed.

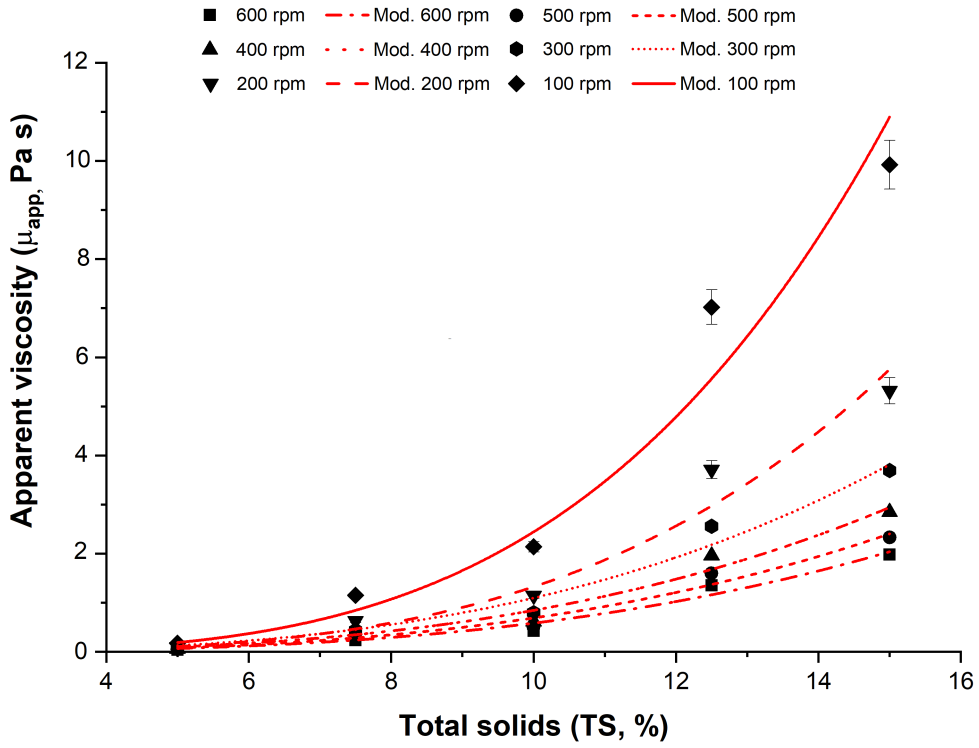

Figure 4.5. Correlation of μ_{app} and TS values upon rotational speed (100-600 rpm) in STRs, equipped with a pitched-blade impeller

μ_{app} was calculated using the Metzer-Otto concept [49], using a k = 10 (hydrofoil) [207]
Power-law fittings curves: y (100 rpm) = 0.48 $x^{3.08}$ (r^2 = 0.976), y (200 rpm) = 0.57 $x^{3.07}$ (r^2 = 0.975), y (300 rpm)= 0.71 $x^{3.07}$ (r^2 = 0.974), y (400 rpm)= 0.93 $x^{3.06}$ (r^2 = 0.972), y (500 rpm) = 0.31 $x^{3.26}$ (r^2 = 0.958) and y (600 rpm) = 0.50 $x^{3.68}$ (r^2 = 0.955)

4.4.1.2 Physical comparison of MSW pulps: Lawrenceville vs Hampden

MSW pulp produced in Lawrenceville and Hampden (Fiberight's demonstration and commercial plants, respectively) were compared in physico-chemical terms (Table 4.3). The processing of feedstocks was conducted following the same methodology, based on the step-wise (front-end separation, pulping and washing) procedure by Fiberight technology. However, MSW is highly heterogeneous and complex due to seasonality, geographical, people's culture and waste management policies [78]. Previous characterisation of both pulps, lignocellulosic and moisture/dry content, showed several differences between Lawrenceville (LV) and Hampden (HD) pulp, predominantly in hemicellulose, lignin and ash fraction. Although glucan (cellulose) content remains unchanged, other components present significant modifications, e.g 12 to 7% hemicellulose for LV and HP pulps, respectively. Additional compositional parameters such as dry matter (analogue of moisture) content showed a 30% decrease between LP (52 %) and HD (38%) pulps. We are unsure which is the rheological contribution of each lignocellulosic component [205], since this also changes upon particle-size, crystallinity etc.. [208]. From the rheological analysis, it was found that pre-conditioning shear rates were too extreme (170 s^{-1}), therefore both MSW pulps exhibit identical viscosities, 0.41 (Lawrenceville) and 0.43 (Hampden) Pa s. Despite this, the steady-state viscosity of 4 % MSW pulps is 4-fold higher ($\sim$ 0.4 to 0.1 Pa) than a 10 %TS pretreated corn stover slurry (PCS), pre-sheared under the same conditions and rheometer geometry [42]. Whilst the power-law parameters (K and n) were within the range. Compared with a 10 % PCS, the consistency indexes for both pulps are much higher (min. 31 Pa s^n) to 18.18 Pa s^n, as are the n values (0.121 to -0.12) [42]. High power-law values with low-solids loading implies that the rheology of MSW slurries is vastly different than PCS, suggesting that the general assumption of "high-solids paradigm" at TS > 15 %TS would be different for MSW-derived feedstocks [2]. Appendix A includes individual flow sweeps of each type of MSW pulp (Fig. SI A.1).

Table 4.3. Physico-chemical parameter (x $\pm$ σ) comparison between Lawrenceville (2017) and Hampden (2019) pulps

	Fiberight's pulps	
Parameter	**Lawrenceville**	**Hampden**
Rheological[1]		
Steady-state viscosity (μ, Pa s)	0.41 $\pm$ 0.13	0.43 $\pm$ 0.08
Yield stress (τ_0, Pa)	7.62 $\pm$ 0.65	9.32 $\pm$ 0.85
Consistency index (K, Pa s^n)	31.0 $\pm$ 3.91	47.2 $\pm$ 11.1
Behaviour index (dimensionless)	0.121 $\pm$ 0.004	0.140 $\pm$ 0.012
Physical[2]		
Crystallinity index (CrI, %)	55.5 $\pm$ 1.58	53.9 $\pm$ 2.50

[1] 4 %TS raw slurries
[2] Oven-dried and cryomilled pulps

MSW-derived pulps have some crystallinity structure (CrI > 50%), probably due to the cardboard and textiles fractions. This index is only an indicator of crystallinity in a substrate, and does not provide information about other factors such as: rigidity, particle-size, morphology or density [209]. Appendix A includes XRD scan of each type of MSW pulp A.2. Compared to a standard compound (e.g. Avicel PH101), the CrI values are significantly lower (average of 54%) than the microcrystalline cellulose equivalent (70-90 %) as measured by the XRD height technique [209]. Despite presenting a lower CrI, MSW-derived pulps are more difficult to degrade by enzymes than Avicel PH101 (95% cellulose) due to high-lignin content and larger particle-size. In comparison to native lignocellulose substrates, e.g. poplar-based woods, the MSW exhibited a similar level of crystallinity ($\sim$ 55%) [210]. Other poplar species, pretreated in by dilute-acid, resulted in a CrI of around 70 % [211]. High CrI (>60 %) were observed in newspaper and cardboard feedstocks, pretreated by a range of methods including milling to dilute-acid [89]. It was noted that chemical-based pretreatments, such as acid or alkali, have a negative effect in the crystallinity index. Supposedly, the hydrolysis of hemicellulose and delignification by severe pretreatments translated as an increase in crystallinity indexes as crystalline cellulose remains as main component of substrate. Chang et al. [210] correlated the digestibility efficiencies during enzymatic hydrolysis of woody biomasses as function of CrI, showing the strong effect in conjunction with lignin content in the recalcitrant structure. Herein, the determination of CrI has been used as qualitative tool for understanding the recalcitrance of MSW-derived pulps and compared with existing feedstocks. To complement, SEM of raw and hydrolysed MSW-pulp slurries can be found in Fig. 4.6.

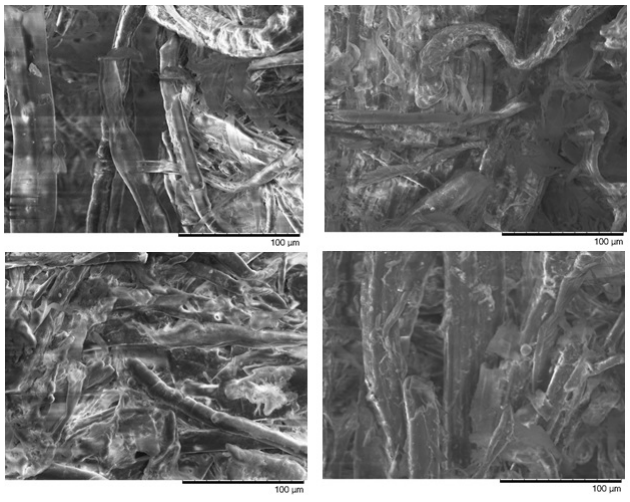

Figure 4.6. Scanning electron microscopy (SEM) imaging of raw and hydrolysed pulps : air-dried (top-left), TO (top-right), T4 (bottom-left) and T48 (bottom-right)

4.4.2 Correlation of off-line glucose and viscosity analysis upon reactor design

4.4.2.1 Parallel bottle reactors

Rolling bottles, e.g. falcon tubes, are alternative reactor configuration to shake flasks or stirred tanks for carrying out enzymatic hydrolysis assays at laboratory scale These laboratory-based experiments are gaining interest across the enzymatic saccharification field as a novel reactor configuration to operate at high-solids loadings [2, 181, 212]. Compared to shake flasks, rolling bottles provide higher conversion yields [115] and easy scalability for commercial applications . In addition, further energy minimisation is achieved as lower rotational speeds are set, max. 80 rpm, to shake flask (200-250 rpm). However, comparing the benefits of horizontal to vertically-orientated reactors, there is not as much information about the rheological profile of hydrolysates processed under these configurations, e.g rolling bottles [146, 213], SSBR [40, 42, 48] and high-solids bioreactor (HSBR) [146].

With this in mind, we undertook an experiment in which the enzymatic saccharification of MSW pulp was performed using rolling bottles with rheological analysis. To ensure the independence of samples, the reactions were each run separately for different times and to determine the power-law properties (K and n), as seen in Fig. 4.7, summarised in Table A.1 as well. Appendix A includes pre-conditioning and flow sweep of each individual sample (Figs. SI A.7, A.8 and A.9. It was noted that both the K and n values showed high standard deviations between triplicate measurements during the first eight hours of hydrolysis. The high variation in measurements could be associated to sensitivity issues around the instrument and/or high substrate heterogeneity. Despite this, almost an 8-fold decrease in K values were observed between 4 to 8 hours of hydrolysis, due to slurry liquefaction (approx. 400 to 50 Pa s^n, respectively), followed by stable K-values. A steeper K-value reduction was observed in the PBR_1 run than the PBR_2 run, which indicates a quicker liquefaction occurred. While, the n indexes evolved inversely to the K-values with distinct behaviour at 8-24 hours of hydrolysis. MSW-derived slurries are well characterised as shear-thinning as exhibiting n indexes below 1, during the course of enzymatic hydrolysis. In theory, an exponential growth in n indexes should be expected, reaching Newtonian fluid conditions after liquefaction [213]. The conversion from non-Newtonian to Newtonian fluid behaviour may occurs under certain circumstances such as complete digestion or operating at low-solids loadings.

Previous investigations have examined the rheological profile of lignocellulosic slurries processed under horizontally-orientated configurations [40, 213]. Using an enzyme dosage of 2.5% w/w (approx. 6 FPU/g cellulose, measured by the filter paper assay on Cellic® CTec3 [154]), similar K-values (50 Pa s^n at 24 hours) were reported in the enzymatic hydrolysis of MSW-derived pulp in rolling bottles, to pretreated corn stovers (PCS) hydrolysates in the SSBR configuration. However, Dasari et al. 2009 [42] displayed K-values of around 50 Pa s^n after 48-hours of 10 %TS

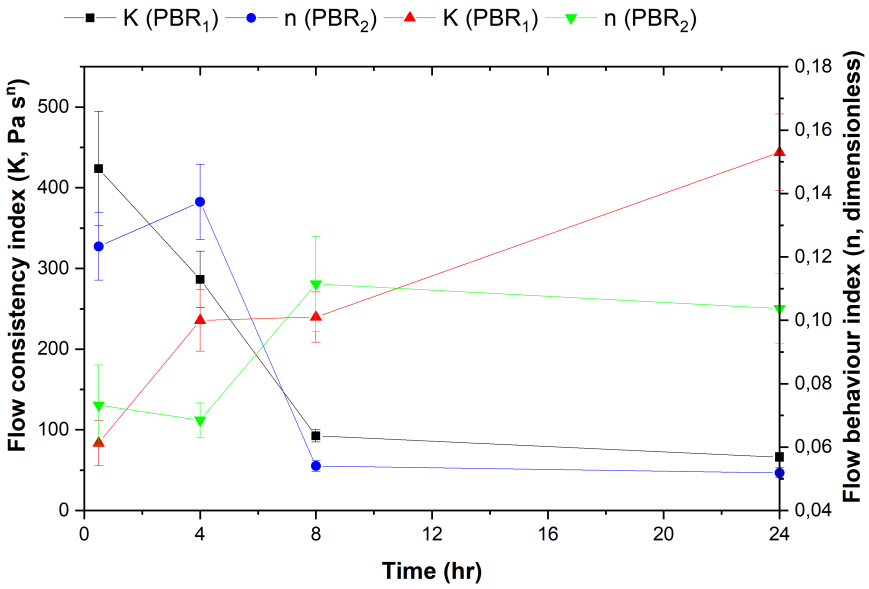

Figure 4.7. Power-law properties (K and n) during PBR hydrolysis experiments

Reaction conditions: 5 %TS, 2.5 % E:S, 0.1 % Fermasure ® XL, pH 5 and 30 rpm.
Error bars represent standard deviation of duplicate two-step method for the rheological analysis

PCS hydrolysis, rotating at 2 rpm with a 15 FPU/g cellulose in the SSBR configuration. With a similar configuration (horizontal rotating reactor, HRR), Du et al. 2017 [213] showed same K-values on 87-hour hydrolysate of 25% PCS, rolling at 100 rpm with 7 FPU/g DM than 0.5-hour hydrolysates of this study. Assuming an enzymatic loading of 3.2 FPU/g DM for MSW-derived hydrolysis, it is demonstrated that 25% PCS enzymatic hydrolysis using CTec2 (90 FPU/ml) needs to double the amount of enzymes and increase by almost 4-fold the hydrolysis time to achieve same the K-values as the initial 5%TS MSW-derived slurries. These comparisons demonstrate that MSW-derived feedstocks (at 5$ TS) exhibit higher consistency indexes than agricultural-based feedstocks (e.g.corn stover), despite of operating at higher solids loadings (10-25 %TS).

To complement the study, apparent viscosities were calculated in conjunction of glucose yields during the course of PBR enzymatic hydrolysis as shown in Fig.4.8. Both parameters followed asymmetric parabolic curves. One hypothesis is that the rapid release of glucose monomers and reduction of slurry viscosity, is associated with the depolymerisation of amorphous cellulose [40]. The remaining crystalline fraction of cellulose is harder to hydrolyse, yielding fewer monomeric sugars after one-day of reaction. In this study, after half an hour of hydrolysis, both MSW slurries presented apparent viscosities of between 5-11 Pa s which decrease rapidly until eight hours of hydrolysis $\sim$ 2.5 and 1 Pa s for PBR_1 and PBR_2, respectively. Following this period, a "plateau effect" was observed with apparent viscosities ranging from 2.5-1 Pa s, which could be associated with the loss of cellulases activity or complete digestion of the MSW-derived slurries. This phenomenon also occurred with

glucose yields, indicating potential end-product inhibition of β-glucosidases by glucose [214]. There are some differences in performance between PBR runs, as glucose yields and kinetics diverged in overall values and trends, respectively. A possible explanation of such high variability could be associated with feedstock heterogeneity.

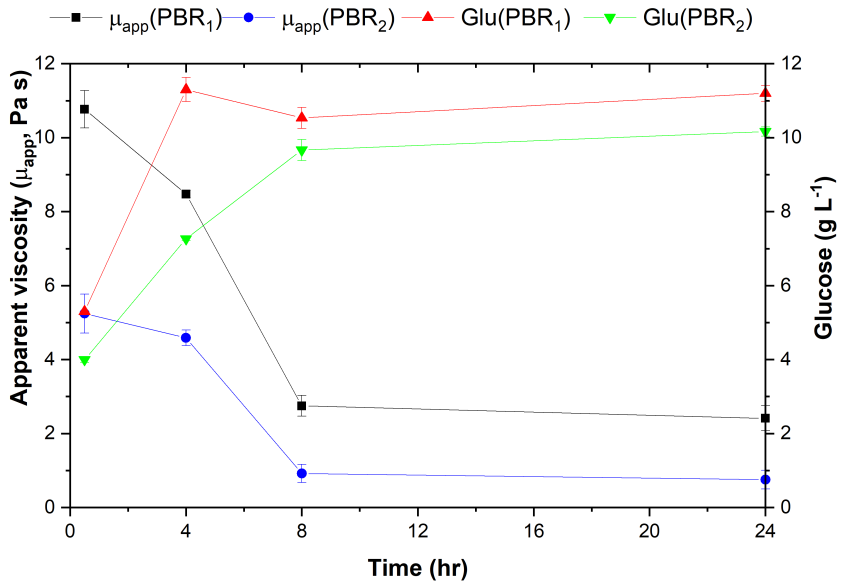

Figure 4.8. Correlation of glucose yields and and viscosity analysis in PBRs, at different solid loadings

Reaction conditions: 5 %TS, 2.5 % E:S, 0.1 % Fermasure ® XL, pH 5 and 30 rpm. Error bars represent standard deviation of rheological measurements and glucose yields duplicates

μ_{app} is a challenging factor to compare, between this study and others since different methods of viscosity determination were applied. Du et al. 2017 [213] recorded apparent viscosities at a fixed a shear rate of 4.8 s^{-1}, without using the corresponding Metzner-Otto concept [49]. Surprisingly, the apparent viscosities were below 3 Pa s at 25% solids, considering that viscosity measurements were not conducted before 15 hours of enzymatic hydrolysis. Although peculiar, a substantial viscosity drop was previously seen between 15 and 38 hours (2500 to 600 and 1500 to 400 mPa s for 7 and 10 FPU/g DM, respectively). The viscosity values started stabilising after 75-hours of enzymatic hydrolysis, showing that high-solids loading require prolonged residence times. Despite this, rolling bottles look like a good alternative to stirred tanks operating at milder conditions ($\sim$ 30 rpm), whilst yielding more monomeric sugars in the absence of internal mixing elements [212].

4.4.2.2 Stirred tank reactors

In 1.5L STRs, the enzymatic hydrolysis MSW-derived pulp was carried out (5-7%TS) with periodic sampling for rheological analysis, throughout the course of hydrolysis. Prior analysis, samples were pre-conditioned for achieving steady-state viscosity

measurements, as seen in Fig. A.4. By fitting of non-Newtonian models in individual hydrolysates, it is demonstrated that MSW slurries are shear-thinning with yield stress behaviour as n indexes are < 1 and $\tau_0 > 0$, respectively, (Fig. A.5 and Fig.A.6). During the course of hydrolysis, higher K and n values are found as increasing solids loadings (Fig. 4.9). These tendencies were also observed in a study by Du et al. [213], in the study of power-law properties of pretreated corn stover hydrolysates (PCS) in two reactors (helical ribbon and rolling bottles). For all cases (5-7 % TS), the evolution of n parameters was in accordance to 25 % (w/w) PCS slurries with 7 FPU/g DM ($\sim$ 3-fold that this study) agitating at 100 rpm, equivalent at 15 to 60 hours of hydrolysis. The increase of n values is associated to an increasing shear-thinning behaviour due to the improvements in biomass liquefaction, once the "viscosity-break" period (4-8 hours) is over. In the lower solids content (5 %TS), flow consistency indexes were in the range of Du et al. [213] work seen in the whole experiment - 35 to 2.5 Pa s^n. However, at 6 and 7 % solids content, K parameters were out of the (100 to 50 Pa s^n) during the first-four hours of the reaction. In the range of 0.1-0.2, n indexes were also reported by Palmqvist et al. [196], consisting of rheological analysis of forestry-based hydrolysates at low (30), middle (60) and high (120) agitation levels in a demonstration-scale reactor. Other authors, Hou et al [215], determined n and K indexes in the range of this study (0.2 and 50 Pa sn, respectively), by a plate-plate rheometer geometry with 5 min preshearing at 100 s^{-1}. Within stirred tank processing, MSW-derived pulps present similar power-law parameters than agricultural feedstocks, but in difference solids regimes (5-7 to 25%TS).

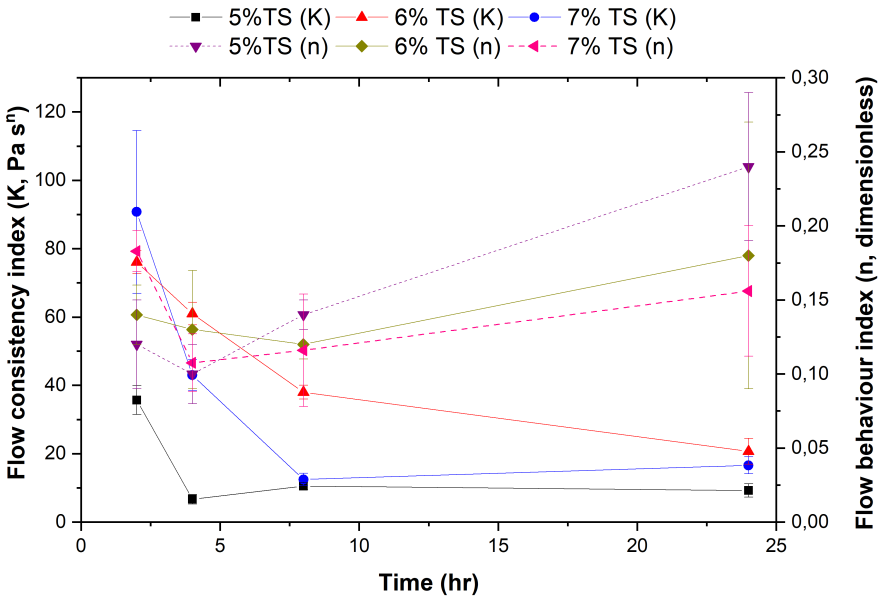

Figure 4.9. Power-law properties (K and n) during STR enzymatic hydrolysis

Reaction conditions: 5-7 %TS, 2 % enzymes loading, 0.1 % tetracycline, 600 rpm and 50 °C. Error bars represent standard deviation of rheological measurement

As seen before (section 4.4.2.1), the evolution between glucose titres and apparent viscosities followed an inverse correlation (Fig. 4.10). For all solid concentrations, the reaction kinetics were similar, a substantial increase in 8 hours and "plateau effect" afterwards, with increasing final glucose titres in accordance to solid loadings: 10 (7%TS), 8.5 (6%TS) and 8 g/L (5%TS). In terms of apparent viscosity, a two-step kinetic behaviour, pronounced at 7 % solids concentrations and slightly less for the other cases (6 and 5 % TS). Even though, each MSW slurry started with very different viscosities, the final values ranged from 0.5 to 0.25 Pa s at 24 hours. It is interesting to observe that apparent viscosities at 24 hours of hydrolysis are independent of solids loadings, indicating that liquefied slurries are similar in rheological terms.

Surprisingly though, similar results were found in the discrete (rheometer) analysis of hydrolysates during the enzymatic saccharification of pretreated corn stover (30 % (w/w), 15 g FPU/g substrate at 150 rpm) employing a helical ribbon impeller bioreactor [215]. Hou et al. [215] compared two methods of apparent viscosity determination, "flow-sweeping" versus an on-site torque method, presenting similar measurements after biomass liquefaction (2 hours). In contrast, several steam-exploded sugarcane hydrolysates processed in a STRs, armed with an elephant-ear type-impeller, presented μapp of 0.1 to 0.02 Pa s, [194]. Moreover, Palmqvist et al. [196] compiled a range of μ_{app} of Norway Spruce hydrolysates as function of impeller geometries, speeds and reactor scales: laboratory (2 kg) and demonstration (4 m^3). Initial average viscosities of 13.5 % solids ranged from 0.16 to 0.53, 0.47 to 0.11 and 0.14 to 0.06 Pa s for the 4 m^3 PBT, 2 kg PBT and 2 kg anchor reactor configuration, respectively. Compared with this study, the initial MSW-related μ_{app} displayed values of 2-10 Pa s, up to 150-fold higher than forestry-based samples. The differences of feedstock and pretreatment conditions, carried out in the Biorefinery Demo Plant (Sweden) [196], are reasonable in explaining such low viscosities compared to 6-7 %TS MSW slurries, even doubling in solid loadings ($\sim$ 13.5). Bearing in mind that MSW-derived pulps are based at 5-7%TS, higher rheological parameters were found than for high-solids studies (13.5-20%). Several physico-chemical factors explain the differences between viscosity readings, e.g particle size, morphology and severity of pretreatment [149]. In comparison with agricultural and forestry feedstocks, neither grinding nor sieving procedures have been conducted in MSW-derived pulps, enabling the presence heterogeneous 10-40 mm particle. And, milder pretreatments (<100 °C and ambient pressure) were performed, in contrast of steam-explosion with SO_2 addition [196].

4.4.2.3 PBR vs STR

The evolution of apparent viscosity and glucose yields during enzymatic hydrolysis of MSW-derived slurries in rolling bottles and stirred tank reactors are displayed in Fig. 4.11. An 80-85 % reduction in viscosity was observed during the first eight hours of enzymatic hydrolysis in both bioreactor configurations. At 4 hours of PBR enzymatic saccharification, the viscosity of the media increased, compared to former

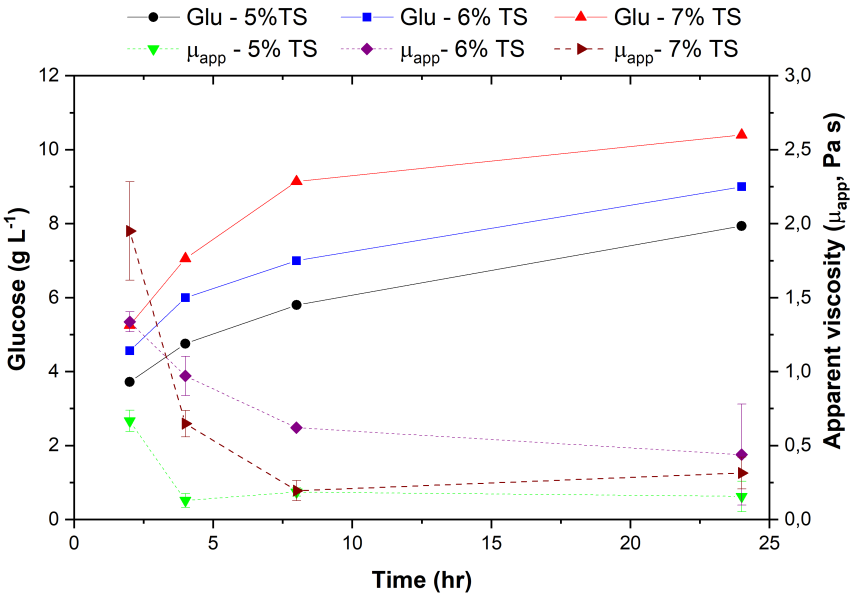

Figure 4.10. Apparent viscosities and glucose yields of enzymatic hydrolysis of MSW-derived pulp in a 1.5L STR

Reaction conditions: 5-7 %TS, 2 % E:S, pH 5, 0.1 % tetracycline (w/w dry pulp), 600 rpm and 50 °C. Error bars represent standard deviation of rheological measurements

analysis. This incongruity might be with uncontrolled operation or heterogeneity of biomass substrate, leading to inefficient liquefaction of media.

Figure 4.11 also shows that the glucose concentration is almost identical despite of the choice of reactor: PBR (10.4 g L^{-1}) and STR (10.2 g L^{-1}), respectively. Although, higher viscosities were observed in the horizontally-orientated geometry, both runs followed the same kinetics. A more gentle mixing approach using rolling bottles, due to absence of internal elements and slower agitation, could lead to higher glucose titers with less shearing on the enzymes in particular β-glucosidases [216]. Interestingly though, it has been reported that rolling bottles performed better than vertical bioreactors at high-solids loadings [146, 213]. But the selection of reactor geometry is independent of bioprocessing performance at low-solids loadings [92].

The determination of power-law (K and n) indexes during the enzymatic hydrolysis in rolling bottles and stirred tank bioreactions is included in Fig. 4.12 as well. Since the calculation of apparent viscosities for each configuration is based on different formulae/theory, direct comparison cannot be pursued [207]. Instead power-law parameters are compared, determined using the same methodology. Despite this, large differences between K and n indexes are observed before eight hours hydrolysis. For instance, at 2 hours, the K-values for STRs are around 100 Pa s^n whilst over 350 Pa s^n for PBRs. After 8 hours biomass liquefaction, the slurry viscosity was considerably diminished as both runs reported similar power-law indices: K of 25-50 Pa s^n and n of 0.01-0.015 (dimensionless). Opposite trends were observed by Du

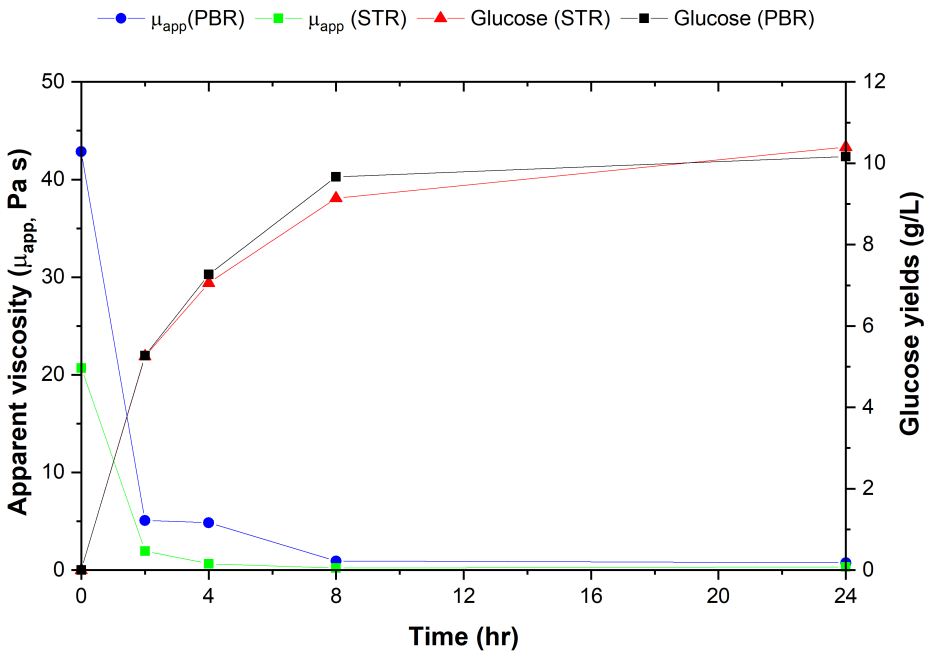

Figure 4.11. Reactor comparison (PBRs vs STRs) of μ_{app} and glucose yields evolution during enzymatic hydrolysis of MSW-pulp

Reaction conditions: 5%TS, 2% E:S. 0.1 %BIT, pH 4.75-5.25 and 50-55 °C. Agitation was set at 30 and 600 rpm for rolling bottle and stirred tank reactions, respectively. Error bars represent standard deviations of duplicate measurement on rheological analysis

et al.[213] in their horizontal bioreactor which exhibited lower K and n indexes than stirred tanks throughout the enzymatic saccharification of pretreated corn stover. Operating at $\sim$ 25% w/w solids loadings, the power-law parameters did not converge until 60 hours of reaction, associated with prolonged biomass liquefaction. At the end of enzymatic hydrolysis (90 hours), the K and n indexes were in the range of 1000 Pa s^n and 0.25, respectively.

4.4.3 *In situ* rheometry

In situ rheometry concerns the study of real-time viscosity evolution during the enzymatic hydrolysis. These studies include effect of solids loadings, particle-sizing, enzyme dosages as well as addition of polymer additives to decrease intrinsic viscosity.

4.4.3.1 Effect of solid and enzyme loadings

Little information is available on real-time evolution of viscosity during the course of enzymatic hydrolysis of biomass [40, 197]. Visually, it was noted that a native substrate looking like wet cardboard was transformed into a muddy-like slurry by the action of enzymes. Understanding the rheological properties and associated kinetics

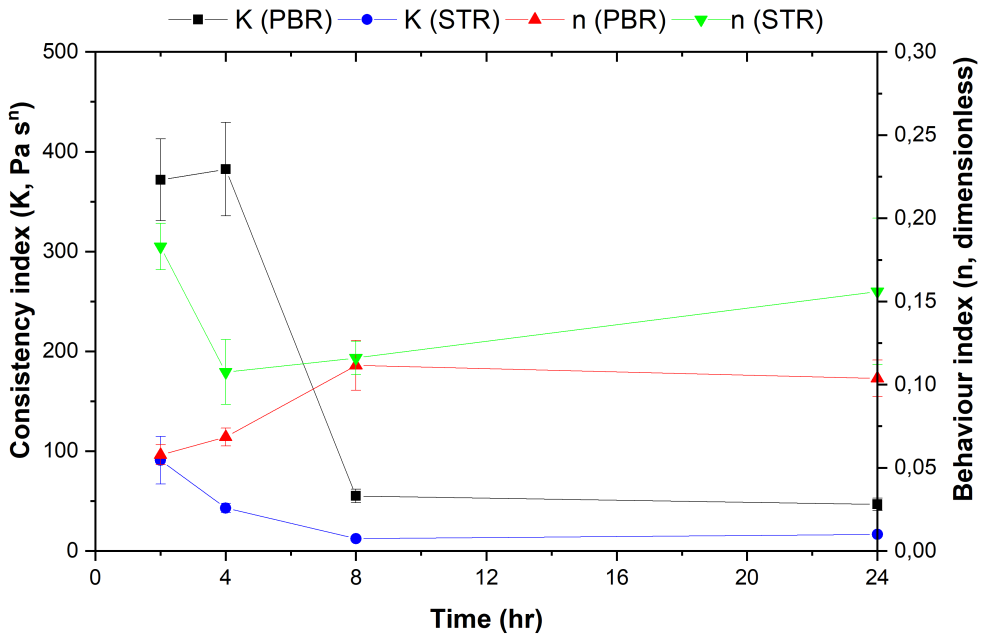

Figure 4.12. Reactor comparison (PBRs vs STRs) of K and n indexes evolution during enzymatic hydrolysis of MSW-pulp

Reaction conditions: 5%TS, 2% E:S. 0.1 %BIT, pH 4.75-5.25 and 50-55 °C. Agitation was set at 30 and 600 rpm for rolling bottle and stirred tank reactions, respectively. Error bars represent standard deviations of duplicate measurement on rheological analysis

is important for addressing the design of bioreactors and operations [149]. To investigate the liquefaction rates at low-solids loadings, *in situ* rheometry was performed during 8 hours of hydrolysis. The Lawrenceville MSW slurries (5 and 6 % TS) were hydrolysed with 5 % enzyme doses at 10 s^{-1}, continuously recording the viscosity measurements (Fig. 4.13). The 1 % increase, from 5 to 6 % solid concentrations, provoke a gentler viscosity reduction (∼0-2 hours) followed by a viscosity "stabilisation at 2-8 hours. In both cases, 5% w/w (approx. 8.33 mg_{prot}/ g_{gluc}) enzyme additions decrease in half the initial slurry viscosity in less than 1 hour: 140 to 70 Pa s and 120 to 60 Pa s for 5 and 6 %TS, respectively. Remarkably, the two-stage kinetics associated with enzymatic hydrolysis of biomass is more pronounced on *in situ* than *ex situ* analysis. In this case, a rapid hydrolysis of amorphous cellulose (1^{st} stage) and slow hydrolysis of crystalline cellulose (2^{nd} stage) [48], is likely to occur during 0-2 and 2-8 hours, respectively.

Compared to other studies, using pre-treated spruce as feedstock and doubling the amount of enzyme [197], *in situ* viscosity measurements also displayed the two-stage kinetics at 10 mg protein/g glucan. This a good example to compare, because they conducted the experiments with the same commercial enzyme cocktail and rheometer configuration. The same trend-line was observed during the hydrolysis of same solids content (2 % solids) at 1 mg protein per g glucan. Surprisingly,

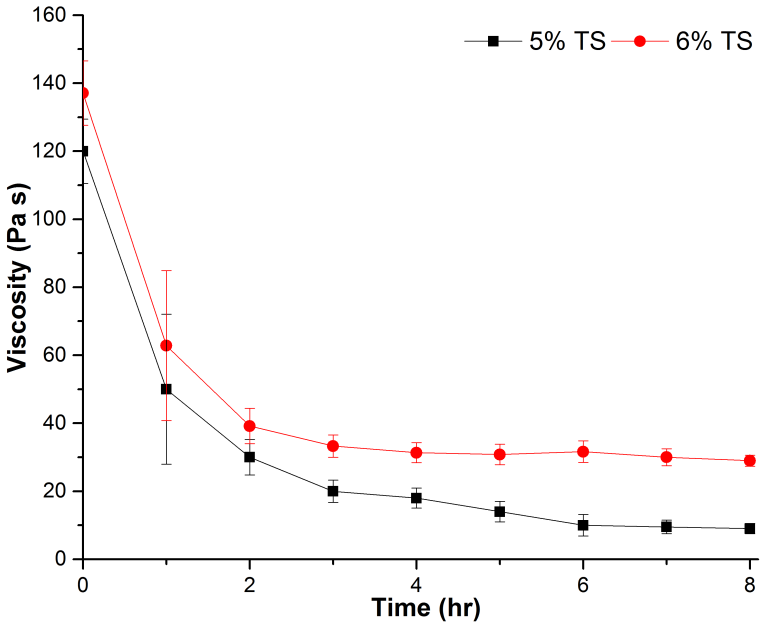

Figure 4.13. *In situ* rheometry of enzymatic hydrolysis of MSW-derived pulp

Reaction conditions: 5-6%TS, 5 % E:S, 0.01 % NaN_3, 900 rpm. MSW pulp was dried (50 ∘C for 2 days), ground by a Nutribullet and 4000 μm < x < 2000 μm sieved. Error bars represent the standard deviation of duplicate runs

close results were observed when substituting CTec3 (a mixture of cellulases, hemicellulases and LPMOs [100]) for purified endogluconases (fungal Cel5A) at 10 mg protein/g glucan. This behaviour was not observed when enzyme concentrations were as low as 0.1 mg protein/g glucan, which could be caused due to the high-initial viscosity of these forestry materials.

To this date, the effect of enzyme loadings on *in situ* viscosity measurements of enzymatic saccharification, has only been explored by Kadic et al. [197]. To evaluate the viscosity evolution as function of enzyme dosage in MSW-derived pulp, duplicate runs of *in situ* rheology experiments were performed with set conditions whilst increasing the amount of enzymes (Fig. 4.14). To decrease the variability of results due high feedstock heterogeneity, MSW-pulps were ground and sieved into particles sizes of 2000 μm < x < 500 μm. In this study, a range of enzyme doses (0.5-2% E:S, equal to 0.8-3.3 $mg_{prot}/\ g_{gluc}$) was investigated in 5% solids loadings for 4 hours at 600 rpm. A control assay was conducted, no enzyme addition, showing an average viscosity of 100 Pa s. Initial viscosity values ranged from 90 to 112 Pa s. As the viscosity readings started after enzyme addition, a difference in initial viscosity is noticed between assays. It can be seen that viscosity evolves as function of enzyme loadings. The "slope" of viscosity over time is multi-factorial, depending on parameters such as solids content, enzyme loadings, feedstocks and rheometer instrumentation etc.. [197]. In a decreasing order: a 1.8, 3.4 and 4.5-fold decrease in viscosity was observed for 0.5, 1 and 2% E:S, respectively, during 4 hours of hydrolysis. Similar trends were also reported by Kadic et al. [197] in the range of 0.1

to 10 mg_{prot}/ g_{gluc}. Although, employing crude endogluconases, a substantial drop in viscosity was observed even at the lowest dosages (0.1 mg_{prot}/ g_{gluc} $\sim$ 0.1 %E:S). Endogluconases binds into the amorphous region of cellulose and hydrolyse into smaller polysaccharide units, but releasing few glucose monomers [197]. As corroborated by Kadic and co-workers , poor glucan conversion (<5%) was exhibited when endogluconases were only added, whilst with CTec3 completed enzymatic digestion at same enzyme dosages (10 mg_{prot}/ g_{gluc} $\sim$ 6% E:S). But, In the absence of cellobiohydrolysases and β-glucosidases, among other enyzmes, *in situ* viscosity measurements using crude endogluconases demonstrated accurate hydrolysis as a multi-enzymatic cocktail [197]. For this, endogluconases are considered as the main responsibles of rapid decrease of viscosity in lignocellulosic biomasses [41].

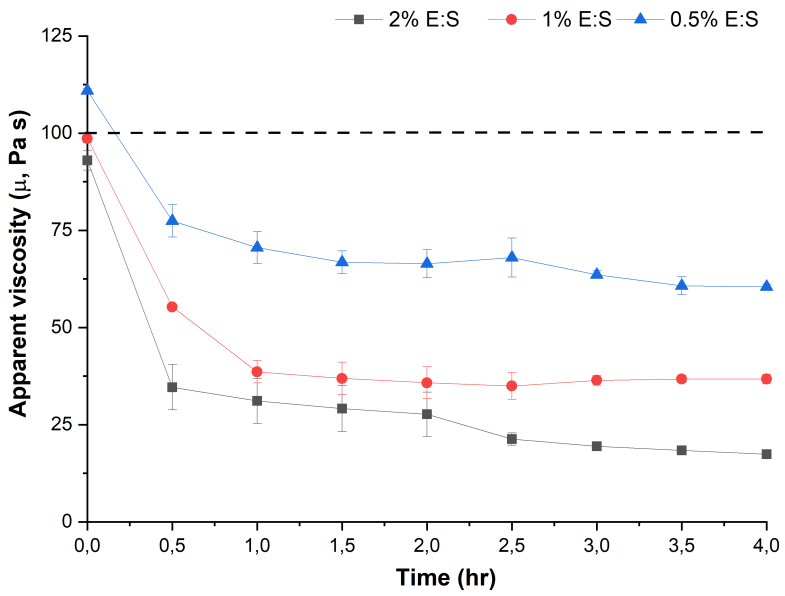

Figure 4.14. *In situ* rheometry of MSW-derived pulp as function of enzyme dosages

Reaction conditions: 5 %TS, 0.01 % NaN_3, 600 rpm MSW pulp ground by a Nutribullet and sieved between 2000 μm < x < 500 μm Error bars represent the standard deviation of duplicate runs

4.4.3.2 Ultra-low enzyme dosages: the effect of particle-size

In situ rheology with ultra-low enzymatic dosages [197] and/or studying the effect of particle-size reduction [40] has not been widely investigated. With this in mind, a combined study involving ultra-low (0.5% w/w) enzyme with unsieved and sieved substrates was proposed for *in situ* study (Fig. 4.15). Interestingly, no major differences were observed if the waste pulp was previously screened through a 500 to 2000 μm mesh size. The averaged viscosity values, per given times, are within the same ranges during the first 3 hours. Remarkably, the sieving of dry pulp does not benefit the viscosity break, even though the accumulation of particles > 2000 μ is avoided.

At these conditions (0.5 % E:S and 10 s^{-1}), the enzymatic saccharification is unimproved by particle-size screening, on the contrary, no clear benefits were observed. In comparison with other studies done with low enzyme doses, similar trends in viscosity evolution were seen, but at different order of magnitude. Kadic et al. [197] monitored the viscosity during the enzymatic saccharification of pretreated spruce at 0.1 mg protein per g glucan, approx. 0.1 % enzyme (w/w dry substrate). Little decrease in viscosity measurements occurred during the hydrolysis (1 hour), 250 to 200 Pa s, and did not showing the "two-stage kinetics" kinetics. Such low enzyme loadings may be insufficient for promoting the hydrolysis of biomass, even though great savings in enzymes costs are achieved.

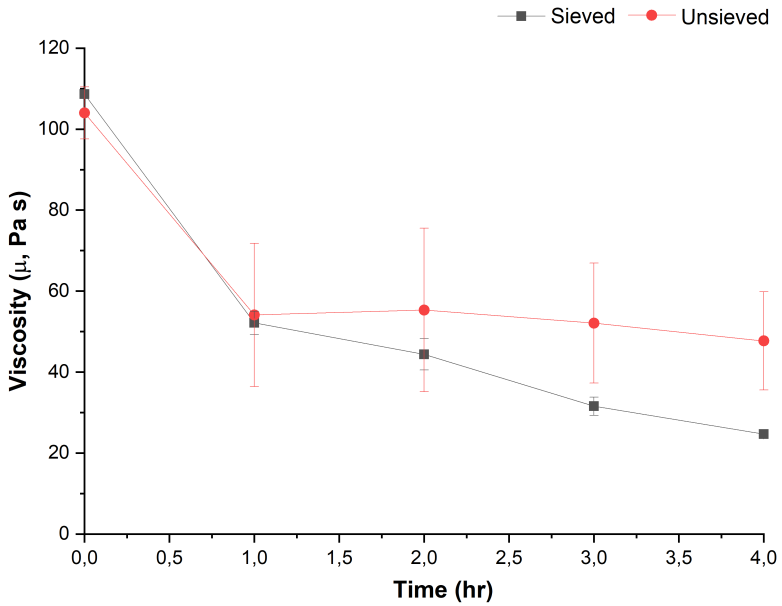

Figure 4.15. In situ rheology of unsieved and sieved MSW slurries with 0.5 % E:S

Reaction conditions: 5 % TS, 0.5 % E:S, pH 4.75-5.25 (adjusted with 6 % H_3PO_4), 50 °C and 10 s^{-1} (600 rpm)

As expected, sieved runs (1000 μm < x < 2000 μm) presented a quicker and more severe reduction in viscosity than unsieved ones. Moreover, less variability in measurements was observed, probably due to higher homogeneity of particle-sizes than raw MSW-pulp. Initial viscosities were around the same range (100 Pa s), equally halved to 50 Pa s but evolved differently until the end of reaction (4 hours): 20 and 50 Pa s for sieved and unsieved runs, respectively. A clear benefit of sieving MSW-derive pulp prior enzymatic hydrolysis is observed, achieving a 5.5 to 2-fold viscosity decrease compared with native biomass. The effect of particle-size reduction in enzymatic hydrolysis of biomasses has been previously investigated, but not with *in situ* rheometry [40]. Dasari et al. [40] compared different particle size ranges (in μm, 150 < x < 180, 104 < x 150 , 75 < x 104 and 33 < x < 75), showing that viscosity decreases as decreases particle-size of slurries. In addition, enzymatic hydrolysis with

smaller particles (33 < x < 75 μm), presented higher glucose yields than the rest of assays.

These sets of studies have demonstrated that ultra-low enzyme additions (e.g. 0.5 %) in enzymatic hydrolysis are dependent on substrate particle-size, but, are insufficient for biomass liquefaction due to the highly-recalcitrant lignocellulosic structure [217], likely to release low glucose concentrations. An additional milling step requires further energy input and risks process cost-effectiveness [17]. Alternatively, the addition of non-catalytic additives such as PEG or Tween [17] to promote viscosity reduction need to be optimised, to balance the processing costs [218]. To operate at ultra-low enzyme doses, it is necessary to improve enzymes formulation for enhancing the reactivity towards recalcitrance cellulose [219]. However, it remains essential to release sufficient glucose and reduce the slurry viscosity for satisfying both commercial and engineering needs.

4.4.3.3 Decreasing stirring speed

To minimise power requirements, decreasing the impeller speed is one option (P= 2 πMN). To date, no studies on *in situ* viscosity measurements have explored the relation between impeller speed and viscosity during enzymatic hydrolysis. An *in situ* run was conducted at 100 rpm whilst maintaining same conditions (5 %TS and 2 % E:S) as previous runs (Fig. 4.14. The viscosity is recorded, averaging measurements hour per hour, and are plotted in Fig. 4.16 during 8 hours of MSW enzymatic saccharification. A decrease in rotational speed leads to 4-fold reduction in viscosity (approx. 600 to 200 Pa s) over 8 hours of hydrolysis. Compared to the 600-rpm run (Fig.4.14), slurry viscosity curve flattens around 200 Pa s, being 10 times higher than when intensive mixing was performed. In addition, the power consumption is halved (2 to 1 W), with a considerable change in the impeller speed. A possible hypothesis is that high torque measurements would be occurring at low tip speed, resulting into high viscosities. The slow impeller velocity does not promote mass-transfer and therefore enzymatic adsorption to the substrate occurs giving in homogeneous liquefaction [73]. These findings were also found in the saccharification of corn stover within a STR, equipped with a Rushton. Even without characterisation by *in situ* rheology, it is evident that poor glucan conversion and mass-transfer occurred is a function of rotational speed [73]. The same authors mentioned that minimum agitation requirements in vertically-orientated reactors should be around 400 rpm, especially once increasing the amount of insoluble solids. Hence, higher rotational speeds are associated with lower slurry viscosities, despite higher power outputs, which was previously evaluated in the rheological characterisation of raw slurries (Fig.4.5).

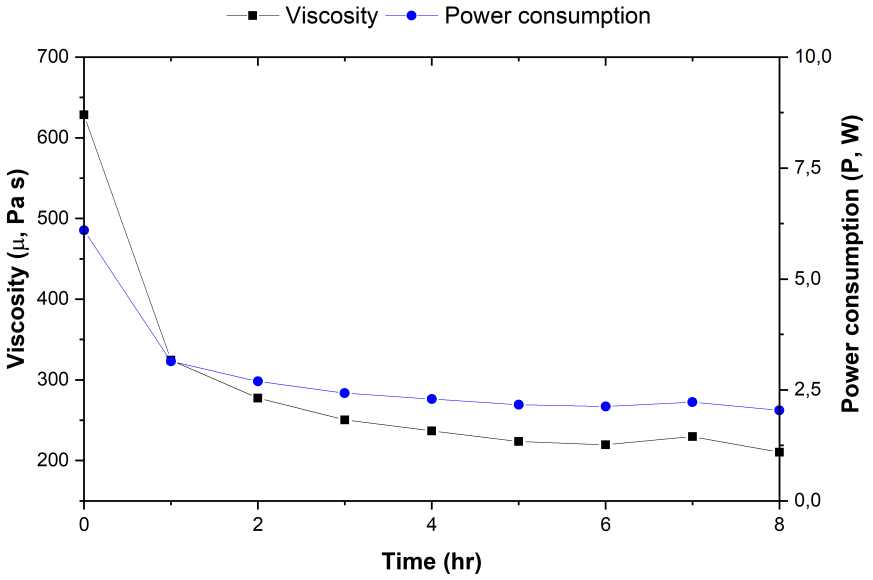

Figure 4.16. *In situ* rheology of 5 %TS unsieved MSW slurries with 2 % E:S at 100 rpm

Reaction conditions: 5 % TS, 2 % E:S, pH 4.75-5.25 (adjusted with 6 % H_3PO_4), 50 °C and 100 rpm

4.4.3.4 Increasing to 10 % solids loadings

Studying the *in situ* rheology of enzymatic hydrolysis of biomass is difficult due to the elevated initial-viscosity of these materials, which cause a risk to the rheometer integrity as well as accurate recording [183]. For this, the gap length (distance between bottom of cup and impeller) rose up to 10000 μm - a 3-fold increase over the instrument specifications (4000 μm). Changing the "tank clearance" prevents case-by-case comparison with previous runs, as it does not reflect the viscosity of the whole slurry, as some particles particles may settle [182]. Despite these issues, the *in situ* viscosity evolution was studied at higher solids loadings (10 %TS), keeping constant the other parameters with previous investigations (enzyme and antimicrobial dosage). But rotational speed was incremented up to 900 rpm to ensure adequate mixing. In Fig. 4.17, a rapid drop in starting viscosity is displayed in less than 15 minutes (0.25 h), <200 to 125 Pa s, following with a more gentle decrease to 75 Pa s at 2 hours of hydrolysis. Power outputs were also plotted in Fig. 4.17, calculated from torque readings as P = 2πMN, for a shear rate of 10 s^{-1}. Differing from viscosity measurements, the power consumption does not suffer such a severe drop in values in two hours, 5 to 2.5 W. However, the power consumption is reduced b half which might indicate some slurry liquefaction.

Few investigations have focused on *in situ* rheometry at solids loadings above 10%TS [41, 197]. Dasari [41] investigated the continuous viscosity readings at 10-13%TS using pretreated sawdust as lignocellulosic material. Severe milling and sieving of particles in the range of 150-180 μm allowed them to carry out the enzymatic hydrolysis, clearly showing the "two-stage" kinetics in a 12-hours period.

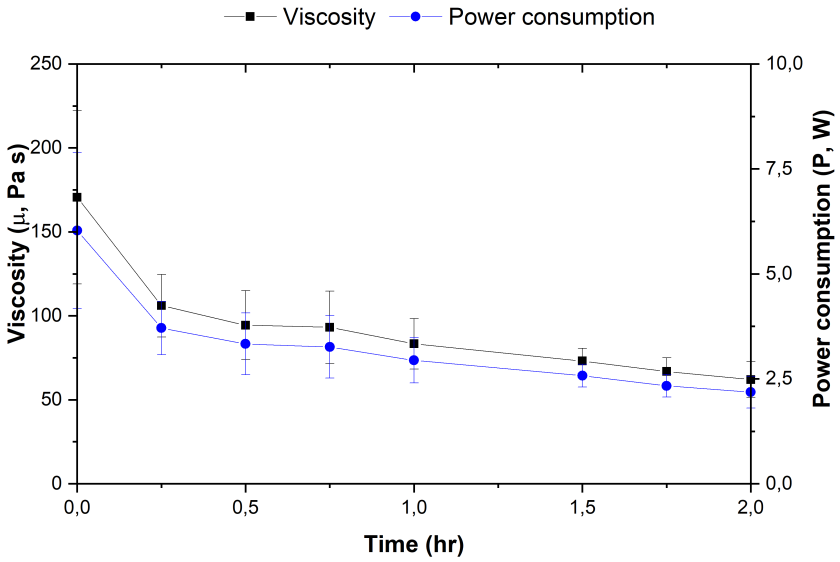

Figure 4.17. *In situ* rheometry of 10 %TS operating at 10000 μm gap

Reaction conditions: 10 %TS, 2 % E:S, 10 s^{-1}, pH 5 (adjusted with 6 % H_3PO_4) and 50 °C

On the other hand, Kadic et al. [197] could not decrease the viscosity of 12% steam pretreated pine slurry by adding enzyme loadings of 10 $mg_{prot}/g_{\ gluc}$ ($\sim$ 6% E:S), neither did they observe the "two-stage kinetics". In contrast to this, after 60 minutes hydrolysis the viscosity measurements was higher than that for the pre-hydrolysis biomass. Both studies demonstrate the technical challenges associated with high-solids enzymatic hydrolysis with *in situ* viscosity measurements due to jamming and wall-slip issues [182], consequently needing severe particle-size reduction.

4.4.3.5 Effect of concentrations of polyethylene glycol (PEG)

Most of the literature focuses the use of PEG for improving conversion rates [220–222], enzymatic mechanisms [223–225] and enzyme recycling [24, 114, 154, 226, 227] within the bioconversion of lignocellulosic biomass into fermentable sugars. Despite the strong evidence of polyethylene glycol (PEG) being a viscosity modifiers[24, 91, 217], few experimental advantages have been reported due to the non-productive bindings of enzymes with lignin [228]. Furthermore, considering the number of investigations that have focused on rheological characterisation of cellulosic standards [229], micro and nanostructures [230–233], there are few that have investigated the binding interactions of polyethylene glycol (PEG), biomass and enzymes.

Herein, we describe our study of the effect of PEG concentrations during the enzymatic hydrolysis of MSW-derived pulp, with *in situ* viscosity measurements (Fig.4.18). Control assays, without PEG addition, were included in each set of experiments. Based on the best results achieved by Puri [36], in regards of use of PEG

additives within enzymatic hydrolysis of MSW-derived pulp, a range of PEG additions were investigated: 0.1-0.05% (Fig. 4.18). 0.05% PEG addition results in lower viscosities than the control, and the 0.1% case after 4 hours of enzymatic saccharfication. Interestingly, a delay in viscosity reduction is observed after the addition of PEG, which depends on the ability of PEG to bind different substrates [225]. No improvement in viscosity reduction was noticed when adding 0.1% PEG. Meanwhile, no difference of 7.5 Pa s in viscosity was observed at 4 hours of hydrolysis, when 0.05% PEG (16 Pa s) was loaded compared to the control assay (23.5 Pa s).

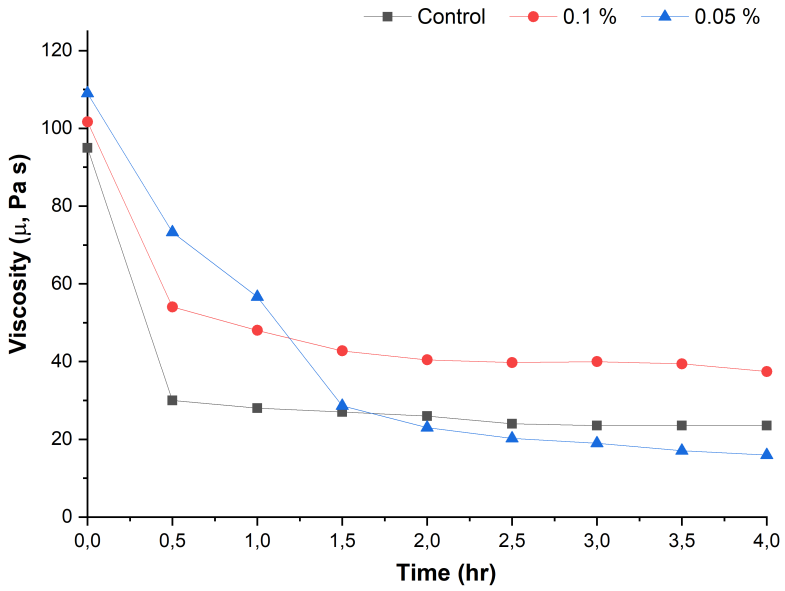

Figure 4.18. *In situ* rheometry during enzymatic hydrolysis of MSW as function of PEG concentration: 0.1-0.05 % (a) and 0.5-0.125 (b)

Reaction conditions: 5% TS, 2% enzyme loading, pH 5 (adjusted with 6 % H_3PO_4) at 10 s^{-1}

There are no studies on the effect of PEG as viscosity reducer during enzymatic hydrolysis of biomass, in a related area. Knutsen et al. [228] demonstrated that adding 2 % (w/w) of PEG 4000 reduces the yield stress of 20 % solids of pretreated corn stover to around 100 Pa, taking as reference the unmodified PCS suspension [228]. Amongst the array of possible polymers, PEG4000 was the most efficient rheology modifiers. The addition of PEG does not affect the thermal stability of endogluconases and β-glucosidases, but diminishes unspecific adsorption of the latter [225]. Rocha and co-workers [225] demonstrated a 32% improvement in glucose yields with the addition of PEG4000, and reduction of the liquefaction time. Although, in an economical assessment, they concluded that cost of additives needs to decreased to boost the commercial feasibility of 2G bioethanol refineries.

4.5 Case studies: independent studies within the Thesis

4.5.1 Fed-batch hydrolysis at Fiberight's demonstration plant: correlation of viscosity with power consumption

As previously described (section 4.3.2), a fed-batch enzymatic hydrolysis of MSW-derived slurries was carried out at Fiberight's demonstration-scale facilities, employing a 6000 litres stirred tank reactor. The evolution of μ_{app} and power-law parameters of hydrolysates throughout the demonstration-scale run is illustrated in Fig. 4.19. Individual flow sweeps of each hydrolysate are included in Appendix A (Figs. SI A.11). The power-law (K and n) parameters fluctuated during the course of the demonstration-scale batch, which could be attributed to the fed-batch strategy (Fig. 4.19a). A clear viscosity reduction is observed at 16 hours of enzymatic hydrolysis, achieving minimum K-values of approx. 50 Pa S^n. As n indexes were kept below 1, it can be stated that the MSW-derived hydrolysates are shear-thinning fluids. In Appendix A, pH/DO monitoring during the demonstration-scale run is also included (Fig. A.10).

The power-law parameters, using a impeller constant of 11 (hydrofoil impeller) [50], were used to calculate the apparent viscosity and compared with on-line monitoring power consumption (Fig.4.19b). For a a different magnitude of scale, it can be appreciated that μ_{app} and P measurements displayed a symmetric profile, demonstrating the strong relationship between both parameters. The maximum viscosity readings of 350 Pa s were found before 8.38% TS fed-batch addition, rapidly decreasing to negligible viscosity. For power consumption, at least 4700 MW are required at this scale. Although it is challenging to make direct correlations between apparent viscosity and power consumption, in particular in MSW-derived slurries, several authors [199, 200] have proposed a power-based method for an *in situ* viscosity method in paper and sugarcane bagasse enzymatic saccharification. However, this method assumes a Newtonian behaviour, therefore cannot be extrapolated in MSW-derived systems. Fluids are affected by multiple factors such as solids contents, enzyme loadings etc. In addition, poor representative sampling (50-ml out of 6000 litres) does not provide the wider rheological profile at demonstration-scale.

Specific power consumption (P_W) was in the range of 0.95-1.15 W L^{-1} (data not shown) throughout the fed-batch hydrolysis (15.43%TS), slightly lower than for industrial applications (1-5 W L^{-1}) [234]. Even achieving P_W values of 1 W L^{-1} , power requirements would account for 5.7 MW. At industrial scale, e.g. 1000 m^{-3}, P_W of 1 W L^{-1} would translate into prohibitive energy requirements for mixing (1 GW). At these scales, the availability of information about power consumption during enzymatic saccharification is scarce, due to non-public disclosure from biorefinery companies. Palmqvist et al. [196] required only 0.18-0.45 W L^{-1} at impeller speed (30 to 120 rpm) for demonstration-scale (4000 L) of pretreated Norway Spruce (13.5%TS). Stirred tank reactors equipped with a pitched-blade impeller in three levels and four baffles, is a feasible option for palliating high energy requirements at these scale.

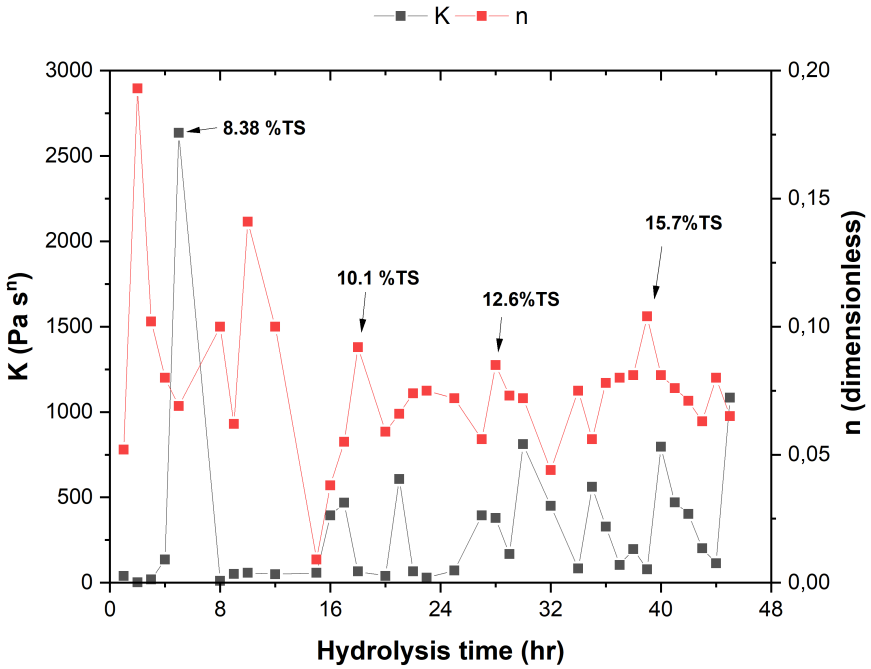

(a)

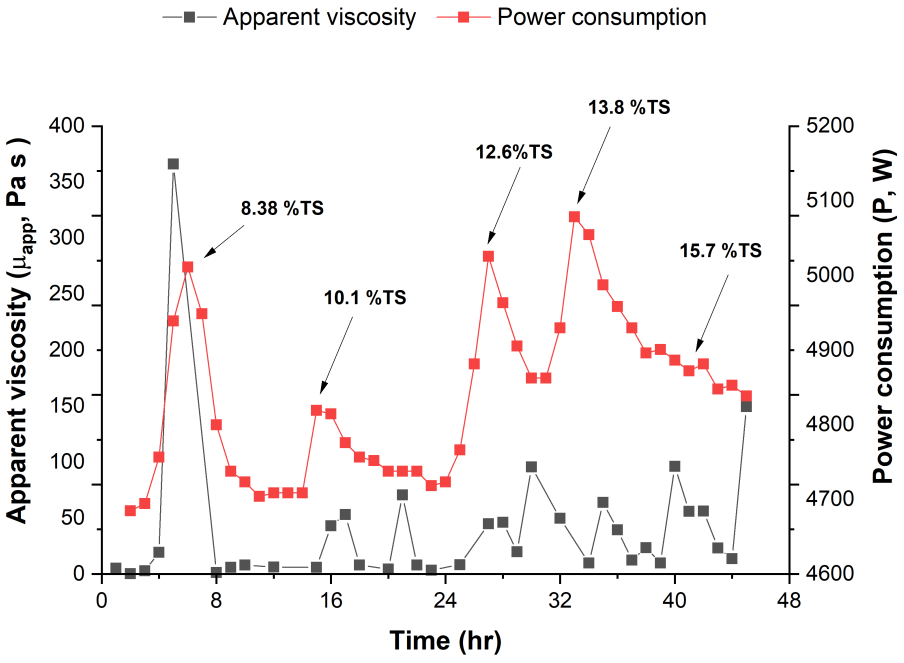

(b)

Figure 4.19. Comparison of rheological parameters and power consumption during the demonstration-scale enzymatic hydrolysis: (a) power-law parameters and (b) apparent viscosity and power consumption

Reaction conditions are depicted in an internal spreadsheet (bx 30103), disclosure of conditions is upon Fiberight's approval Arrows represent spike of solid loadings within fed-batch mode, the completed feeding strategy is described above (Table 4.2)

Other studies have calculated specific power consumption by modelling tools: 2.5 to 9.8 W L^{-1} [235] and 0.52-2.63 W L^{-1} [234]. Further improvements in power minimisation are still needed to make stirred tank competitive in terms of power efficiency for high-solids enzymatic hydrolysis [234].

From the demonstration-scale batch, some hydrolysates were also subjected to the determination of area and volume-based particle-size distribution (Fig 4.20). In one side, Fig 4.20a does not show a binomial distribution as seen in the literature [58, 187, 205], two major peaks are presented at around 100 and 700 μm in all hydrolysates. However, throughout the enzymatic saccharification, the volume of the second peak decreases to less than 2 %. A possible hypothesis is that oligosaccharides are still present in the hydrolysate broth due unproductive depolymerisation into monomers [236, 237]. After 10-hour of hydrolysis, the "shoulder" distribution around 500 μm is likely to disappear if completed lignocellulosic digestion is achieved. Although, alternative experimental methods as size-exclusion chromatography (SEC) would elucidate on this matter [236, 238]. In the case of area-based PSD, a substantial drop of surface % is observed at the larger particle sizes (1000 to 100 μ) during the first 10 hours. At 2 and 4h, a binomial distribution is observed with a peak at around 50 μ. Wiman et al. [205] conducted similar studies with pretreated softwood hydrolysates, displaying a decrease in area and volume percentages above 100 μm during the course of hydrolysis. Interestingly, a clear Gaussian distribution was observe with the absence of the "shoulder effect". Compared with MSW-derived pulps (12% hemicellulose), pretreated Norway Spruce contains only 0.5 % of this fraction. Therefore, the "shoulder effect" could be attributed to the presence of hemicellulosic fraction, as either lignin and cellulose were presented in both investigations.

To provide an average particle-size of hydrolysates during the course of hydrolysis, volume-based and area-based mean can be calculated. Table 4.4 summarises of both mean diameters according to an arbitrary classification of particle fractions (fine, medium and coarse), adapted from Kadic et al. [58]. In general terms, D_{43} and D_{32} decrease during the studied times as expected due the enzymatic degradation in substrates. Kadic et al. [58] plotted the area-based mean diameter during the enzymatic hydrolysis of spruce and giant reed (13% WIS for both) at different impellers speeds (100, 300 and 600 rpm) and cellulose-to-glucose (%) conversion. A major drop in D_{32} is observed, 33 to 18 μm, compared with above-mentioned study (less than 10 μm) in the same time-frame. Another study based on native and dilute acid pretreated poplar examined particle size distribution by meshing at various sieves sizes [211]. They determined the volume of the particle size as the ratio of pore size; < 50 μm (small), between 50 to 74 μm (middle) and > 74 μm (large), divided by the total hydrolysate volume. Depending upon the nature of the substrate, the particle size distribution change (pretreated poplar) or not (native) as: small and middle volume fractions increased and large one diminished.

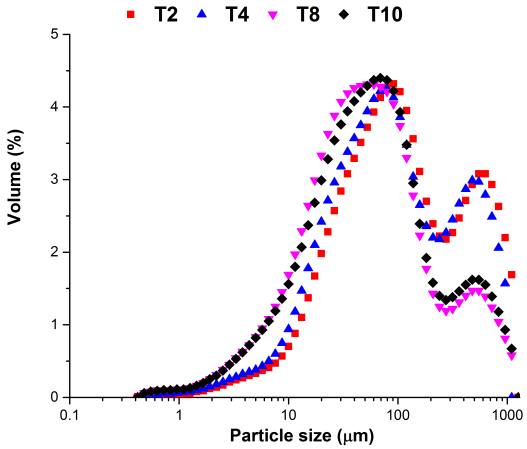

(a)

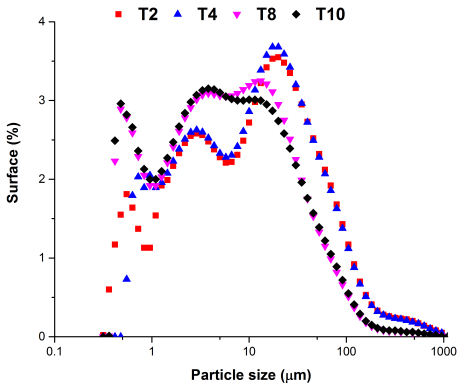

(b)

Figure 4.20. Particle-size analysis of demonstration-scale hydrolysates

Total solids per time: 0.78 (2 hours), 5.42 (4 hours), 8.07 (8 hours) and 8.16% TS (10 hours). Reaction conditions are depicted in an internal spreadsheet (bx 30103), disclosure of conditions is upon Fiberight's approval

4.5.2 Louisville placement stage: continuous viscosity measurements

Continuous (*in situ*) viscosity measurements of ball-milled MSW-derived slurries (10-20 % TS) were conducted for 8 hours (Fig. 4.21). Each set of experiments behaved differently depending upon the solids concentrations: quick and slow viscosity reduction for 10 and 20% solid enzymatic hydrolysis, respectively. At higher solids loadings, a 77% viscosity reduction was observed in the first two hours (1800 to 300 Pa s), improving to a 99 % viscosity decrease when halving the amounts of solids (10%TS). As commented upon earlier, little information is available in regards of *in situ* viscosity measurements within a rheometer at moderate and high-solids loadings [197, 198]. Kadic et al. 2018 [197] hydrolysed 12 %TS with 10 mg protein/g cellulose of CTec3 whilst providing *in situ* viscosity measurements. Despite using the same enzyme cocktail and close enzyme dosages (10 to 8 mg protein/g cellulose), only a 20% viscosity reduction was observed during steam-pretreated pine hydrolysis with severe agitation (160.7 s^{-1}). With another scope, Coffman et al. 2018

Table 4.4. Particle-size distribution and averages ($D_{4,3}$ and $D_{3,2}$) of demonstration-scale hydrolysates

	Volume-based				Area-based			
Time (hr)	**$D_{4,3}$ (μm)**	**Fine (%)**	**Mid (%)**	**Coarse (%)**	**$D_{3,2}$ (μm)**	**Fine (%)**	**Mid (%)**	**Coarse (%)**
2	207	4.0	45.6	50.3	33.2	46.9	47.1	6.0
4	201	7.1	55.3	37.6	32.6	46.3	47.9	5.8
6	209	6.2	54.4	39.3	29.8	49.5	45.0	5.5
8	115	10.0	60.4	29.6	17.4	61.3	36.7	2.1
10	125	9.7	57.9	32.3	17.9	62.4	35.3	2.3

Nomenclature: Volume-based ($D_{4,3}$) and surface-based) ($D_{3,2}$) are mean averages. Fine, mid and coarse fractions consist of particle size < 10 (fine), 10 < x < 100 (medium) and > 100 (coarse) μm, respectively.

[198] presented liquefaction rates of 4-8 hours on 30 % w/w Avicel hydrolysis with a 5-fold increase in enzyme dosages (40 to 8 mg protein/g cellulose). Same study investigated the viscosity reduction of 18 % ionic liquid (IL) pretreated switchgrass at same operational conditions, exhibiting a 6-hour liquefaction rate. Although, the liquefaction rates were determined by a novel approach, based on viscoelastic principles and *in situ* oscillatory measurements, Coffman et al. [198] used excessive amounts of enzymes. Biomass sieving through (at least) a 2 μm mesh seems mandatory for *in situ* viscosity measurements at high-solids solids. Otherwise, excessive axial forces would result into potential damage and malfunctioning of the rheometer instrument.

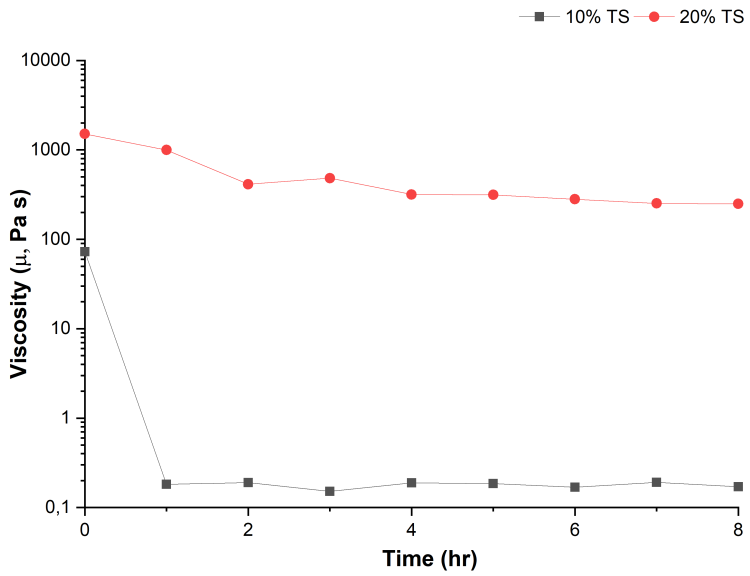

Figure 4.21. Continuous viscosity measurements during the enzymatic hydrolysis of MSW-derived slurries (ball-milled, approx. 150 μm

Reaction conditions: 10-20 % TS, 5 % E:S, 0.1% NaN_3 at 50 °C and 10 s^{-1}

At similar solids (10% TS) and enzyme loadings (15 FPU/g cellulose) than Dasari [41], viscosity measurements of MSW-pulp during enzymatic saccharification presented different results than sieved red-oak saw dust (33 μm < x $\leq$ 75 μm). The ball-milled MSW pulp was sieved through 150 μm to determine particle-size and compared with the forestry residue slurry. Despite this, the MSW-derived pulp slurry contained coarser particles, and a 99% viscosity reduction was observed while only a 50 % for the forestry-based assay. Several reasons could explain the discrepancies on viscosity evolution/values of both assays: pre-processing, enzyme cocktail and nature of feedstock [205]. The so-called "two-stage" kinetics profile was appreciated for MSW-derived hydrolysis , but not for red-oak sawdust case. It is possible that efficient viscosity reduction does not occur in biomasses with fine particles (<100 μm), as slurry media is already liquefied. Another hypothesis as suggested by Dasari et al. [40] is that cellulose fragmentation is limited into a certain extent by cellulases in the presence of micrometric particles.

4.5.3 OPTOMS: *in situ* and *ex situ* viscosity measurements during fed-batch enzymatic hydrolysis

Changes of apparent viscosity were characterised during fed-batch hydrolysis (B79 and B80 OPTOMS runs) by *in situ* and *ex situ* methods (Fig. 4.3.4). A second graph, Fig. 4.22b, was included to better illustrate *in situ* viscosity fluctuations during 24-hours of fed-batch hydrolysis. A simple approach for the determination of *in situ* viscosity based on power-based measurements is described in the methodology section 2.18. Power-law properties (K and n) and individual flow sweeps for B79 and B80 fed-batch runs can be found in Appendix A (Table SI A.2) Although, it is challenging to compare continuous and discrete viscosity records, substantial discrepancies in initial μ_{app} values matched for B80 runs for both type of viscosity analysis ($\sim$ 5 Pa s) at 5-hour of reaction. The *in situ* rheometry stopped after one-day of monitoring as minimum values of 0.075 Nm are necessary for torque-metering (see www.ika.com, vendor's description). In theory, *in situ* μ records would decrease until the end of reaction within the range of *ex situ* μ values (approx. 1-5 Pa s). The unexpected arise of viscosity at 24-hour occurs after re-starting the agitator for sample withdrawal. Pre-conditioning and flow sweeps of each B79 and B80 hydrolysates are included in Appendix A (Fig. SI A.12, A.13 and A.14)

As *in situ* viscosity measurements are calculated from torque-sensor readings, "viscosity spikes" occurred when increasing solids loadings as part of fed-batch strategy [194]. In particular, several increments on viscosity were observed for a 6-hour period in relation of fed-batch strategy (6, 9, 12, 13, 14, 15 and 16% TS) as indicated in Fig. 4.22b. Similar trends were reported by Cardona et al. [202] on fed-batch hydrolysis of Solka-floc (a delignified powdered cellulose) suspensions using a magnetic resonance imaging (MRI) set-up for on-line yield stress measurements. Interestingly, after 4 hours of hydrolysis, slurry media exhibits lower viscosities even operating at twice as much solids loadings than the start of reaction. Periodic aliquot addition

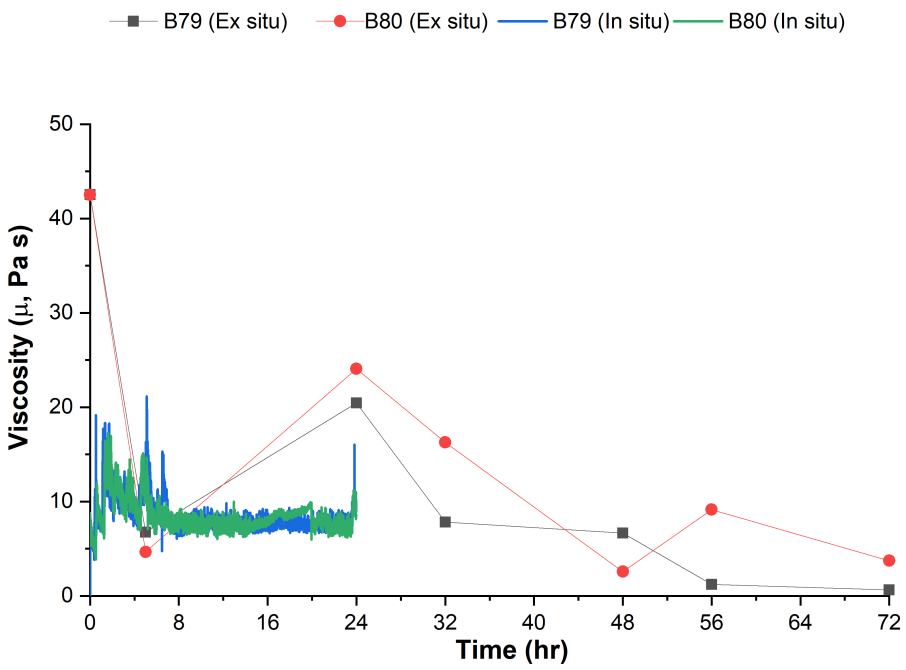

(a)

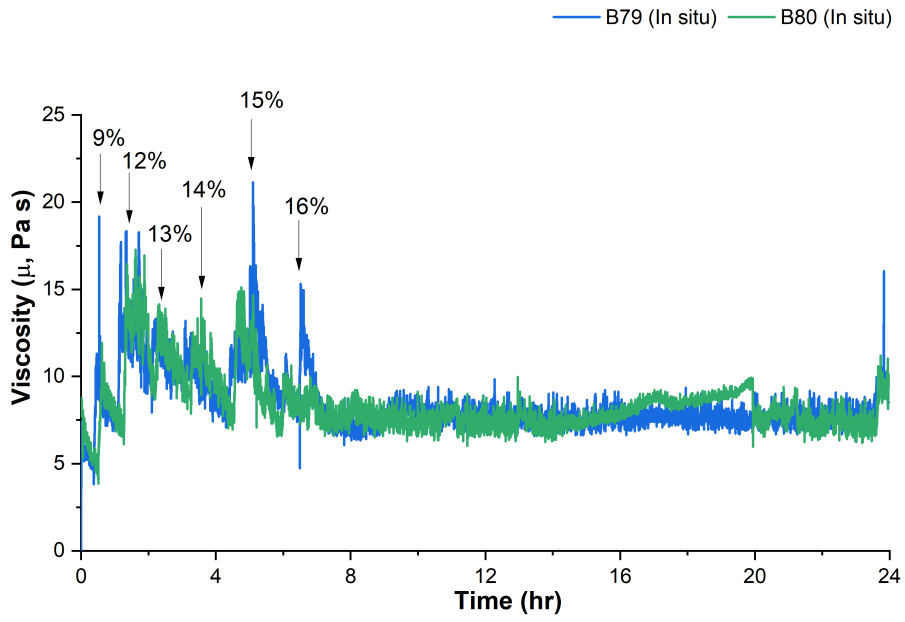

(b)

Figure 4.22. Comparison of *in situ* and *ex situ* viscosity analysis during a pilot-scale hydrolysis assay: (a) combined and (b) one-day *in situ* monitoring
In Fig.4.22b, arrows timing of aliquots addition in accordance of total solids

(solids + enzymes) alleviates high-initial viscosity of the system, allowing to easily operate at high-solids regimes within stirred tank bioreactors. By indirect methods, Liu et al. 2015 [239] determined system viscosity changes in accordance of gradual or whole enzyme additions with increasing solids loadings (15, 23 and 30 %) and 8-10 hours feeding time. Surprisingly, batch-enzyme addition with periodic solids addition resulted into lower viscosities and accelerates liquefaction rates by 2-fold as the initial slurry liquefies better.

To date, few studies have compared the evolution of viscosity by direct and indirect means during the enzymatic hydrolysis of biomass. Time-course apparent viscosities were measured at 150 rpm by on-site and off-site methods on 30 % w/w of pretreated corn stover hydrolysed for 12-hours with 10 mg protein/g DM [215]. In this study, on-line viscosities (calculated as $\mu = \pi M/73.56ND^3$) were in the range of rheometer-based (off-line measurements) after 2 hours of hydrolysis. Other combinations of *in situ* and *ex situ* viscosimetric and morphogranulometric techniques have been performed to understand the mechanistic relationship during enzymatic hydrolysis of cellulose suspensions [199, 200]. An *in situ* rheometry system based on concepts of Metzner-Otto and Rieger and Novak was proposed for the determination of viscosity of various paper-based suspensions [199]. Within 2 hours of starting hydrolysis (liquefaction rate), slurry viscosity decreased (*in situ* by 100-fold while diameter of fibrils decrease two-fold (*ex situ*). More recently, Le et al. 2017 [200] demonstrated a strong correlation of viscosity with the fraction of coarse particle in both sugarcane bagasse and filter paper hydrolysates. The combination of viscosimetric and morphogranulometric could elucidate the mechanistic effects by cellulases during biomass hydrolysis, therefore improving biorefining of lignocellulosic feedstocks.

4.6 Chapter summary

This chapter provides a literature analysis of rheology in lignocellulose biomass processing, which among other aspects are included as publication in the *Renewable and Sustainable Energy Reviews Journal*: "High-solid loading processing of lignocellulosic biomass to enhance bioconversion under biorefinery concept: Effects of mass and momentum transfer".

The research methodology is expanded from Chapter 2 (Materials and Methods), including the specifications for PBR assays and case studies. The results and discussion sections are split between: raw slurries, offline viscosity analysis, *in situ* rheometry and case studies. Key messages/findings per results section are summarised as follows:

Raw slurries

- Yield stress increase exponentially upon total solids in the range of 5-15 %TS

- A power-law relation was formulated to correlate yield stress with TS: τ_0 = 1.5 $\times$ 10^{-2} $TS^{4.2}$
- Apparent viscosity is proportional to solids concentration in stirred tanks < 600 rpm of impeller speed
- Lawrenceville and Hampden MSW pulps present similar physico-chemical properties, despite being different sources

Off-line viscosity analysis

- The determination of power-law parameters are used as viscosity and non-Newtonian indicators
- For PBRs, apparent viscosity of hydrolysates during enzymatic hydrolysis was calculated with a modified version of shear rate formulation
- Meanwhile in stirred tanks with pitched-blade geometries, the Metzner-Otto concept was used for the determination of apparent viscosity
- A rheological and process comparison was established between bioreactors, showing slower viscosity reduction for PBR than STRs but releasing same amount of sugars
- Inclusion of glucose measurements showed that glucose titers evolve indirectly to viscosity reduction during enzymatic hydrolysis
- A time-frame of 4-8 hours was identified as liquefaction rate for solids loadings ranging from 4-5%TS

***In situ* rheometry**

- The two-stage kinetics profile, partially seen in off-line viscosity analysis, was verified in these type of studies but at faster rates (2-4 hours)
- *In situ* rheometry was conducted to study the differences on kinetics upon total solids, enzyme loadings, surfactants additions, among other operational conditions
- At same total solids (5%TS), an approx. 33, 45, 60 % viscosity reduction was observed for 0.5, 1 and 2 % E:S in a period of 30 minutes.
- At same enzyme loadings (5 % E:S), a 1% increase on solid concentration (5 to 6 %TS) experiences same viscosity reduction (70 %) in four hours of hydrolysis.
- At same solids and enzyme loadings (5% TS and 2% E:S), sieving through (1000 μm) have a negative effect on liquefaction rates compared to an untreated waste biomass

- *In situ* rheometry of medium-solids loadings (10%TS) were achieved by increasing gap height of rheometer, but viscosity readings were underestimated as operating in non-calibrated conditions
- The decrease of viscosity readings are promoted by 0.1% PEG addition, although, associated costs of additives do not optimise the cost-effectiveness of enzymatic saccharification

Case studies

- At demonstration-scale, apparent viscosity and power consumption evolved in a proportional relationship during operation. Particle-size distribution of MSW slurries was also examined, showing its time-dependence during enzymatic hydrolysis.
- High-solids *in situ* rheometry was achieved via ball-milling of MSW-derived pulps, but these systems are not realistic at industrial scale due to excessive energy consumption
- An on-line method, coupling the mixing theory with torque-metry, was proposed to record viscosity measurements according to power consumption for a fed-batch hydrolysis at pilot-scale

Chapter 5

Reactor design and operation for enzymatic saccharification of MSW-derived pulp

5.1 Introduction

While industrial bioprocessing is consolidated for the manufacturing of application such as food, feed and pharmaceuticals, the conversion of MSW-based feedstocks to high-value products is still under development. It is dependent upon of funding and subsidies with factors such as enzyme costs, feedstock recalcitrance, power usage and carbon-trading [240]. The process (enzymatic hydrolysis) is conducted in bioreactors , engineering elements where the reaction occurs, to meet; the requirements of a biological system, ensure high processing yields and commercially viable productivity. Accurate design of bioreactors is of importance in optimising the productive volume of the vessel whilst minimising input costs such as enzymes and agitation rates [212]. The commercialisation of lignocellulosic sugars is only achievable at high-solids loadings [2], and optimised bioreactor designs and operability play a key role in addressing this. Moreover, bioreactors must provide adequate mixing, control of operational parameters and being scalable for the industrialisation of lignocellulosic-derived sugars.

5.2 Literature review

Several authors have extensively reviewed bioreactor designs for the bioconversion of lignocellulose biomass into fermentable sugars and subsequent production of high-value products [212, 241]. Designs for high-solids have been discussed [2, 92, 242], which include pilot-scale operation. For enzymatic saccharification, bioreactor designs are classified according to the author's suggestion, not as in other areas (e.g. solid-state fermentation). For instance, Liguori et al. [241] summarised bioreactor options for the conversion of dedicated energy crops (*Arundo Donax*), corn stover, wheat straw and alternative biomass (e.g. mesquite wood, switchgrass). The novelty of this work was the description of reactor components and properties in various

operation modes (batch, fed-batch and continuous), specific conversion pathways of lignocellulose to sugars for ethanol fermentation: separate hydrolysis and fermentation (SHF), simultaneous saccharification and fermentation (SSF), simultaneous saccharification and co-fermentation (SSCF) and consolidated bioprocessing (CBP). More recently, Pino et al. [212] focused the revision of bioreactor designs in two typology of bioreactors (stirred tank and membrane bioreactors). Within the first group of bioreactors, attention was made to describing agitation systems, energy consumption and mixing time as operational factors. For membrane bioreactors (MBR), the emphasis was put in system configuration and set-up of operational parameters and volume distribution for accurate product removal, briefly mentioning the economics of these bioreactors. A third group of analysis (operation strategies) described the basics of enzyme recycling and high-solids loadings, with horizontal bioreactors as the preferred option for this. Interestingly, a separate group of bioreactors known as pneumatically agitated (airlift and bubble columns) were presented as promising options for lignocellulosic bioprocessing due to lack of mechanical mixing, which leads to lower energy consumption. Although, both pneumatically agitated bioreactor configurations are still under development for enzymatic hydrolysis, since they require in-depth design of multi-phasic systems and determination of optimal performance parameters (e.g mass-transfer coefficient). With this in mind, a summarised version of the available literature is provided, focusing on modes of operation and reactor designs with a scope in high-solids loadings. Reactor designs are split between two groups depending on the vessel orientation: vertical (stirred tanks) and horizontal (scraped, paddle and rotatory) bioreactors. The main operational and variable parameters (power consumption and mixing time) are described with a common approach for both configurations. However, these novel bioreactor designs and auxiliary operations (e.g.enzyme recycling) are not discussed as being beyond the scope of this study.

5.2.1 Modes of operation

Regardless of reactor configuration and geometry, three main modes of operation are involved in enzymatic saccharification in accordance of feeding strategy: batch, fed-batch and continuous. A representation of each mode is illustrated in Fig.5.1, showing the substrate concentration over processing time as function of each mode. All modes of operation have been studied for the enzymatic hydrolysis by experimental and computational methods [212], the latter using differential equations for calculating mass balances as depicted in section 2.10. Table 5.1 summarises main characteristics of each mode of operation for the enzymatic hydrolysis of biomass, as adapted from cell culturing techniques.

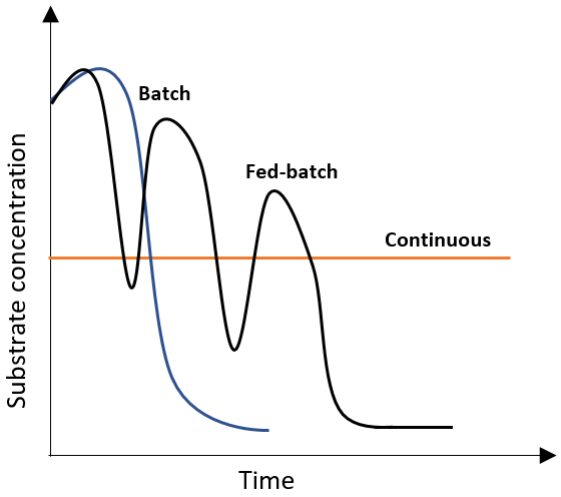

Figure 5.1. Representation of substrate concentration over time per mode of operation

5.2.1.1 Batch mode

Batch mode, also known as discontinuous processing, consists of a single and initial feed of lignocellulosic substrate and enzymes. Slurry media conditions evolve as function of retention time, being a closed system where the volume remains constant throughout reaction. Batch enzymatic hydrolysis dominates, being the preferred method of processing due its simplicity and passive mode of operation. Although, releasing more monomeric sugars than continuous processing, batch processing is based on extended residence times (> 7 days) and is limited to a certain threshold of solid loadings, hampered by high lignocellulosic viscosity. Consequently, excessive amounts of energy are required and glucose production rates decrease exponentially over time. Both variables leads to poor application of batch enzymatic hydrolysis at industrial scale [243, 244].

5.2.1.2 Fed-batch mode

Fed-batch, semi-batch or semi-continuous terms are used for defining the intermittent addition of substrate and/or enzymes during the saccharification process. This provides an alternative to batch processing, as it promotes mass-transfer leading to higher conversion yields. The gradual loading of lignocellulosic substrates alleviate the initial high-viscosity and enhances mixing in the system, consequently, , higher solids loadings are achieved [245]. Furthermore, unproductive enzyme binding and a decrease in inhibition problems are minimised due to the addition of fresh substrate [202]. Many fed-batch strategies have been performed in enzymatic hydrolysis, changing the timing of the feeding and type of aliquot. Modenbach A.A and Nokes S.E [92] reviewed a wide range of fed-batch hydrolysis studies with agricultural residues at high-solids loadings.

5.2.1.3 Continuous mode

In a continuous mode of operation, substrates feeding and product removal occur at the same flow-rate, resulting in a constant working volume. Consequently, the biological reaction does not change its reactivity achieving "steady-state", where the inlet and outlet concentration remain unchanged. It is noted that substrate inhibition in continuous systems is reduced since less undesirable compounds are found [246]. Moreover, reaction control (pH and temperature) is simpler in continuous mode than batch due to reaching steady-state. However, the continuous enzymatic hydrolysis of biomass is still under development, hindered by the fluid characteristics of biomass (e.g. recalcitrant nature and elevated initial viscosity). The design of an efficient bioreactor and auxiliaries is essential for the "flowability" of product materials and deployment of lignocellulosic bioprocessing [15].

Table 5.1. Overview of characteristics per mode of operation for enzymatic hydrolysis of biomass

Characteristics	Batch	Fed-batch	Continuous
Addition of fresh inlets	No	Yes	Yes
Slurry volume	Constant	Increases	Constant
Removal of product	No	No	Yes
Product inhibition	High	Medium	Low
Slurry media conditions	Unsteady	Unsteady	Steady-state
Glucose yield	Moderate	High	Low
CAPEX	Low	Low	High
OPEX	Intermediate	Low	High

5.2.2 Stirred tank reactors

Stirred tank reactors, abbreviated as STRs, are common equipment for carrying out enzymatic hydrolysis as in many other biotechnology applications [247]. STRs are constituted with a cylindrical vessel equipped with one impeller which is powered by an overhead agitator system, as seen in Fig 5.2. These type of reactors provide vigorous and consistent mixing, achieving a certain degree of homogeneity throughout the vessel. For preventing the formation of vortex and stagnant regions, some panels known as baffles can be attached in the wall of the vessel. The number (1 to 4) and shape (e.g. beavertail, concave, rectangular) of baffles influence mixing behaviours and power input in the system [248]. Fig 5.3 illustrates the flow patterns on unbaffled and baffled STRs, showing considerable differences on mixing regimes. The selection of principal dimensions (height, diameter) of bioreactor elements are key factors for reactor design. Garcia-Ochoa et al. [247] recommended the establishment of 0.3-0.6 ratio between the diameter of the impeller and diameter of the tank (D/T). Meanwhile, the ratio between height and diameter of tank is set around 2:1 or 3:1. Other geometric recommendations include impeller and baffles dimensions and their positioning towards the wall of the vessel [44].

STRs can be built from various materials (hard-plastics, glass and stainless steel), however, glass is the preferred option for laboratory-scale bioreactors. Depending

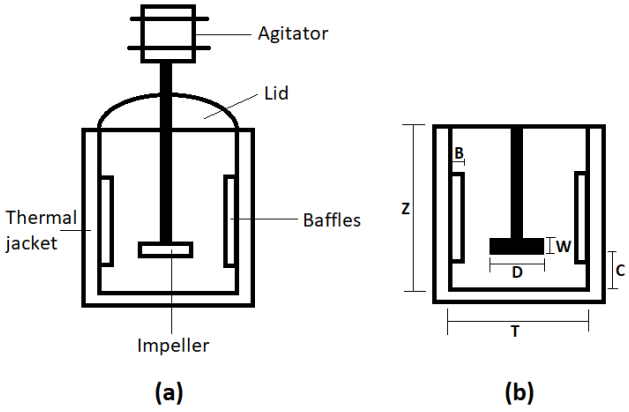

Figure 5.2. Schematic diagram of a stirred tank reactor: (a) structure and (b) dimensions

Nomenclature: T is vessel diameter, Z is vessel height, D is impeller diameter, C is clearance distance and B baffle width (longitude units)

on the reactor scale, a particular heating device is used for keeping a constant temperature: incubators, water-jackets or serpentines. At volumes below a litre, Erlenmeyer flasks fitted in an orbital incubator are used as stirred tank reactor, with supply of hot air. The main drawbacks of this system are the loss of temperature during withdrawal of samples and poorer air convection than liquid-based devices. At bench-scale, glass-lined vessels with an integrated thermal-jackets, where a thermal liquid (water or oil) is recirculated from an external heating bath. From pilot to commercial scale, jacketed-vessels are also equipped with an internal serpentine for providing additional heating and avoid heat-transfer limitations during the operation.

5.2.2.1 Types of impellers

Numerous types of impellers have been used for agitation purposes in the chemical industry [249]. Impellers are classified upon the mixing patterns that generate: axial (down to up) or radial (side to side). Fig 5.4 shows the typical impeller configurations for the enzymatic hydrolysis of lignocellulosic feedstocks. Although, new agitation systems are constantly appearing for processing of lignocellulosic biomass, e.g S-shaped and segmented helical impellers [241]. The need of mixing in lignocellulosic processing is to achieve a certain degree of homogeneity for promoting mass and heat transfer, therefore, enabling the effective adsorption of enzymes into the substrate [149]. The typical impeller choices for the enzymatic hydrolysis of lignocellulosic biomass are pitched-blades (PBTs) and Rushton turbines [212], resembling as a helicopter helix and disk-type with six blades, respectively, as seen in Figs. 5.4a-b. Both geometries are used for controlling the gas dispersion (dissolved oxygen) and formation of bubbles of oxygen in fermentation processes, adapted for enzymatic saccharification. However, these types of impellers are inefficient for mixing of highly viscous feedstocks. The so-called cavity effect or formation of dead-zones

is observed when employing both impeller geometries [250]. In addition, excessive amounts of electricity are required during operation. Several investigations for the enzymatic hydrolysis of biomass, forestry and [58, 196, 251–253] and agricultural [194] feedstocks, have compared the mixing performance of pitched-blades and/or Rushton turbines with alternative mixing devices (e.g. anchor). Regardless of the operational conditions, PBTs resulted in higher power consumption (2.25 to 1.55 W L^{-1}) and lower hydrolysis yields (28.8 to 30.1%) than anchor-type impellers [196]. Similarly, Rushton turbines under-performed to elephant-ear impellers in power consumption, mixing time and cellulose conversion [254]. For instance, using Rushton turbines less than 60% of cellulose was converted into glucose at 470 rpm, whilst, over 75% was achieved by the elephant-ear geometry. Hence, both conventional impellers are not recommended for bioconversion of lignocellulose substrates as they exhibit low bioprocessing efficacy.

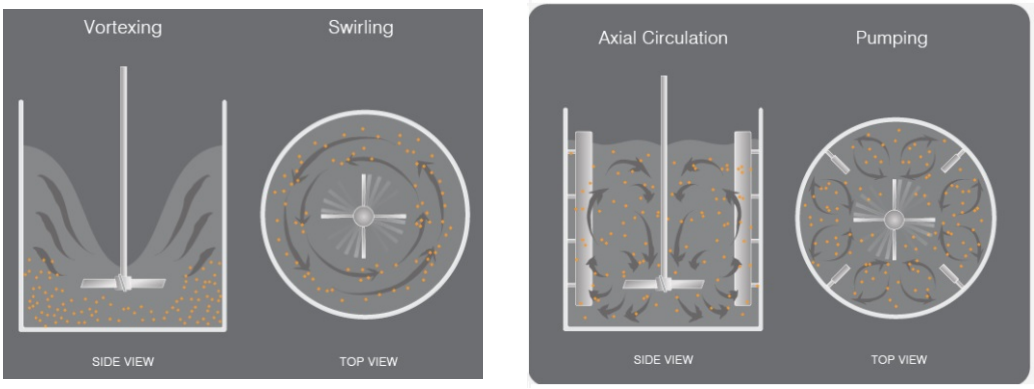

(a) Unbaffled STR

(b) Baffled STR

Figure 5.3. Flow patterns in unbaffled (a) and baffled (b) stirred tank reactors [255]

Based on the unsuitability of pitched-blade and Rushton turbines in the mixing of lignocellulosic feedstocks, novel impeller configurations are employed (Figs. 5.4c-g. The first group of hydrofoil impellers (Fig. 5.4c) offer efficient mixing and solids suspension in low shear environments. They are commercialised under different trademark names (e.g. Lightinin A315, *APV LE* hydrofoil and *Chemineer HE-3*), and made of stainless steel [44]. McFarlane and Nienow [256–259] released a series of four papers, comparing the agitation performance of hydrofoil-based impellers (*Prochem Maxflo T* and *Lightinin A315*) with Rushton turbines. The mixing-related parameter (mass-transfer and power consumption) were tested with each, and the hydrofoil impellers outperformed Rushton turbines when dealing with various mixtures (air-water, coalescence and cellulosic model compounds). Focusing on lignocellulosic slurries, Benz G [260] demonstrated that hydrofoil impellers can significantly reduce the capital and operational costs compared to pitched-blade ones. They require 60% less energy and costs the half than pitched-blade, due to the lower torque requirements.

Helically agitated reactors (Fig 5.4c) can be found as single (spiral-shape) or double (DNA-shape) helix ribbon impellers. They are high surface area mixing elements

with a particular mode of mixing, lifting the substrate from the bottom to the top of the vessel. Many investigations are available, using a double helical ribbon impeller for several biorefinery applications: pretreatment, enzymatic hydrolysis, SHF and SSF [215, 261, 262]. In the State Key Laboratory in China, a 5-L bioreactor equipped with helical stirring has been employed in multiple investigation for high-solids processing of corn stover. Same group of researchers have studied mixing-related parameters by experimental and computational [263–265]. In France, Battista et al [266, 267] compared mixing time, power consumption and glucose concentrations in batch test of a wide range of impellers, including single and double helical, for the enzymatic hydrolysis of wheat straw. It was found that increasing the complexity and diameter of impellers led to better performance of the lignocellulosic operation, as double helicoidal impellers outperforms in all three studied parameters. Helical-based impellers are useful tools for high-solids mixing, showing better performance than the other impellers, but several considerations have to be taken into account. Helical ribbon geometries are unsuitable for industrial bioprocessing, being limited to a certain scale with prohibitive manufacturing costs [268], therefore, are restricted for bench-scale applications.

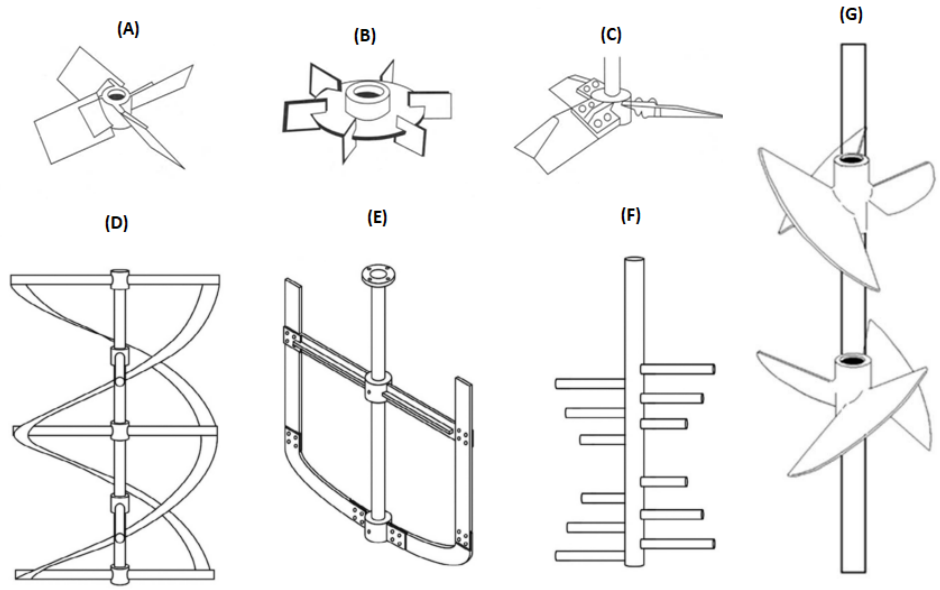

Figure 5.4. Typical impeller configurations for enzymatic hydrolysis of biomass: (a) hydrofoil, (b) Rushton turbine, (c) 4-blade 45° pitched blade (4BP), (d) double helical ribbon, (e) anchor, (f) peg-mixer and (g) elephant-ear. Adapted from Penney W [269] and Pino M.S et al [212].

The anchor (Fig 5.4e) is another type of impeller, named after looking like the ship's anchor, employed in many applications. They are one of the preferred options, alongside helical, requiring less power and generating less shear than other designs [270]. Anchor-type impellers are wall-scraping, ideal for viscous fluids which avoid the stagnation of the material on the tank walls. Some examples can be found in the

literature, although, anchors are uncommonly used for enzymatic saccharification: switchgrass [271], Norway spruce [196, 272] and giant reed [196, 273] and wheat straw [266, 267]. It is noted that the wide diameter of the anchor, promotes homogeneous mixing throughout the medium due a better power dissipation. However, as with helical-based geometries, poor scalability impedes them being real options for industrial biorefining [274].

The last two type of impellers, peg-mixer and elephant-ear (Figs. 5.4f-g), have been employed in enzymatic saccharification but less frequently. The peg-mixers are impellers adapted from the pulp and paper industry, employed during bleaching and pulping processes [275]. At laboratory scale, some examples of peg-mixers (Fig. 5.4f) are reported for the bioconversion of renewable feedstocks: unbleached Kraft pulp (UBKP) and organosolv pretreated poplar (OPP) [275] as well as agave bagasse [151]. Zhang et al. [275] processed two hardwood residues with up to 20% substrate consistency at 20 rpm, yielding 140 g L^{-1} in only 48 hours. By employing peg-mixers, cellulose conversion of 60% were achieved. On the other hand, Caspeta et al. [151] enzymatically degraded agave bagasse at 20 and 30% TS levels in a series of 30 ml peg-mixer for 80h, agitating at 150 rpm. Agave bagasse was ethanosolv pretreated prior digestion. The most elevated glucose concentrations (200 g/L) and cellulose conversion (90 %) were found at 30% TS, in specific pretreatment conditions. Although, enzymatic hydrolysis of biomass using peg-mixers have shown the highest glucose titers, there still a lack of information about related power consumption. Hence, further investigation of mixing-related and techno-economic aspects are still needed for satisfying the industrial bioprocessing of lignocelluloses.

In contrast, the "elephant-ear" turbines are modified versions of pitched blades with a down-pumping and up-pumping modes of mixing [276]. Elephant ear impellers showed promising results on average shear rates compared with Rushton turbines [276] in bioreactor processing. Based on this study, Correa et al. [254] selected elephant ear geometries for the enzymatic hydrolysis of steam-exploded sugarcane bagasse. Two versions of elephant ear impellers, down-pumping and up-pumping, were used for the providing both axial and radial flows. Several combinations of elephant-ear with/without Rushton turbines were studied [194, 254]. The combination of down and up-pumping elephant impellers showed the highest energy efficiency and glucose conversion yields in this process. A scale-up protocol was proposed using a scale-up factor of 1000, to design a geometrically similar reactor from the 3-L laboratory version (3 m^3). Maintenance of power consumption per unit (P/V) was taken into account as scale-up criterion, for the determination of mixing-time at the larger scale. Scaling-up by 1000 times results into in a 4-fold increment in mixing-time. Furthermore, using elephant ear impellers alleviate the formation of lignocellulosic-based inhibitor during enzymatic saccharification as less dead zones and accumulation of inhibitors are formed.

5.2.3 Horizontal reactors

Horizontal reactors have become an alternative to stirred tank reactors for the high-solids enzymatic hydrolysis of lignocellulosic feedstocks [92, 149]. These type of reactors are used in other industrial processes such as waste management [277], food [278] and biotechnological applications [43]. In contrast to stirred tank reactors, the horizontal orientation allows gravitational or free-fall mixing, requiring less energy consumption [213]. The horizontal orientation of the reactor offers many advantages over stirred tanks: minimisation of particle settlement, accumulation of re-agents [17], better aeration and solids distribution than stirred tanks [279]. In contrast, larger footprints and higher manufacturing costs are associated with the decommission of horizontal reactor [43]. Mitchell et al. [43] proposed a classification based on aeration, mixing and stirring features in horizontal bioreactors for solid-state fermentation. Regarding bioconversion of lignocellulosic feedstocks, independent studies by Kadic et al. [196] and Modenbach et al. [92] have categorised horizontal reactors into four groups, depending upon the reactor design: rotating paddle reactors, scraped surface bioreactors, rotary drum bioreactors and roller bottle reactors (Figure 5.5). This categorisation will be used for the literature analysis, including most the relevant studies, which are typically unaerated and continuously-mixed bioreactors for the enzymatic hydrolysis of lignocellulosic feedstocks.

5.2.3.1 Paddle reactors

Paddle reactors (Fig. 5.5a) are horizontal reactors structured with several blades (paddles), which are perpendicularly attached to the rotating shaft. The mixing capabilities are increased by free-fall mixing from the scraping action of the paddles, which removes substrate from the reactor walls. The sectional-type of agitation promotes heat-transfer as achieving well-mixed conditions throughout the vessel. Paddles (dryers) reactors have been employed for decades in the fine and speciality chemicals industry [44], among other applications, currently commercialised by a range of companies such as Heinkel and Bachiller. For the enzymatic hydrolysis of lignocelluloses, Jorgensen et al. [93] developed a pilot-scale (280 L) paddle reactors for high-solids pretreatment, enzymatic saccharification and fermentation of wheat straw into ethanol. The paddle reactor is divided into 5 filling chambers of 60x20 cm each, operating via free-fall mixing which reduces the need for mechanical agitation. Surprisingly, cellulose conversion is independent of the rotational speed and working volume in the paddle reactor geometry. Free-fall mixing was programmed with a change of direction (clock-wise to anti-clock wise, and vice versa) every two minutes during the whole operation. Thus, avoiding the formation of "dead zones" of unreacted lignocellulosic substrate and poor enzyme adsorption. More recently, the integrated biomass utilisation system (IBUS) project managed by DONG Energy (Denmark), adapted the pilot-scale version of the paddle reactor for research and development [283] and scale-up [284], with volumes of 400 L and 11 m^3, respectively.

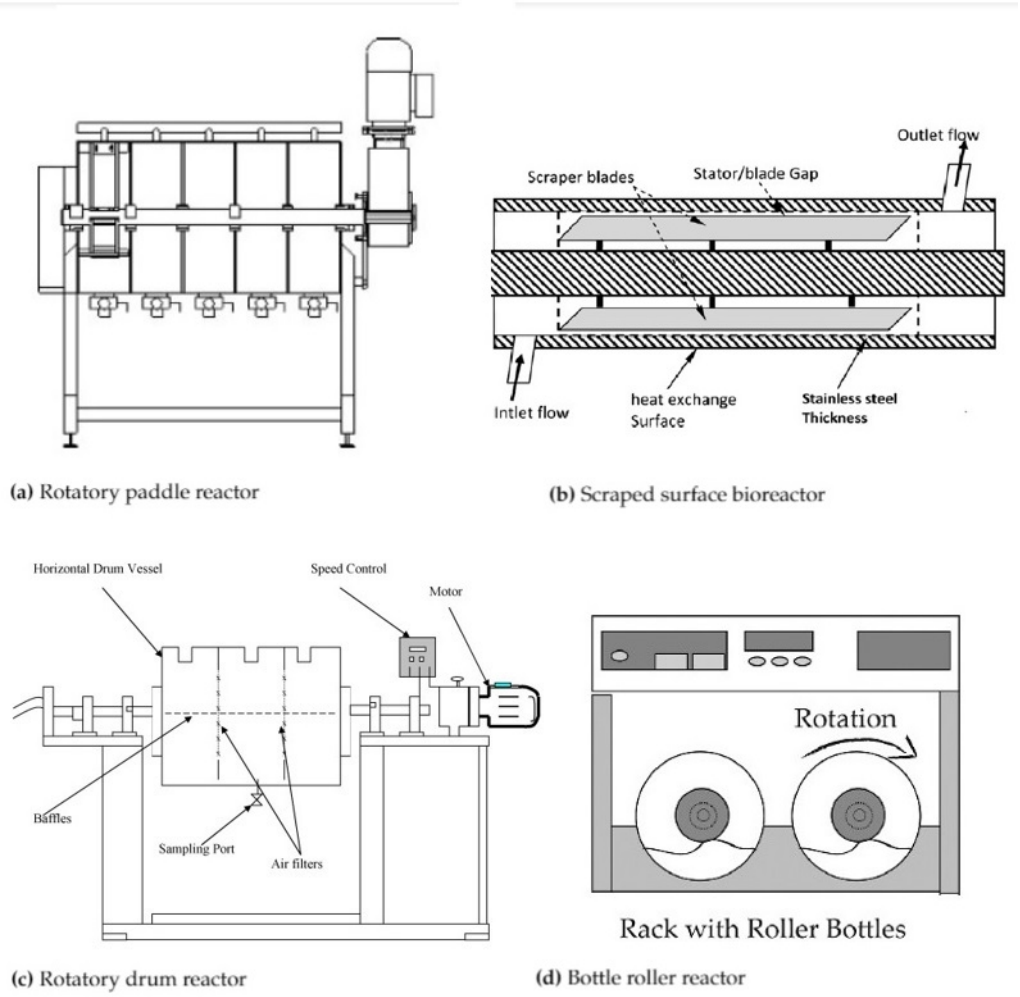

Figure 5.5. Different concepts of horizontal reactors employed for enzymatic hydrolysis of biomass: (a) rotating paddle reactors [93], (b) scraped surface bioreactor [280], (c) rotary drum reactor horizontal rotating bioreactor [281] and (d) roller bottle reactors [282]

Insoluble solids of 20-40% were set as maximum threshold for wheat straw biorefining, showing the high efficiency of these reactor designs for high-solids loadings. In 2012, an integrated biorefinery producing; 2G ethanol, lignin pellets and molasses was built in Kalundbordg (Denmark), based on the IBUS process [284]. Following on from this, a full-scale plant (5-12 times) the capacity of Kalundborg plant, will be commissioned upon policy and market directives in the KACELLE project [17].

5.2.3.2 Scraped surface bioreactors

Scraped surface bioreactor (SSBR), Fig 5.5b, is a similar type than paddle reactor, but with scraped blades attached in parallel instead of perpendicular to the rotational axis. The scraping action of the blades avoids stagnation of substrate on the wall, consequently, heat-transfer is promoted throughout the vessel. SSBRs offers the above-mentioned benefits such as low power consumption, low particles of particles and efficient operability at high-solids loadings [242]. These type of reactors

are adapted from scraped surface heat ex-changers (SSHE), that are widely used in the food industry with their efficient mixing of high viscous materials (cream cheese, peanut better etc..) [280]. Researchers have focused on the study of heat-transfer performance [285–287] or fluid dynamics Newtonian (water or polyalkylene glycol) and Non-Newtonian (carboxymethyl cellulose and tomato puree) fluids during a SSHE operation [278, 288]. An 8 L SSBR was self-designed by Dasari et al. [41, 42] and employed for the enzymatic saccharification of pretreated sawdust and corn stover. High-solids loadings, ranging from 15 to 25 % TS, were investigated under the SSBR configuration, resulting in high glucose titers (above 80 g L^{-1}) than when processed in shaken flasks [42]. The system operated at 2 rpm to minimise the power consumption, whilst maintaining good mixing with those solids regimes. Interestingly, less than 0.6 W L were required for initial mixing of 20% lignocellulosic slurries, showing great advantages over stirred tank reactors: infeasible at high-solids mixing or excessive power input (1.5 W $^{-1}$) at low-solids loadings [181].

5.2.3.3 Rotatory drum reactors

Rotatory drum bioreactors (RDBs) are another type of horizontal vessel in which the substrate tumbles by the action of a rotating shaft (Fig.5.5c). RDBs are also free-fall mixing, as paddle reactors, but with the absence of attached "impellers" on the shaft. Typically, the reactor design is a cylindrical vessel which is positioned parallel to the floor, although alternative designs in shapes (cones or v-shape) and degrees of inclination ($< 45°$) are also available [43]. There are several advantages of processing with RDBs compared to stirred tanks: larger surface area, feasibility with high-solids loadings ($\sim$ 20% or higher) and lower operational costs (power consumption, maintenance and volume) [279]. RDBs have been employed for centuries in the powder technology for cement formulation, fine chemicals and food applications [289]. From that, rotating drum biorectors have been explored for multiple bio-based areas such as cell culturing [290], solid-state fermentation [43], bioleaching [279] and composting [120]. For instance, Mitchell et al. wrote the book "*Solid-State Fermentation Bioreactors: Fundamentals of Design and Operation*", as guideline for bioreactor design and operability for solid-state fermentation. A broad overview of bioreactor configurations, putting a strong emphasis on the design of RDBs, and modelling microbial processes was covered. For the lignocellulosic biorefinery, RDBs have been mainly employed for the production of crude cellulases [281, 291], with a few examples of ethanol fermentation are also present [241, 292, 293].

To promote aeration and mass/heat transfer, internal mixing elements (baffles or lifters) are attached to the rotating drum bioreactor. As in stirred tank reactors, the baffles introduce mixing to avoid stagnation of the substrate onto the tank wall, non-formation of "dead zones" [255]. The effect of the baffles has been studied during operation of rotating drum bioreactors since the last century for fermentation processes in RDBs [294]. Mitchell et al. [43] reviewed different baffle designs in RDBs, looking at the fluid dynamics s over unbaffled vessels. Factors such as the

number, shape, size and position affect the mixing mechanism, and the bioreactor performance [248]. Liu et al. [295] demonstrated that equipping a rotating drum with 8 baffles mounted vertically, led to better mass-transfer during microbial oxidation by *Acidithiobacillus ferrooxidans* as a bioleaching process. Furthermore, they correlated an increase in power consumption with the increase in number and width of the baffles. A more mechanistic study was conducted by Jiang et al. [248], who investigated the mixing performance of granulated materials by four baffle designs (single, cross-type or flake-ice shapes). Better mixing performance resulted in non-single baffle shapes, which were optimised by their size. There is no evidence for an investigation to the effect in RDBs in lignocellulosic biorefining. A preliminary study by Roche et al. [146] was carried out with the intention of studying the presence of baffles (0 or 4) and other operational parameters. In contrast, conversion yields of pretreated corn stover into glucose were reported, the effect of the baffles was not reported. Further research is needed to test these hypothesis that baffles are beneficial, as they have demonstrated great advantages in solid-state fermentation [43] or bioleaching [294, 296].

5.2.3.4 Rolling bottle reactors

A laboratory version of RDBs, known as rolling bottle reactors, can be used for early-stage or scale-down studies. The experimental set-up consists of horizontal jars place on a roller apparatus, which is enclosed in an incubator for temperature control. The reactor sizes can be varied from 15 ml (centrifuge tubes) up to 4 L (wide-mouth polypropylene bottles) rotating at maximum rates of 80 rpm. As previously described, baffles can be attached to the walls and alumina grinding balls can be introduced to enhance the mixing performance [146]. Rolling bottle reactors (RBRs) are commonly employed for cell culturing, particle formulation and other applications in a laboratory environment [297]. Compared with RDBs, more studies have been reported with RBRs for the enzymatic hydrolysis of lignocellulosic biomass [115, 146, 228]. Roche et al. [115, 146] demonstrated the suitability of RBRs for gentle mixing of high-solids processing compared to shake flasks and paddle reactors. The roller apparatus can be decked with numerous reaction vessels at once, which offer great versatility and saves time for screening parameters. For instance, Knutsen et al. [228] simultaneously investigated the effect of > 20 viscosity modifiers in pretreated corn stover. In addition, RBRs are simple, robust and scalable designs which facilitate the research and development of a specific process whilst minimising operational costs.

5.2.4 Comparison of reactor configurations

A comparison between stirred tank and horizontal reactors is proposed for enzymatic saccharification of lignocellulosic biomass, shown in Table 5.2.

Table 5.2. Comparison of main features for stirred tank and horizontal reactors

Reactor configuration	Advantages	Drawbacks
Stirred tank reactors	• Higher scalability scaling • Easier installation of probes • Easier scale-up	• Higher power consumption • High-solids limitation • Poorer mass and heat transfer
Horizontal reactors	• Low power consumption • More suitable for high-solids • Higher footprint	• Difficulties for on-line monitoring • Lower scalability • Higher CapEX

5.2.5 Bioreactor designs for high-solid loadings

Several bioreactor designs have been employed to overcome the problem of high-solids loadings: peg-mixers, helical ribbon stirred tanks, paddle, scraped and rolling bottle reactors [2, 17, 212]. Table 5.3 shows examples used in high-solids enzymatic saccharification of lignocellulosic feedstocks, including: reactor design, reaction conditions, pretreatment and process yields. In batch mode, few designs are capable of efficient operation with low energy requirements (above-mentioned). Any type of reactor works *per se* with high-solids loadings using a fed-batch feeding strategy [92]. Da Silva et al. [2] summarised a list of reactor and impeller designs for batch high-solids loadings in the range of 20-40%. Horizontal reactors that encompass from paddle to rotatory/rolling, are selected for hydrolysing lignocellulosic slurries at 30-40%. In the vertical orientation, only helical ribbon (segmented and helical) and peg-mixer are suitable designs for high-solids loadings. Some examples have been reported using shake flasks, though the ability of hydrolysis above 20% w/w is more influenced by the pretreatment than the orbital type of mixing [40]. With the same feedstock and pretreatment strategy, hydrolysis yields of 52% were achieved by employing a paddle dryer [298] in comparison a home-made version [93] using 40% w/w of steam-exploded wheat straw. Although, higher hydrolysis yields have been reported in the enzymatic hydrolysis of agave bagasse by peg-mixers (90%) [151], direct comparison cannot be established, differing on: feedstock, pretreatment. For the commercialisation of lignocellulosic sugars, other aspects such as manufacturing and operational costs of each design play a significant role on determining the techno-economics [299], hence, it is difficult to conclude with a preferred "high-solids" reactor option.

5.3 Analysis of operational parameters: power consumption and mixing

Several parameters need to be determined for the satisfactory operability of bioreactors: pH, DO, temperature, conductivity [212]. In particular, two operational parameters are used as indicators for determining the bioreactor performance: power consumption and mixing time.

Table 5.3. Overview of high-solids loading enzymatic hydrolysis studies upon reactor design and operation

Reactor design			**Hydrolysis conditions**							
Type	*Feeding*	*Scale (volume)*	*Solids*	*Duration*	*Enzymes*	*Agitation*	*Feedstock*	*Pre-treatment*	*Glucose yields (efficiency %)*	*Reference*
In-line mixer	Fed-batch	Pilot (250k gallons)	20 % DM	24h (SSF of 84h)	On-site enzymes, 7 FPU	NR	Corn stover	NaOH and H_2SO_4	50 g/L, 90%	[147, 299]
Paddle reactor	Batch	Pilot (40L)	25 % DM	25h (SSF of 74h)	C/β mix, 7 FPU	6.6 rpm	Wheat straw	IBUS*	50 %, 45 g/kg	[93]
Paddle reactor	Batch	Pilot (400L)	27% DM	6h (SSF of 240h)	C/β mix, 41 FPU	2.5-16.5 rpm	Wheat straw	IBUS[1]	40 g/kg, 50%	[283]
Rotary drum reactor	Fed-batch	Lab-scale (NR)	25% DM	6h (SSF of 240h)	CTec2, 7 FPU	100 rpm	Corn stover	H_2SO_4/ steam explosion	80 g/kg, 65%	[213]
STR with a helical impeller	Fed-batch	Lab-scale (NR)	25% DM	6h (SSF of 240h)	CTec2, 7 FPU	100 rpm	Corn stover	H_2SO_4/ steam explosion	75 g/kg, 60%	[213]

[1] A hydrothermal pretreatment is performed in the IBUS (Integrated Biomass and Utilisation System) related projects, combining stem-explosion plus water washing
Scale includes laboratory, pilot, demonstration and commercial
DM is dry matter (%), FPU is filter paper unit (FPU/g substrate) and CBU is cellobiose unit (CBU/ g substrate), SSF is simultaneous saccharification and fermentation and NR is not reported

Table : continued

Reactor design			**Hydrolysis conditions**							
Type	*Feeding*	*Scale (volume)*	*Solids*	*Duration*	*Enzymes*	*Agitation*	*Feedstock*	*Pre-treatment*	*Glucose yields (efficiency %)*	*Reference*
STR with a hydrofoil impeller	Batch	Pilot (200L)	20-30%DM	48h	10 different mixtures[2]	NR	Poplar wood chips	Steam-explosion at 200-208 °C for 5-9 min	15-49 g/L (16-45%)	[72]
STR with a peg-mixer	Batch	Lab (0.9L)	20% DM	100h	C/β (100 FPU)	20 rpm	Hardwood kraft pulp and poplar wood chips	Organosolv: 50% EtOH, 1.25% H_2SO_4 at 170 °C for 60 min	140 g/L (95%)	[275]
STR with a peg-mixer	Batch	Lab (30ml)	30%DM	80h	NS5013 (10 FPU) + NS50010 (20 CBU)	150 rpm	Agave bagasse	Ethanosolv: 50% EtOH and 0.5 % H_2SO_4 at 160 °C for 10 min	80 g/L (90 %)	[151]
STR with a modified Rushton turbine	Batch	Lab (1L)	20% DM	45h	Zylase^R (15-31mg enzyme g^{-1}glucan)	50-500 rpm	Corn stover	Dilute acid/steam explosion method	30-65 g/L (% NR)	[73]

[2] This work combined different commercial enzymatic cocktails: Cellic CTec (Novozymes), Novo188 (Novozymes), AlternafuelAF 100L (Dyadic), AlternafuelAF 200L (Dyadic), Accellerase 1500 (Genencor) and Multifect xylanase (Genencor)
Scale includes laboratory, pilot, demonstration and commercial
DM is dry matter (%), FPU is filter paper unit (FPU/g substrate) and CBU is cellobiose unit (CBU/ g substrate), SSF is simultaneous saccharification and fermentation and NR is not reported

In bioprocessing, power consumption refers to the electric energy (W) consumed during the running of engineering components: mixing, heating/cooling and purification steps. Minimisation of the power consumption is key for enhancing the profitability of industrial bioprocesses. In this study, power draw focuses on the energy requirements related to the agitator system. For the measurement of power consumption, a wide range of tools are available, split into four groups: electric, calorimetric, reaction torque and reaction strain [300]. Ascanio et al. [300] reviewed the principal options (dynamometers and torque meters), amongst others things, describing their advantages and drawbacks. The selection of a preferred technique includes the ease of installing and wide torque range coverage. Although, certain limitations are intrinsic (e.g. recording of power consumption per individual impeller) . For this, strain gauges are available for measuring the power input of each impeller, despite their elevated market costs. Nonetheless, Benz proposed a laboratory protocol for the determination of multi-impeller systems based on torque readings and theoretical derivation for slurry mixing [301].

During the biochemical conversion of biomass to monomeric sugars, a sensor device coupled between the agitator system and rotational shaft (torque-metering) is the main technique for measuring the energy consumption [42, 196, 215, 262, 264–267, 272]. However, a few studies have used dynamometers instead [194, 254]. Torque-metering, the force that causes an object (fluid) to rotate on an axis is measured (M, Nm). Consequently, power consumption is determined as a function of rotational speed ($P = 2\pi MN$). Power consumption is commonly reported in watt units (W), but a modified version (specific power consumption, P_w) can be used instead (W L^{-1}), allowing the accurate comparison between independent studies. As a "rule of thumb", power consumption range from 1-3 W L^{-1} for ensuring the viability of industrial bioconversion of lignocelluloses [234]. If P_w measurements are displayed, the power to ratio volume can be derived from power recording and reactor volume. Under the same reaction conditions, several researchers have compared the specific power consumption at different impeller geometries [194, 196, 266, 267]. So far, Battista et al. [266, 267] has presented the most comprehensive study on the influence of impeller's geometry in batch/fed-batch tests at set conditions. For instance, in batch; anchor, paravisc and double helicoidal impellers require 3.0, 3.5 and 2.8 W L^{-1}, respectively, at 250 rpm in a stirred tank reactor. While, a range of P_w values were reported in fed-batch for hydrofoil (6.0 W L^{-1}), marine (6.0 W L^{-1}), anchor (3.3 W L^{-1}), paravisc (4.0 W L^{-1}) and double helicoidal impellers (2.7 6.0 W L^{-1}) at 80 rpm. In addition, other impeller geometries were compared during initial enzymatic saccharification (values at time 0): pitched-blade (2.5 W L^{-1}) to anchor (1.55 W L^{-1}) [196], Rushton (3 W L^{-1}) to elephant-ear (3.25 W L^{-1}). As power consumption varies upon many parameters (feedstock nature, pretreatment method etc..) [149], broad statements cannot be made, unless same reactions are used.

Mixing times (also referred as blend times), are an experimental factor that determine the time required for achieving a certain degree of homogeneity (e.g. 90

%) after injecting a tracer in a vessel. This key parameter for examining the mixing performance of processing unit, as well, as for scaling-up purposes [212]. In stirred tank reactors, various theoretical expressions have been depicted for the determination of mixing time or equivalent factor as function of reactor dimensions and dimensionless in turbulent regime [44] and laminar [302] regimes without aeration, respectively. Ascanio et al. [303] widely proposed a broad spectrum of experimental techniques for the empirical determination of mixing-time, classified as: (1) degree of flow disturbance and (2) type of collected data . (intrusive or non-intrusive) The first group encompass non-intrusive methods (e.g. colorimetry or thermography) where the flow is not disturbed by the action of external elements, whilst, intrusive (e.g. pH or conductometry) alter the flow patterns during mixing. Secondly, direct measurements (colorimetry or conductometry) are those taken from human or probe intervention, in contrast, to indirect measurements (e.g. thermography) where the acquired data is processed to an image. Ascanio et al.[303] summarised the main operating principles, advantages and disadvantages of six mixing-time techniques: colorimetry, electrical resistance tomography, thermography and probe-based (pH or conductometry). Moreover, several factors were compared, from accuracy and reproducibility to sampling speed, performed using the above-mentioned techniques. From a practical perspective, colorimetry stands outs as the most common technique in stirred vessels [304], based on the addition of dye during mixing to visualise the time required for achieving completed colouring, among other features such as solid patterns, dead zones or caverns. Although, being a simple and cost-effective technique to implement, it is subjected to human eye subjectivity and works only for transparent systems.

With this in mind, as opaque systems, lignocellulosic slurries would require specific techniques for mixing-time analysis: pH pulse [267], temperature pulse [254] conductometry [305] or monitoring tracer concentration [264] methods. In these methods, mixing time is estimated as time required for achieving 95% of corresponding final value after addition of external agent, e.g. pH after base addition. For instance, Battista et al. [267] determined mixing time of a wheat straw slurry by pH pulse method (10 ml of 2N NaOH), in a stirred tank reactor (2.2 L working volume) as function of several impeller geometries: hydrofoil, marine, anchor, paravisc and double helicoidal. In batch mode (250 rpm), mixing time decrease as increasing complexity and diameter of impeller: anchor (27s), paravisc (29s) and double helicoidal (8.5s). The same experiments were performed with the other geometries in fed-batch mode (half of working volume), resulting in the best performance by the helical-based configuration (7.2s). A temperature pulse method ws carried out by Correa et al.[254], to study the changes of agitation rates within various dual impeller configuration (Rushton and elephant-ear) in stirred tank reactors. A direct correlation was observed between the increasing stirring speed and decreasing mixing time, which was more pronounced in vessels equipped with the elephant-ear (33.2 s at 753 rpm) than Rushton turbines (161 s at 753 rpm). Using computational

fluid dynamics, Zhang et al. [264] simulated the mixing-time by the trace concentration method in helically-agitated systems, scaled-up by a 10 factor (5, 50 and 500 L) as a function of solid loading. At agitations rates of 50 rpm, the medium scale (50 L) displayed a higher mixing time than 5 and 500 L versions, e.g. 82 s compared to 80 and 64 s,respectively. Apart from stirred tanks, mixing time has also been analysed in other configurations such as scraped surface bioreactors [305]. Using conductometry, Ghorbanian et al. [305] showed an exponential relationship between the total solids and mixing time: 402 (7.5%TS), 2165 (12.5%TS) and 5502 (17.5 % TS) minutes. High-solids operation under a SSBr configuration led to longer mixing times than in stirred tanks. Overall, analysis of mixing time is a useful technique for improving performance in lignocellulosic biorefining.

5.4 Results and discussion

Objective: To investigate the application of various reactor designs for transitioning from batch to continuous mode of operation

5.4.1 Stirred tank reactor

In this section, the two investigations used stirred tank reactors and experiments were conducted by following the methodology previously described: power consumption (section 2.5.2 and mixing-time (section 2.8.2). The design of the reactor employed vessels is also included in Chapter 2 (section 5.2).

5.4.1.1 Power consumption

The specific power (P_w) was measured during enzymatic saccharification assays of MSW-pulps (5-7% TS), as seen in Fig .5.6. Due to technical problems, the torque-metering of the 7 %TS run stopped within the eighth hour, but was re-started prior to completion of the hydrolysis. It is noted that the initial P_w increases as a function of the solids content; 2.25, 2 and 1.5 W L^{-1} for 7, 6 and 5%TS. A severe drop (40-50%) in power consumption occurs after 8-hours of enzyme addition for each assay, mainly associated with biomass liquefaction [40]. However, the slope of the power consumption curve (0-8 hours) varies in accordance with solids loadings, similarly with the timing of constant P_w values. As the slurry viscosity decreases, less power input is necessary for impeller mixing. Final specific power outputs were of 0.5, 0.75 and 1.5 W L^{-1} for 5, 6 and 7% TS, respectively. Compared with Correa et al. [194], similar P/V outputs were recorded during the enzymatic saccharification of steam-exploded sugarcane bagasse in STRs, equipped with dual elephant-ear impeller geometry. Despite working under different conditions; solids loadings (5 to 20%TS), enzyme doses (3.3 to 10 FPU $g_{biomass}$) and rotational speeds (500 to 470 rpm), resulted in P_w measurements in the range of 1.5-2 W L^{-1}. In another study,

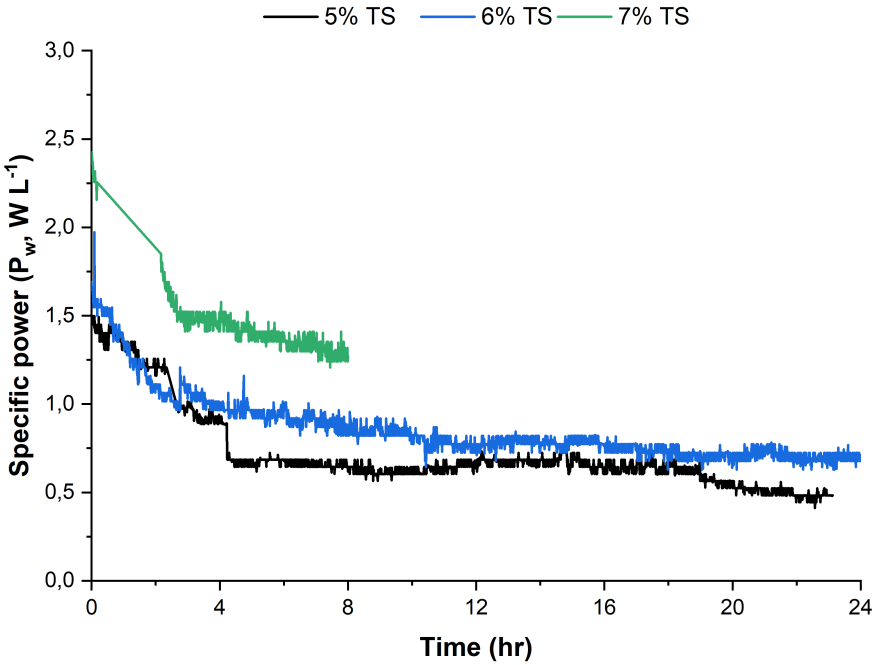

Figure 5.6. Specific power (P_w) monitoring during enzymatic saccharification assays (5-7% TS) in STRs

Reaction conditions: 5-7 %TS, 2 % enzymes loading, 0.1 % tetracycline, 500-600 rpm and 50 °C
Note: glucose yields were 8, 9 and 10 g L^{-1} for 5,6 and 7% TS, respectively, at 24-hours of hydrolysis

[196] showed P_w outputs ranging from 0.5-1.5 W L^{-1}, during the enzymatic saccharification of 10%w/w Norway spruce at 72 hours. Despite both impeller geometries (pitched-blade and anchor impellers) were stirring at 200 rpm, different power outputs were resulted: 2.25 and 1.55 W L^{-1}, respectively. By combining the key findings, it was demonstrated that pitched-blade turbines are the least efficient impellers for the minimising power consumption during enzymatic saccharification of biomass [196]. Other impeller geometries as elephant-ear or anchor are more suitable for bioconversion of lignocellulosic substrates in STRs, as indicated by displaying P_w measurements of 1.5 W L^{-1} at solid loadings 2 or 4 times higher than this study.

Another factor, total energy consumption (E) was estimated by Eq. 5.1. The E values (in Wh L^{-1}) were 16.6 (5 % TS), 20.6 (6 % TS) and 32.6 (7 % TS) for the different total solids. Lower energy consumption was estimated (16.6-32.6 Wh L^{-1}) to Correa et al. [194] reporting 140-160 Wh L^{-1} during a working at high-solids sugarcane bagasse hydrolysis (20 % TS) in 96 hours with different feeding strategies. Direct comparisons are not realistic due vast discrepancies on feedstock, solids loadings, residence time and feeding strategies. Despite some variations in impeller geometries (single pitched-blade versus double elephant-ear) and stirring speed (600 to 470 rpm), a 10-fold increase of energy outputs, likely attributed to the high-solids

operation. Total energy consumption varies many parameters during enzymatic saccharification: feedstock, pretreatment, particle-size and enzymatic cocktail/loading [196].

$$\epsilon = \int_a^b P_w(t) \times \, dt \tag{5.1}$$

5.4.1.2 Mixing time

In a 1.5L stirred tank reactor (80% working volume), the mixing time was determined in water and 5% TS MSW-pup slurry solutions, as can be seen in Fig. 5.7. The time to reach 95% of final conductivity is used as an indicator for achieving complete homogenisation of the system, indicated by corresponding arrows. In a complementary figure (Appendix B, Fig. SI B.1), ratio of C_t per C_0 was plotted during experimentation to show when "95% of final trace concentration was achieved, which represents the "mixing-time".

A high degree of homogeneity was achieved in 1.5 and 9.3 minutes for water and 5% MSW-pulp solutions, respectively. For water, there is a disparity between the results depending upon the mixing-time method and reactor geometry within the literature [266, 305]. The same methodology was employed in the SSBR configuration by Ghorbanian et al. [305], reporting a mixing-time of 36 min by rotating at 2 rpm. Large changes in the rotational speed and size of vessel are the main reasons of a 22-fold increase in t_m, compared to our study. In contrast, Battista et al. [266] investigated the mixing-time in water (among other straw-miscanthus-water mixtures in batch and fed-batch strategies) by the pH pulse method, indicating that only 3.3 s were needed to achieve complete homogeneity of the system. Although, effective blending was achieve by using a helicoidal impeller geometry, only by stirring at 50 rpm. It is difficult to explain a 30-fold decrease in mixing-time,compared with this study, as reported by Battista et al. [266]. Some potential reasons may be attributed to using higher tracer concentration (0.3 to 0.1% w/w) and a different re-agent (NaOH to NaCl).

For the MSW-pulp slurry (5%TS), similar t_m were found by Correa et al. [254] prior to hydrolysis of steam-exploded sugarcane bagasse (10%TS), employing dual Rushton and Rushton/elephant ear turbine configurations at 470 and 188 rpm, respectively. At same solids loadings, the t_m decreased by about 12 times if dual elephant ear (updraft and downdraft) impellers were equipped. Contrary to this, Rushton turbines led to longer mixing times when rotating from 94 to 753 rpm range. Battista et al. [267] studied the effect of impeller configuration on mixing-time in a series of batch and fed-batch experiments of wheat straw slurries at high-solids loadings (20% w/w). A correlation between the impeller factors (design complexity and diameter) was observed to dictate mixing-time at the pre-hydrolysis step. At 200 rpm, the double helical impeller (D = 140 mm and H = 160 mm) needed only 10

s for achieving 95% mixing time, whilst, a four-bladed hydrofoil (D = 90 mm and H = 20 mm) took around 60 s. Herein, as observed in the power consumption studies, it shows that pitched-blade turbines are inefficient impellers for achieving good mixing in lignocellulosic slurries. Alternative geometries such as helical or elephant-ear lead to lower mixing-time, therefore, a more rapid distribution of enzymes throughout the slurry.

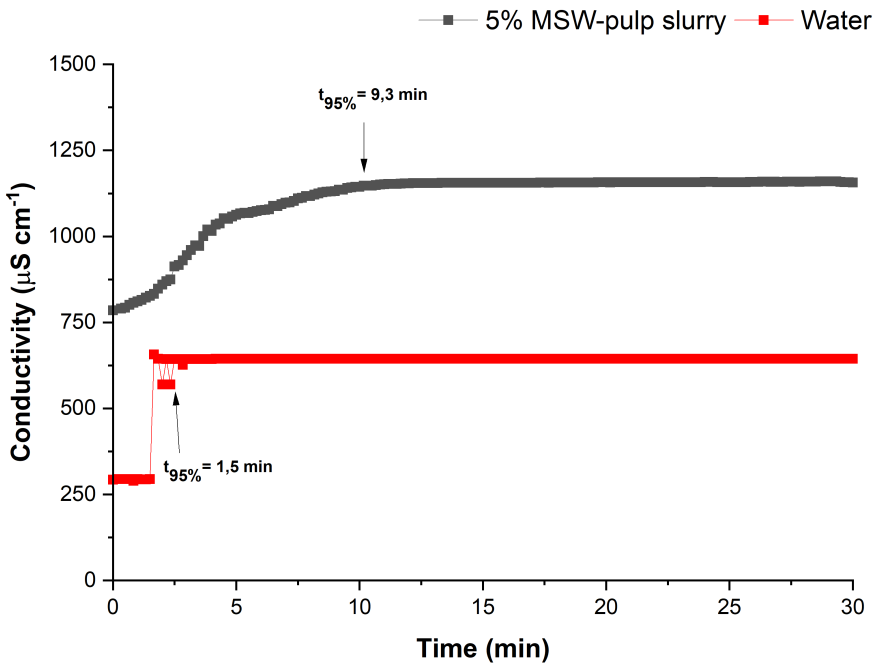

Figure 5.7. Conductivity measurements as function of time for water and MSW-pulp solutions after trace injection

Reaction conditions: water (200 rpm) and MSW-pulp (600 rpm) on a single pitched-blade turbine (40mm diameter)

5.4.2 Scrape surface bioreactor: a placement stage

A scraped surface bioreactor, previously designed and assessed by Dasari and coworkers [41, 42], was tested for the enzymatic saccharification of MSW-pulp slurries (Fig. 5.8). Five different runs were carried out with periodic analysis of glucose concentrations (Fig. 5.8): (1) 15 %TS raw batch, (2) 7.5 + 7.5 % TS raw fed-batch, (3) 15 % batch and (4) 5 + 10 % TS fed-batch and (5) 10 + 5 + 5 % TS fed-batch. Initially, the reaction was conducted with raw MSW-pulp in batch (no.1) and fed-batch modes (no.2). Untreated lignocellulosic feedstock with coarse particles hinders high-solids enzymatic saccharification as the scraped surface bioreactor struggled to operate. Using untreated MSW-pulp resulted in glucose yields of above 35 g L^{-1} for over 48 hours, despite the feeding strategy. In order to make a more amendable substrate,

MSW-pulp was dried and shredded, obtaining a cotton-like material. A batch hydrolysis assay (no.3) was carried out and compared with the raw homologous reaction. By shredding the lignocellulosic substrate, a 20 g L^{-1} glucose uplift (40 to 60 g L^{-1}) was achieved, indicating the beneficial effect of particle-size reduction. Dasari et al. [40] demonstrated that size reduction by disk milling improved the enzymatic saccharification of biomass 2-fold as result of better enzyme adsorption. To tackle the initial viscosity and efficiently operate at high-solids loadings, the enzymatic hydrolysis of biomass has been investigated in fed-batch mode [92]. Modenbach et al. [92] highlighted that amount of solids and timing of addition are important factors for maintaining high conversion rates throughout the reaction, for the reactor performance. Herein, two fed-batch strategies were investigated: no. 4 (5 + 10 %TS) and no. 5 (10 + 5 + 5 % TS).

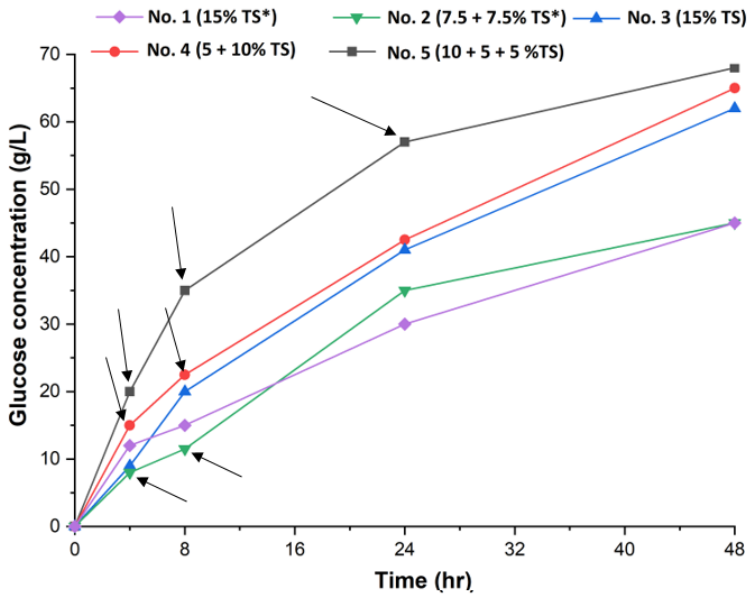

Figure 5.8. Enzymatic hydrolysis of MSW-pulp in the Dasari's SSBR configuration: glucose yields

Reaction conditions: 5% E:S, 0.1% NaN_3, 10 rpm, 50 %V, 50 °C and pH 4.75-5.25
*Represent batches using raw MSW pulp, otherwise, with shredded MSW pulp. And arrows the timing of feeding for fed-batch experiments

According to Puri et al. [32], fed-batch processing improves the initial glucose yields over operating in batch, but final glucose titers are in the same range (65 to 63 g L^{-1}). To pursue 20% solids loadings, an alternative fed-batch strategy (exp. no. 5) was investigated with a gradual three-aliquot addition. Initial loading of 10% solids resulted in the highest glucose titers of all runs, achieving glucose levels of 20 g L^{-1} in only 4 hours of reaction. In 48 hours, an impressive concentration of 70 g L^{-1} was achieved, which is close to the commercial requirements [2]. It is worth mentioning that elevated glucose yields, in particular using shredded pulp, could be attributed to an excessive use of cellulases [155]. However at these loadings

(5% (w/w)), approximately 10-15 FPU/g cellulose [154], the enzymes cost should be less $2/kg for the viable production of cellulosic ethanol from lignocellulosic sugars [306].

5.4.2.1 Power characterisation: ramp-up and monitoring

Power consumption was measured throughout three hydrolysis assays , as seen in Fig 5.9. The resulting power consumption was normalised to working volume, described here as specific power consumption (P_w, W L^{-1}). As expected, enzymatic hydrolysis with untreated MSW-pulp exhibited the highest initial P_w measurements of around 1.5 W L^{-1}. Untreated slurries contain an agglomeration of particles and high viscosities, leading to low mass-transfer and an excess of the power [73]. In enzymatic saccharification experiments with shredded pulp, experiments no. 2 and 3, the specific power consumption was 0.3 and 0.6 W L^{-1}, respectively. The low viscosity of treated MSW-pulp and the presence of finer particles promotes reactor mixing, resulting in lower energy requirements. The feeding strategy also has an impact on power measurements [194]. Single feeding (batch) of lignocellulose slurries requires larger amounts of power due to mixing of the whole slurry, compared to split solids addition in fed-batch mode [307]. As indicated in the literature, fed-batch strategies minimise power consumption since the substrates is rapidly liquified, demanding low torque for agitation [254]. According to Hou et al. [215], there is a severe drop in the power usage during the first eight hours of hydrolysis since most of the lignocellulosic biomass is being degraded to monomeric sugars. Once the biomass is liquified (4-8 hours), slurry mixing is improved due to the lower intrinsic viscosity, therefore, little torque is recorded. After 24 hours of reaction, negligible levels of torque are measured, since the torque-sensor is not sensitive enough below the minimum detection limits associated to this sensor.

As observed in Fig. 5.10, the power consumption is directly proportional to the rotational speed for most of the batch and fed-batch hydrolysis experiments. There is a correlation between power consumption (W) and agitation (rpm). This trend is clearly seen at the 15 %TS batch assay, dark blue and green lines. The fed-batch hydrolysis (10 + 5 +5 %TS) exhibited 50% less power consumption compared to Dasari's study using 10 %TS. Halving the working volume (3L) during fed-batch would have a major effect in P_w than in batch (7L). Pretreating (shredding) the MSW pulp also had a positive effect, lowering the power requirements during saccharification at same solid loadings. A 50 % difference in power consumption (5 to 2.5 W, raw and shredded, respectively) is reported at maximum stirring speeds (10 rpm). Physical pretreatments reduce the particle size and initial viscosity, thus, less torque is needed during hydrolysis of these feedstocks [308]. Similar power outputs were reported using untreated MSW-pulp slurries in comparison with Dasari et al [41], at same solids loadings. Unfortunately, increasing the rotational speed with power measurements were not conducted below 10 % TS, except with the empty tank. In

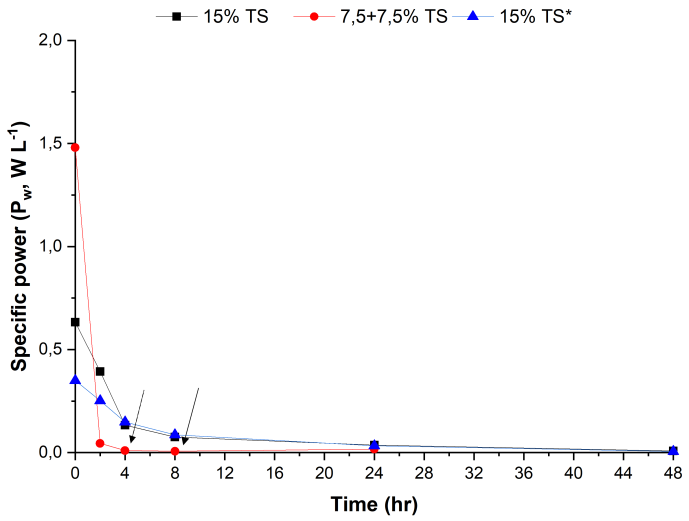

Figure 5.9. Specific power consumption during enzymatic hydrolysis in the Dasari's SSBR configuration

Reaction conditions: 5% E:S, 0.1% NaN_3, 10 rpm, 80 %V (except 40+40%V for the fed-batch assay), 50 °C and pH 4.75-5.25.*Represent batches using raw MSW pulp, and the arrows the fed-batch feeding

absence of working volume, power consumption is not linearly proportional to rotational speed, e.g less than 1 and 3 watts for 4 and 10 rpm, respectively. This study shows that MSW pulp has an increased energy consumption over corn stover [41], even at lower solids loadings due to nature of feedstock and pretreatment method on the agricultural residue.

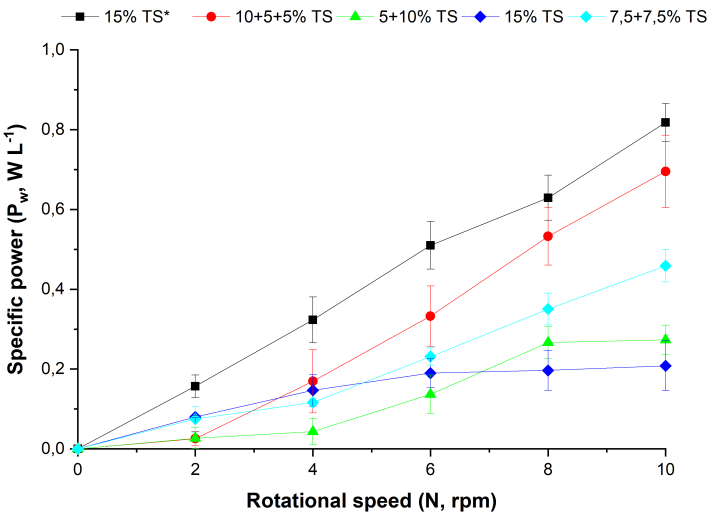

5

Figure 5.10. Specific power consumption as function of rotational speed depending on feeding strategy in the Dasari's SSBR configuration, prior enzyme addition)

Note: working volume of batch, fed-batch (2 aliquots) and fed-batch (3 aliquots) assays were 80, 40 and 26%, respectively, and the *represent batches using raw MSW pulp

5.4.3 Home-made SSBR

This section discusses the investigations using the home-made SSBR as described in the section 2.3.3.2, with corresponding multi-parameter monitoring included in the Appendix B. Unless otherwise stated, the enzymatic hydrolysis of MSW-pulp was carried out as a two-stage hydrolysis (SSBR and stirred tank reactor) with 2-3 aliquot additions and purges. This approach is referred as "semi-continuous" hydrolysis. The timing of the 250-ml aliquot purging/loading is shown for each study. To increase the solids content (15%TS), a fed-batch reaction was conducted, consisting on two aliquot addition 7.5 and 22.5% TS at 4 and 8 hours, respectively. After one-day of reaction, 1 L of SSBR hydrolysate was transferred into a stirred tank reactor for starting the secondary hydrolysis.

5.4.3.1 Batch hydrolysis

A batch hydrolysis was carried out with specific power consumption monitoring and discrete analysis of sugar monomers (Fig.5.11).Setting the reaction mass at constant temperature of 50-55 °C during was achieved by installing a "coiled-tubing jacket", described in section 2.3.3.2. Multi-parameter monitoring of pH/DO and temperature is included in Appendix B (Fig. SI B.2), showing adequate conditioning throughout the hydrolysis experiment. Even with the simplicity of this SSBR, better control of slurry media conditions were performed compared with previous experiments in a SSBR set-up (section 5.4.2). Compared with a reaction in Dasari's SSBR configuration (Fig.5.9), a lower specific power consumption (0.3 to 1.5 W L^{-1}) was recorded at the beginning enzymatic saccharification, operating at similar TS values (7.5-8%). Although, measurements of P_w fluctuated throughout the enzymatic hydrolysis, likely due to back-mixing problems, and the so-called "two-stage kinetics" was not observed. At 17-hours of hydrolysis, moderate yields of sugar monomers were observed (6.5 and 2 g L^{-1} for glucose and xylose, respectively), not comparable with the homologous SSBR configuration (section 5.4.2). In that case, 20 g L^{-1} of glucose titers (Fig.5.8) were achieved in the same time-frame, but with an extra addition of cellulases (5% E:S). Better reaction control is needed in the SSBR, as approx. 6 g L^{-1} glucose were yielded in 17 hours of hydrolysis, compared with a similar reaction run in a stirred tank reactor by Climent Barba et al. [47]). Although resulting into low specific power consumption, greater reaction control is needed to achieve higher sugar titers.

5.4.3.2 Two-stage hydrolysis: no refilling

With the aim of designing a more efficient two-stage enzymatic hydrolysis, duplicate assays were conducted with periodic sampling of hydrolysates for glucose and xylose titers analysis (Fig. 5.12. Multi-parameter monitoring of pH and temperature is included in Appendix B (Fig. SI B.3), showing adequate reaction control. Despite presenting acceptable levels of glucose (10-12 g L^{-1}) and xylose (3-4 g L^{-1})

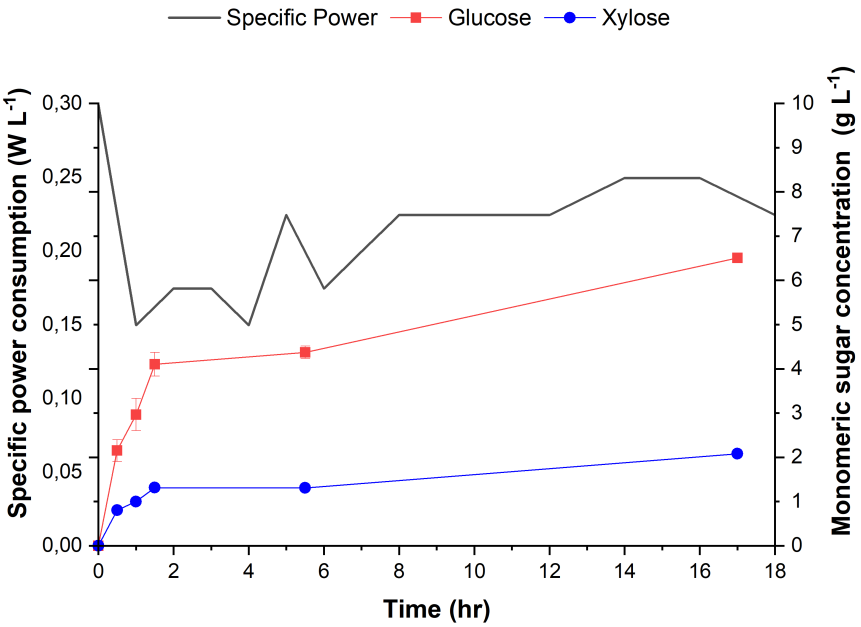

Figure 5.11. Batch enzymatic hydrolysis of MSW-pulp in the home-made SSBR configuration: specific power consumption, glucose and xylose yields analysis

Reaction conditions: 8%TS, 2%E:S, 0.1%BIT, 30% V, 50 rpm, 50° and pH 4.75-5.25. Error bars represent standard deviations of samples, withdrawn from the left, mid and right sampling ports

titers in 24-hours, a decline in sugar monomers is noted thereafter. Discharging a fraction (1L) of SSBR to STR, for carrying on with the enzymatic hydrolysis, did not enhance the release of monomeric sugars. On the contrary, it slightly decreased or plateau in the case of glucose and xylose, respectively. Loss of sugars is mainly attributed to microbial contamination [309], although other factors such as oxidation and acidification may also occurring [124]. Integration of pH/DO monitoring coupled with the analysis of organic acids as contamination control tools, would promote the preservation of sugar syrup and avoid microbial contamination [47]. The so-called "plateau effect" is expected at 24-72 hours depending on solids loadings as suggested by Puri [36]. Implying a completed solubilisation of structural carbohydrates and end-product inhibition to cellulases [236]. Therefore, it is of great importance to control reaction conditions as well as mitigate bacterial contamination, specially in a multi-stage hydrolysis (non-sterility between phases).

5.4.3.3 Semi-continuous hydrolysis: 2 aliquots

In order to increase the production of lignocellulosic sugars without employing larger bioreactor vessels, a two-stage hydrolysis was proposed, consisting on: (i) transfer of hydrolysate from SSBR to STR (purging) and (ii) an equivalent addition of fresh substrate (feeding). Further details are depicted in the corresponding section

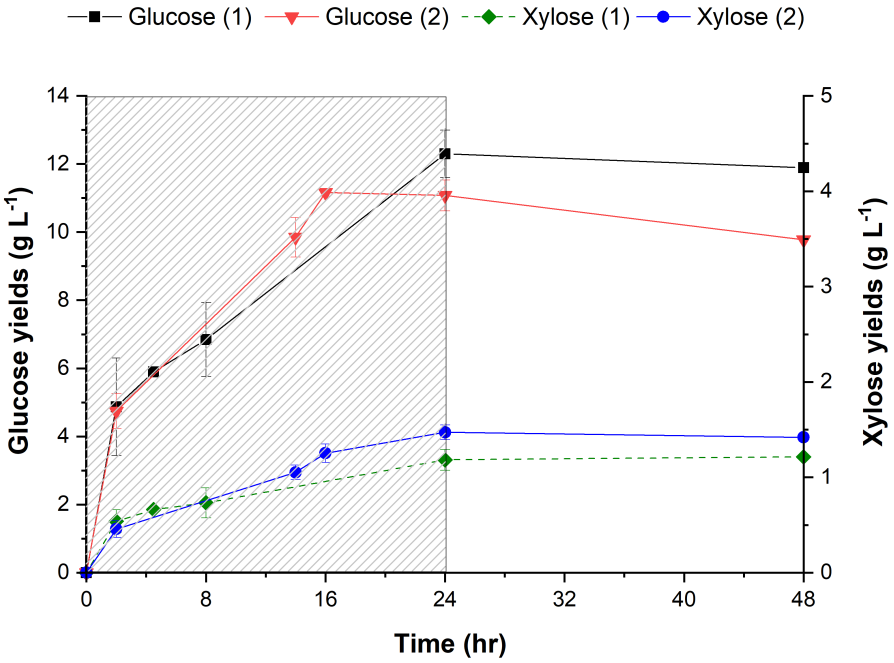

Figure 5.12. Two-stage enzymatic hydrolysis of MSW-pulp in the home-made SSBR configuration

Reaction conditions:8%TS, 2%E:S, 0.1%BIT, 35%V, 30 rpm (300 rpm STR), 50 °C and pH 4.75-5.25
Error bars represent standard deviations of samples, withdrawn from the left, mid and right sampling ports; where numbering is for trial 1 and 2, respectively. In the graph, hatched and non-hatched areas represent timing of primary (SSBR) and secondary (STR) hydrolysis, respectively.

2.4 of Materials and Methods. To overcome potential technical constraints, a preliminary test was run with discrete analysis of sugar monomers whilst monitoring key operational parameters (pH/DO and temperatures) as included in the Appendix B (Fig. SI B.4). Both purged aliquot, 250-ml (4hr) and 150-ml (8hr) were transferred to a secondary enzymatic hydrolysis or a shaker incubator, without addition enzymes. Final hydrolysates (24 hours) were analysed to determine their densities (approx. 1.1 g/L) and the percentage of constitutive fractions (supernatants, insoluble solids, filtrate), where the moisture content of filtrate (PHS) was also determined. Slurry components are represented in pie charts (Appendix B, Fig. SI B.5), composed of 98% and 2% of liquid and solid fraction, respectively, for both secondary hydrolysis aliquots.

Constant pH and temperature readings were achieved over-night (8-16 hours) by periodic NaOH addition and sealing of the water-bath (Fig. B.6. Adjusting the reaction conditions throughout the enzymatic hydrolysis, resulted in good performance of the system (Fig. 5.13). As observed in Fig. 5.13, a 4-fold reduction (0.2 to 0.05 W L^{-1}) in specific power consumption occurred in about 4 hours, with a small increase up to 0.075 W L^{-1} after the first "aliquot substitution"). When adding fresh substrate (with the consequent purging) for the second-time, a minor increment to 0.06 W L^{-1}

was reported. Despite showing several zero P_w values due to stopping the motor for sampling, a clear "two-stage" kinetic was noticed which accounts for an efficient lignocellulosic saccharification [41]. At 4-hours, P_w values approx. reached minimum levels, which translates into a sufficient slurry liquefaction, enabling the purging/feeding operation. In the primary hydrolysis reactors, a constant glucose production rate of 0.5 g L^{-1} h^{-1}, indicated a certain degree of steady-state was reached - main characteristics of continuous bioprocessing [15]. Moreover, in the secondary hydrolysis reactor, the "plateau effect" was avoided during the whole reaction as glucose titers increased from 4 to 7 g L^{-1} after the semi-continuous period. The same glucose concentrations were found in the primary hydrolysis reactor as well. Although higher solids loadings and productivity rates/yields are targeted, this work illustrates that a batch time of 4 hours is enough prior setting the semi-continuous hydrolysis.

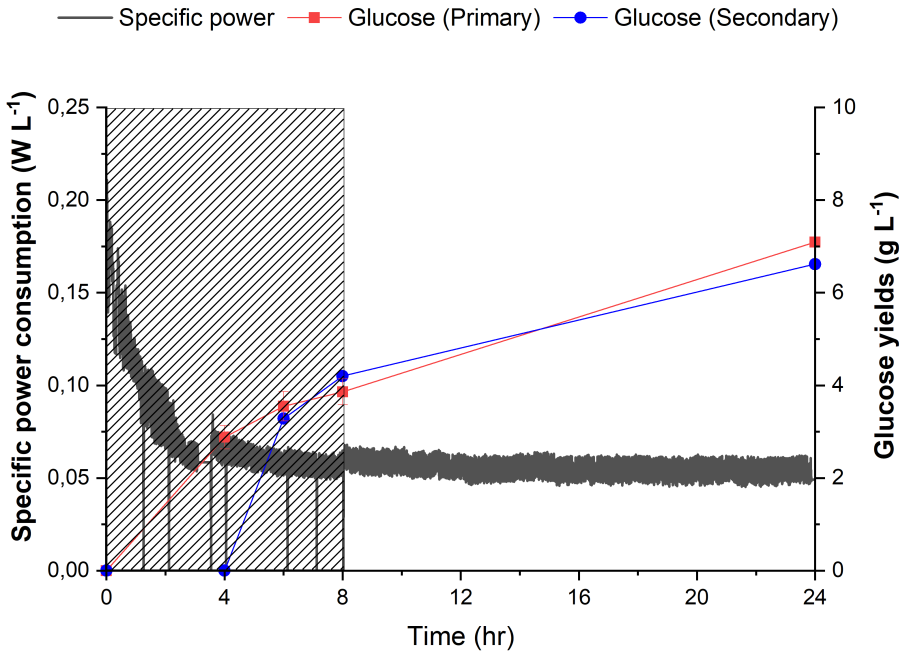

Figure 5.13. Semi-continuous enzymatic hydrolysis of MSW-pulp in the home-made SSBR configuration: specific power consumption and glucose yields analysis

Reaction conditions: 5%TS, 2%E:S, 0.01%BIT, 40%V, 30 rpm (100 rpm STR), 50 °C and pH 4.75-5.25
Hatched box represents timing of semi-continuous hydrolysis period

5.4.3.4 Semi-continuous hydrolysis: 3 aliquots

A variation of the previous experimentation was investigated in triplicate, with constant volume (500 ml) and more frequent "aliquot substitution" (2 hours), to study the effect of shorter residence times. Discrete analysis of the glucose yields of in the primary (SSBR) and secondary (STR) hydrolysis reactors throughout the two-stage

enzymatic saccharification can be found in section 5.14. It was observed that the glucose yields increase in linear proportion to hydrolysis time, when adding fresh aliquots for 8 hours. This implies stable productivity rates of $\sim$ 0.5 g L^{-1} showing a pseudo-steady-state [310]. Except for the third replicate, similar kinetics were observed and final glucose titers yielded within the same range of 7-8 g L^{-1} at 24 hours). For the secondary hydrolysis, high repeatibility of the kinetics and yields were seen, but with some loss of sugars. In contrast to the primary SSBR hydrolysis (Fig. B.7), additional release of fermentable sugars was not observed after transfer, stabilising at 7-8 g L^{-1}. This phenomenon suggest that cellulases are being deactivated, thus incapacitating the further conversion of biomass to sugars [154].

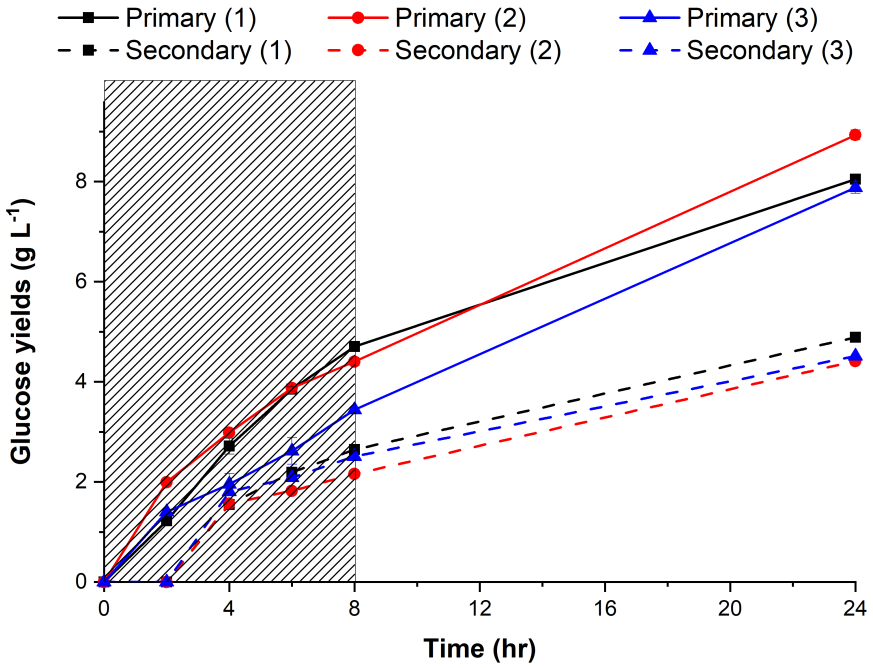

Figure 5.14. Glucose analysis during semi-continuous (3 aliquots) enzymatic hydrolysis of MSW-pulp in the home-made SSBR configuration

Reaction conditions: 5%TS, 2%E:S, 0.01%BIT, 40%V, 30 rpm (100 rpm STR), 50 °C and pH 4.75-5.25.
Trial 1,2,3 are triplicate experiments
Hatched boxes represent semi-continuous and fed-batch for the primary and secondary hydrolysis, respectively

Monitoring of the specific power consumption was done during the two-stage enzymatic saccharification, and each run was plotted in Fig. 5.15. Despite some differences between batches, nearly constant P_w measurements are observed ranging from 0.15 to 0.10 W L^{-1} for the semi-continuous hydrolysis period (8 hours). Zero-value P_w measurements were related to stopping the agitator for sampling as commented upon earlier. Once the SSBR operates in batch (8-24 hours), the power consumption is halved except for replicate 3, where the records oscillate until the end of reaction. A possible explanation behind such high P_w fluctuations could be

related to deviation of torque sensors (± 4 N cm^{-1}) and frequency of monitoring (every 30s). While, power consumption ranged between 0.12 to 0.15, 0.07 to 0.1 and 0.06 to 0.1 W L^{-1} for replicate 1, 2 and 3, respectively, during semi-continuous mode. Power consumption reached steady-state for 8 hours, indicating that continuous processing was achieved for this period of time [243]. Considering the manual approach to this experiment, power consumption was kept constant during purging of processed slurry and feeding of fresh substrate. With implementation of an automated pump system as Stickel et al. [21], the entering and exiting flow-rates can be better controlled which allows operation in steady-state conditions for an extended period of time.

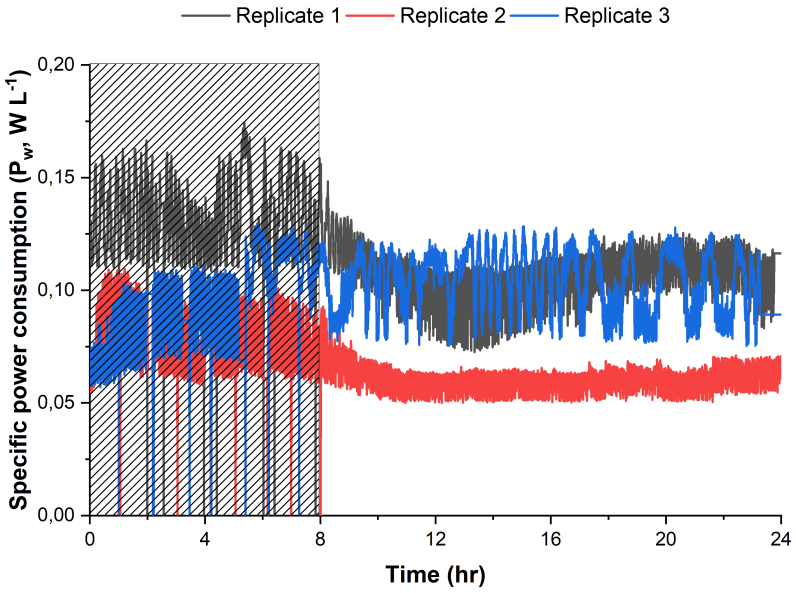

Figure 5.15. Specific power consumption during semi-continuous (3 aliquots) enzymatic hydrolysis of MSW-pulp in the home-made SSBR configuration

Reaction conditions: 5%TS, 2%E:S, 0.01%BIT, 40%V, 30 rpm (100 rpm STR), 50 °C and pH 4.75-5.25.
Trial 1,2,3 are triplicate experiments
Hatched boxes represent semi-continuous and fed-batch for the primary and secondary hydrolysis, respectively

5.4.3.5 Fed-batch hydrolysis

To operate at high-solids loadings (15%TS), a fed-batch hydrolysis was conducted, consisting of: a 2 L addition at 7.5% TS (time 0 h) and 0.5 L addition at 22.5 %TS (time 8 h) for filling 35% of tank volume. After 24-hours, a 1 L of hydrolysate was transferred to a STR for secondary hydrolysis. Continuous and discrete analysis of the specific power consumption and glucose yields were assessed during fed-batch and secondary hydrolysis assays (Fig.5.16). pH/DO and temperature parameters were only monitored in the SSBR configuration for 24-hours of hydrolysis (Fig. SI B.8). It

is worth mentioning that the pH and temperature were kept within optimum conditions for Cellic® CTec3 enzyme cocktail [100]. Despite the addition of fresh substrate, DO measurements show oxygen depletion tending towards anaerobic thresholds at 20-24 hours of hydrolysis, indicating a potential source of microbial contamination [47].

Fig.5.16 shows that P_w measurements were about 1.5 W L^{-1} at the 1^{st} aliquot (7.5% TS, 2L) addition (time zero). The MSW-derived slurry rapidly liquified, requiring less power for mixing, approximately a 12-fold decrease in only 2 hours (1.5 to 0.125 W L^{-1}). The power consumption increased up to 0.5 W L^{-1} as result of feeding the second aliquot (22.5 %TS, 0.5 L). Surprisingly, such an amount of concentrated MSW slurry provokes a 4-fold increment in P_w measurements in the system, despite such small volume addition. In the STR, agitation of 1-L of liquified MSW-pulp slurry (time 8 hours) requires a specific power consumption about 10 times (2.5 W L^{-1}) larger than in the SSBR (0.25 W L^{-1}). Also, the viscosity reduction is slower as taking 10 hours to fall below 1 W L^{-1}, whereas, occurring in only 0.5 hour in the SSBR configuration. Integrating the SSBR with STR using a fed-batch feeding strategy enabled the operability at high-solids loadings. Moreover, the two-stage enzymatic hydrolysis system results in a low power usages than single-phase hydrolysis, reducing the operational costs [262]. This experiment demonstrated the feasibility of solids loadings above 15% w/w by fed-batch and horizontal configurations, which are minimum requirements for a commercial system [2].

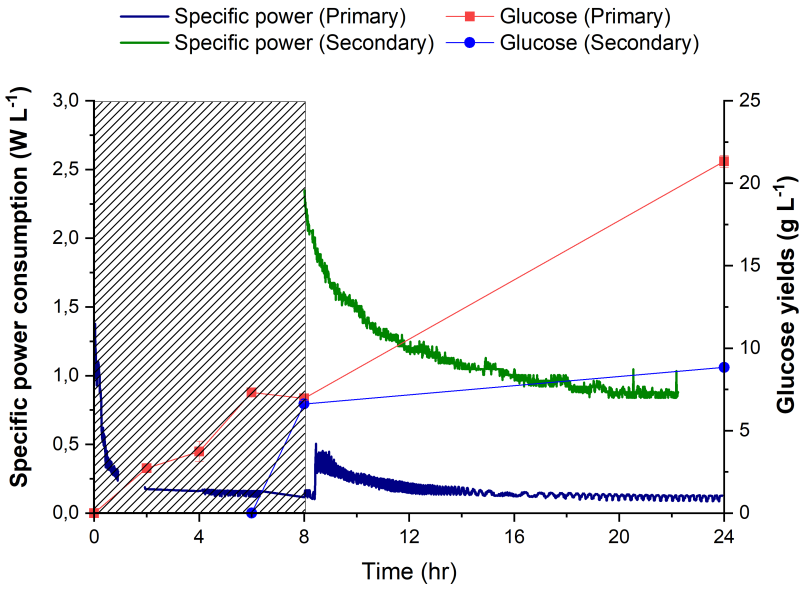

Figure 5.16. Fed-batch high-solids enzymatic saccharification of MSW-pulp in the home-made SSBR configuration: glucose yields and specific power consumption

Reaction conditions: 15% TS (7.8/2.5L and 22.5%TS/0.5L at 8h), 2% E:S, 0.01% BIT, 30 rpm (300 rpm STR), 40 %V, 50 °C and pH 4.75-5.25
Hatched boxes represent semi-continuous fed-batch period of time

For glucose yields (Fig.5.16), two distinct reaction kinetics are observed depending upon the primary or secondary hydrolysis reactors. As achieved in earlier semi-continuous runs, glucose yields evolved linearly over the time, reaching steady-state conditions. In contrast, the glucose titers plateau experienced after transfer to the secondary hydrolysis tank, indicating end-product inhibition [72]. In batch mode, the evolution of glucose concentrations follows the Michaelis-Menten kinetics [139]. Before 24 hours, the lignocellulosic feedstock is not exhausted as further monomeric sugars should be released. Despite this, the fed-batch approach doubled the productivity rates (0.5 to 1 g L^{-1} h^{-1}) compared to batch reactions, which were kept constant in the first hydrolysis step. From 8 to 24 hours hydrolysis, the glucose concentrations increased to 20 g L^{-1} after feeding fresh substrate into the SSBR. In parallel, the STR glucose concentrations plateaued at $\sim$ 9 g L^{-1}, indicating possible product inhibition. The transfer of slurries between tanks by manual handling does not promote enzymatic saccharification, which could be attributed to an exhaustion of lignocellulosic sugar sources. One possible operating error was inefficient pumping of the lignocellulosic slurry, potentially leaving the unhydrolysed fraction at the bottom or side of SSBR. Therefore, fewer solids were left in the STR for the hydrolysis. To overcome this, better reaction control [47] and pumping strategies [21] should be implemented to enable a two-stage enzymatic hydrolysis.

5.4.4 Rolling bottles as rotary drum reactors

This section includes experimentation using the set-up as described in the Materials and Methods section 2.3.4.

5.4.4.1 Baffle effect in glucose and adsorption yields

The inclusion of baffles in bioreactors for enzymatic hydrolysis of lignocellulosic feedstocks has received little attention, despite the community is being well-aware of their advantages for improving processing yields [212]. For instance, Correa et al. [194, 254] investigated different operational parameters of steam-exploded sugarcane bagasse hydrolysis (power consumption, biomass conversion, mixing time) in a homemade stirred tank reactor equipped with four baffles. More recently, other authors have evaluated the effect of including baffles for enzymatic hydrolysis of biomass [146, 311]. In a stirred tank reactor, Kinnarinen et al [311] showed no experimental uncertainty in glucose yields at 8-12% solids contents of saccharifying cardboard waste if baffles were included with of double propeller and Rushton turbine impeller geometries. A similar effect was reported by Roche et al. 2009 [146] in rotating jars equipped with 0 to 4 baffles during enzymatic hydrolysis of pretreated corn stover at high-solid loadings. It is not clear why the effect of baffles was neutral during these studies, since baffles have been utilised for enhancing good mixing and processes from cell culturing to bioleaching [295]. A plausible explanation could

be related to substrate stagnation due coarse particles, and, heterogeneous mixing behaviour at high-solids [183].

To verify the benefits of including baffles as means for increasing glucose yields in MSW-pulp enzymatic saccharification, several hydrolysis experiments were conducted with 0, 1 and 3 baffles under the same reaction conditions (Fig. 5.17). The design and installation of baffles is described in section 5.3, and was performed in accordance of with guidelines for rotary drum reactors [43]. Little difference was observed during 24 hours of enzymatic saccharification within the two groups of experiments, yielding glucose yields from 50 to 60 g L^{-1}. However, from 24 to 48 hours, a significant increase in glucose titers was seen in the baffled reactors, after biomass liquefaction. At high-solids loadings, it is suggested that baffles do not improve mixing features in the first stages of enzymatic hydrolysis, due to viscosity of slurries. Once liquified, mass and heat transfer is enhanced by the use of baffled reactors. As demonstrated in the literature [294], better aeration is achieved by incorporating baffles, consequently, more oxygen is accessible for the LPMO enzymes. Although, it is unclear what is the electron acceptor in the LPMO oxidation mechanism (molecular oxygen or peroxide) [124], an oxygen source enhances this type of enzymatic activity, and better aeration promotes the saccharification.

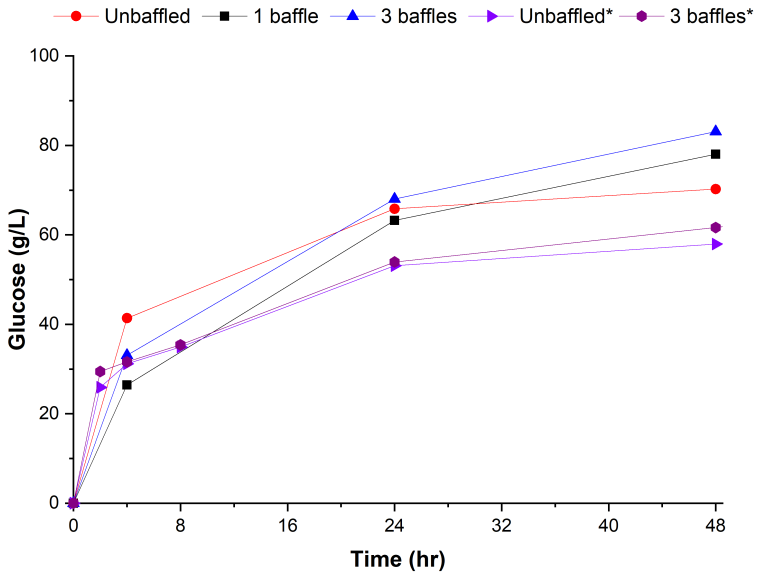

Figure 5.17. Baffle effect (unbaffled, 1 and 3 baffles) on glucose yields during enzymatic hydrolysis of MSW-derived slurries

Reaction conditions: 20%TS, 2% E:S, 0.1% BIT, 30 rpm, 50 °C and pH 4.75-5.25
* represent hydrolysis experiments with natural pH control control and using older enzyme cocktails

To determine whether enzyme adsorption to the substrate is a factor of in enhancing glucose yields [154] in baffle reactors, the protein content was analysed in the lignocellulosic hydrolysates (Fig.5.18). The determination of protein content (in %) enabled the calculation of enzyme adsorption (section 2.9.5.1), as ratio between

free and neat enzyme in units of protein mass. Initially, $\sim$ 600 mg of protein were loaded, but this rapidly adsorbs to the substrate (2 hours), decreasing the concentration of free enzymes by a factor of 3 and 6 for unbaffled and 3 baffled runs, respectively. However, enzyme adsorption was incomplete as more than 100 mg protein were still present in the hydrolysate broth, unattached to the substrate. The difficulties of adjusting optimum conditions throughout the slurry, and the presence of highly coarse particles may be associated with an incomplete enzyme adsorption [24].

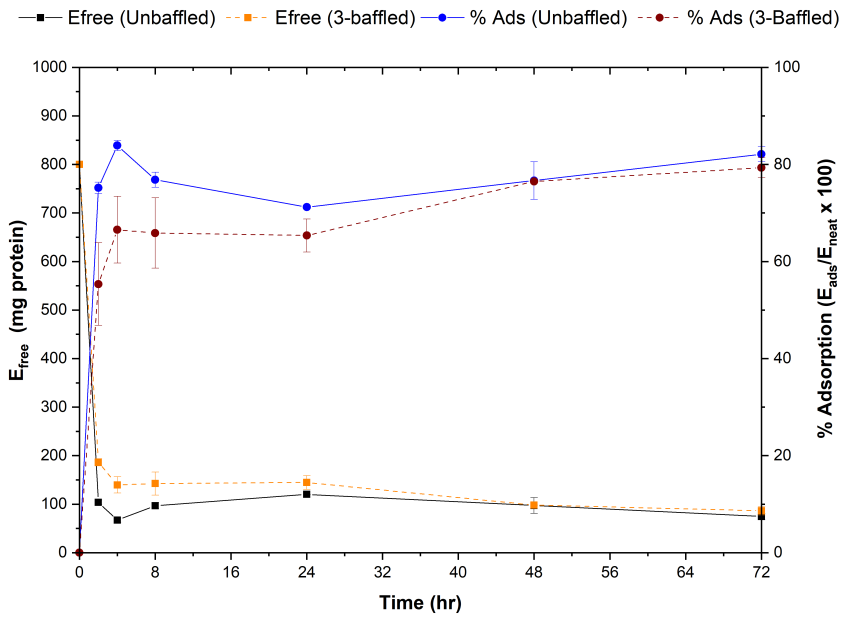

Figure 5.18. Baffle effect (unbaffled and 3 baffles) on enzyme adsorption during enzymatic hydrolysis of MSW-derived slurries

Reaction conditions: 20%TS, 2% E:S, 0.1% BIT, 30 rpm, 50 °C and pH 4.75-5.25. Error bars represent the standard deviations (σ) of triplicates from each hydrolysates collected at discrete time-points

In both runs, the percentage of enzyme adsorbed surpassed 60% in only 4 hours of reaction (Fig.5.18). The presence baffles results into higher enzyme adsorption than unbaffled tanks for at least two days of reaction. However, unbaffled baffles presented an increase on enzyme adsorption (Fig. 5.18, no improvements on glucose yields were observed (Fig. 5.17). Roughly 80% enzyme adsorption was achieved in the two reactor configuration. It is reported that cellulases adsorb within the first 10-15 minutes of hydrolysis [212]. This could also be occurring in the MSW pulp saccharification with Cellic CTec3 cocktails, as seen in other studies of starch-based feedstocks with commercial enzymes formulations [312]. More frequent and earlier analysis of protein content is needed to corroborate this fast enzyme adsorption.

5.4.5 Pseudo-flow hydrolysis: manual continuous mode

Due to high capital cost, high slurry viscosity and poor flowability, it was not possible to conduct a continuous enzymatic hydrolysis of MSW-pulp. Model compounds (e.g. Avicel®) could have been used instead, for setting-up a continuous system, but it would not be representative an industrial system for MSW-pulp. To mimic a continuous enzymatic saccharification with MSW-pulp slurries, an intermediate process was designed known as "pseudo-flow hydrolysis". The pseudo-flow procedure is widely described in the Materials and Method (section 2.6).

With this in mind, pseudo-hydrolysis experiments were carried out in duplicate (exp. no. 1 and 2) for 50-72h, with discrete analysis of monomeric sugars (glucose and xylose) in 2-L rotary drum (Fig. 5.19). The purged slurry was transferred to a second unit, for continuing the reaction (Fig. 5.20). Keeping optimum pH values throughout the experiments was achieved as illustrated in Fig. B.9. At the same time, mass flow rates were calculated off-line, to show that the volume was constant in the primary reactor, equally purged in both secondary vessels (Fig. B.10 with corresponding densities (Fig. B.11)

It was noticed that a "pseudo-steady-state" was achieved during 1-4 space volumes (around 16 hours) for glucose and xylose yields, more precisely in the latter sugar monomer. A higher glucose variability in batches could be that it is more prone to biological contamination than xylose as described in Chapter 3. On average, around 25 and 5 g L^{-1} of glucose and xylose yields were released during the pseudo-flow period. When moving to batch, concentrations of the sugar monomers increased proportionally up to 80 and 24 g L^{-1} in 76 hours (batch 1). Meanwhile, for the second run, approximately 54 and 13 g L^{-1} were released for glucose and xylose, respectively, at 52 hours. The shorter batch residence time of batch no.2 was associated to facilities closure due to COVID-19 pandemic.

Steady-state continuous enzymatic hydrolysis (CEH) has been previously set by Stickel et al. 2018 [21], in the enzymatic hydrolysis of 5-10%TS pretreated corn stover in a membrane-reactor system. Better purge control with a series of pumps and membrane recirculation led the achieve steady-state mode within 1-2 space-volumes, at 2-5% solids loadings. More recently, improvements in either enzymes (20 to 10 mg protein g enzyme) and solids (5 to 8.5%TS) were achieved with same feedstocks and CEH set-up [22]. Despite the simplicity of the approach, in this study, near steady-state was reached using high-solids loadings of MSW-pulp slurries. In comparison with to other studies, the system has better bioprocessing equipment and milder conditions [21, 22]. Both runs showed high repeatibility with 90% confidence interval at most data-points, despite the non-automation of the system.

In the secondary tanks, partially-liquified slurries were further saccharifying in fed-batch mode (Fig.5.20), in parallel of the primary stages. Due to volume constraints, 500-ml of purged aliquot was divided in two vessels, therefore, average values of sugar monomers are plotted in Fig. 5.20 with the standard deviations. The second experiment showed a higher variability in the results, suggesting that

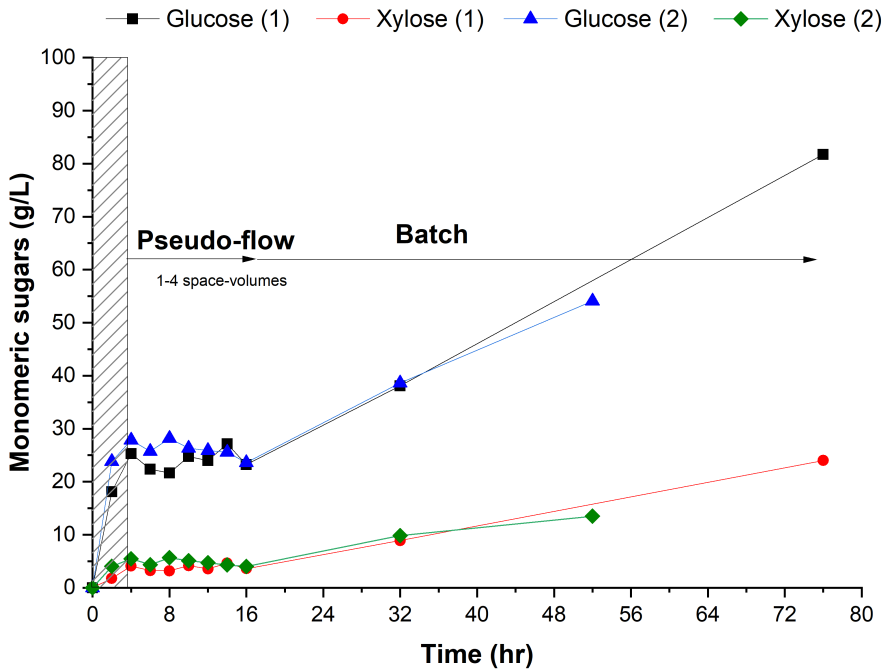

Figure 5.19. Pseudo-flow enzymatic hydrolysis (batch 1): monomeric sugars in primary and secondary hydrolysis reactors

Reaction conditions: 20% TS, 2% E:S, 0.01% BIT, 30 rpm, 80 %V, 50 °C and pH 4.75-5.25
The hatched box zone represents the start-up (batch) time of 4 hours [1]

sampling errors occurred during the high-solids operation [149], but, not in the first pseudo-flow hydrolysis test. As recommended by Modenbach et al. [17], fed-batch hydrolysis overcomes viscosity limitations due better mixing, and in consequence, higher glucose titers are yielded in comparison to batch hydrolysis. Surprisingly, a 10 g L^{-1} difference was observed between exp. 1 and 2 at 52 hours of hydrolysis: 85 to 75 g L^{-1}, respectively. Several factors could explain the improvements in glucose yields, e.g. high feedstock heterogeneity or less product inhibition [145]. Furthermore, greater control of the slurry-media conditions (Appendix B, Fig. SIB.9b) for the optimal activity of enzymes was achieved as result of familiarity with the new process design. Puri et al. [32] demonstrated that a two-stage enzymatic hydrolysis of MSW-pulp improved the glucose yields in comparison with a conventional single-stage system. In our case, no additional processes were needed (intermediate fermentation or wash step with/without β-glucosidase addition), as means to enhance process yields in comparison with the previous study [32]. The "pseudo-flow hydrolysis", employing rotatory drum reactors, has demonstrated that high-solids enzymatic hydrolysis of a MSW-pulp can be converted from batch to continuous. Even without process automation, the commercial requirements in terms of glucose yields (80 g L^{-1}) were satisfied as requirement for a commercial exploitation [2].

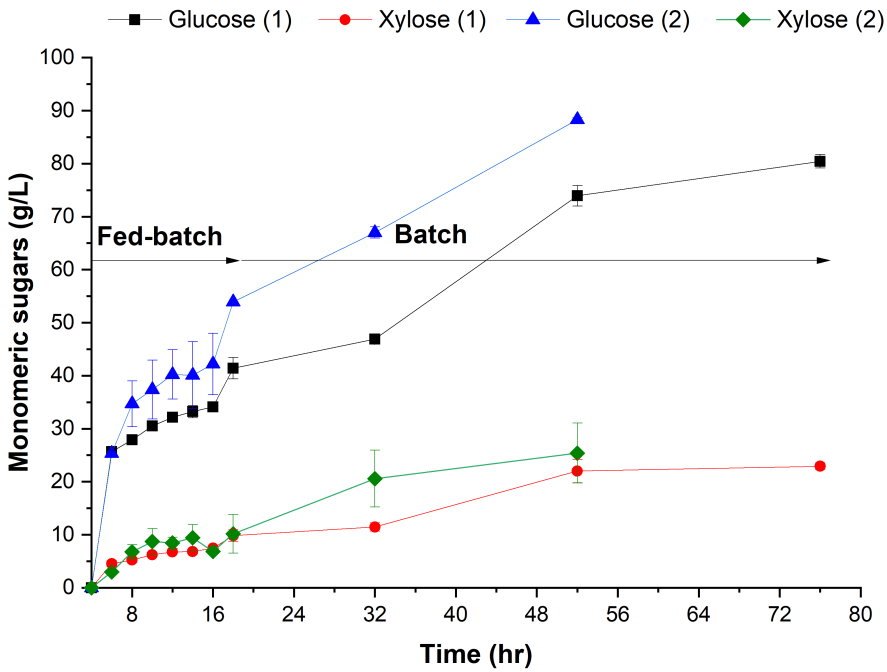

Figure 5.20. Pseudo-flow enzymatic hydrolysis (batch 2) of MSW-derived pulp: monomerics sugars in primary and secondary hydrolysis reactors

Reaction conditions: 20% TS, 2% E:S, 0.01% BIT, 30 rpm, 80 %V, 50 °C and pH 4.75-5.25. Error bars represent standard deviations (σ of average measurements, per experiment, in secondary hydrolysis stages

5.4.6 Reactor comparison

Based on previous findings (Chapters 3-5), the main parameters for each reactor are compared, based on batch processing (Table 5.4). Due to their poor scalability, shake flasks were not included despite being used (Chapter 3), and, operational parameters (e.g. power consumption in mixing) could be theoretically calculated [313, 314]. Hence, the four reactor designs described in Chapter 2 (section 2.3) are compared. Seven process parameter/aspects were selected and determined for each reactor design, abbreviated as; STR, SSBR, home-made SSBR and RDB (Table 5.4).

The solids loadings (TS) is one of most important factors in enzymatic hydrolysis, as higher loadings lead to higher sugar concentrations, minimising capital and operational costs [93]. As commented earlier, operating with solids above 15 % w/w is required for yielding around 80-100 g L^{-1} of glucose, the "commercial threshold" of lignocellulosic sugars [2]. By reviewing and investigating the high-solids regime and suitability of bioreactors (section 3.2.3 and 5.2.5), the maximum TS values were compared per configuration for each batch mode (Table 5.4): RDB (25%) SSBR (15%), home-made SSBR (12 %) and STR (10%). As expected, horizontal reactors were able to handle higher solids contents, in particular RDBs followed by scraped surface bioreactors (Dasari's and our home-made, but not by stirred tanks. In batch, horizontal reactors and STRs equipped with helical or peg-mixers can handle high-solids

Table 5.4. Comparative study of reactor design on operational parameters in batch enzymatic hydrolysis of MSW-derived slurries

	STR	SSBR	Home-made SSBR	RDB
Max. TS (%)	10	15	12	25
Glucose yields[a] (g L^{-1})	10	NA	12	14
Initial P_w (W/L)[a]	2.5 (600 rpm)	1.5 (10 rpm)	1.25 (30 rpm)	3.25 (30 rpm)[b]
E_f (g glucose Wh^{-1})	0.31	3.33[c]	4.00	0.17[4]
Footprint (cm^2/L)	100	250	120	200
Probe/sampling ports	4	4	12	0
Others	Qvis & FTIR	NA	Qvis & FTIR	NA

Legend: SSBR is Dasari's SSBR configuration, E_f is energy efficiency, NA is not applied and Qvis is an in-line viscometer
[a] 7.5-8 %TS, 2% E:S and 0.1% anti-microbial, 50-55 °C and pH 4.75-5.25, [b] determined by a dual-plug meter device at 30 rpm (independent of TS value) and [c] normalised measurements at 5% E:S

loadings [2]. The vertically-orientated reactors with a pitched-blade impeller are not functional for solid loadings above 10% (in batch), due to inefficient mixing leading to poor mass/energy transfer [146].

Glucose is the main product of enzymatic saccharification of biomass, whose concentration depends on numerous factors : reactor performance, carbohydrate fraction, enzyme loading/type, total solids etc.. [275]. To simplify the comparison between reactor designs, final glucose titers (24 hours) were normalised for solid loadings at same enzyme doses (Table 5.4): SSBR (20 g L^{-1}/g substrate) < RDB (14 g L^{-1}/g substrate) < iPRD SSBR (12 g L^{-1}/g substrate) < STR (10 g L^{-1}/g substrate). Since the SSBR assays were run with 5% E:S, associated glucose yields are excluded for comparison. Approximately 10-14 g L^{-1} glucose concentrations were released depending upon the reactor choice at reaction conditions of: 7.5-8% TS, 2% E:S and 0.1% antimicrobial addition (e.g. BIT). Notwithstanding, these differences at 2-4 g L^{-1} glucose concentration, the economical viability of enzymatic hydrolysis would depend upon the choice of reactor design.

Initial power consumption (P_w, in W L^{-1}), as throughout the hydrolysis process, is an important factor for evaluating the energy efficiency upon the reactor configurations (Table 5.4). Higher agitation rates result in more power consumption through mixing ($P = 2\pi MN$), the P_w values were normalised by rotational speed. Apart from the RDB design, determined by a dual-plug meter (3.25 W L^{-1} at 30 rpm), the rest of the P_w measurements were estimated by torque-meter. With this in mind, the reactors designs were ranked according to the normalised specific power consumption: 1.25, 1.5 and 2.5 W L^{-1} for home-made SSBR, SSBR and STR, respectively. As a "rule of thumb", the specific power consumption are typically in the range of 1-5 W L^{-1} [234]. Even at the lower end, the power requirements for industrial application would be prohibitive. Table 5.4 also include rotational speeds for the calculation of normalised specific power consumption for the STR (600 rpm) , SSBR (10 rpm), home-made SSBR and RDB (30 rpm) configurations. It is worth mentioning that STR requires 600 rpms for mixing, compared to only 10 and 30 rpm for SSBR and home-made SSBR configurations, respectively. Stirring at 600 rpm, mixing "dead zones"

were observed in the stirred tank prior liquefaction.

RDBs would require a torque-based measurement to include them in a direct comparison. No information in regards of power consumption has been found on RDBs for enzymatic hydrolysis of biomass [241]. In other biorefineries such as anaerobic digestion treatment of MSW, the energy analysis of RDBs is well-reported [277]. Zhang et al. [315] reviewed a range of US facilities for the production of MSW-derived feedstocks into biogas, consuming from 0.04 to 0.1 W L^{-1} (Appendix B, Table SIB.1). Similar values of P_w are also found in the powder technology, e.g. Liu et al. [295] investigated the power consumption of employing RDB for bioleaching of 10% w/w of Al_2O_3 slurries at 10 rpm, indicating that P/V measurements remained below 0.4 W L^{-1}.

The ratio between glucose yields and total energy consumption (Eq. 5.1), known as energy efficiency (in g L^{-1} Wh^{-1}), represents the overall energy consumption in mixing per mass production of sugar. This parameter dictates the energy-efficiency of enzymatic saccharification. With this in mind, high quantities of sugars with minimal energy output are targeted. Reactor designs were ranked upon energy efficiency: home-made SSBR (4 g Wh^{-1}) < SSBR (3.3 g Wh^{-1}) < STR (0.31 g Wh^{-1}) < RDB (81 g Wh^{-1}). Due to differences on enzymes dosages and electrical measurements in SSBR and RDB, respectively, it would be accurate to only compare the home-made SSBR and STR set-ups in terms of energy efficiency. For an enzymatic saccharification of 24 hours, the STR represents a 10-fold decrease in energy efficiency (0.31 g Wh^{-1}) over the home-made SSBR (4 g Wh^{-1}). The faster rotational speed but less mixing efficiency are key factors for accounting to such low E_f in stirred tanks. On the contrary, in the home-made SSBR configuration, lignocellulosic sugars are released more efficiently and with a gentle agitation. Dasari et al [42] reported energy efficiencies, ranging from 7-15 g glucose Wh, during enzymatic saccharification of pretreated corn stover (10-25%). This study highlight the need for high-solids regimes as electricity outputs vastly decrease per mass of sugar.

In industrial processes, the footprint is a term used to describe the area (space) taken by a manufacturing unit for on-site operation. A compact design, occupies less space horizontally. In plant commissioning, taller units are preferred to wider ones, as vertical spacing is cheaper than horizontal. Therefore, smaller footprints are more attractive for plant design and operation lowering the capital and operational expenditures. At laboratory scale, the footprint of the various reactor designs employed was calculated, and normalised to the reactor volume (Table 5.4). The footprint was estimated as the area per volume of reactor set-up, including agitator and heating systems: 100 (STR), 250 (SSBR), 120 (home-made SSBR) and 200 cm^2 L^{-1} (RDB), respectively. Both STR and home-made SSBR stand out in terms of footprinting, halving the space required for operation over the other designs. Stirred tanks are well-known for their compact design, but surprisingly, the home-made SSBR design showed a smaller footprint. The home-made SSBR design was based on Dasari's SSBR (section 5.4.2), so the footprint could be further enhanced. The

others configurations were not optimised in terms of footprint due to their simple or off-shelf designs, e.g the RDB design as PP bottle place on a roller apparatus.

Other aspects related to reactor operation were included to showcase the ability of the reactor configurations regarding *in situ* monitoring and sampling during enzymatic saccharification. A high number of sampling/probe ports facilitates the reactor control and monitoring, providing more or less information on key analytical parameters. Table 5.4 summarises the number of probe/sampling ports per reactor design: 4, 4, 12 and 0 for the STR, SSBR, home-made SSBR and RDB, respectively. In addition to this, there is the possibility of attaching unconventional probes (Qvis and FTIR) by modifying the reactor lids, offering scientific information on alternative disciplines.

5.4.7 Comparison between modes of operation

From the previous results (Figs. 5.17, 5.19 and Fig.5.20), the process parameters for the three modes of operation (batch, fed-batch, pseudo-flow) were compared (Fig.5.21). All data-points were taken from reactions that were conducted at same reaction conditions and reactor geometry. In the pseudo-flow hydrolysis, steady-state mode was not feasible for longer residence times (48 hours), due to the manual nature of the operation, but considered for comparative purposes. With this in mind, glucose yields are 80 $\pm$ 0.92, 63 $\pm$ 1.2 and 25 $\pm$ 0.8 g L^{-1} for batch, fed-batch and pseudo-flow hydrolysis experiments at 48 hours of reaction. An approximated 30% improvement is observed when hydrolysing MSW-derived pulp in fed-batch over the batch strategy, and a 20% increment over pseudo-flow hydrolysis. Highly-concentrated sugar syrups (above 80 g L^{-1}) are desired for the commercialisation of lignocellulosic sugars and derivatives [2], enabling the minimisation of downstream costs (e.g. distillation). Although, the glucose titers is a key aspect, it is not the only indicator for evaluating the feasibility of a lignocellulosic biorefineries [15], e.g. mass production and productivity rates.

Productivity is an important factor for the successful deployment of industrial bioprocessing [316]. In this case, a glucose productivity of $\sim$ 12 g L^{-1} h^{-1} was achieved by the pseudo-flow hydrolysis after 48 hours, greatly exceeding the batch and fed-batch productivities: 1.2 and 1.5 g L^{-1} h^{-1}, respectively. The rapid hydrolysis of amorphous cellulose results in the highest production rates within 2-4 hours of enzymatic saccharification[237], and is maintained during the pseudo-flow hydrolysis period. On the contrary, an exponential decay was seen in batch and fed-batch hydrolysis, achieving final productivities of $\leq$ 2 g L^{-1} h^{-1}. One of the benefits of converting the enzymatic hydrolysis from batch (or fed-batch) to continuous is the achievement of 6-fold higher productivity rates. However, further modification of the continuous processing systems is necessary to produce glucose titers for commercial applications (min. 80 g L^{-1}), whilst enhancing the production rates.

In addition, another group of parameters were estimated upon mode of operation (Table 5.5). From the home-made SSBR runs (section 2.3.3.2), the operational

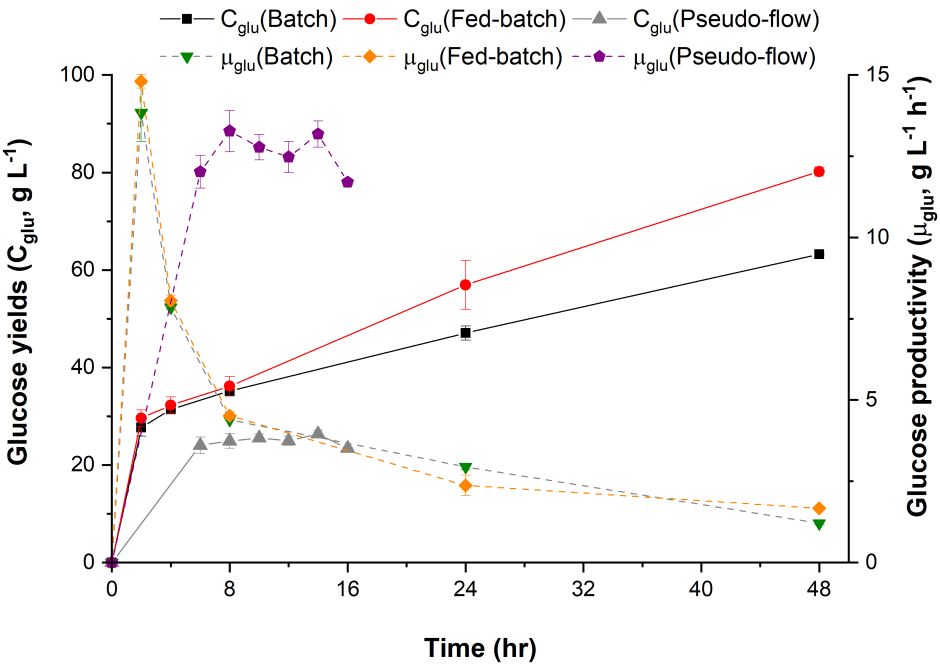

Figure 5.21. Comparison of glucose yields and rates during enzymatic hydrolysis of MSW-derived slurries per mode of operation: batch, fed-batch and pseudo-flow

Reaction conditions: 20% TS, 2% E:S, 0.01% BIT, 30 rpm, 50 %V, 50 °C and pH 4.75-5.25
Error bars represent standard deviation of duplicate experiments. All hydrolysis experiments were conducted in a 2-L drum rector

parameters were extrapolated to a residence time of 24 hours, except for continuous processing (4 hours). Values were normalised to total solids (torque) or total solids and processed volume (total energy) in order to establish direct comparisons between modes of operation. Higher torque measurements were recorded in the continuous process (10 N cm^{-1}), due to short residence time (4 hours). In contrast, in batch and fed-batch, the torque measurements were 6 and 4 N cm^{-1}, respectively. In the same reaction conditions, the torque evolves differently upon feeding strategy and length of time [303]. However, a larger production of sugars minimises the energy consumption (1.5 Wh L^{-1}) in continuous over batch (15.4 Wh L^{-1}) and fed-batch (10.5 Wh L^{-1}), where even higher torque measurements were recorded. As commented upon previously, the fed-batch results to low energy consumption, herein reported as lower torque and total energy measurements over batch and continuous processing.

5.5 Chapter summary

In this chapter, various topics of around reactor design and operation were investigated and these are summarised as follows.

Stirred tank reactors showed poor suitability to high-solids loading due to high-initial viscosity leading to poor mass and heat transfer. Moreover, elevated power

Table 5.5. Comparison of operational parameters during enzymatic hydrolysis of MSW-pulp in the home-made SSBR configuration depending on mode of operation: batch, fed-batch and continuous

	Batch	Fed-batch	Continuous
Batch time (h)	24	16	4
Downtime (h)	4	12	4
Torque (M, N cm^{-1})	6	4	10
Total energy consumption[a] (ϵ, Wh L^{-1})	15.4	10.5	1.50

[a] ϵ is the integral of specific power consumption (set at specific batch-time) per a total of 24 hours, measured with a torque-sensor attached to the SSBR configuration

inputs ranging from 1 to 3 W L^{-1} were observed even at 5-7%TS. These power requirements are prohibitive for industrial processing, and would be accentuated at higher solids loadings. In the literature, mitigation of the "solids-effect" is addressed by employing helical ribbon impellers and/or a fed-batch strategy, but both give poor scalability.

A scraped surface bioreactor was assayed with different feeding strategies of MSW-pulp aliquots during a placement stage at the University of Louisville (Kentucky, USA). Although, facing some technical barriers during testing, Dasari's SSBR configuration allowed operation at high-solids loadings (also in batch) which was previously impossible in STRs. Additional advantages of STRS are low specific power consumption (>1 W L^{-1}) , mainly due low agitation rates (10 rpms).

A *home-made SSBR* was designed and built based upon placement's experience. Multi-parameter pH and temperature monitoring were set along the whole vessel was achieved, and "coiled-tube" heating system was used to maintain the reaction at 50-55 °C. A semi-continuous hydrolysis was carried out for 8 hours, and was validated with high repeatability between batches.

Testing of *rotary drum reactors* as roller bottles was successfully proven at high-solids loadings, as previously stated in the literature. Installation of baffles increased the glucose yields after one-day of reaction due to claimed benefits in improving aeration and mixing, the former issue was potentially related to LPMO activity. Using baffles, no advantages were observed for enhancing enzyme adsorption, on the contrary, it decreased during 8-24 hour of enzymatic saccharification.

Based on the previous findings, a *pseudo-flow hydrolysis* was successfully conducted to mimic a steady-state reaction with rotary drum reactors. Even operating by hand, high repeatibility was noted between the two runs with increasing amounts of resulting sugars in the secondary hydrolysis reactor compared to a single-phase assay. This work has provided guidelines for designing an automated continuous design for enhancing the commercialisation of MSW-derived slurries into lignocellulosic sugars.

Reactor configurations were compared showing that STRs are unfavourable options for processing lignocellulosic biomass via enzymatic hydrolysis, due to the excessive power and mixing-time requirements. Neither high-solids loadings nor low

power inputs and mixing-times were achieved using this geometry. Whereas, the horizontally-orientated reactors (scraped surface and rotary drum bioreactors) were demonstrated to be successful with high-solids enzymatic hydrolysis. Notwithstanding, each horizontal configuration has a particular drawback: solids content below 15%TS and absence of on-line monitoring for the SSBR and RDB, respectively.

Regarding *modes of operation*, continuous processing stands out in terms of productivity and energy costs per unit of processed volume. Considering the downtime costs and accurate process design (further elaborated in Chapter 6), these show greater commercial viability for both the batch and fed-batch strategies. Through modelling and techno-economic analysis, the best design for the two-stage hydrolysis will be indicated as well as pointing out the associated plant expenditures (capital and operational), revenues and profits.

Overall, this chapter has looked at reactor designs (stirred tanks vs horizontal reactors) and operations (batch, fed-batch and continuous), comparing the main process aspects for the enzymatic hydrolysis of a MSW-pulp slurry. The main advantages and disadvantages of selecting one or other configuration is described, highlighting the suitability of horizontal reactors for high-solids bioprocessing with low energy consumption. Moreover, a pseudo-flow hydrolysis was designed and tested for mimicking continuous processing, showing that steady-state conditions can be achieved after 3 space-volumes and productivity rates were enhanced over batch and fed-batch hydrolysis modes.

Chapter 6

Optimisation, modelling and techno-economic assessment for scaling-up

6.1 Introduction

This chapter covers the investigations of various methodologies for the optimisation, modelling and techno-economic evaluation of enzymatic saccharification of MSW-pulp systems. Each section includes the corresponding literature analysis, research methodology and result/discussion.

6.2 Literature review

6.2.1 Process optimisation

In enzymatic hydrolysis of biomass, as in any type of reaction, optimisation consists on the selection of an option that comes closest to an economic optimum performance/operation. The criteria behind the economic objective involves fulfilling certain restrictions, conditions, design equations, whilst respecting the limits of the system [317]. In the context of enzymatic hydrolysis, maximum glucose yields with minimal enzymes dosages and power requirements are targeted as optimisation factors. Finding the optimum parameters has many solutions, sometimes becoming endless. Process optimisation can be conducted by multiple methods (hands-on and computer-aided), including the real-time application of mathematical algorithms [318]. To simplify, we reviewed two optimisation approaches, one-variable-at-a-time (OVAT) and design of experiments (DoE), the latter including response surface methodologies (RSM) has common tools for optimising the bioconversion of biomass to glucose.

6.2.1.1 One-variable-at-the-time in enzymatic hydrolysis

Prior to the introduction of DoE tools, experiments were optimised by an OVAT approach as means for studying the effect of only one variable (e.g. rotational speed)

whilst keeping the rest constant during experimentation. In lignocellulosic biorefining, many aspects can be optimised such as pretreatment conditions and optimum cellulase conditions. Commonly, OVAT approaches can be found in studies, entitled as the effect" or "effect", for the optimisation of operational parameters concerning reactor performance: rotational speed, power consumption and reactor volume.

As power consumption is a function of rotational speed (P= 2π =MN), affected by reactor design and impeller geometry [194]. The effect of stirring speed on conversion yields, among other parameters such as power consumption, particle-size distribution and mass-transfer [58, 73, 196, 251], has been widely investigated in the enzymatic hydrolysis of agricultural and forestry residues. Wojtusik et al. [73] investigated the mass-transfer and conversion yields as function of stirring speed, for enzymatic hydrolysis of corn stover, concluding that best results were obtained at 500 rpm. Working with forestry residues, Palmqvist et al. [196, 251] reported maximum conversion yields at same agitation rates (500 rpm), but consuming the largest amounts of energy. Corroborated by Kadic et al. [58], stirring speeds of at least 500-600 rpm are required for adequate mixing of solids loadings above 13% TS in stirred tanks reactors equipped with pitched-blades.

In a paddle reactor, Jorgensen et al. [93] showed that cellulose conversion during 24 hours of the enzymatic hydrolysis of wheat straw, was independent of rotational speed (4 to 12 rpm). Similar results were found by Kadic et al. [58] after 96-hours of hydrolysis forestry residues in a stirred tank reactor, stirring at various rates: 600, 300 and 100 rpm. In contrast, a positive effect in conversion rates is observed when hydrolysing at high enzyme dosages (min. 20 FPU/ b substrate). Palqmvist et al. [251] reported that conversion rates increase as function of rotational speed in same systems [58]. Using PCS as raw material, Wojtusik et al. [73] demonstrated that apart of the positive relationship between rotational speed and conversion yields, a minimum agitation rate of 300 rpm was necessary for guaranteeing mass transfer. were needed for enhancing the mass-transfer.

Alternative mixing methods have been proposed, in contrast to to continuous agitation, for the optimisation of low energy requirements whilst enhancing the release of fermentable sugars from lignocellulosic biomass: e.g. intermittent mixing, short mixing times etc. Intermittent mixing is common practice in the RDB operations [296], e.g. solid-state fermentation. Since continuous mixing can potentially shear proteins (i.e. cellulases) and increases power inputs, intermittent mixing can be employed for overcoming these issues associated to the enzymatic hydrolysis [115, 148, 319, 320]. A wide range of intermittent mixing strategies have been conducted, e.g. mixing for 4 hours plus no agitation or one mixing hour per day. Roche et al. [146] investigated a vast array of possibilities, concluding that effective initial mixing and continued is necessary for achieving high conversion rates, but in continuous mode. Previously, it has been found that intermittent mixing (510 rpm for 1 min and 0 rpm for 5 min) can turn into equal cellulose conversions than continuous stirring at 510 rpm [148]. Same results were suggested by Ingesson et al. [320], in the enzymatic

hydrolysis of low-solids cellulose in shaken flasks.

On the other hand, Liu et al. [262] evaluated the effect of intensive mixing time, ranging from 0 to 48 hours, within a two-stage hydrolysis of corn stover at high solids loadings. Interestingly, no great differences in glucose yields and carbohydrate conversion rates were observed despite of varying the mixing times at a 30% solids enzymatic hydrolysis. However, at least 48 and 3 hours were required for achieving maximum conversion yield when hydrolysing 20 and 25%TS, respectively. At short mixing times, energy saving up to 60% can be achieved in comparison with single-stage and continuous mixing systems. These alternative mixing techniques have proven to be as effective as continuous agitation for providing sufficient mixing on the enzymatic hydrolysis, and can be set for the optimisation (minimisation) of energy consumption.

Another important parameter is the the working volume, which has a direct impact in both capital and operational costs, i.e. a higher working volume would reduce equipment and operational expenditures per processed unit [93]. Moreover, at high-solids loadings additional reductions in overall costs can be pursued as previously discussed in Chapter 2. Jorgensen et al. [93] evaluated the effect of chamber filling from 3 to 12 kg per assay, showing no significant correlation to either cellulose conversions and relative ethanol yields at 23-25% TS. Although, the authors mentioned that even high degrees of fillings to 14.5 kg, revealed no decreases in yields. To date, no others publications have studied the effect of working (filling) volume into conversion rates in enzymatic hydrolysis of biomasses.

6.2.1.2 Design of experiments: a new optimisation tool for enzymatic saccharification

Design of experiments, abbreviated as DoE, is a statistical tool for the optimisation of processes which is conducted via a range of software (LINDO, Minitab, MODDE). The advantages of DoEs over OVAT approaches is finding the optimum reaction conditions and interactions between parameters whilst minimising the amount of necessary experiments [63]. There are two main groups of DoE studies depending on the approach: screening and response surface methodology with 2^k full-factorial and CCF as preferred methodologies, respectively. In biofuel production, DoE methodologies have attracted interest as a rapid tool for the optimisation of whole biorefinery pathways and associated processes, e.g. conditions during harvesting to evaporation temperature on end-product purification [321]. Generally, the main objective is the maximisation of sugar outputs with minimum addition of re-agents (enzymes, additives etc.). Focusing on the biochemical conversion of lignocelluloses to sugars, DoE studies are commonly found under the terminology "optimisation" or "design of experiments" in areas of pretreatments [117, 312, 322–327] formulation of cellulases [219, 328], enzyme operability [148, 329] and enzymatic hydrolysis [155, 330]. In terms of pretreatment methods, optimisation studies focus on H_2SO_4-hydrolysis [117, 312, 322, 323] as preferential option, although some examples of: AFEX [324],

organosolv [325] and alkaline [326, 327] pretreatments are found. In these respects, three main operational parameters (temperature, pressure and concentration of reagent) are optimised for: (i) maximum sugar release, (ii) higher delignification and (iii) less formation of lignocellulosic by-products. For instance, Rezende [325] found that acid-alkaline pretreatment with 4.5% w/v NaOH, 85 °C and ball milling time of 100 min, enabled the highest release of glucose from grass biomasses compared to acid-organosolv pretreatment techniques.

The use of home-made enzyme mixtures is gaining interest as alternative to commercial cocktails, due to higher feedstock selectivity and non-dependence of enzyme manufacturers [68, 331]. With individual enzymes secreted by *T.ressei*, Zhou et al. [328] conducted a central composite design (CDD) experimental design in order to determine the optimum formulation. Other researchers have investigated the enzyme supplementation of crude enzymes into commercial mixtures for the enhancement of sugar titers [219]. Reaction conditions (pH and temperature) of alternative enzymes to *Trichoderma* are optimised via experimental designs. For instance, Zambare et al. [329] determined the enzymatic hydrolysis of PCS, using *Penicillum pinophilum* crude cellulases, was operating under optimum conditions at pH of 4.5, 10%TS and 20 FPU g^{-1} DM as solid loadings. In contrast, three variables (pH, temperature and residence time) were optimised as function of cellulose conversion by Tengborg et al. [148]. The RSM approach, showed that pH 4.9, 38 °C and 144h were ideal parameters for the enzymatic hydrolysis of softwood with a mixture of commercial enzyme solutions: Celluclast 2L and Novozyme 188.

Other DoE studies have investigated the influence of enzyme loading, rotational speed and solid contents in the bioconversion of biomass to monomeric sugars [155, 330]. Interestingly, Mussatto et al. [155] found that doubling the agitation speed (100 to 200 rpm) has a negative effect on the enzymatic saccharification of brewer's spent grains, independently of enzyme and solid loadings. According to the 2^3 full-factorial design, glucose yields and cellulose conversions of 93.1 and 99.4%, respectively, were identified at 100 rpm, 45 FPU/g and 2% w/w. As expected, lower agitation rates and solids contents with higher enzyme dosages, are the optimum conditions for such enzymatic hydrolysis. In another study, the interactions between enzyme doses, tip speed and power consumption were investigated for the cellulolysis of filter paper with the Flashesyme^{TM} Plus 2G, a rare commercial cocktail [330]. Using a multiple linear regression model, a conventional method for fitting the data, enabled the determination of relative effect of the three mentioned parameters on glucose concentration, feeding period and energy consumption. As expected, enzyme loadings play an important role on increasing the release of monomeric sugars, decrease liquefaction rates and energy requirements. It can be concluded that DoE is a useful tool for optimisation of conditions and determination of interactions with a robust statistical analysis, whilst minimising the amount of experiments, in consequence time and costs.

6.2.2 Process modelling

Simulation of chemical engineering processes is becoming an attractive option for modelling processes, in complement of laboratory experimentation. In these regards, main commercial software are AspenPlus and HYSYS, facilitating the determination of mass/energy balances for evaluating the engineering costs of the system. Although, computational tools accelerate simulation, experimentation is still needed to incorporate processing aspects such as feedstock composition, system assumption etc.. In lignocellulosic biorefineries, two main models are used for designing the necessary equations which are then incorporated to the simulation: stoichiometry and mathematical models. This following sections pretends to review both methodologies as well as provide meaningful examples within the biochemical conversion of biomass.

6.2.2.1 Stoichiometry

It is challenging to establish stoichiometric relationship of the enzymatic hydrolysis of biomass as a conventional reaction (A+B $\longrightarrow$ C+D), due to the multi-factorial characteristic of the system (raw materials and enzymes), several attempts have been made for simplifying the process. A list of individual reactions to illustrate the hydrolysis of lignocellulosic compounds into their monomeric equivalents was proposed by Humbirdt et al. [147] for the three stages of cellulosic ethanol fermentation: pretreatment, enzymatic hydrolysis and fermentation. In particular, enzymatic hydrolysis can be depicted with the following reactions (Eq. 6.1-**??**):

$$(Glucan)_n + n\,H_2O \longrightarrow n\,Glucose \tag{6.1}$$

$$Cellobiose + n\,H_2O \longrightarrow 2\,Glucose \tag{6.2}$$

$$(Xylan)_n + n\,H_2O \longrightarrow n\,Xylose \tag{6.3}$$

$$(Arabinan)_n + n\,H_2O \longrightarrow n\,Arabinose \tag{6.4}$$

$$(Mannan)_n + n\,H_2O \longrightarrow n\,Mannose \tag{6.5}$$

$$(Lignin)_n \longrightarrow n\,Soluble\,lignin \tag{6.6}$$

The side-reactions can also be incorporated in process modelling of the enzymatic hydrolysis, to calculate the inhibition of monosaccharides to undesirable compounds. Microbial contamination results into the formation of lactic acid, from monosaccharides sources as seen in Eq.6.7. Release of other inhibitors such as weak acids (acetic, levulinic, formic, succinic) and phenolics (coumaric, vanillic and benzoic acids), among other compounds, were neglected in the stoichiometry of pretreatment and enzymatic hydrolysis stages. However, dehydratation of saccharides to furfurans (glucan and fructose to HMF and xylan to furfural, respectively) were considered in the pretreatment, to reflect the sugar degradation due to high acidic and high temperatures. During fermentation, three main components are yielded from glucose and xylose and co-fermentation products (glycerol, succinic acid and xylitol), apart from ethanol and carbon dioxide. In this case, further reactions take place to balance out the cell mass of *Z.mobilis* with the nitrogen sources.

$$Glucose \longrightarrow 2\, Lactic\, acid \tag{6.7}$$

$$3\, Xylose \longrightarrow 5\, Lactic\, acid \tag{6.8}$$

$$3\, Arabinose \longrightarrow 5\, Lactic\, acid \tag{6.9}$$

$$Galactose \longrightarrow 2\, Lactic\, acid \tag{6.10}$$

$$Mannose \longrightarrow 2\, Lactic\, acid \tag{6.11}$$

Stoichiometric equations to describe cellulosic hydrolysis to monosaccharides via acid, catalyst or enzymes, has been proposed to simplify the biomass conversion route. Although, they are based on pure cellulosic substrate with the absence of lignin fraction, and simple depolymerisation mechanisms. Primary stoichiometric equations of cellulose and hemicellulose to glucose and xylose, respectively, followed by ethanol fermentation are depicted as follows (Eq.6.12-6.13):

Glucan to Glucose

$$n\, C_6H_{10}O_5 + n\, H_2O \longrightarrow n\, C_6H_{12}O_6 \tag{6.12}$$

Xylan to Xylose

$$C_5H_8O_4 + n\,H_2O \longrightarrow nC_5H_{10}O_5 \tag{6.13}$$

A partial fractionation of cellulose to oligosaccharides, cellobiose formation and its hydrolysis to glucose was formulated as well [48]. Following expressions depict the cellulose to glucose conversion, through cellobiose formation and hydrolysis (Eq.6.14-6.16).

Cellulose to oligosaccharides

$$(C_6H_{10}O_5)_n + H_2O - enzyme \longrightarrow n(C_6H_{10}O_5)_{n-1} + C_6H_{12}O_6 \tag{6.14}$$

Cellobiose formation

$$(C_6H_{10}O_5)_n + H_2O - enzyme \longrightarrow n(C_6H_{10}O_5)_{n-2} + C_{12}H_{22}O_{11} \tag{6.15}$$

Cellobiose to glucose

$$C_{12}H_{22}O_{11} + H_2O - enzyme \longrightarrow 2\,C_6H_{12}O_6 \tag{6.16}$$

6.2.2.2 Mathematical models

In addition to the use of stoichiometry, mathematical models have been used for representing the reaction mechanism during the enzymatic hydrolysis of biomass. In addition, the enzymatic saccharification can be modelled in batch, fed-batch and continuous mode [246], by the integration differential equations for determining mass and energy balances. Based on structural features and functions, mathematical models were classified into four categories: (1) nonmechanistic model; (2) semimechanistic model; (3) functionally based model; (4) structurally based model. Jeoh et al. [332] provide an updated version for filtering mechanistic models into two categories: "enzyme-centric" and "substrate-centric". Achieving a completely realistic kinetic model is not possible to date, due to the catalytic characteristics of enzymes and physical complexity of lignocellulose feedstocks. For instance, Zheng et al.[60]

included a series of assumptions for the derivatization of rate equation, ranging from uniform enzymatic attack to amorphous and crystalline cellulose fraction to non-adsorption of β-glucosidases onto lignin, among others that simplify the enzymatic mechanisms. Despite the numerous advances on creating mathematical models, kinetic modelling of lignocellulose hydrolysis is limited, as not being representative enough and applied for scaling-up purposes, as occurring with the stoichiometry.

6.2.3 Techno-economic assessment

Techno-economic assessment (TEA) is a methodology for the determination of the economic evaluation of an industrial process, with a holistic approach. In general terms, TEA involves the determination of mass/energy balances via process modelling and consequent economics costs of engineering components and operations. It is used as predictive tool to evaluate the techno-economic viability of a project, e.g product value, return on investment, logistics, storage and plant decommissioning). In biorefineries, TEA are conducted for estimating an approximate selling prices of a product (e.g. ethanol) in order to competed with current commodities at industrial scale [4]. Although, TEAs can prevent the economic losses by predicting the performance of a plant, several assumptions are implied which would not be realistic in the market. Most of assumptions include constant raw materials prices, theoretical process yields and financial assumptions such as linear depreciation and income tax rates. External factors such as ethanol market prices are difficult to forecast, and will have an important impact on the overall economics.

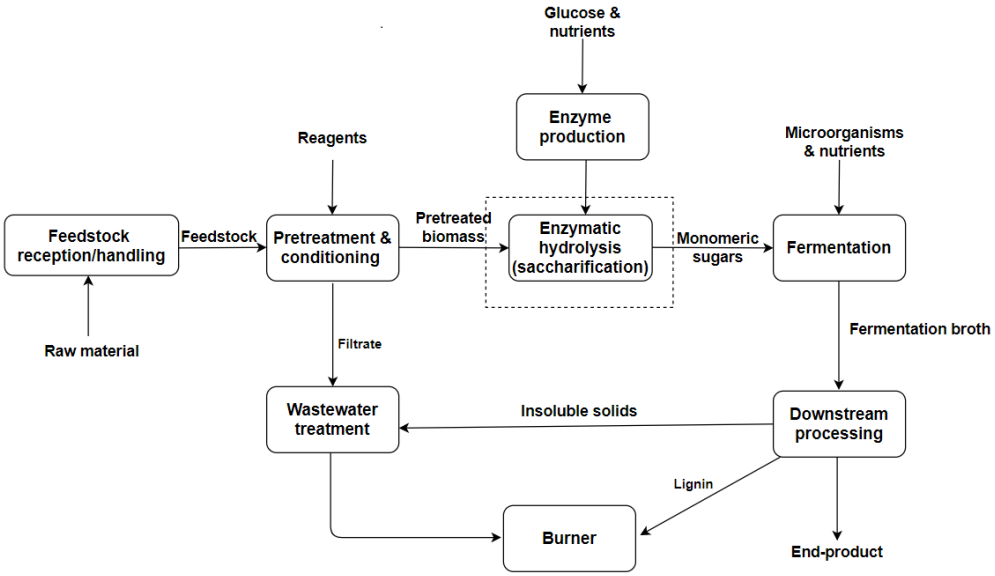

Figure 6.1. Schematic diagram of an integrated cellulosic ethanol biorefinery

Due to the scope of this work, the revision of TEA studies is focused on cellulosic ethanol plants, although some examples of bioconversion to hydrocarbon fuels are

also discussed as including the enzymatic hydrolysis. Performing a precise techno-economic assessment of future plant is vital for ensuring the commercial viability of the project and save costs during plant design. The common methodology for carrying out a TEA is by following a standard production cost, focusing on the incurred costs for the production of a finished product. Due to the complexity of techno-economic assessment of cellulosic ethanol plants, it is recommend to use an alternative methodology that includes geographical location, supply-chain an others aspects [333]. Gnansounou and Dauriat [333] proposed a multi-disciplinary approach (technical, economic and environmental) for assessing the viability of commercial cellulosic ethanol plants, complemented with Target Costing, Value Resource and Value Engineering practices. By employing the alternative strategy, a more accurate economic analysis of cellulosic biorefineries is achieved, reducing the perceived risks by the investors. As part of a consistent review, Gnansounou et al. [333] illustrated the key techno-economic aspects cellulosic ethanol plants in the US and Europe, focusing on: competition between resources, value of feedstock, value of product, co-products and intermediates and consideration of value-chain. Interestingly, in this case, biomass costs are highly significant than enzyme costs in the overall production economics.

Early work on TEA started in the US for cellulosic ethanol plants using corn stover due several reasons: high carbohydrate content, established supply-chain and public subsidies on plant crops [334]. Even though, these type of plants were operating since the 80s, TEA investigations did not take place until commencing the beginning of the millennium [235]. Most of this work has been carried by the NREL institution [299, 335–339] as technical reports and peer-review publications. At pilot and commercial scale, NREL's core technology is a dilute-acid pretreatment followed by SSF, integrated with auxiliary processes such as wastewater treatment and biomass combustion as by-product valorisation streams [235]. A preliminary TEA by Wooley et al. [235] predicted ethanol production costs ranging from 0.15 to 0.25 USD L^{-1} in year 2015. This work was based on NREL plant design [204], was capable of producing 250.000 m^3 per annum of bioethanol. Later on, Aden et al. [340] incorporated a co-current dilute-acid pretreatment and separate hydrolysis and fermentation, meeting ethanol selling prices by Wooley et al. [235]. Several variations on pretreatment stage, fermentation and downstream process were investigated by Kazi et al. [336, 337], but exceeding previous commercials costs of 1 USD per litre of ethanol. More recently, Humbird et al. [338] demonstrated that by including an on-site enzyme production and co-fermentation steps, ethanol prices can be cut in half to $ 0.5 L^{-1} of ethanol.

Recent NREL R&D investigated the bioconversion of lignocellulosic sugars to hydrocarbon fuels via catalytic upgrading, as alternative to ethanol fermentation with a market price of $ 0.66 USD per litre [299, 339]. The two new pathways were defined, both including deacetylation and mechanical refining (DMR), and whole-slurry batch or continuous enzymatic hydrolysis for butanediol and butyric acid

fermentation, respectively. Either alcohol and acid streams were further upgraded to hydrocarbon fuels, with estimated commercial values of 1.5 and 2.5 USD L^{-1}, respectively. Alternatives uses to burning lignin, such as lignin recycling and conversion to equivalent monomers, was also investigated in these reports. These investigations demonstrated that hydrocarbon fuels are still underdevelopment and at market disadvantage towards cellulosic ethanol.

After corn stover, sugarcane is the dominant feedstock for ethanol production with Brazil as leading sugarcane production of 700 million tonnes per annum [341]. Most ethanol is food-based, due to the large history of sugar-mills from sugarcane, consequently with an established infrastructures and supply-chain. Although, sugar mills are being retrofitted to utilise the resulting residues (sugarcane bagasse) as raw material for additional ethanol titers [342, 343]. To determine the viability of integrated sugarcane biorefineries, first (1G) and second (2G) generation, TEA investigation have been conducted focusing on determining the MESP for cellulosic ethanol [343, 344]. MacRelli et al. [343] investigated the effect of heat integration, sugarcane leaves as raw material, enzyme dosages and energy-efficient equipment in several 1G+2G scenarios via process modelling. It was concluded that integrated sugarcane bioethanol is competitive (without subsidies) to 1G starch-based bioethanol production in Europe, as minimum ethanol selling price (MESP) down to 0.40 USD L^{-1} were achieved. A comparison of techno-economic performance for thermochemical and biochemical conversion of sugarcane residues was performed by Seabra et al. [344]. The two technologies presented quite similar MESPS, 0.318 and 0.329 USD L^{-1} for biochemical and thermochemical conversion, respectively. Other researches have identified the technical bottlenecks and economic feasibility of dilute acid pretreatment on the cellulosic ethanol part [342]. The cost-effectiveness of the process is mainly driven by solids loadings in pretreatment step, enzymatic hydrolysis time and possibility of pentose fermentation. For achieving the best economic performance, the optimum conditions are required (10%TS, 24 h enzymatic hydrolysis time and co-fermentation of pentoses) as economic viability is at risk by increasing use of chemicals, especially during pretreatment and neutralisation steps. This shows that integrated sugarcane-based, utilising all parts of sugarcane bagasse residues, is vital for achieving the best results from a techno-economic point of view to displace 1G bioethanol refineries [342, 343].

The use of forestry residues as alternative to corn stover and sugarcane, is widely adopted in countries with an established forestry and logging industry [345]. In Sweden, softwood-to-ethanol conversion has been investigated during the last decades from a techno-economic point of view techno-economic analysis [345–349]. Due to the recalcitrance of feedstock, gaseous impregnation of $S0_2$ at low-temperatures (<50 °C) followed by steam-explosion is the chosen pretreatment, as patented by Lund University [345, 347, 348]. Initial investigations on process simulation resulted into 0.57 to 0.63 USD L^{-1} for cellulosic bioethanol refinery operating by SSF and

SHF, respectively [348]. Further improvements on energy integration of softwood-to-ethanol plants, particularly in evaporation stages and anaerobic digestion, led to a reduction in ethanol selling prices to 0.54 USD L^{-1} [345]. Instead of softwood, Frankó et al. [346] examined the future potential of different forestry residue such as sawdust, hog fuel or early thinnings, among others. Based on previous TEA methodologies [345, 347, 349], minimum ethanol selling price (MESP) as function of net present value (NPV) was determined, ranging from 0.77 to 1.52 USD L^{-1} [346]. Apart from sawdust and shavings, negative NPVs were reported in all cases, making the process non-viable. It was found that the negative cost-effectiveness of cellulosic ethanol from forestry-residues is attributed to an increasing bark content, resulting into poor sugar yields during enzymatic hydrolysis.

6.3 Experimental methodology

6.3.1 Process optimisation

Process optimisation was conducted by either 2^3 or 2^4 full-factorial experimental design by a statistical software named MODDE 12.1 (Umetrics, Sartorius, Sweden). A series of experiments per study were assayed in rotary drum reactors (50-ml and 2L) as described in section 2.5. Data-processing and statistical analysis was also performed with this software. In each optimisation study (list below), specific factors and responses are included accordingly.

6.3.2 Use of kinetics for predicting glucose yields

Unless otherwise stated, an enzymatic hydrolysis assay of MSW-pulp was run in a 2-L rotary drum reactors for 72 hours, to determine the reaction kinetics at the following conditions: 25%TS, 2% E:S, 0.1 % BIT and 30 rpm. A power-law model ($y=ax^b$) was fitted into the discrete analysis of glucose yields (experimental data) and used for prediction of glucose yields based on mode of operation (Chapter 2, section 2.10).

6.3.3 Sweet spot design - finding the optimum operational settings

The sweet spot design involves conducting a 3^3 full-factorial experimental design by MODDE 12.1 (Umetrics, Sartorius, Sweden software), showing 9 combinations of experiments as summarised in Table 6.1. Glucose yields were determined by following methodology of kinetics section 6.3.2 per each TS, and energy efficiency calculated as the ratio of mass glucose per total energy consumption (g glucose Wh^{-1}). Once the experimental data is acquired, the sweet spot tool of MODDE software is run to determine experimental space which satisfies certain criteria [350]. Three criteria are set based on commercial requirements of lignocellulosic sugars [2], increase rates of continuous over batch processing [15] and energy efficiency of horizontal reactors [41] with low and high end values as found in the literature:

- **criteria 1:** glucose yields of 80 to 120 g L^{-1} [2]
- **criteria 2:** glucose rates of 1 to 2 g L^{-1} h^{-1} [15]
- **criteria 3:** energy efficiency of 0.1 to 0.4 g glucose Wh^{-1} [41]

Table 6.1. 3^3 full-factorial experimental design for sweet spot determination: glucose yields, rates and energy efficiency upon total solids and batch-time

No. exp	TS (%)	RT (hr)	Glu (g L^{-1})	r_{Glu} (g L^{-1} h^{-1})	Glu_{eff} (g $W^{-1}h^{-1}$)
N1	20	2	10.1	5.07	0,92
N2	25	2	8.97	4.48	0.81
N3	20	120	51.5	0.42	0.07
N4	25	120	75.3	0.62	0.11
N5	20	60	39.1	0.65	0.11
N6	25	60	52.5	0.87	0.15
N7	22.5	2	11.0	5.52	1.00
N8	22.5	120	43.9	0.36	0.06
N9	22.5	60	34.8	0.58	0.10

6.3.4 Techno-economic assessment

A techno-economic assessment is a step-wise methodology for the economical analysis of processing unit, herein enzymatic hydrolysis of MSW-derived pulp to fermentable sugars. It includes from process design, determination of mass/energy balances passing to costs estimation of each investigated system. In this study, several reactor configurations are compared (batch, fed-batch and continuous) for bioprocessing of MSW-pulp into monomeric sugars at pilot and demonstration-scale. The following methodology includes each step (process design, mass/energy balances, costs estimation and economical analysis) on the techno-economic assessment, with a list of assumptions and used data-sets.

6.3.4.1 Process design

The process design of a two-stage hydrolysis, liquefaction and saccharification steps, is carried out by using the τ = W_V/Q expression for a fixed volume and residence time. As seen in Table 6.2, the residence time of liquefaction reactor dictates flow-rates as well as residence time and volume of secondary hydrolysis tank. In steady-state, the Q_{in} is equal to Q_{out} as reaction mass rate is 0 (subsection 2.10). In this study, four configurations are investigated as two-stage systems (liquefaction/saccharification reactor) with set residence times per stage: (i) 6/48, (ii) 12/42, (iii) 18/36 and (iv) 24/30 h. The volume of saccharification reactor is determined according to saccharification residence time, difference between liquefaction and total residence time. Table 6.2 summarises process design (flow-rate, residence time and working volume) of four continuous two-stage systems, employed for process modelling/simulation.

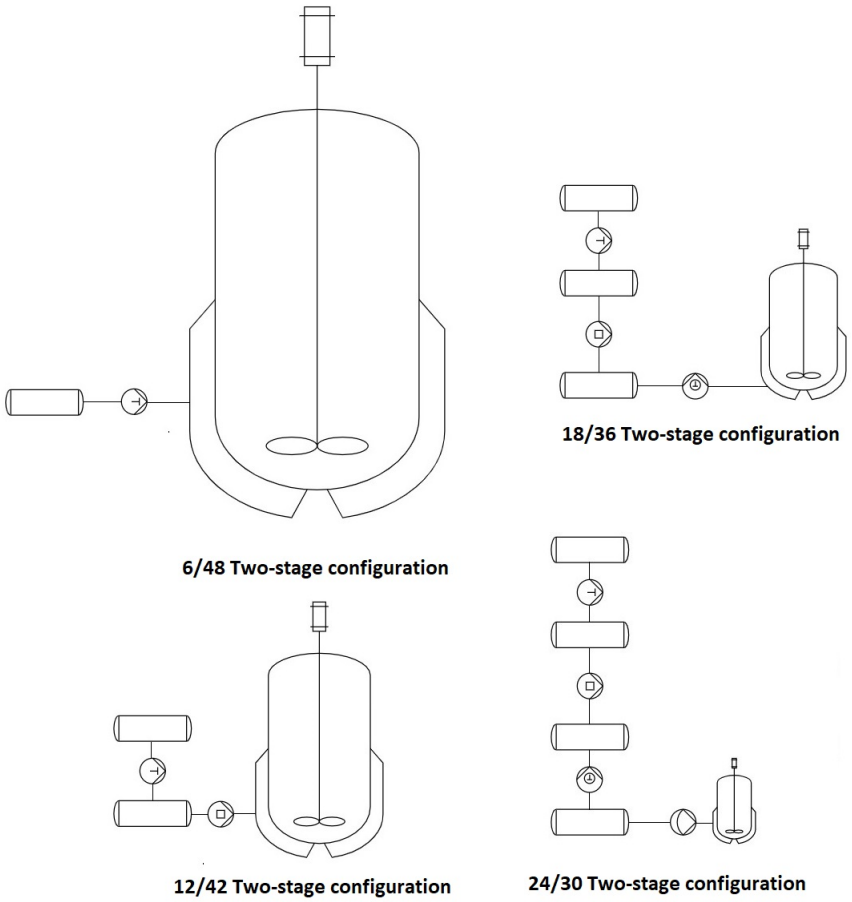

Figure 6.2. Schematic diagram of two-stage continuous enzymatic saccharification: primary (drum) and secondary (stirred tank) reactors interconnected with positive displacement pumps

As embracing an industrial scope, residence times of liquefaction bioreactors are limited to 6 hours per liquefaction reactor. Thus; 1, 2, 3 and 4 bioreactors are configured for the 6/48, 12/36, 18/40 and 24/30 two-stage configurations, respectively, connected by pumps between them (Fig. 6.2). A modified version of the 6/48 two-stage configuration in form of liquefaction bioreactor plus 3 CSTR in series, connected with pump accordingly, is proposed for volume reduction of saccharification reactor (Fig. 6.3).

6.3.4.2 Mass and energy balances

A robust mass and energy (M&E) balances was generated using Excel (Microsoft Office) for both scales, in accordance to process design (section 6.2). Unless otherwise stated, the reaction conditions of enzymatic saccharification of MSW pulp are 25 % TS, 2 % E:S, 0.01 % BIT (w/dry substrate) and 0.001 % H_3PO_4 (v/working volume). The inlet and outlet mass balances were calculated according to reaction kinetics (section 6.3.2), adjusted per mode of operation (Eq. 6.17. A residence time (RT) of 54 hours was set for the continuous systems, whilst 120 hours for batch and fed-batch

Table 6.2. Two-stage process design for continuous MSW hydrolysis at pilot and demonstration scales

Liquefaction (primary) reactor			**Saccharification (secondary) reactor**	
W_V (L)	**Q (L hr^{-1})**	**τ (hr)**	**W_V (L))**	**τ (hr)**
Pilot-scale				
24	4.0	6	192	48
	2.0	12	105	42
	1.33	18	60	36
	1.0	24	37.5	30
W_V (m^3)	**Q (m^3 hr^{-1})**	**τ (hr)**	**W_V (m^3)**	**τ (hr)**
Demonstration-scale				
40	6.6	6	320	48
	3.3	12	140	42
	2.2	18	80.0	36
	1.6	24	50.0	30

W_V is working volume and Q is equal for both processes

designs. Moreover, a correction factor (a) of 1 and 1.2 was included in the prediction of glucose yields for the batch and fed-batch mode, respectively. Once for the continuous processing, the steady-time is reached after 3 space-volumes (162 hours) of finishing the batch start-up period (54 hours).

$$Glu = [14.469 \times RT^{0.446}] \times a \tag{6.17}$$

The annual mass balances for batch and fed-batch designs is calculated upon a down-time of 48 hour per batch, thus total running time of 8736 hours or 52 batches per annum. Meanwhile, the annual running time in steady-state (TSS) is calculated by Eq.6.18, considering the start-up batch-time and space-volumes to reach steady-state:

$$TSS = (t_{yr}) - RT - t_{3SV} \tag{6.18}$$

Where t_{yr} is annual duration (8760 hours), RT is residence time (54 hours) and t_{3SV} is time to reach steady-state, equal to 3 space-volumes (162 hours). While the energy input is the sum of bioengineering processes (mixing, heating and pumping) per step (Eq. 6.19. Due to the absence of experimental techniques for on-site determination of the energy requirements, the power demand is taken as reference from the technical description of the vendor. Table 6.3 summarises the individual power requirements of reactor configuration at fixed operational conditions:

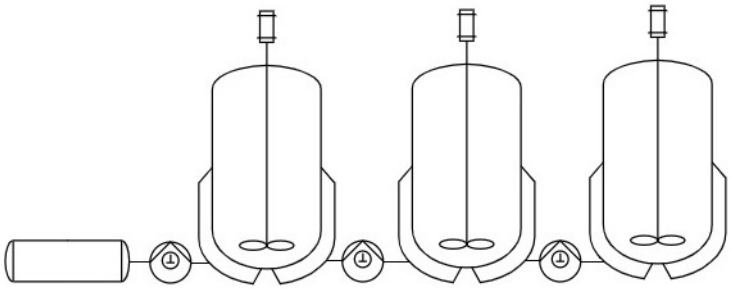

Figure 6.3. Schematic diagram of the modified two-stage configuration (6/48h), secondary hydrolysis as series of CSTRs

Note: residence time of each secondary hydrolysis reactor is of 16 hours (48/3))

$$P_n = \int_0^t (P_{R1} + P_{H1} + P_{P1}) \times t_1 .....(P_{Rn} + P_{Hn} + P_{Pn}) \times t_n \tag{6.19}$$

Where P_n is sum of power per hydrolysis step (liquefaction and saccharification) P_{Rn} is the power of n reactor (stirring, kW), P_{Hn} the power of n thermostat (heating, kW), P_{Pn} the power of n positive cavity pump (pumping, kW) and t_n the running time (in h). The energy balances per processing time (P_n) are determined as the sum of all engineering components and activities within the enzymatic hydrolysis process by Eq. 6.19. Likewise, power demands for the demonstration-scale energy balances are summarised in Table 6.4. If not available or found in the technical description, the power requirements are calculated by the "scale-up rule" (Eq.6.20).

Table 6.3. Power demand of bioprocessing equipment at pilot-scale

Stage,scale	P (kW)	Reference
Liquefaction		
Rotary drum reactor (30 L)	0.55	https://tinyurl.com/1i7pp574
Thermostat bath (12 L)	2	https://tinyurl.com/4yvqpyjs
Positive displacement pump (1 L h^{-1})	0.37	https://tinyurl.com/zgu7wbo0
Saccharification,		
Stirred tank reactor (50 L)	0.25	https://tinyurl.com/1i7pp574
Thermostat bath (12 L)	2	https://tinyurl.com/4yvqpyjs
Positive displacement pump (1 L h^{-1})	0.37	https://tinyurl.com/zgu7wbo0

$$P_{V2} = \frac{V2}{V1}^{0.50} \times P_{V1} \tag{6.20}$$

Where P_1 is reference power demand , P_2 is scaled power demand , V_1 is reference reactor volume and V_2 is scaled reactor volume. A list of assumptions were made for estimating the mass/energy balances of all combinations of continuous, batch and fed-batch systems for the bioconversion of MSW-pulp into glucose:

- Upstream (waste reception to pulping and feeding of raw materials), downstream (recovery and purification) and storage processes are neglected
- Lignocellulosic composition of MSW pulp remains constant [36, 47]
- Physico-chemical characteristics of rest of re-agents remained unchanged
- Volume of H_3PO_4 is equal to a thousand part of working volume, and, NaOH a half of H3PO_4 to balance the pH throughout the bioprocessing
- Pumping energy (liquefaction and saccharification) does not take into account the differences in slurry viscosity
- A downtime (DT) of 2 days per year and per batch is estimated for two-stage continuous and batch/fed-batch hydrolysis
- Downtime costs, ranging from 5 to 20% of total OpEx [351], are estimated on a mid-range level (10%).
- Steady-state is not achieved until 3 space-volumes after the batch period, e.g. 162 hour for a 54 residence time.
- No depreciation, labour, maintenance or any other indirect costs are included in the cost estimation.

Table 6.4. Power demand of bioprocessing equipment at demonstration scale

Stage,scale	P (kW)	Reference
Liquefaction		
Rotary drum reactor (50 m^3)	30	https://tinyurl.com/hiw01otr
Thermostat bath* (12 m^3)	15	https://tinyurl.com/1k0t0iqy
Positive displacement pump (2 m^3 h^{-1})	1.0	https://tinyurl.com/552vydop
Saccharification,		
Stirred tank reactor (20 m^3)	62.5	https://tinyurl.com/17uchigt
Thermostat bath* (12 m^3)	36	https://tinyurl.com/1k0t0iqy
Positive displacement pump (2 m^3 h^{-1})	1.0	https://tinyurl.com/552vydop

* Volume of heating jacket is a third of reactor volume and power demand is scaled-up from a 200 L model

6.3.4.3 Costs estimation

The capital expenditures (CapEx) and operating expenses (OpEx) are the sum of bioprocessing equipment and M&E components, individually taken from the world's largest online B2B market place: www.alibaba.com. The costs of bioprocessing equipment for the CapEx determination are summarised in Table 6.5, selected as reference values upon the process design (section 6.3.4.1). The "scale-up rule" with an index (n) of 0.55 (Eq. 6.21) is used for the determination of each bioprocessing equipment based on its volume. In contrast, the M&E components costs (raw materials, electricity and revenue streams) are chosen according to chemical suppliers

and literature values, summarised in Table 6.6. Two complementary parameters, return of investment (ROI, in %) and payback period (PP, in yr) are calculated from profit (revenue - OpEx) and CapEx by employing Eq. 6.22 and Eq. 6.23.

Table 6.5. Costs of bioprocessing equipment at pilot and demonstration scales

Item	Price (£)	V* or Q	References
Pilot-scale			
Liquefaction			
Rotary drum reactor	2100	30 L	https://tinyurl.com/yteu8o4h
Thermostat bath**	500	12 L	https://tinyurl.com/ytz26q3j
Positive displacement pump	500	1-4 L h^{-1}	https://tinyurl.com/552vydop
Saccharification,			
Stirred tank reactor	1500	50 L	https://tinyurl.com/98j519n7
Thermostat bath**	500	16 L	https://tinyurl.com/ytz26q3j
Positive displacement pump	500	1-4 L h^{-1}	https://tinyurl.com/zgu7wbo0
Demonstration-scale			
Liquefaction			
Rotary drum reactor	200000	50 m^3	https://tinyurl.com/hiw01otr
Thermostat bath**	10000	16 m^3	https://tinyurl.com/4yvqpyjs
Positive displacement pump	3000	1.6 m^3 h^{-1}	https://tinyurl.com/zgu7wbo0
Saccharification,			
Stirred tank reactor	100000	78 m^3	https://tinyurl.com/1i7pp574
Thermostat bath**	15000	20 m^3	https://tinyurl.com/4yvqpyjs
Positive displacement pump	3000	1-4 m^3 h^{-1}	https://tinyurl.com/zgu7wbo0

* Reactor volume is 20% larger than working volume, where the difference volume is the head-space
** Thermostat bath volume is equal of jacketed volume, which is a third of reactor volume

$$Cost\ size2 = Cost\ size1 \frac{Size2}{Size1}^n \tag{6.21}$$

Table 6.6. Costs of re-agents, products and electricity in bulk

Item	Cost per unit	Reference
Raw materials		
Cellic® CTec3[a]	£1.5/kg	[240]
Tap water	£0.01L^{-1}	[352]
1,2-benzisothiozalinone	£0.7/kg	https://tinyurl.com/6m9zhbk8
Sodium hydroxide	£0.2/kg	https://tinyurl.com/4natyhgj
Phosphoric acid	£0.5L^{-1}	https://tinyurl.com/1jwcvyvj
Electricity[b]	£0.01/kWh	[353]
Revenues		
Glucose[c]	£0.4/kg	https://tinyurl.com/2fd7ok9v
PHS[d]	£0.25/kg	https://tinyurl.com/85crydsx

[a] A cellulase cocktail is taken as reference for the Cellic® CTec3 pricing
[a] Based on natural gas combustion plus a combined-cycle gas turbine (CCGT)
[c] Based on food-grade glucose, obtained from sugarcane
[d] Based on demonstration-grade lignin, a by-product of wood processing by sulfite pulping
All URL links are taken from alibaba.com, including average prices of high-purity grades (> 95 %)

$$ROI = \frac{Profit}{CapEx} \times 100\% \tag{6.22}$$

$$PP = \frac{1}{ROI} \times 100 \tag{6.23}$$

6.3.4.4 Sensitivity analysis via DoE

At pilot-scale, the sensitivity analysis involved a 2^3 full-factorial with one centre-point, by the statistical software MODDE 12.1 (Umetrics, Sartorius, Sweden). Four main parameters were set as factors with the next ranging costs: rotary drum reactor (£2000-50000), enzymes (£1-5/kg), sugar (£0.1-0.5/kg) and PHS (£-0.025-0.25/kg). Where CapEx, OpEx, Revenue, Profit, ROI and PP are set as responses. Economic analysis was carried out for the 6/48 continuous configuration as a combination of 17 experiments as seen in Table 6.7.

Table 6.7. 2^3 full-factorial for the sensitivity analysis at pilot-scale

Exp no.	Enzymes (£/kg)	Horizontal reactor (£)	Sugar (£/kg)	PHS (£/kg)
1	-1	-1	-1	-1
2	1	-1	-1	-1
3	-1	1	-1	-1
4	1	1	-1	-1
5	-1	-1	1	-1
6	1	-1	1	-1
7	-1	1	1	-1
8	1	1	1	-1
9	-1	-1	-1	1
10	1	-1	-1	1
11	-1	1	-1	1
12	1	1	-1	1
13	-1	-1	1	1
14	1	-1	1	1
15	-1	1	1	1
16	1	1	1	1
17	0	0	0	0

Enzymes: £1/kg (-1), £3/kg (0) and £5/kg (+1)
Horizontal reactor: £2000 (-1), £26000 (0) and £50000 (+1)
Sugar: £0.1/kg (-1), £0.3/kg (0) and £0.5/kg (+1)
PHS: £-0.025/kg (-1), £0.1125/kg (0) and £0.25/kg (+1)

For the demonstration-scale, same methodology was employed but with fixed horizontal reactor costs. Therefore, only three factors were studied (enzymes, sugar and PHS costs), analysing their effects to OpEX, revenue and profit in the 6/48 configuration. Table 6.8 summarises the conditions of 15 experiments.

Table 6.8. 2^3 full-factorial for the sensitivity analysis at demonstration-scale

Exp no.	Enzymes (£/kg)	Sugar (£/kg)	PHS (£/kg)
1	-1	-1	-1
2	1	-1	-1
3	-1	-1	-1
4	1	-1	-1
5	-1	1	-1
6	1	1	-1
7	-1	1	-1
8	1	1	-1
9	-1	-1	1
10	1	-1	1
11	-1	-1	1
12	1	-1	1
13	-1	1	1
14	1	1	1
15	-1	1	1

Enzymes: £1/kg (-1), £2/kg (0) and £4/kg (+1)
Sugar: £0.2/kg (-1), £0.3/kg (0) and £0.4/kg (+1)
PHS: £0.5/kg (-1), £0.1125/kg (0) and £0.25/kg (+1)

6.4 Results and discussion

6.4.1 Optimising enzymatic hydrolysis of MSW-pulp

6.4.1.1 Decreasing mixing-related energy: 5-10 %TS

To diminish the deactivation of cellulases caused by strong flow pattern [354] and decreasing power requirements of continuous mixing, alternative mixing strategies have been proposed [225, 320]. In this context, a 2^3 full-factorial experimental with three centre points was designed as combination of 11 experiments. Moderate stirring speeds (1-30 rpm) and total solids (5-10%TS) were chosen as thresholds, but extreme agitation times (15-1440 min) were set to evaluate their effect of short or prolonged mixing times on enzymatic hydrolysis. Table 6.9 summarises experimental design by including factors (agitation time, rotational speed and total solids) and responses (glucose yields at time 1 and 24 and normalised energy consumption) per each enzymatic hydrolysis experiment. Since energy consumption was not measured by torque-metering (dual-plug device instead), the total energy consumption is normalised per TS (E_{TS}, in W h TS^{-1}) , thus, considering the effect of solids loadings. To complement the experimental design, statistical analysis consisting on summary of fit (r^2, q^2, model validity and reproducibility) and observed vs predicted plots was included in Appendix C (Table C.1 and Fig. C.1), respectively. Except for the model validity (<0.1), showing lack-of-fit in either T1 and T24 responses; other statistics showed that the model was: highly-significant ($r^2 > 0.92$), good-quality ($q^2 > 0.5$) and highly-reproducible (reproducibility > 0.99) [355].

The results showed that 1-hour glucose yields (T1 Glu) ranged from 2.62-4.96, 7.1-7.2 and 9.9-11. g L^{-1} for 5, 7.5 and 10 % solids content, respectively. At 24

Table 6.9. 2^3 full-factorial for examining minimum mixing requirements

	Factors			Responses		
Exp. no.	**N_t (min)**	**N (rpm)**	**TS (%)**	**T1 Glu (g L^{-1})**	**T24 Glu (g L^{-1})**	**E_{TS} (W h TS^{-1}**
N1	15.00	1.0	5.0	5.25	28.5	0.32
N2	1440	1.0	5.0	6.42	37.2	31.2
N3	15.00	30	5.0	12.6	35.0	0.36
N4	1440	30	5.0	7.20	28.0	35.0
N5	15.00	1.0	10	9.93	62.0	0.16
N6	1440	1.0	10	21.8	73.7	15.6
N7	15.00	30	10	19.8	68.3	0.18
N8	1440	30	10	23.6	70.1	17.5
N9*	727.5	15	7.5	14.2	61.1	10.9
N10*	727.5	15	7.5	14.0	58.2	10.9
N11*	727.5	15	7.5	14.4	60.1	10.9

Reaction conditions: 5%E:S, 50-ml falcon tubes, 50 °C and pH 4.75-5.25. *centre-points of the experimental design

hours of hydrolysis, final glucose yields (T24 Glu) increased as increasing TS values : 14-18 (5 %TS), 29-30 (7.5 %TS) and 31-36 g L^{-1} (10 %TS). Despite operating at low-medium solids loadings, high concentrations of glucose were found which can be attributed to a high enzyme usage (5% E:S) [148]. Apart from the centre-point experiments, a slight variation (10-20%) in glucose yields was observed independently on the mixing strategy per TS. However, there was a vast difference in total energy consumption between experiments with short mixing-times (< 0.5 Wh TS^{-1}) or continuous agitation (> 14 Wh TS^{-1}). Even the intermediate cases (N9-N11) present a normalised energy consumption 30 (0.36 Wh TS^{-1}) to 68 (0.16 Wh TS^{-1})times higher than 15-min agitation cases (11 to 0. Wh TS^{-1}). The energy consumption is an important factor for dictating the energy-efficiency of the process (mass product per energy) [149]. This may suggest that severe mixing is not an essential requirement for carrying out the enzymatic hydrolysis [146]. Therefore, it is preferred to set short agitation times as consuming less power per unit of glucose, e.g. N5 and N7 to N6 and N8 experiments.

The response contour plots showed the effect of N and N_t per response (T1 Glu, T24 Glu and E_{TS}) for 7.5% TS in Fig. 6.4. Maximum initial glucose yields (T1) of 7.5 g L^{-} were achieved within 22.5-30.0 rpm (N) and 600-1440 minutes (N_t), coloured in red (Fig. 6.4a). These results suggest that minimum mixing requirements of 600 min at 30 rpm or 1440 min at 22.5 rpm, are necessary for achieving the optimal enzymatic saccharification at these reaction conditions. A direct linear relationship of glucose yields and N and N^t is depicted at 7%TS, but rotational speed is less significant in T1 glucose yields at 10% TS. In contrast, highest T1 glucose titers (4.4 g L^{-1}) were yielded by a short (15 minutes) and fast (30 rpm) mixing strategy at low-solids loadings (5%TS). It is well known that degree of mixing is dependent on total solids [148]. At low-solids loadings, slurry media behaves as a liquid, consequently, not mass-transfer limited in comparison with and it is not as mass-transfer limited than at higher solid contents [17].

(a)

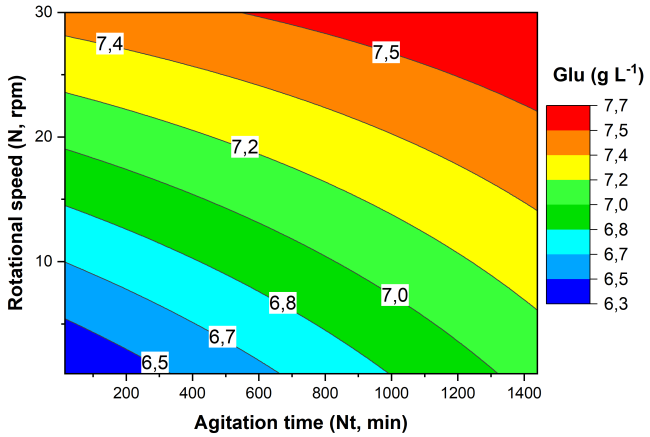

(b)

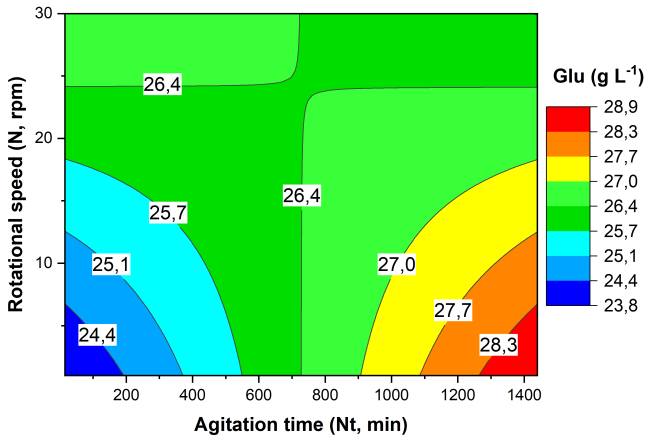

(c)

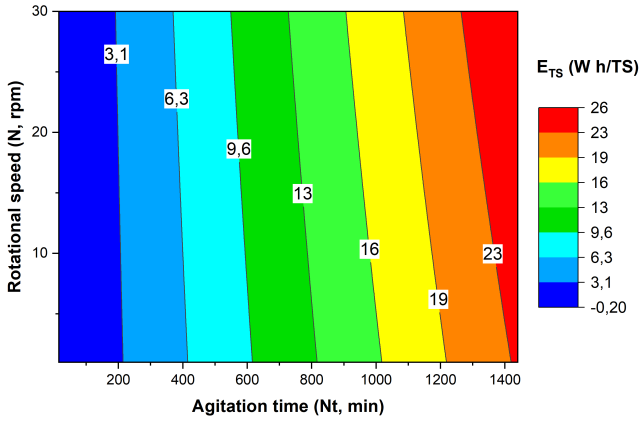

Figure 6.4. Response contours of DoE for examining the minimum mixing requirements: initial glucose yields (a), final glucose yields (b) and total energy consumption (c)

Once the enzymatic hydrolysis progresses (T24 glucose yields), N and N_t relationship is very different than for the one-hour glucose titers (Fig.6.4b). In this case, maximum T24 glucose yields of (28.3 g L^{-1}), red-zone) are achieved low (approx. 5 rpm) and extensive agitation periods (1300-1440 minutes). These results contradict Wojtusik et al. [73], which concluded that quicker agitation rates lead to higher mass-transfer and cellulose conversion at 20% w/w. Although, this statement may be applied for an enzymatic saccharification of pretreated corn stover under a stirred tank reactor configuration, but not when using rolling bottles as other authors suggested [146].

In Fig. 6.4c, it is noticed that E is a function of N and Nt, but agitation time has a more significant impact than stirring speed. Approximately a 110-fold energy reduction, 35.0 and 0.32 Wh TS^{-1} for N4 to N1, respectively, can be achieved with little initial agitation whilst reaching similar glucose levels (14 g L^{-1}). Doubling the amount of total solids halves normalised energy consumption compared with 5%TS, as less energy is needed per solids unit. Even intermediate mixing regimes (exp N9-N11) led to 11 W h TS^{-1}, yielding same glucose titers than 10%TS experiments with little agitation. From this, a more cost-effective strategy can be proposed in order to operate at higher solids loadings whilst saving on the energy demand.

To evaluate the effect of each factor per response, coefficient plots with a 95% confidence were plotted (Appendix C, Fig. C.2). The box plots showed that stirring speed has a positive effect of +0.5 g L^{-1} on initial glucose yields, whereas, no effect was seen for final glucose yields. Agitation time positively effects both glucose yields by 0.5-1 g L^{-1}. For E_{TS}, no comparison of positive effect (12 W h TS^{-1}) of N^t can be made with rest of variables. This work suggest that for energy-efficient deconstruction of biomass to sugar, intensive and short agitation followed by gentle mixing throughout enzymatic saccharification is sufficient [146].

6.4.2 Process modelling and simulation

6.4.2.1 Determination of reaction kinetics

A high-solids enzymatic hydrolysis (25% TS) of MSW-derived pulp was conducted, as described in section 6.3.2, where a power-law model was fitted into experimental data. for further data-extrapolation (Fig. 6.5). Fitted curve is formulated as $y = 14.469\ x^{0.446}$; where y is glucose concentration (g L^{-1}) at given time (h, x axis). This expression enables the prediction of glucose yields as function of reaction time with great accuracy as demonstrated by a coefficient of regression (r^2) < 0.98.

6.4.2.2 Modelling of production parameters of each operation mode

To complement the previous study (Chapter 5, section 5.5), additional production parameters were predicted via reaction kinetics for each mode of operation (Eq. 6.17. Table 6.10 summarises glucose yields, rates and production based on a lab-scale (2 L) version of enzymatic saccharification of MSW-pulp. For each mode of operation,

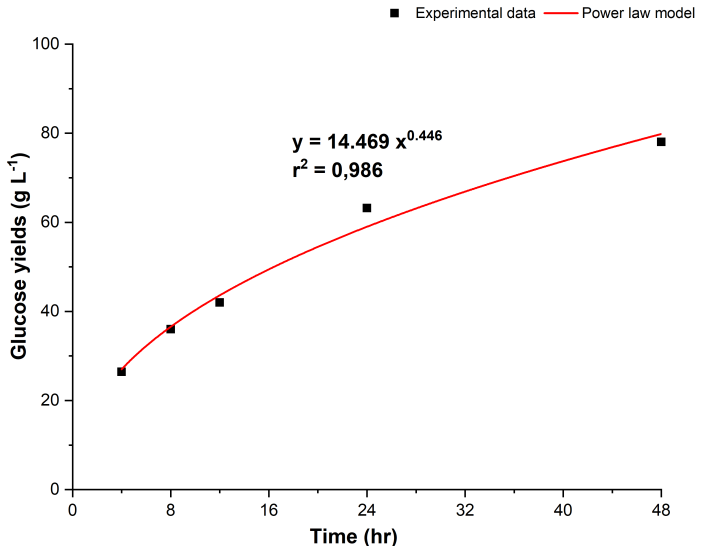

Figure 6.5. Kinetic analysis of batch hydrolysis of MSW-derived slurries in 2-L drum reactors : experimental and modelling glucose yields and rates

Reaction conditions: 25% TS, 2% E:S, 0.01% BIT, 30 rpm, 80 %V, 50 °C and pH 4.75-5.25

a residence time of 120 hours for the batch and fed-batch systems was set, whilst, a 6/48 (54 hours) configuration for the continuous mode.

Table 6.10. Comparison of modelled parameters of he enzymatic hydrolysis of MSW-pulp per mode of operation: batch, fed-batch and continuous

	Batch	Fed-batch	Continuous
Glucose yield (g L^{-1})	120	140	102
Glucose rate (g $L^{-1}h^{-1}$)	1	1.25	2
Glucose mass production (g)	240	260	1683
Residence time (h)		120	54

Reaction conditions: 25% TS, 2% E:S, 0.01% BIT, 30 rpm, 80 %V, 50 °C and pH 4.75-5.25.

As observed in Table 6.10, continuous processing improves the main process-related parameters of the enzymatic hydrolysis of MSW-pulp, in comparison to batch and fed-batch modes. Although lower glucose yields were reported (102 g L^{-1}) mainly due a shorter residence time and associated losses until reaching steady-state, overall glucose rates (2 g L^{-1} h^{-1}) and mass production (1683 g) are higher in continuous mode. In particular, a 7 and 6.5-fold increase is observed in MSW-derived sugar production, when enzymatic saccharification operates in continuous, compared to batch or fed-batch, respectively. This study also indicates that fed-batching is more advantageous than batch processing as all modelled parameters are higher [17]. Although being a more laborious feeding strategy, fed-batch offers significant improvements in glucose yields (140 to 120 g L^{-1}), rates (1.5 and 2 L^{-1} h^{-1}) and mass production (260 to 240 g) to batch.

Similar results were reported by Ghorbanpour and Miccio [310], for the comparison of batch, fed-batch and continuous enzymatic hydrolysis of orange peel wastes (OPW) by mathematical modelling. The rate equations per mode of OPW enzymatic hydrolysis were calculated by previous determination of Michaelis-Menten constants followed by a Lineweaver-Burk data transformation and linearisation. Despite the numerous assumptions, constant reaction conditions (temperature, volume, density, composition) and simple kinetics, three ideal reactors (batch, fed-batch and continuous) were modelled using MATLAB®, showing an evident advantage of continuous processing as achieving higher production of galacturonic acid compared to batch and fed-batch. This work is a useful tool for the prediction of process yields, e.g. modelling of industrial bioprocesses.

6.4.2.3 Sweet spotting: finding of optimum conditions

In Fig. 6.6, the sweet spot is represented as a light-green area, where all three criteria are met according to the set limits (see note in Fig. 6.6). Data-extrapolation points out that the "sweet spot" lies around residence times of 54-65 hours and total solids of 24.6-25 %. At above 24.6%TS, prolonged residence times (120 hr) are not necessary to achieve acceptable levels of sugar concentrations, indicating that a more cost-effective operation is possible. In addition, these requisites can be achieved with low enzyme loadings (2% E:S) and agitation rates (10-30 rpm). Consequently, these sweet spot conditions of 25%TS (solids loadings) and 54 hours (total batch time) are selected as guidelines for carrying out the process design of continuous MSW hydrolysis.

To date, sweet spot optimisation tools are poorly employed in the biorefineries area. This term is more commonly used in sustainability studies where three key pillars (social, economic and environmental) are combined and achieved for certain process/product [356]. But some publications can be found in regards of ethanol/gasoline optimum blending. The U.S department of Energy concluded that "sweet spot" of ethanol blending was between 25 and 40% as meeting emissions, price and infrastructure requirements [357]. Some mentions of sweet-spot have been made in other biorefining areas, but not fully investigated. At the IBioC, it was mentioned that one of the feedstock challenges for industrial wastes/residues for biorefining is finding the sweet spot between volume, process and demand [358]. Although, making these statements, no evidence of sweet spot optimisation has been found.

6.4.3 Techno-economic assessment at pilot-scale

6.4.3.1 M&E balances

Annual mass/energy (M&E) balances of the best-performing configuration (6/48 two-stage continuous system) are shown in Fig. 6.7. M&E balances of remaining configurations are included in Appendix C. In addition to the inlet and outlet mass

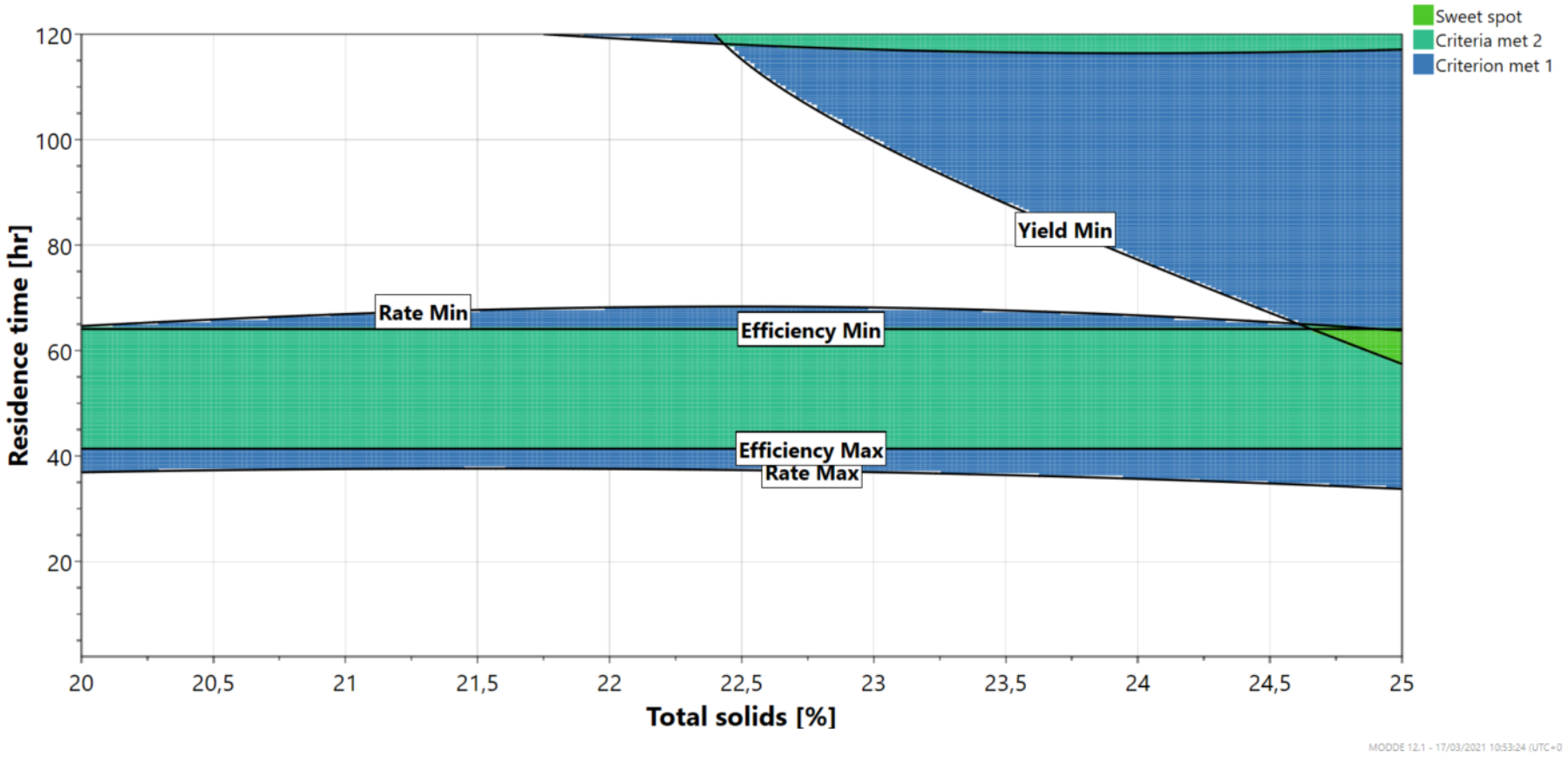

Figure 6.6. Sweet spot plot design of residence time vs total solids for three response variables: glucose yields, rates and efficiency

For three response variables either none, one, two or all three criteria can be satisfied. This is illustrated by the white area (none), dark blue area (one), turquoise area (two) and the light green area also known as the sweet spot (all three). Thresholds of responses are: yield (50-75 g L^{-1}), rates (0.5-2 g L^{-1} h^{-1}) and efficiency (0.1-0.3 g glucose kW^{-1} $^{-1}$
Note: labels represent lower and upper thresholds of each criteria (above-mentioned) as function of residence time and total solids

flows, an intermediate flow is included as the mass flow after the liquefaction step. In the 6/48 two-stage continuous system around 8.5 tonnes of MSW-pulp are processed per annum (tpa) in a dry basis, totalling 34 tpa of MSW-pulp slurry. For the process simulation, the lignocellulosic composition of MSW-pulp is glucan (55%), xylan (12 %), galactan/araban/mannan (6%, GAM), lignin (24%) and ash (3%), as reported previously [32, 47]. The annual product is a lignocellulosic slurry made of 3.1 tpa of glucose, PHS as solid residues (3.3 tpa) and wastewater as by-product (27 tpa). As the kinetic analysis focused only on the prediction of glucose yields, the rest of monosaccharides (and oligosaccharides) concentration are excluded in the product stream. Whereas, enzymes (170 kg) and sum of re-agents ($\sim$ 15 kg) represents a small portion on annual mass flows. For the energy balances, most of energy consumption is required for heating ($\sim$ 60%), mixing ($\sim$ 22%) and pumping ($\sim$ 15%) processes, totalling 14 and 12 GW for the liquefaction and saccharification step, respectively.

At laboratory and pilot-scale, M&E balances of enzymatic hydrolsyis are not commonly performed due to early-stage development and non-maturity of processes, although some examples can be found: corn stover [359], agave-based feedstock [79, 324] and switchgrass [191, 271]. Others authors [86] incorporated experimental data for process simulation and life cycle assessment of MSW to butanol and ethanol. Recently, a research group of the *Lawrence Berkeley National Laboratory* are commonly including mass balances of the bioconversion of biomasses to sugars via ionic liquid processes [79, 191, 271, 324, 360, 361]. Mass flows enabled the comparison between different sugar-producing routes from biomass. For instance, an alternative conversion of lignocelluloses to sugars via addition of hydrochloric acid (acidolysis) was developed in conjunction of ionic liquid pretreatments [360, 361]. Compared to enzymatic hydrolysis, more effective deconstruction of corn stover/grasses/non-recyclable paper mixtures is achieved via acidolysis, however, more severe conditions are necessary (4 N HCl and 105 °C). By establishing M&E flows, accurate techno-economic evaluations of lignocellulosic biorefineries can be acquired with experimental data, without depending completely on theoretical yields [348].

M&E balances of all investigated systems are summarised in Table 6.11, grouping input/output flows and depicting some efficiency-based parameters. By far, the 6/48 design outperforms the rest of two-stage continuous systems by 2 (12/42), 3 (18/36) and 4 (24/30) times in mass flows (feedstock, water, enzymes and re-agents). For instance, a 2-fold increase on feedstock inlets was observed by the 6/48 operation (8.5 tpa) instead of the 12/42 (4.2 tpa). Differences on processing capabilities are varying in proportion of flow-rates as set in the process design (Table 6.3.4.1) - 4.0 l h^{-1} (6/48), 2.0 l h^{-1} (12/42), 1.3 l h^{-1} (18/36) and 1 l h^{-1} (24/30). The 6/48 configuration has an annual revenue stream (sugar and PHS) 2, 3 and 4 higher than 12/42, 18/36 and 24/30 , respectively. The mass production is based on process design

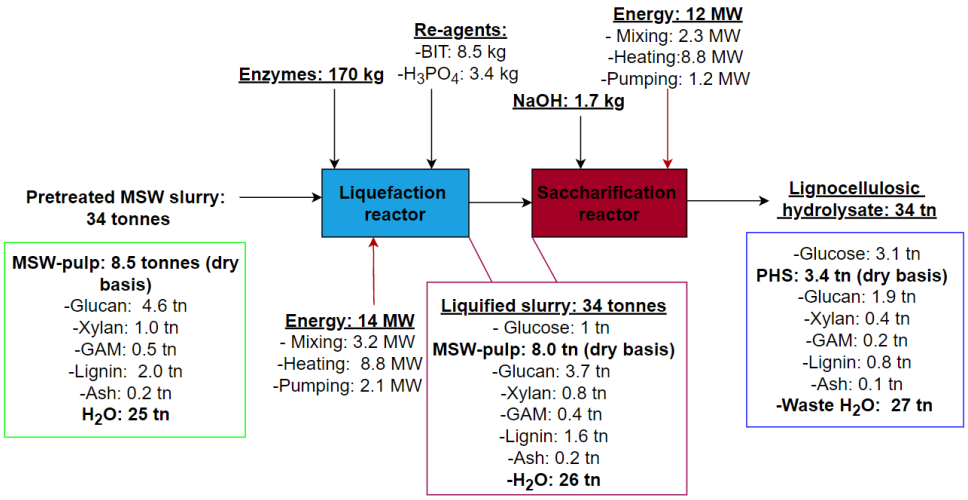

Figure 6.7. M&E balance diagram of best-performing pilot-scale configuration (6/48 two-stage continuous)

Liquefaction reactor: V = 30 L, RT = 6 hours and Q = 4 l h^{-1}
Saccharification reactor V = 230 L, RT = 48 hours and Q = 4 l h^{-1}
Legend: GAM is Galactan/Arabanan/Mannan as fraction of minor sugars

which has a direct impact into the CapEx, e.g. number/size of engineering equipment [362]. For a full techno-economic evaluation, experimental trials are necessary for establishing a more robust M&E balance.

Furthermore, the bioprocessing energy (sum of liquefaction and saccharification bioreactor energy requirements) of 6/48 configuration is significantly lower (25 MW) than other two-stage continuous systems: 35 (12/42), 45 (18/36) and 55 MW (24/30). Appendix C includes the individual power demands per equipment of each investigate configuration (Table C.2). Increasing the number of liquefaction reactors (and pumps) results into a higher energy demands due to mixing and heating, even though, smaller vessels are employed for the saccharification step. According to the energy demands per engineering component (Table 6.3), the electricity requirements for heating are 4 times higher than mixing. Consequently, bioreactor designs with more vessels result into higher energy consumption. This statement is only valid when power consumption is not measured as function of slurry viscosity, thus having an impact on mixing and pumping processes [196]. In theory, shorter liquefaction times results into highly-viscous substrates, therefore, higher energy requirements. As possible solution is to incorporate a correction factor per mixing stage (liquefaction and sacharification) in accordance to viscosity reduction during enzymatic saccharification of previous investigation working at high-solids loadings [42, 58, 251]. Although, these correction factors would not be accurate for the enzymatic hydrolysis of MSW-pulp, it would provide a further adjustments in the real values.

To complement the M%E balances, energy and enzyme efficiencies were calculated per investigated configuration. But the energy efficiencies vary depending on the configuration: 0.12, 0.04, 0.02 and 0.01 tn glucose MW^{-1} for 6/48, 12/42, 18/36

and 24/30 configuration, respectively. According to Dasari et al. [40], energy efficiencies of 10-25% w/w enzymatic hydrolysis of pretreated corn stover was in the range of 0.15-0.20 tn glucose MW^{-1}, highlighting that that 20% solids was the optimum solid level as the glucose release compensated the higher energy requirements. Whilst, Correa et al. [194] reported values of 0.23-0.35 tn glucose MW^{-1} in sugarcane bagasse hydrolysis under different feeding strategies. Even one of our reference systems (fed-batch) displayed energy efficiency values of 0.03 tn glucose MW^{-1}, at least double what was reported. So, the two-stage continuous systems showed that energy-efficiency can be improved over batch and fed-batch strategies.

Enzyme productivity was also calculated alongside energy efficiency, as indicator of efficiency in regards of enzyme dosages. Not much evidence of this parameter has been reported, but it has gained importance, in particular in enzyme recycling studies [114]. In a fed-batch processing followed by enzyme recycling, Visser et al. [114] determined enzyme productivities in the range of 3.78-2.56 g sugar/mg enzyme protein, depending on enzyme loadings for a solids content of 12% w/v. Home-made enzyme extracts, 50:50 (v/v) from filamentous fungi were used with low filter paper activities (5.7 FPU/ml). Therefore, lower enzyme efficiencies are displayed in comparison with our study (14-20 g glucose mg^{-1} enzyme protein), using commercial enzyme blends (Cellic CTec3) with FPase activity of 120 FPU/ml [209]. More active enzyme formulations are required for enhancing the cost-effectiveness of the system, through achieving considerable enzyme savings whilst guaranteeing an efficient enzymatic saccharification [221].

Table 6.11. Summary of M&E balances of the pilot-scale configurations

	Two-stage continuous					
	6/48	**12/42**	**18/36**	**24/30**	**Batch**	**Fed-batch**
Input						
Feedstock (tn)	8.5	4.2	2.7	2.0	1.5	1.5
Water (tn)	25	12	8.3	6.2	4.7	4.7
Enzymes (kg)	170	84.6	55.9	41.4	31.5	31.5
Re-agents[a] (kg)	13	6.7	4.4	3.3	2.5	2.5
Bioprocessing energy[b] (MW)	25	35	45	55	11	26
Output						
Glucose (tn)	3.1	1.5	1.0	7.6	6.9	8.2
PHS (tn)	3.4	1.7	1.1	8.2	6.3	6.3
Wastewater (tn)	27	13	9.0	6.6	4.9	4.8
Energy eff. (tn glucose MW^{-1})	0.12	0.04	0.02	0.01	0.05	0.03
Enzyme prod. (g glucose mg^{-1} enzy. protein[c])	14	14	14	14	16	20

[a] Re-agents include BIT (antimicrobial agent), H_3PO_4 and NaOH (pH adjusters)
[b] Bioprocessing energy includes mixing, heating and pumping per stage
[c] A protein content of 110 mg BSa ml^{-1} was determined for Cellic CTec3, by the Bradford assay

Compared with the reference cases (batch and fed-batch), a 5-fold increase on total production (8496 to 1576 kg yr^{-1}) is observed by operating with the 6/48 system. Although, batch hydrolysis halves bioprocessing energy (12 MW) to 6/48 (25 MW) and fed-batch (26 MW) system, particularly due to being structured as one

230L stirred tanks. The incorporation of a second stage, makes the fed-batch system to produce around 130 kg per year more than batch design (828 to 692 kg yr^{-1}), but with a lower energy-efficiency (0.03 kg glucose kW^{-1}) than batch design (0.05 kg glucose kW^{-1}). It is well-known that batch and fed-batch systems result in higher conversion yields than continuous processing, mainly due to operating at longer residence times [305]. The release of glucose yields during different modes of operation (batch, fed-batch and continuous) has been compared for the enzymatic saccharification of corn stover [21, 22] and orange peel wastes [310]. Although insoluble solids loadings were not set equally, due to "clogging" issues during the continuous process, Stickel et al. [21] showed that batch hydrolysis yielded over 10 g glucose per g biomass (at 10%TS) whilst only 0.44 g glucose per g biomass in continuous (5% TS). A sudden decrease in glucose concentrations is observed when switching from batch to continuous, taking several hours until reaching steady-state. More recently, Lischeske and Stickel [22] reported that final glucose concentrations of 5 and 7.5%TS acid-pretreated corn stover were significantly higher in batch than continuous mode, 22.5 to 12.5 g L^{-1} and 40 to 22 g L^{-1}, respectively. On the other hand, Ghorbanpour Khamseh and Miccio [310] modelled that galacturonic acid concentrations decreases from 0.3 to 0.15 g/kg biomass during orange peel hydrolysis, when changing from batch to continuous operation. A similar behaviour was observed in the mass production of the pectin-derived acid, 0.15 to 0.14 g, if processing in batch or fed-batch, respectively. It is widely accepted that poorer process yields are achieved in continuous than batch or fed-batch processing.

6.4.3.2 Economic analysis

The economical analysis consists on the determination of CapEx, OpEx, revenue and profit for the above-mentioned pilot-scale configurations (Fig. 6.8). As seen in M&E balances, 6/48 resulted into highest product turnovers with high energy-efficiency. This translates into the highest profit margins, ranging from £1,800 to 2,300 depending on the inclusion of energy costs. Despite reporting such profitability, 6/48 systems accounts for highest CapEx (£1,500) and OpEx (£1,200) values as structured with a 240-L STR and high usage of enzymes and re-agents, respectively. The two-stage design reduces the equipment costs by employing one horizontal reactor instead of two, but higher associated costs are observed due employing a 240-L STR. Interestingly, one of the reference systems (fed-batch) has same CapEx than 6/48 configuration, but its profits is reduced by a 8-fold ($\sim$ £500) due to lower production and low downtime costs. Downtime, understood as time than the plant is not operating, accounts for large sums of money which can be approximately 10% of OpEx including the loss of productivity but also adding start-up costs (cleaning, re-filling, heating etc..) [363]. Both CapEx and OpEX of other two-stage continuous configurations, decrease by 20-30% but leading to lower profitability rates. Despite presenting highest levels CapEx (£1,500) and OpEx (£1200), the modified version of 6/48 configuration generated an annual revenue of £3000 being the most profitable design (Fig.

6.8). The substitution of 3 CSTR of lower volume (80L) instead of a larger 230 L, decreases the CapEx by £2000 (£10 to £8k), even considering the installation of slurry pumps. This bioreactor design is more advantageous from techno-economic viewpoint, as higher profits are achieved with lower initial investment (CapEx) [243]. The two-stage 12/42 configuration is the second option in accordance to economics followed by the reference batch system, both with profits below £1000 at pilot-scale. In contrast, remaining three options (18/36, 24/30 and Fed-batch reference) are unfeasible for enzymatic saccharification of MSW-pulp as presenting negative profits. It is worth mentioning that either 24/30 and fed-batch reference present same-range CapEx values than 6/48 cases, but with a 8-fold reduction in revenues.

At pilot-scale, CapEx and revenue are not commonly estimated due to the early-stage development of processes, considered as non-profitable and immature technologies, but not at industrial stages [338, 364]. Rajendran and Murthy [364] assessed the economic viability of biorefining Banagrass and Energy cane into valuable fuels, chemicals and energy. Different 60,000 dry MT/yr processing plants were simulated by SuperPro for cost estimation, to then determine the economic parameters. Even considering the whole supply-chain, CapEx and revenue values can be extrapolated to put our study into perspective. From transportation into downstream processing, several products (ethanol, ethly acetate, ethylene, hexane and energy) are manufactured from Bananagrass and EnergyCane, with capital costs and revenues ranging from £500-600 and £200-500 per tonne of feedstock (Banagrass and Energy cane), respectively. Within biorefinery platforms, a conventional dilute-acid pretreatment followed by simultaneous saccharification and fermentation process, is compared as looking closer than system to our study. Biorefining of banagrass or energy cane enables the co-production of gypsum, energy and ethanol; accounting for OpEx and revenues in the range of £175-200 per tonne. Cellulosic biorefineries operate under small profit margins as being greatly dependent on ethanol market prices, therefore, diversifying into a portfolio of products [364]. To contextualise, we achieved OpEx and revenues in the range of £300-350 and £950-1100 per tonnage, respectively, even in the reference systems (batch and fed-batch). However, rest of biorefinery pathways are missing in the cost estimation (MSW-pulp pretreatment, downstream processing, waste water treatment and PHS burning), which would greatly changed the process economics.

The determination of CapEx and revenues are independent of electricity costs, but not the OpEx and profit calculations. In Fig. 6.8, standard deviations are included in average OpEx and profit values depending on energy costs (£0.01 or 0 kWh). Electricity represents around 20% of operational costs, whilst the rest accounts for chemicals (pH adjusters) and enzymes, playing a certain role on the economics. For instance, four investigated configurations (18/36, batch and fed-batch) are closely to become viable by including energy costs. Others are directly unfeasible, i.e 24/30, as presenting negative profit values. Saying that, average

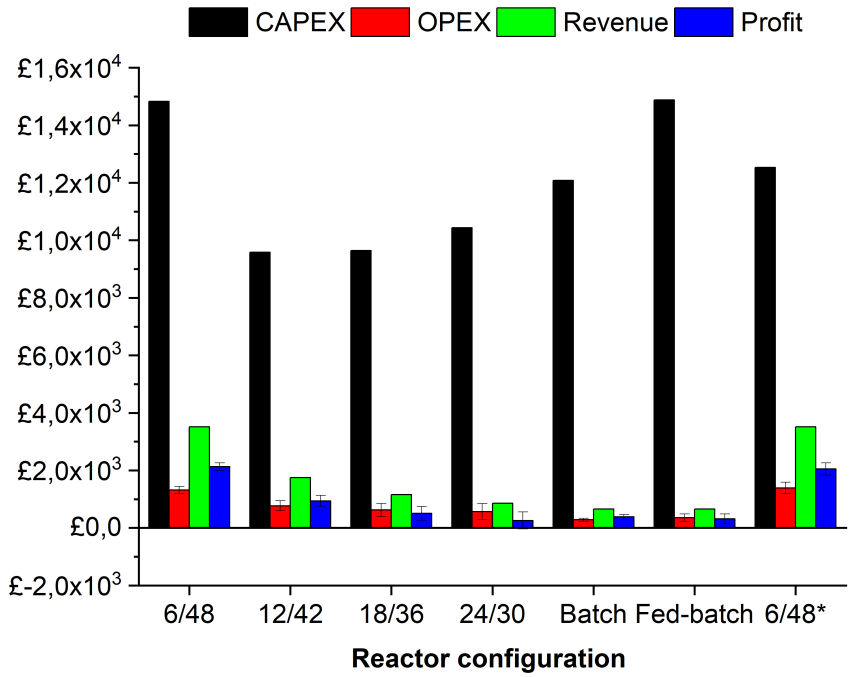

Figure 6.8. Economic analysis (CapEx, OpEx, revenue and profit) of pilot-scale configurations

Error bars represent standard deviation (±) of average values (with and without electricity costs)

OpEx/profit values decreased as function of revenue per bioprocessing configuration: 6/48 (£1500/£2100), 6/48* (£1400/£2050) 12/42 (£770/£940), 18/36 (£620/503), 24/30 (£560/250), batch (£280/380) and fed-batch (£353/315), respectively. Kazi et al. [336] demonstrated that ethanol product values are poorly affected by an electricity price in the range of 0.06 to 0.04 $/kW. h. At this tight range, no major differences are observed, but vast changes in electricity prices plays an important role on overall economics. To overcome electricity costs, a common approach in biorefineries is the integration of utilities processes such as biogas production or biomass combustion, from by-product stream for self-electricity production [147]. Wastewater produced during pretreatment and purification steps can be degraded via anaerobic digestion, whilst, the remaining solids are burnt for electricity generation. Other auxiliary processes commonly installed in biorefineries are heat-exchangers, in order to avoid heat losses, and ensure a better heat integration.

From the economic analysis of Fig. 6.8, return on investment (ROI) and payback period (PP) are determined as described in section 6.22. As profit does not include CapEx, these two parameters would elucidate better on the viability of each studied system. The effect of energy costs into both economic indicators is evaluated for each configurations, and foreseen an scenario with self-electricity scenario. As observed in Fig. 6.8, the energy plays an important role on OpEx making some reactor configuration feasible or not depending on this factor. Interestingly, ROI and PP of

both 6/48 configurations increase by 22% when excluding energy inputs. In average a 15-22% ROI and 4-6 years PP is estimated in both energy scenarios. For the rest of configurations, ROI/PP is ranked in a decreasing order as the profit results: 12/42 < Batch < 18/36 < Fed-batch < 24/30. Negative values of both ROI and PP were determined for 18/36, 24/30 and Fed-batch configuration with energy costs. On the other hand, the worst-performing reactor improved both economic indicators, but presenting ROI and PP of approx. 4-7% and 13-25 years, respectively. The determination of ROI and PP demonstrates the viability or not the investigated reactor configuration, and can be used as criteria for selecting the most cost-effective option for enzymatic saccharification of MSW-pulp at pilot-scale.

ROI and PP are common financial indicators for evaluating the rentability of a product/process. In one side, ROI reflects the efficiency of an investment being made, whilst, PP is the necessary time until reimbursing the capital investment. Techno-economic studies of lignocellulosic biorefineries include ROI and PP for the economic analysis, with assumed values [336, 338] or determined via cash flows [364, 365]. Kazi et al. [336] stipulated a 10% ROI for the production of 2000 MMg day^{-1} cellulosic ethanol, via a two-stage dilute acid and hydrolysis process coupled with fermentation. Other authors, Piccolo and Bezzo [365] compared two lignocellulosic biorefineries (enzymatic hydrolysis and fermentation to gasification), capable of processing 700,000 tpa of dry biomass wood into ethanol. Several economic indexes were calculated for both technologies, ranging from 20.5 to 32.5% for a PP of 10 and 5 years, respectively. As indicated from these reviewed publications, ROI and PP around 10-30 % and 5-10 years, respectively, are attractive enough for market investors. Therefore, only the 6/48 presents adequate economic feasibility, followed closely to the 12/42, which would need of some adjustments to reach this investment attraction.

Table 6.12. Financial analysis of pilot-scale configurations

	With energy costs		Without energy costs	
Reactor configuration	**ROI (%)**	**PP (yr)**	**ROI (%)**	**PP (yr)**
6/48	13	7.42	15	6.57
12/42	8.2	12.2	12	8.16
18/36	2.9	35	8.0	12.4
24/30	-0.3	-298	5.4	18.2
Batch	2.5	39.5	3.9	25.1
Fed-batch	10	103	3.3	29.6
6/48*	16	6.38	19	5.19

6.4.3.3 Sensitivity analysis

This study investigates the effect of ROI upon key parameters of the system, demonstrating minimum economic requirements and illustrating the potential scenarios of viable 6/48 continuous hydrolysis at pilot-scale. Hence, a sensitivity analysis was

performed by plotting a 4-D response countour plot (Fig. 6.9 from responses of experimental design at 6/48 pilot-scale configuration (Table 6.7). Due to exhibiting a best-performance in techno-economic terms, the 6/48 configuration is chosen for the sensitivity analysis. Contour plots of ROI (%) are mapped as function of enzyme (x axis) and horizontal reactor (y axis), according to three levels of sugar (£0.1, 0.3 and 0.5 kg^{-1}) and PHS costs (£-0.025, 0.1125 and 0.25 kg^{-1}). For each factor, a range of values (with the median as intermediate point) are set based on worst to best favourable market-conditions, to visualise the effect of extreme limits to ROI percentages.

As seen in Fig. 6.9, pilot-scale 6/48 continuous enzymatic hydrolysis of MSW-pulp is not feasible from an economical viewpoint (ROI ≤ 0) at different sugar/PHS costs combinations: £0.1 kg^{-1}/£-0.025 kg^{-1}, £0.1 kg^{-1}/£0.1125 kg^{-1} and £0.2 kg^{-1}/£-0.025 kg^{-1} (Figs. 6.9d,g,h). Despite of horizontal reactor costs, the process becomes viable at enzyme costs ranging from £1-1.6 kg^{-1} and £1-4.25 kg^{-1} when sugar/PHS costs are £0.3 kg^{-1}/£-0.025-0.1125 kg^{-1} (Figs.6.9e,i). Similar contour plots are mapped for Figs. 6.9a,f - showing that 5% ROI are achieved at horizontal reactors and enzyme costs below £25000/unit and £3/kg, respectively. In the case of Fig. 6.9f, the range of enzyme costs is significantly wider (£1-4/kg), increasing the economics flexibility of the process. As expected, higher ROIs are found at £0.3-0.5 kg^{-1} sugar costs at least at PHS £0.25/kg (Fig. 6.9b,c). Highest ROI (15%) are predicted at £1-2.75/kg of enzyme values when revenue streams are commercialised by the maximum prices (£0.5/kg and £0.25/kg for sugar and PHS, respectively). Rajendran and Murthy [364] carried out a sensitivity analysis of important process within different lignocellulosic biorefineries, using Banagrass and Energy cane as feedstock. Depending on the conversion pathway, ROI fluctuates from -5 to 10% ROI. Product selling prices, equivalent to sugar and PHS cost in this study, followed by plant capacity are considered the most important factors. Interestingly, ROI did not fluctuate much in accordance to enzymes costs (3-6%), in comparison with ethanol price (0 to 10%).

6.4.4 Techno-economic assessment of demonstration scale

A TEA study was performed for a demonstration plant, approximately 13000 times larger than the pilot-case version. The same methodology was employed for the determination of material and energy balances, financial analysis, but taking into account the corresponding process design and bioprocessing equipment costs.

6.4.4.1 M&E balance

As before, only the M&E balance of 6/48 two-stage continuous system was represented as being the most productive bioprocessing option (Fig. 6.10. This configuration processes 14.1 kt of pretreated MSW-pulp (14.1 kt), totalling 56.4 kt as slurry

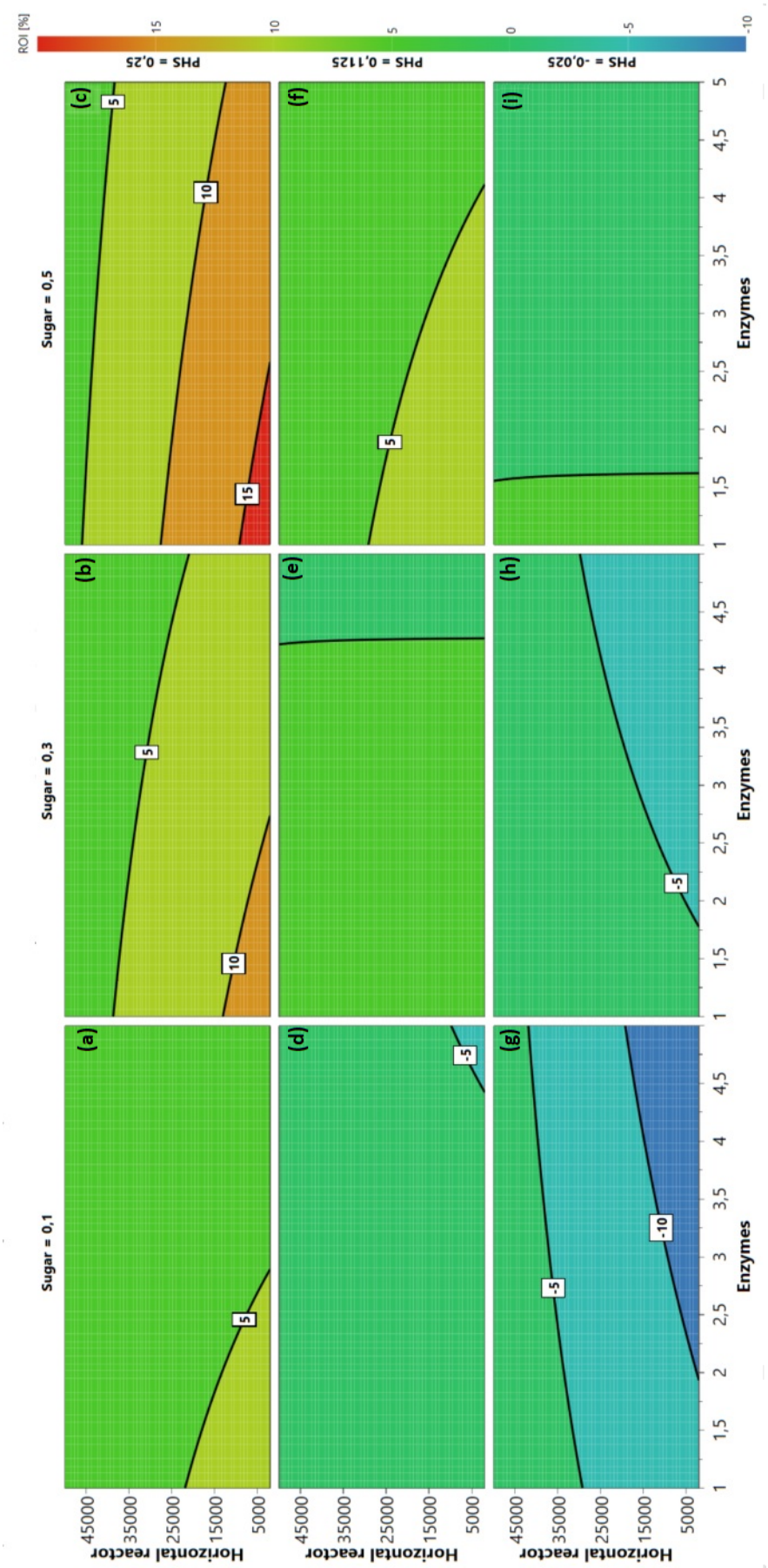

Figure 6.9. Sensitivity analysis (4-D contour plot) of 6/48 pilot-scale configuration, mapping ROI as function of horizontal reactor and enzyme costs for three levels of sugar and PHS costs

which then converts to 5.22, 11.3 and 45.5 kt of sugar, PHS and waste water, respectively. The pretreated MSW pulp is pH-adjusted with H_3PO_4 (5.64 tpa) and BIT added (35.3 tpa) for tackling the inherent microbial contamination. Once conditioned, pH and temperature, optimum conditions are achieved for starting the enzymatic saccharification with loading 282 tpa of enzymes. In the first stage, the aims is to reduce the initial viscosity of lignocellulosic slurry thus low conversion rates are expected for a short residence time (6 hour). An intermediate mass flow (liquefied slurry) is pumped for carrying on the enzymatic saccharification. Where additional 48 hours are necessary for increasing glucose titers to 102 g L^{-1}, achieved by gentle agitation in the stirred tank reactor. The release of organic acids tends to reduce the pH below the optimum threshold, in consequence, NaOH (2.82 tn) is added. The outlet stream contains a highly-concentrated sugar hydrolysate and solid fraction (PHS), made of recalcitrant carbohydrates and high lignin content. The hydrolysis broth also contains other monosaccharides (e.g. xylose and mannose) and oligosaccharides, but were not calculated in the mass flows as excluded in kinetic analysis. As seen in Fig. 6.10, most of energy demand (1.6 GW) is required in the saccharification stage, mainly for mixing of 400 m^3 stirred tank reactor. Only 0.3 GW for liquefaction as set for horizontal agitation, vessel heating and pumping of liquefied slurry. Roughly, 6/48 M&E balances are comparable with a cellulosic biorefinery plant [366], processing 20 kt per annum of dry forestry residues to ethanol. Similar inputs, enzymes (0.8 to 1.2 tonnes per hour) to this study were used, for degrading various forestry residues into fermentable sugars. Although, including additional engineering processes (pretreatment, fermentation, combustion and anaerobic digestion), this techno-economic study by Franko et al. [366] will be used as comparison.

Flow-sheet diagrams of the rest of investigated configurations are included in Appendix C (Fig. C.8-C.12). However, a summary of M&E balances showing the main inlet and outlet flows was included in Table 6.13. Appendix C includes the individual power demands per equipment of each investigated configuration (Table C.3). Annual material balances for the two-stage continuous configurations (12/42, 18/36 and 24/30) are approximately a half (28.0 kt), third (18.5 kt) and fifth (13.7 kt) of 6/48 lignocellulosic processing, which is 56.4 kt. These trends are kept constant in respect of other material balances such as water, enzymes and re-agents, despite normalising per total masses. In batch and fed-batch (two-stage) systems, a similar difference in processing capabilities are observed to the 6/48 case (13.1 to 56.4 kt per year), showing the advantages of two-stage continuous system with a shorter liquefaction (6 hours) and longer saccharification (48 hours) two-stage continuous system. The batch reference system also needs around 4/5 parts (1.64 GW) of bioprocessing energy. Surprisingly, the two-stage fed-batch system the worst configuration as displaying high energy requirements (2.64 GW) and poor lignocellulosic processing (13.4 kt). In the outlet stream, same differences on processing capabilities are observed between 6/48 configuration (5.22 kt sugar) and rest of designs: 12/32

(2.60 kt sugar), 18/36 (1.72 kt sugar), 24/30 (1.27 kt sugar), batch (1.44 kt sugar) and fed-batch (1.73 kt sugar) configurations. Complementary, PHS and wastewater are yielded in same proportion compared with the 6/48 configuration (Table 6.13), e.g. 11.3 and 5.6 kt of PHS or 45.5 and 22.7 km^3 of waste water for 6/48 and 12/42, respectively.

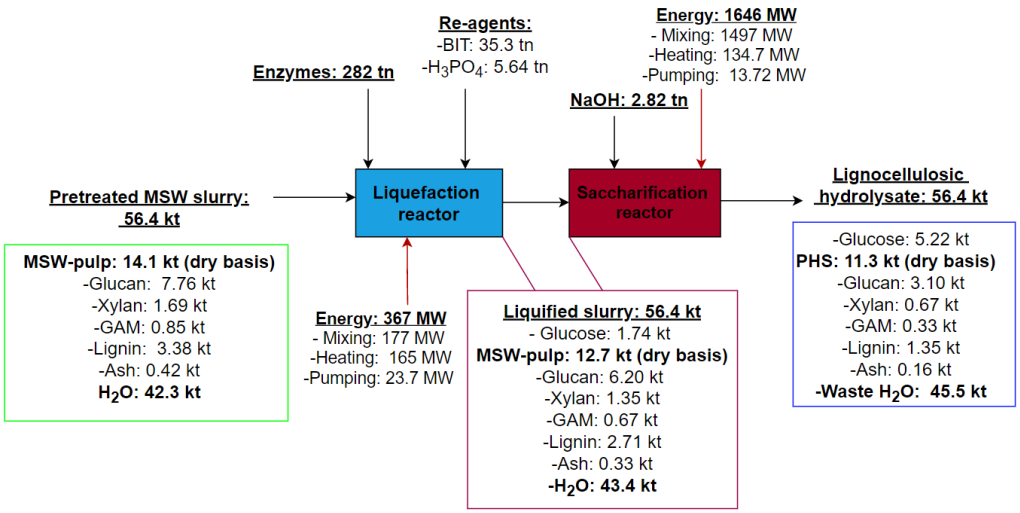

Figure 6.10. M&E balance diagram of best-performing demonstration-scale configuration (6/48 two-stage continuous)

Liquefaction reactor: V = 40 m^3 , RT = 6 hours and Q = 6.6 m^3 h^{-1}
Saccharification reactor V = 400 m^3, RT = 48 hours and Q = 6.6 m^3 h^{-1}
Legend: GAM is Galactan/Arabanan/Mannan as fraction of minor sugars

In industrial bioprocessing, among other industries, high energy-efficiencies are targeted to lower operational costs and environmental impacts [343]. The process design and operability have a huge impact on energy-efficiency of each system, dictated by the size of equipment and associated energy demand. In these regards, energy efficiencies of investigated configurations are compared as follows: 6/48 (2.59 kt glucose GW^{-1}) 12/42 (1.77 kt glucose GW^{-1}), 18/36 (1.16 kt glucose GW^{-1}), 24/30 (0.78 kt glucose GW^{-1}), batch (0.88 kt glucose GW^{-1}) and fed-batch (0.65 kt glucose GW^{-1}). As expected, the highest energy efficiency was reported by the 6/48 configuration as exhibiting the highest sugar production with moderate energy requirements. In contrast, fed-batch systems accounts for the lowest energy-efficiency despite of using same reactor configuration. The low productivity (1.73 tpa) in conjunction with highest energy demand (2.64 GW) leads to a ratio of less than 1 kt glucose per GW consumed (0.65). Rest of investigated configurations were at least 60% lower in energy-efficiency, decreasing linearly as function of decreasing sugar production. Interestingly, the 24/30 configuration consumes as much as energy than reference systems for producing same quantities of lignocellulosic sugars per mass unit. On the other hand, enzyme efficiencies remained constant for all two-stage continuous configurations (14 g glucose mg^{-1} enzy. protein). But, higher ratios are

reported for the batch and fed-batch systems: 16 and 20 g glucose mg^{-1} enzy. protein, respectively.

Different Swedish researchers [345, 346, 349] investigated the techno-economic viability of forestry-based biorefineries for manufacturing of ethanol, electricity and biogas. Ethanol is produced via SO_2 pretreatment plus simultaneous saccharification and fermentation with on-site yeast cultivation from softwood residues in scales ranging from 150 to 250 kt per annum. Despite using a shared model for process simulation, each author has adapted it accordingly. Energy demand (efficiency) understood as energy input per produced ethanol has been determined in three studies, reporting values of 13.5 to 34.6 [366], 0.9 to 21.3 [345] and 11-14 [349] MJ per kg or l of ethanol. For instance, Franko et al. [366] depicted energy demands with high variability according on raw material used for biorefining (from sawdust to hog fuel), which are equivalent to $\sim$ 1-2 kt per GW^{-1}. Although, both biorefinery models are not directly comparable, these back-of-the-envelope calculation shows that three two-stage continuous systems (6/48, 12/42 and 18/36) are as energy-efficient as robust biorefinery models.

Table 6.13. Summary of annual M&E balances of the demonstration-scale configurations

	6/48	**12/42**	**18/36**	**24/30**	**Batch**	**Fed-batch**
Input						
Feedstock (kt)	14.1	7.10	4.70	3.50	3.25	3.25
Water (km^3)	42.3	21.0	13.9	10.3	9.85	9.85
Enzymes (tn)	282	140	92.9	68.8	65.7	65.7
Re-agents (tn)	43.7	21.8	14.4	10.7	10.2	10.2
Bioprocessing energy (GW)	2.01	1.46	1.47	1.62	1.64	2.64
Output						
Glucose (kt)	5.22	2.60	1.72	1.27	1.44	1.73
PHS (kt)	11.3	5.6	3.7	2.8	2.6	2.6
Wastewater (km^3)	45.5	22.7	15.0	11.1	10.4	10.4
Energy efficiency (kt glucose GW^{-1})[c]	2.59	1.77	1.16	0.78	0.88	0.65
Enzyme prod. (g glucose mg^{-1} enzy. protein[c])	14	14	14	14	16	20

[a] The re-agents stream includes BIT (antimicrobial agent) and H_3PO_4/NaOH (pH adjusters)
[b] Bioprocessing energy includes mixing, heating and pumping per each stage (liquefaction and saccharification)
[c] Energy efficiency is ratio between Glucose (kt) and Bioprocessing energy (GW))
[c] A protein content of 110 mg BSa ml^{-1} was determined for Cellic CTec3, by the Bradford assay

6.4.4.2 Economic analysis

It is noted that CapEx increases as function of number of engineering components, mainly driven by higher costs of horizontal reactor (£200k) in difference with the rest of equipment. Consequently, process designs with more horizontal reactors results into higher CapEx, despite of being set-up with smaller stirred tank reactors. Generally, CapEx slightly exceeds £1m (24/30 two-stage configuration) but diminishes among continuous systems as function of liquefaction time: £772k (18/36), £556k (12/42) and £489k (6/48). Employing one CSTR (400 m^3) into three CSTRS (133 m^3)

does not account for smaller CapEx (£497k), as incurring additional costs on heating and pumping equipment. Recently, Davis et al. [339] demonstrated that CSTR in series account for higher capital costs than single reactors, which also estimated a difference of more than £30m depending on batch (£10m) or continuous (£43m) enzymatic hydrolysis to produce lignocellulosic sugars for manufacturing butyric acid and 2,3-butanediol, respectively. The batch system is more economic than rest of configurations (£244k), due to its bioengineering simplicity (one 400 m^3 STR) and absence of transfer pump between stages. The two-stage fed-batch system presents same CapEx than 6/48 configuration (£489k), as showing an identical design - 50 m^3 (liquefaction reactor) and 400 m^3 (saccharification reactor). Humbird et al. [147] included a list of vendor's quotes on mechanical equipment, showing that only the hydrolysis and fermentation stage costs around £21m for converting 773 kt per annum of corn stover into ethanol. Among these costs, saccharification tank (250,000 gallons) and transfer pump (352 gallons per minute) account for £5.6m and £80,000, respectively. For instance, the 6/48 configuration costs around £150,000 only considering the 400 m^3 STR connected with a purged pump (6.6 m^3), approx. £500,000 in total. In a case-by-case comparison, a lower CapEX per processed biomass ratio is seen in Humbird's study (£7200/kt) to our study (£10000/kt).

In contrast, OpEx increases as increasing overall M&E balances, ranked as follows per bioprocessing configuration: £1.4m (6/48), £706k (12/42), £472k (18/36) and £355k (24/30), £350k (Fed-batch) and £340k (Fed-batch). The modified version of 6/48 ($6/48^{-1}$) present similar OpEx values than the conventional design (£1.4m). Only a 2% increase is noted if electricity costs are included or not for all configurations, e.g. £1.41 to £1.39m for 6/48 with and without energy costs. It is well noted that OpeX of lignocellulosic biorefineries is mainly affected by the costs of enzymes, representing around 16-20% of total operational costs. In this study, a higher contribution is calculated (Data not shown) of around 40% since the rest of commodities are very affordable with prices lower than £1/kg. Despite elevated OpEx values, the superior processing capacity of the 6/48 (and 6/48*) configuration translates well into a higher revenue stream (£5.8m), which doubles the 12/42 system (£2.9m). Revenues descend for rest of configurations to: £1.9m (18/36), £1.42 (24/30). In reference systems, the revenues varies upon final glucose concentrations as the same sugar production is achieved. The fed-batch strategy yields higher glucose titers (146 g L^{-1}) than batch hydrolysis (122 g L^{-1}), resulting into a higher revenue stream (£1.6m to £1.5m, respectively). These revenue streams are calculated at favourable market conditions for sugar and PHS price, but within commercial prices. As most lignocellulosic slurry is made of water, additional downstream processing and purification is needed to acquire the highly-concentrated sugar syrups. Therefore, not much product is left. As PHS constitutes around 25% of whole slurry, the feasibility or not to sell competitively in the market would have a huge impact on the revenue stream. For instance, the revenue stream of 6/48 configuration would be of £2.3m (Data not shown) if PHS is not sold.

Rajendran and Murthy [364] reported OpEx in the range of £10-35m for biorefining 60 kt per annum of Banagrass and EnergyCane into bioproducts including ethanol, ethyl acetate, dodecane, hexane and electricity. For a SSF-based conversion platform, OpEx were approximately £10m which is the equivalent of £16 x 10^3 per kt per annum. Among our investigated systems, maximum OpEx to feedstock ratios of £100 x 10^3/kt are calculated, a 6-fold increase to the Banagrass/Energycane ethanol production. Similar values were calculated for the revenue streams, showing the higher economic potential of biorefining of agricultural residues into ethanol, gypsum and electricity. These great differences can be attributed to an unrealistic enzyme cost, £0.36/kg, set by Rajendran and Murthy [364]. Yang et al.[240] highlighted that the Department of Energy Biomass Program pretended to meet an enzyme costs goal of £1.5/kg at minimum. It seems impossible that enzyme manufactures could go down to £0.36/kg as commented, thus, the OpEx will not be entirely accurate at this point.

For the continuous systems, profit decreases as previously observed in the calculation of revenue streams: £4.4m (6/48), £2.2m (12/42), £1.4m (18/36) and £1.07m (24/30). A considerable economic advantage is noticed by fed-batch (£1.23m) instead of batch processing (£1.12m). As profit is calculated only based on the enzymatic hydrolysis of biomass, it is challenging to compared with other biorefineries which encompass the whole process [299, 339]. Notwithstanding, the profitability of the process is mainly driven by enzymes costs, which itself is affected by commercial agreements upon choice of cocktail, volume required, frequency of supply etc. The commercialisation of co-products such as lignocellulosic sugar and PHS operates in tight margins, dictating the profitability of the whole process. The rest of bulk commodities are used in less quantities and due to their low and stable commercial prices, do not affect as much the generated profits. The variability of profits according to enzyme, sugar and PHS costs is assessed in the following section, by conducting a sensitivity analysis. Hence, presented results are only subjected to components cost as depicted in Table 6.6. Compared with SSF-based forestry residues biorefineries, generating profit by selling ethanol and co-products (pellets, biogas and electricity), profit margins ranged from £280-425m in a 20-year time-span as function of raw materials is used (e.g. sawdust and shaving, early thinnings) [366]. A 200 kt per annum cellulosic ethanol biorefinery would make approx. £100,000 per kt dry biomass, 3 times less than our best-performing system (6/48, £300,000/kt MSW pulp). In this case, excluding additional capital and operational costs in pretreatment and fermentation steps results into higher profits per unit of processed biomass. Qualitatively, the MSW-to-sugars process is more profitable than SSF-based forestry biorefinery, but further inclusion of financial parameters and performance of in-depth techno-economic assessment is needed to make final conclusions.

From the economic analysis of Fig. 6.11, return on investment (ROI) and payback period (PP) are estimated as described in section 6.22. Table 6.14 summarises ROI and PP values according to each bioprocessing configuration, including the effect

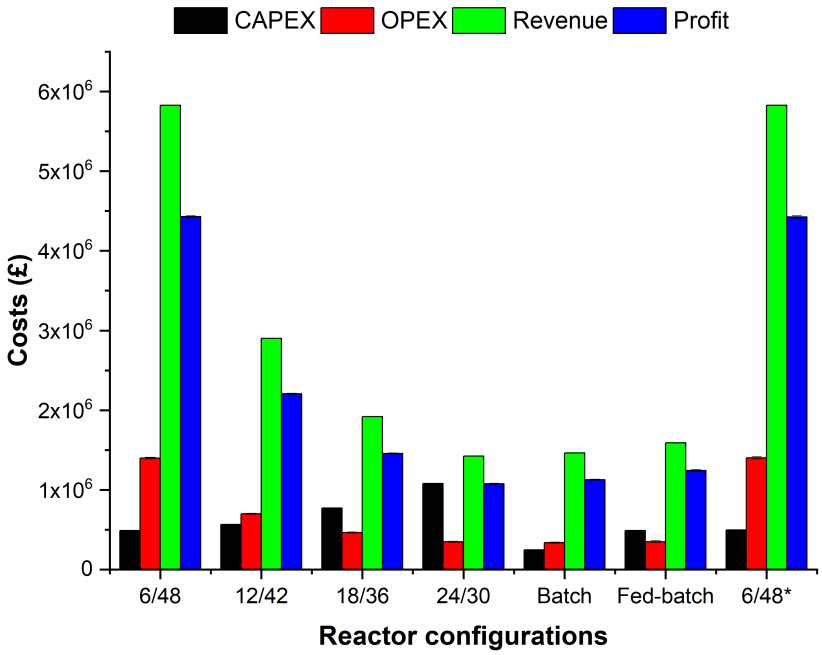

Figure 6.11. Economic analysis (CapEx, OpEx, revenue and profit) of demonstration-scale configurations

Error bars represent standard deviation (±) of average values (with and without electricity costs)

of electricity costs. Both parameters are determined to examine the effect of capital costs in dictating the financials per bioprocessing configuration. As unrealistic values were determined by using enzymes, sugars and PHS costs from Table 6.6, these conditions were modified to achieve a more close-to-reality case. Generally, higher ROI and lower PP values are reported in process designs with higher profits but lower CapEx ratios, and viceversa: 42 %/2.39 years (6/48), 17 %/5.82 years (12/42), 8 %/13.0 years (18/36) and 4.00 %/27.9 years (24/30). Whilst for reference systems, two well defined results are found: 30 %/3.33 years (Batch) and 22 %/4.52 years (Fed-batch). From the investors viewpoint, even including energy costs, only the 6/48 and 6/48* configurations are more attractive than reference batch system (ROI = 30 % and PP = 3.33 years), as presenting higher ROIs (42 and 39%) and lower PPs (2.39 and 2.54), respectively. As occurring with the profitability, a supplementary sensitivity analysis is required for studying ROI and PPs values in a wide range of conditions, including the worst-case scenarios (i.e. highest enzymes but lower sugar/PHS costs). At advantageous economic conditions, e.g. £0.35/kg of enzymes, Rajendran and Murthy [364] estimated that utilising hexoses and pentoses for ethyl acetate production from Banagrass led to ROI and PP of 8.93% and 11.2 years, respectively. Even at detrimental economic costs for enzymes and product, all investigate configurations improved ROI (20-42%) and PP (5-10 years) results than previous example. Including additional financial factors, such as labour costs and interests

rates, would have an impact on promising ROI/PP results and may provide a more realistic picture.

Table 6.14. Financial analysis of demonstration-scale configurations

	With energy costs		Without energy costs	
Reactor configuration	**ROI (%)**	**PP (yr)**	**ROI (%)**	**PP (yr)**
Two-stage (6/48)	46	2.18	42	2.39
Two-stage (12/42)	20	5.05	17	5.82
Two-stage (18/36)	10	10.43	8	13.03
Two-stage (24/30)	5	19.6	4	27.9
Batch	37	2.74	30	3.33
Two-stage (Fed-batch)	28	3.63	22	4.52
Modified Two-stage (6/48)	45	2.21	39	2.54

ROI and PP were calculated for the following costs: enzymes (£5/kg), sugar (£0.15/kg) and PHS (£0.1/kg)

6.4.4.3 Sensitivity analysis

At demonstration-scale, the sensitivity analysis was shown as a 4-D response countour plot (Fig. 6.12 for the 6/48 configuration. The response on profit was obtained by running the TEA study for different combinations of enzymes, sugar and PHS costs. And, contour plots of profit (£) are mapped as function of enzyme (x axis) and sugar costs (y axis), both in £/kg, according to three levels of PHS costs sugar (£0, 0.125 and 0.25 kg^{-1}). Colour coding represents the ranges of profit margins by a £1m difference, and including negative scenarios. As seen in Fig. 6.12, the profitability of 6/48 two-stage continuous system is a function of all three factors (enzymes, sugar and PHS costs), where different scenarios are available for viability at demonstration-scale. According to Kazi et et al. [336], product value of ethanol (as indicator of profitability) is more sensitive to enzyme costs followed by feedstock cost, varying from $1.2 to 1.8 and $1.2 to 1.45 per liter of ethanol, respectively. A difference of fifty cents of a dollars could make feasible or not the biorefining of corn stover to ethanol at commercial-scale, as manufacturing millions of litres leading to multi-million profits or losses.

At unfavourable conditions (PHS prices of £0/kg). the enzymatic hydrolysis of MSW-pulp starts being viable at sugar prices of at least £0.24/kg and minimal enzymes costs (£1/kg). But this scenario is not realistic due to such low enzymes costs, highlighting the need of making some profit with the PHS stream. An intermediate case, PHS price equal to £0.125/kg, offers greater flexibility in terms of profit as being more robust. Independently of enzyme and sugar costs, positive profit values are observed throughout the contour plot. Sensible market prices of £4/kg (ref) and £0.3/kg (ref) for enzymes and sugar, respectively, would result into profits of over £2m. At more advantageous conditions, PHS price of £0.25/kg, a minimum profit of £3m is achieved independently of all costs. Further improvements on biotechnology manufacturing are necessary to decrease the prices of enzymes around £1.5/kg

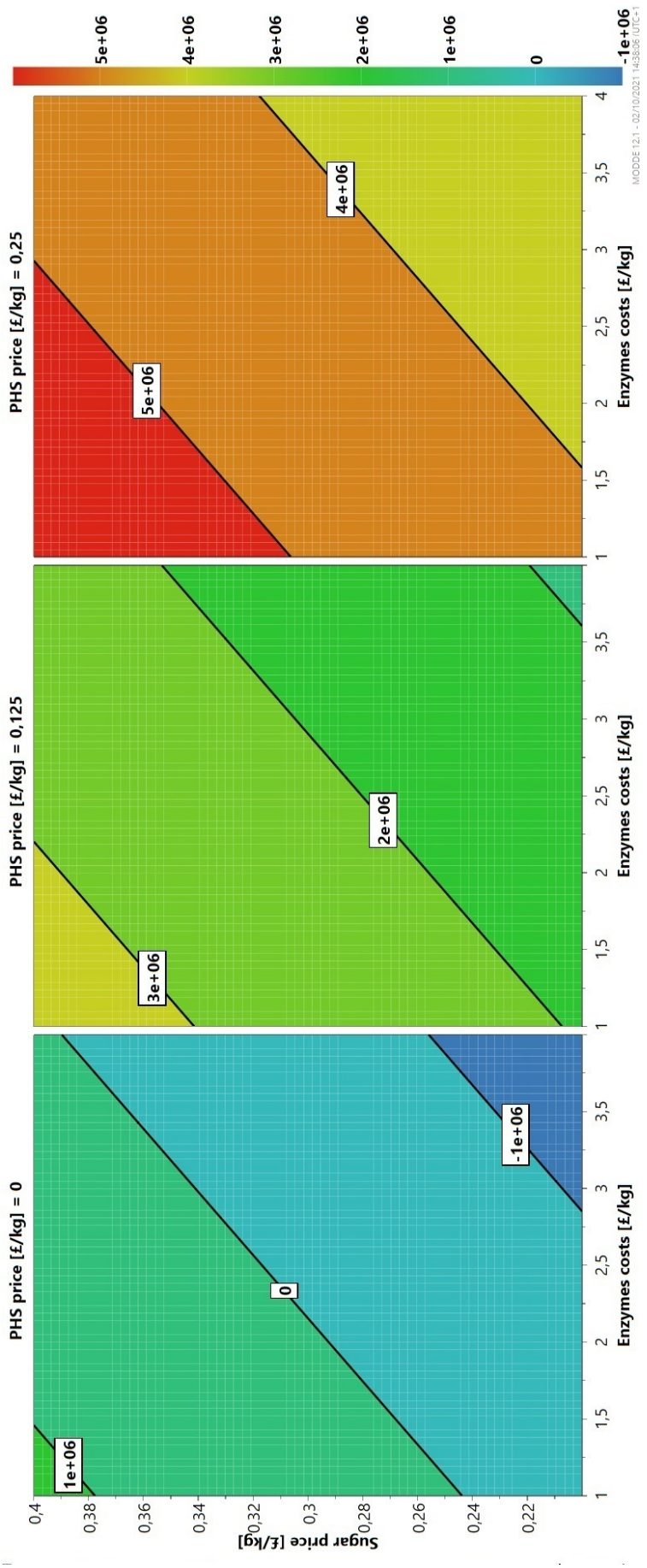

Figure 6.12. Sensitivity analysis (4-D contour plots) of the 6/48 demonstration-scale configuration, mapping profits as function of enzymes and sugar costs for three levels

as minimum requirement for the viability of cellulosic ethanol. However, even doubling the enzymes costs to £3/kg with a moderate sugar price of £0.3/kg would turn into the highest profit levels of over £5m. Notwithstanding, it is recommended of PHS purification in order to satisfy the market requirements, otherwise, the feasibility of the process cannot be achieved.

6.5 Conclusions

In this chapter, three main areas were researched for the scale-up of enzymatic hydrolysis of MSW-pulp into fermentable sugars: optimisation, process modelling and techno-economic assessment.

Optimisation encompassed the use of DoE for the determination of optimum conditions upon reactor operability for the release of fermentable sugars from MSW with the highest energy-efficient. As demonstrated, intensive and continuous mixing is not necessary for undergoing the enzymatic saccharification. At solids loadings ranging from 5 to 10%TS, short mixing times (15 minutes) are sufficient for promoting the enzymatic saccharification as enzymes adsorb into the substrate. Moreover, agitation rates can be decreased from 30 to 1 rpm, whilst producing the required concentrations. This work has demonstrated that alternative mixing strategies enhance energy-efficiency of the system, whilst yielding the necessary amounts of sugars.

Process modelling and simulation based on reaction kinetics, have enabled the prediction of glucose yields depending on different modes of operation: batch, fed-batch and continuous. Consequently, productivity advantages by operating in continuous mode have been validated. In addition, the prediction of reaction parameters (glucose yields, glucose rates and energy efficiency) lead to optimum settings in regards of the design of continuous system. This study suggests that residence times of 54 hours and 25%TS are adequate for designing continuous system, whilst meeting industrial process requirements

Through a simple techno-economic assessment, using process modelling and simulation, a comparative study between novel bioprocess and base-line study was performed. Based on commercial costs, the financial analysis per configuration was evaluated at pilot and semi-industrial scale, showing that the 6/48 two-stage continuous system outperforms over the rest of designs. The annual production of lignocellulosic sugars was enhanced by 7 times using this strategy over the reference systems, accounting for £1m profits at demonstration scale under the set economics.

Chapter 7

Conclusions and future work

7.1 Research summary

The main findings of the Thesis are summarised as follows, grouping the highlights of all "results" chapters:

- **High-solids loading enzymatic hydrolysis** was effectively pursued by a rotatory drum reactor, and 25% TS were identified as the upper threshold limit. With this solids loadings, it is recommended to conduct multi-sampling and through pH-adjustment for reliable analysis and accurate reaction control. Therefore, highly-concentrated sugar syrups ($\sim$ 80 g L^{-1}) can be achieved with cost-effective additions of enzymes and re-agents (pH-adjusters and antimicrobial agents) with low agitation rates (10 rpm).

- **Intrinsic biological contamination** of MSW substrates was tackled *in situ* by employing a home-made automated dosing system, integrated in the enzymatic hydrolysis process. The bespoke application is based on pH/DO levels as metric for predicting microbial contamination and reaction control, correlated with the analysis of organic acids. Amongst the tested compounds and concentrations, 0.01% w/w dry substrate weight of 1,2-benzisothiazolinone (BIT) is the preferred option as yielding the highest glucose titers whilst minimising the release of organic acid (lactic acid), and eliminating most of microbial population. The main findings of this study were included in the paper I [47].

- **The challenges of using MSW** as lignocellulosic material for enzymatic hydrolysis were evaluated and a new classification was proposed from the literature: surrogate materials, mixed wastes and single-stream. The physico-chemical characteristics of MSW slurries were determined and compared with conventional lignocellulosic substrates, to showcase the additional complexity of bioprocessing these materials. Commercial examples of MSW biorefineries were also discussed, putting in context the Fiberight Ltd. technology. These aspects were included in the paper II submission.

- **The rheology of MSW-pulp slurries** (raw and hydrolysate) was characterised, identifying the lignocellulosic dilutions as Non-Newtonian fluids with a shear-thinning with yield stress behaviour (Herschel-Bulkley). Through sweep flow tests, several correlations were achieved of solids loadings as function of rheological parameters, and these as function of operational parameters such as rotational speed. Moreover, the *in situ* rheometry enabled to acquire real-time viscosity data during enzymatic saccharification of MSW-pulp, showing the different liquefaction rates depending on an array of parameters: total solids, enzyme loadings, particle-size, rotational speed etc.. A literature analysis of the rheology profile of high-solids for the bioconversion (pretreatment, enzymatic hydrolysis and fermentation) of lignocellulosic biomass into high-value products was provided, which took part in the paper III submission.

- **A pseudo-flow hydrolysis** was successfully conducted to mimic continuous operability of a high-solids MSW enzymatic hydrolysis by rotary drum bioreactors. By manual handling, steady-state was achieved during 12 hours (3 space-volumes), yielding around 25 g L^{-1}. Liquefied slurry was periodically fed into a secondary tank for carrying on the enzymatic saccharification, resulting into higher glucose yields (80-90 g L^{-1}) than in batch mode (65 g L^{-1}).

- **Reactor design and modes of operation** were widely investigated and compared via: laboratory experimentation, process modelling and literature analysis. Amongst the reactor designs, the home-made SSBR outperforms in all studied parameters (power minimisation, energy efficiency, low footprint and access to in-line monitoring), except for total solids. For operating at high-solids loadings, the rotary drum bioreactors are more suitable than home-made SSBR. With regards of modes of operation, continuous enzymatic hydrolysis results into higher productivity rates, mass production whilst requiring less energy per processed unit.

- **Process optimisation** demonstrated that severe and agitation rates are not required for releasing the required glucose titers during enzymatic hydrolysis. By setting-up a 15-min agitation time at 30 rpm, power consumption is reduced by a 120-fold whilst energy efficiency improved by a 120-fold in comparison with continuous agitation strategies. This mixing strategy is applicable at 5-10% solids loadings, and may be of interest for certain applications where energy demand is critical on the feasibility of the system

- **A simple techno-economic evaluation** was performed to compare various bioprocessing configurations (two-stage continuous, batch and fed-batch) at both pilot and demonstration-scale, within the industrial requirements of Fiberight Ltd. From the techno-economic assessment, it was demonstrated that the 6/48 configurations is the most preferred option for setting an enzymatic hydrolysis of MSW-pulp, as showing 7-fold higher productivity rates and profits than

the reference systems. From an investor's perspective, the 6/48 configuration also present additional financial advantages than the rest of designs due to showing great differences in ROIs and PPs.

7.2 Contributions to knowledge

This Thesis pretends to contribute to different knowledge areas within the bioprocessing of lignocellulosic feedstocks such as bioreactor design, rheology and application of reaction control and monitoring. To follow, several aspects of this Thesis are summarised to show the contribution per area:

Automated reaction control and monitoring as means towards smart biomanufacturing has been investigated in several studies. By application of bespoke and licensed applications, it was possible to offer real-time and automated reaction control and monitoring systems for: (i) tackling of microbial contamination, (ii) recording of sugar concentrations and (iii) power optimisation during enzymatic hydrolysis of MSW-pulp. Some of these applications are available on-demand, whilst, the methodology for using others are described in paper I [47]. These on-line techniques are of great importance for reaction control and parameter monitoring in other biotechnological areas as studying common reaction parameters (pH, DO and power consumption).

MSW is a challenging feedstock for enzymatic hydrolysis due to its higher crystallinity, degree of biological infection and heterogeneity than the rest of lignocellulosic feedstocks. In this study, the difficulties to use MSW as starting materials have been overcome by setting-up of efficient antimicrobial strategies and efficient bioreactor design and operation. The different experimental studies have demonstrated the different behaviour of MSW within the high-solids regime, and contradicts the general statements on lignocellulosic rheology (e.g. "pumping" requirements, power-law parameters etc.). This study provides the know-how of efficiently using MSW as lignocellulosic feedstock, which enables its expansion within the biorefineries sector.

Working at high-solids loadings is one the requirements for commercialisation of lignocellulosic sugars. Herein, demonstrated by the application of rotary drum bioreactors as dealing with high-solids loadings, whilst minimising power consumption (mixing). Up to 25% solids loadings, the enzymatic hydrolysis of MSW-pulp to glucose in concentrations above 80 g L^{-1} was achieved under strict industrial requirements. The insights of reaction control and sampling under these conditions have also been discussed, which is useful for shifting from academic to industrial environment, and promote the scaling-up of this technology. Further literature review in high-solids loadings within the bioconversion of lignocellulose into glucose-derived products, encompassing from pretreatment to fermentation, has been conducted with a rheological and computational fluid dynamics (CFD) perspective (paper III).

The guidelines for bioreactor conversion from batch to continuous and operation at high-solids loadings have been assessed during the Thesis. Basics of reactor design and operability in accordance with rheological characteristics of MSW-pulp are discussed, which open an umbrella of possibilities for bioprocessing of high-solids and high-viscous lignocellulosic feedstocks. Through process modelling, the advantages of continuous over batch and fed-batch processing has been demonstrated and validated with the previous laboratory experimentation. Moreover, a simple techno-economic assessment has been described which can also be used in closely allied areas without the need of licensed software.

Apart from the knowledge contributions in form of journal articles, some investigations carried out within this Thesis have supported the development of two grant projects: OPTOMS (104391) and Bio-integrated Valorisation of India's Municipal Solid Waste to Renewable Feedstocks (BB/S011986/1). In the OPTOMS project, the rheological characterisation of MSW-slurries was used for conducting a CFD study to quantify the limitations of employing a stirred tank reactor design due excessive power consumption and long mixing time. Moreover, an on-line rheological analysis approach was proposed with torque-metering to show the effect of fed-batch feeding and agitation strategies throughout a 10-L enzymatic hydrolysis of MSW-pulp. Determination of slurry viscosity is an important factor for Fiberight Ltd. as helps on reactor design, scale-up and optimisation of the MSW-to-sugars process. The suitability of rotary drum reactors for processing of high-solids loadings has been applied in both grant projects. For the "India/UK MSW" project, the literature review on MSW feedstocks has enabled to better understand the challenges of processing these type of feedstocks, which complements with the expertise on bioreactor design on high-solids enzymatic hydrolyses.

7.3 Further work

- **Open-access automated reaction control and monitoring**

  Smart biomanufacturing is one of the areas under-development of the *Industry 4.0* to upgrade the production processes whilst decreasing the environmental impacts of bio-based processes. Due to software limitations, an automated reaction control and monitoring systems is not available to date. Through graphical programming, a bespoke application can be designed which allows real-time pH and DO monitoring for functioning of the integrated control system (patent no. WO2019/220092A1 [367]) and temperature profile with open-source accessibility. These bespoke applications would improve bioprocessing operability and minimise dependence of license vendor's for the automation and optimisation of processes.

- **On-line rheological analysis**

By combining the background of agitation/mixing and rheology with the application of bespoke software, an on-line rheological analysis method can be developed for recording of real-time viscosity measurements upon reactor design. These systems were of great importance for avoiding the dependence of off-shelf viscosity probes and overcoming the lack of open-access software. Understanding the real-time viscosity profile of each bioprocessing operation prior scaling-up, would support the plant design and optimisation of capital costs for the next scaling-up steps.

- **Bench-scale continuous bioreactor: a prototype**

  From the main results in rheology, bioreactor design and reaction control, a bench-scale prototype can be designed and built for assaying a continuous enzymatic hydrolysis of MSW-pulp at high-solids loadings. The rheological background allows to conduct an accurate process design and set-up of bioengineering activities. Deploying such continuous hydrolysis reactors would improve the de-risking of the technology and provides the guidelines for scale-up.

- **A full techno-economic assessment**

  The economical indicators of various bioprocessing configurations were determined and compared to indicated which is the best system from a techno-economic viewpoint. But, further process modelling is required for commercialisation. The application of software such as AspenPlus (plant design and economical analysis), Crystal ball (uncertainty and sensitivity analysis) and GaBi (life cycle assessment) are required for evaluating the market-based and environmental profile of the two-stage continuous enzymatic configuration. These methodologies can be also used for the rest of biorefining system, to show the techno-economic viability and environmental advantages of a waste biorefinery over other conventional waste management practices (e.g incineration or anaerobic digestion).

References

1. Rosales-Calderon, O. & Arantes, V. A review on commercial-scale high-value products that can be produced alongside cellulosic ethanol. *Biotechnology for Biofuels* **12** (2019).
2. Da Silva, A., Espinheira, R., Teixeira, R., De Souza, M., Ferreira-Leitão, V. & Bon, E. Constraints and advances in high-solids enzymatic hydrolysis of lignocellulosic biomass: A critical review. *Biotechnology for Biofuels* **13,** 58 (2020).
3. Balan, V., Chiaramonti, D. & Kumar, S. Review of US and EU initiatives toward development, demonstration, and commercialization of lignocellulosic biofuels. *Biofuels, Bioproducts and Biorefining* **7,** 732–759 (2013).
4. Sadhukhan, J., Ng, K. & Martinez, E. *Biorefineries and Chemical Processes* 676 (2013).
5. Kobayashi, H. & Fukuoka, A. Synthesis and utilisation of sugar compounds derived from lignocellulosic biomass. *Green Chemistry* **15,** 1740–1763 (2013).
6. Bettenhausen, C. Rhamnolipids rise as a green surfactant. *ACS Chemical & Engineering News* **98,** 1–6 (2020).
7. UKRI. *Commercialisation of MSW derived sugars for the production of thermoset resins*
8. LBNet & BBRSC. *UKBioChem10: The ten green chemicals which can create growth, jobs and trade for the UK* tech. rep. (2018).
9. Werpy, T. & Petersen, G. Top Value Added Chemicals from Biomass: Volume I – Results of Screening for Potential Candidates from Sugars and Synthesis Gas. Office of Scientific and Technical Information (OSTI). *Office of Scientific and Technical Information,* 69 (2004).
10. Bozell, J. J. & Petersen, G. R. Technology development for the production of biobased products from biorefinery carbohydrates—the US Department of Energy's "top 10" revisited. *Green Chemistry* **12,** 539–55 (2010).
11. Chandel, A. K., Garlapati, V. K., Singh, A. K., Antunes, F. A. F. & da Silva, S. S. The path forward for lignocellulose biorefineries: Bottlenecks, solutions, and perspective on commercialization. *Bioresource Technology* **264,** 370–381 (2018).
12. De Jong, E., Stichnothe, H., Bell, G., Henning Jørgensen, M., de Bari, I., Jacco van Haveren, E., Lindorfer, J. & an der Johannes Kepler, E. *Bio-Based Chemicals A 2020 Update Bio-Based Chemicals With input from: (pdf version) Published by IEA Bioenergy* tech. rep. (2020).
13. Spekreijse, J., Lammens, T., Parisi, C., Ronzon, T. & Vis, M. Insights into the European market for bio-based chemicals Factsheets for 10 bio-based product categories. *European Commission Joint Research Centre* (2019).
14. Van Ree, R., De Jong, E. & Kwant, K. *Task 42 Bio-based Chemicals: value added products from biorefineries* tech. rep. (2012).

15. Brethauer, S. & Wyman, C. Review: Continuous hydrolysis and fermentation for cellulosic ethanol production. *Bioresource Technology* **101,** 4862–4874 (2010).

16. Carr, M. E., Black, L. T. & Bagby, M. O. Continuous enzymatic liquefaction of starch for saccharification. *Biotechnology and Bioengineering* **24,** 2441–2449 (1982).

17. Modenbach, A. & Nokes, S. The use of high-solids loadings in biomass pretreatment-a review. *Biotechnology and Bioengineering* **109,** 1430–1442 (2012).

18. Ishihara, M., Uemura, S., Hayashi, N. & Shimizu, K. Semicontinuous enzymatic hydrolysis of lignocelluloses. *Biotechnology and Bioengineering* **37,** 948–954 (1991).

19. Bélafi-Bakó, K., Koutinas, A., Nemestóthy, N., Gubicza, L. & Webb, C. Continuous enzymatic cellulose hydrolysis in a tubular membrane bioreactor. *Enzyme and Microbial Technology* **38,** 155–161 (2006).

20. Gurram, R. N. R. & Menkhaus, T. T. J. Continuous enzymatic hydrolysis of lignocellulosic biomass with simultaneous detoxification and enzyme recovery. *Applied Biochemistry and Biotechnology* **173,** 1319–1335 (2014).

21. Stickel, J. J., Adhikari, B., Sievers, D. A. & Pellegrino, J. Continuous enzymatic hydrolysis of lignocellulosic biomass in a membrane-reactor system. *Journal of Chemical Technology and Biotechnology* **93,** 2181–2190 (2018).

22. Lischeske, J. J. & Stickel, J. J. A two-phase substrate model for enzymatic hydrolysis of lignocellulose: Application to batch and continuous reactors. *Biotechnology for Biofuels* **12** (2019).

23. Yang, M., Li, W., Liu, B., Li, Q. & Xing, J. High-concentration sugars production from corn stover based on combined pretreatments and fed-batch process. *Bioresource Technology* **101,** 4884–4888 (2010).

24. Jørgensen, H. & Pinelo, M. Enzyme recycling in lignocellulosic biorefineries. *Biofuels, Bioproducts and Biorefining* **11,** 150–167 (2017).

25. Bhaskar, T., Pandey, A., Rene, E. & Tsang, D. *Waste Biorefinery Integrating Biorefineries for Waste Valorisation* **9,** 1689–1699 (2020).

26. Waldron, K. *Bioalcohol Production* 365–390 (2010).

27. Hassen, A., Belguith, K., Jedidi, N., Cherif, A., Cherif, M. & Boudabous, A. Microbial characterization during composting of municipal solid waste. *Bioresource Technology* **80,** 217–225 (2001).

28. Ibbett, R., Tucker, G., McKechnie, J. & Meng, F. Enzyme digestion of biofiber from mechanical heat treated municipal solid waste: Accessing kinetic and rheological design data using a pilot-scale high-solids mixer. *Biomass and Bioenergy* **143,** 105817 (2020).

29. Izaguirre, J. K., da Fonseca, M. M. R., Fernandes, P., Villarán, M. C., Castañón, S. & Cesário, M. T. Upgrading the organic fraction of municipal solid waste to poly(3-hydroxybutyrate). *Bioresource Technology* **290,** 121785 (2019).

30. Loizidou, M., Alamanou, D. G., Sotiropoulos, A., Lytras, C., Mamma, D., Malamis, D. & Kekos, D. Pilot Scale System of Two Horizontal Rotating Bioreactors for Bioethanol Production from Household Food Waste at High Solid Concentrations. *Waste and Biomass Valorization* **8,** 1709–1719 (2017).

31. Ghanavati, H., Nahvi, I. & Karimi, K. Organic fraction of municipal solid waste as a suitable feedstock for the production of lipid by oleaginous yeast cryptococcus aerius. *Waste Management* **38,** 141–148 (2015).

32. Puri, D. J., Heaven, S. & Banks, C. J. C. Improving the performance of enzymes in hydrolysis of high solids paper pulp derived from MSW. *Biotechnology for Biofuels* **6,** 107 (2013).
33. Gerber, S., Oganesoff, E., Gerber, M. & Stuart-Paul, C. *Wet pulping system and method for producing cellulosic insulation with low ash content* 2010.
34. Pendse, H., Bilodeau, M., Luce, A., Waite, D., Town Fuel and Fiber & Atwell, J. S. *Technology Review Fiberight Process for MRC* tech. rep. (The University of Maine, 2015).
35. WRAP. PAS 110: Specification for whole digestate, separated liquor and separated fibre derived from the anaerobic digestion of source-segregated biodegradable materials, 46 (2010).
36. Puri, D. *Optimisation of the production of fermentable sugars using paper pulp derived from municipal solid waste (MSW)* PhD thesis (2014).
37. Fiberight Limited. *Reducing contamination risk and increasing yields in the production of platform sugars from UK MSW* 2016.
38. *Fiberight, LLC – Leading the Way Forward – Leading the Way Forward: www.fiberight.com*
39. Limayem, A. & Ricke, S. Lignocellulosic biomass for bioethanol production: Current perspectives, potential issues and future prospects. *Progress in Energy and Combustion Science* **38,** 449–467 (2012).
40. Dasari, R. K. & Eric Berson, R. The effect of particle size on hydrolysis reaction rates and rheological properties in cellulosic slurries. *Applied Biochemistry and Biotechnology* **137-140,** 289–299 (2007).
41. Dasari, R. *High-solids saccharification and viscosity studies in a scraped surface bio-reactor .* PhD thesis (2008).
42. Dasari, R., Dunaway, K. & Berson, E. A scraped surface bioreactor for enzymatic saccharification of pretreated corn stover slurries. *Energy and Fuels* **23,** 492–497 (2009).
43. Mitchell, D. A., Krieger, N. & Berovic, M. *Solid State Fermentation Bioreactors* 482 (2006).
44. Atiemo-Obeng, V., Penney, W. R. & Armenante, P. in *Handbook of Industrial Mixing. Science and Practice* 543–585 (2004).
45. Mason, W. P. Viscosity and shear elasticity measurements of liquids by means of shear vibrating crystals. *Journal of Colloid Science* **3,** 147–162 (1948).
46. Wynn, E. J. Relationship between particle-size and chord-length distributions in focused beam reflectance measurement: Stability of direct inversion and weighting. *Powder Technology* **133,** 125–133 (2003).
47. Climent Barba, F., Chacón, M. G., Reynolds, W. R., Puri, D. J., Bourne, R. A. & Blacker, A. J. Improved conversion of residual MSW biomass waste to sugars using online process monitoring and integrated contamination control. *Bioresource Technology Reports* **13,** 100612 (2020).
48. Dunaway, K. W., Dasari, R. K., Bennett, N. G. & Eric Berson, R. Characterization of changes in viscosity and insoluble solids content during enzymatic saccharification of pretreated corn stover slurries. *Bioresource Technology* **101,** 3575–3582 (2010).
49. Metzner, A. B. & Otto, R. E. Agitation of non-Newtonian fluids. *AIChE Journal* **3,** 3–10 (1957).

50. Bakker, A. & Gates, L. E. Properly choose mechanical agitators for viscous liquids. *Chemical Engineering Progress* **91,** 25–34 (1995).

51. Foucault, S. P., Ascanio, G. & Tanguy, P. A. Power characteristics in coaxial mixing: Newtonian and non-newtonian fluids. *Industrial and Engineering Chemistry Research* **44,** 5036–5043 (2005).

52. Sluiter, A., Hames, B., Hyman, D., Payne, C., Ruiz, R., Scarlata, C., Sluiter, J., Templeton, D. & Nrel, J. Determination of total solids in biomass and total dissolved solids in liquid process samples. *National Renewable Energy Laboratory (NREL),* 9 (2008).

53. BSI Standard Publication. *Characterization of waste - Sampling of waste materials - Part 3: Guidance on procedures for sub-sampling in the field* 2006.

54. Sluiter, A., Hames, B., Ruiz, R., Scarlata, C., Sluiter, J., Templeton, D. & Crocker, D. Determination of structural carbohydrates and lignin in Biomass. *Laboratory Analytical Procedure (LAP),* 17 (2012).

55. Basumallick, L. & Rohrer, J. Determination of Uronic Acids and Wood Sugars in Wood-Based Hydrolysates. *Fisher Scientific,* 2–7 (2017).

56. Wing, R. E. & Freer, S. N. Use of trifluoroacetic acid to prepare cellodextrins. *Carbohydrate Polymers* **4,** 323–333 (1984).

57. Bradford, M. M. *A Rapid and Sensitive Method for the Quantitation of Microgram Quantities of Protein Utilizing the Principle of Protein-Dye Binding* tech. rep. (1976), 248–254.

58. Kadić, A., Palmqvist, B. & Lidén, G. Effects of agitation on particle-size distribution and enzymatic hydrolysis of pretreated spruce and giant reed. *Biotechnology for Biofuels* **7,** 77 (2014).

59. Segal, L., Creely, J. J., Martin, A. E. & Conrad, C. M. An Empirical Method for Estimating the Degree of Crystallinity of Native Cellulose Using the X-Ray Diffractometer. *Textile Research Journal* **29,** 786–794 (1959).

60. Zheng, Y., Pan, Z., Zhang, R. & Jenkins, B. B. M. Kinetic modeling for enzymatic hydrolysis of pretreated creeping wild ryegrass. *Biotechnology and Bioengineering* **102,** 1558–1569 (2009).

61. Gusakov, A. V., Sinitsyn, A. P. & Klyosov, A. A. Kinetics of the enzymatic hydrolysis of cellulose: 1. A mathematical model for a batch reactor process. *Enzyme and Microbial Technology* **7,** 346–352 (1985).

62. Tsai, C. T., Morales-Rodriguez, R., Sin, G. & Meyer, A. S. A dynamic model for cellulosic biomass hydrolysis: A comprehensive analysis and validation of hydrolysis and product inhibition mechanisms. *Applied Biochemistry and Biotechnology* **172,** 2815–2837 (2014).

63. Leardi, R. Experimental design in chemistry: A tutorial. *Analytica Chimica Acta* **652,** 161–172 (2009).

64. Science and Technology Select Committee. *Waste or resource? Stimulating a bioeconomy* tech. rep. February (House of lords, 2014).

65. Hazar, Y. in *Lignocellulose Conversion: Enzymatic and Microbial Tools for Bioethanol Production* 21–38 (2013).

66. Bajpai, P. Pretreatment of Lignocellulosic Biomass for Biofuel Production. *SpringerBriefs in Green Chemistry for Sustainability* **34,** 86 (2016).

67. Bischof, R. H., Ramoni, J. & Seiboth, B. Cellulases and beyond: The first 70 years of the enzyme producer Trichoderma reesei. *Microbial Cell Factories* **15,** 106 (2016).

68. Lopes, A. M., Ferreira Filho, E. X. & Moreira, L. R. An update on enzymatic cocktails for lignocellulose breakdown. *Journal of Applied Microbiology* **125,** 632–645 (2018).

69. Beeson, W., Vu, V., Span, E., Phillips, C. & Marletta, M. Cellulose Degradation by Polysaccharide Monooxygenases. *Annual Review of Biochemistry* **84,** 923–946 (2015).

70. Bissaro, B., Røhr, Å., Müller, G., Chylenski, P., Skaugen, M., Forsberg, Z., Horn, S., Vaaje-Kolstad, G. & Eijsink, V. Oxidative cleavage of polysaccharides by monocopper enzymes depends on H2O2. *Nature Chemical Biology* **13,** 1123–1128 (2017).

71. Dimarogona, M., Topakas, E. & Christakopoulos, P. *Recalcitrant polysaccharide degradation by novel oxidative biocatalysts* 2013.

72. Di Risio, S., Hu, C., Saville, B., Liao, D. & Lortie, J. Large-scale, high- solids enzymatic hydrolysis of steam-exploded poplar. *Biofuels, Bioproducts and Biorefining* **6,** 246–256 (2012).

73. Wojtusik, M., Zurita, M., Villar, J., Ladero, M. & Garcia-Ochoa, F. Influence of fluid dynamic conditions on enzymatic hydrolysis of lignocellulosic biomass: Effect of mass transfer rate. *Bioresource Technology* **216,** 28–35 (2016).

74. Wojtusik, M., Zurita, M., Villar, J. C., Ladero, M. & Garcia-Ochoa, F. Enzymatic saccharification of acid pretreated corn stover: Empirical and fractal kinetic modelling. *Bioresource Technology* **220,** 110–116 (2016).

75. Wojtusik, M., Villar, J. C., Ladero, M. & Garcia-Ochoa, F. Physico-chemical kinetic modelling of hydrolysis of a steam-explosion pre-treated corn stover: A two-step approach. *Bioresource Technology* **268,** 592–598 (2018).

76. Chundawat, S. P., Lipton, M. S., Purvine, S. O., Uppugundla, N., Gao, D., Balan, V. & Dale, B. E. Proteomics-based compositional analysis of complex cellulase-hemicellulase mixtures. *Journal of Proteome Research* **10,** 4365–4372 (2011).

77. Yang, S., Ding, W. & Chen, H. Enzymatic hydrolysis of rice straw in a tubular reactor coupled with UF membrane. *Process Biochemistry* **41,** 721–725 (2006).

78. Mahmoodi, P., Karimi, K. & Taherzadeh, M. J. Efficient conversion of municipal solid waste to biofuel by simultaneous dilute-acid hydrolysis of starch and pretreatment of lignocelluloses. *Energy Conversion and Management* **166,** 569–578 (2018).

79. Sun, N., Xu, F., Sathitsuksanoh, N., Thompson, V. S., Cafferty, K., Li, C., Tanjore, D., Narani, A., Pray, T. R., Simmons, B. A. & Singh, S. Blending municipal solid waste with corn stover for sugar production using ionic liquid process. *Bioresource Technology* **186,** 200–206 (2015).

80. EPRS. *Towards a circular economy-Waste management in the EU STUDY Science and Technology Options Assessment* tech. rep. (2017), 1–140.

81. Li, A. & Khraisheh, M. Rubbish or resources: An investigation of converting municipal solid waste (MSW) to bio-ethanol production. *WIT Transactions on Ecology and the Environment* **109,** 115–122 (2008).

82. Jensen, J. W., Felby, C., Jørgensen, H., Rønsch, G. Ø., Nørholm, N. D., Liang, L., Li, C., Xu, F., He, Q., Yan, J., Luong, T., Simmons, B. A., Pray, T. R., Singh, S., Thompson, V. S. & Sun, N. Enzymatic processing of municipal solid waste. *Waste Management* **30,** 2497–2503 (2010).

83. Li, A. & Khraisheh, M. Bioenergy II: Bio-ethanol from municipal solid waste (MSW): The role of biomass properties and structures during the ethanol conversion process. *International Journal of Chemical Reactor Engineering* **8** (2010).

84. Li, A., Antizar-Ladislao, B. & Khraisheh, M. Bioconversion of municipal solid waste to glucose for bio-ethanol production. *Bioprocess and Biosystems Engineering* **30,** 189–196 (2007).

85. Schmitt, E., Bura, R., Gustafson, R., Cooper, J. & Vajzovic, A. Converting lignocellulosic solid waste into ethanol for the State of Washington: An investigation of treatment technologies and environmental impacts. *Bioresource Technology* **104,** 400–409 (2012).

86. Meng, F., Ibbett, R., de Vrije, T., Metcalf, P., Tucker, G. & McKechnie, J. Process simulation and life cycle assessment of converting autoclaved municipal solid waste into butanol and ethanol as transport fuels. *Waste Management* **89,** 177–189 (2019).

87. J. Abdullah, J. & Greetham, D. Optimizing Cellulase Production from Municipal Solid Waste (MSW) using Solid State Fermentation (SSF). *Journal of Fundamentals of Renewable Energy and Applications* **06,** 3 (2016).

88. Brooks, T. A. & Ingram, L. O. Conversion of Mixed Waste Office Paper to Ethanol by Genetically Engineered Klebsiella oxytoca Strain P2. *Biotechnology Progress* **11,** 619–625 (1995).

89. Rivers, D. B. & Emert, G. H. Factors affecting the enzymatic hydrolysis of municipal-solid-waste components. *Biotechnology and Bioengineering* **31,** 278–281 (1988).

90. Sotaniemi, V. H., Tikkanen, T., Pasanen, A., Taskila, S. & Ojamo, H. Effect of enzyme and substrate dosing strategies on mixing and hydrolysis of old corrugated cardboard. *Biomass Conversion and Biorefinery* **5,** 141–148 (2015).

91. Jørgensen, H., Kristensen, J. & Felby, C. Enzymatic conversion of lignocellulose into fermentable sugars: challenges and opportunities. *Biofuels, Bioproducts and Biorefining* **6,** 246–256 (2012).

92. Modenbach, A. & Nokes, S. Enzymatic hydrolysis of biomass at high-solids loadings – A review. *Biomass and Bioenergy* **56,** 526–544 (2013).

93. Jørgensen, H., Vibe-Pedersen, J., Larsen, J. & Felby, C. Liquefaction of Lignocellulose at High-Solids Concentrations. *Biotechnology and Bioengineering* **96,** 862–870 (2007).

94. Isikgor, F. H., Becer, C. R. & Remzi Becer, C. Lignocellulosic biomass: a sustainable platform for the production of bio-based chemicals and polymers. *Polymer Chemistry* **6,** 4497–4559 (2015).

95. Piotrowski, J., Zhang, Y., Bates, D., Keating, D., Sato, T., Ong, I. & Landick, R. Death by a thousand cuts: the challenges and diverse landscape of lignocellulosic hydrolysate inhibitors. *Frontiers in Microbiology* **5,** 90 (2014).

96. Chheda, J. N., Román-Leshkov, Y. & Dumesic, J. A. Production of 5-hydroxymethylfurfural and furfural by dehydration of biomass-derived mono- and poly-saccharides. *Green Chemistry* **9,** 342–350 (2007).

97. Aguilar, R., Ramírez, J. A., Garrote, G. & Vázquez, M. Kinetic study of the acid hydrolysis of sugar cane bagasse. *Journal of Food Engineering* **55,** 309–318 (2002).

98. Van der Pol, E. C., Bakker, R. R., Baets, P. & Eggink, G. By-products resulting from lignocellulose pretreatment and their inhibitory effect on fermentations for (bio)chemicals and fuels. *Applied Microbiology and Biotechnology* **98,** 9579–9593 (2014).

99. Jönsson, L. L. J. & Martín, C. Pretreatment of lignocellulose: Formation of inhibitory by-products and strategies for minimizing their effects. *Bioresource Technology* **199,** 103–112 (2016).

100. Novozymes. Novozymes Cellic® CTec3 - Secure your plant's lowest total cost. *Novozymes,* 1–6 (2012).

101. Jönsson, L., Alriksson, B. & Nilvebrant, N. *Bioconversion of lignocellulose: Inhibitors and detoxification* 2013.

102. Doelle, H. in *Bacterial Metabolism* 129–198 (Elsevier, 1969).

103. Sun, T. & Altenbuchner, J. Characterization of a mannose utilization system in bacillus subtilis. *Journal of Bacteriology* **192,** 2128–2139 (2010).

104. Chai, Y., Beauregard, P. B., Vlamakis, H., Losick, R. & Kolter, R. Galactose metabolism plays a crucial role in biofilm formation by Bacillus subtilis. *mBio* **3** (2012).

105. Baldomà, L. & Aguilar, J. Metabolism of L-fucose and L-rhamnose in Escherichia coli: aerobic-anaerobic regulation of L-lactaldehyde dissimilation. *Journal of bacteriology* **170,** 416–421 (1988).

106. LeBlanc, D. J. & Mortlock, R. P. Metabolism of D-arabinose: a new pathway in Escherichia coli. *Journal of Bacteriology* **106,** 90–96 (1971).

107. Muthaiyan, A., Limayem, A. & Ricke, S. Antimicrobial strategies for limiting bacterial contaminants in fuel bioethanol fermentations. *Progress in Energy and Combustion Science* **37,** 351–370 (2011).

108. Rich, J. O., Leathers, T. D., Bischoff, K. M., Anderson, A. M. & Nunnally, M. S. Biofilm formation and ethanol inhibition by bacterial contaminants of biofuel fermentation. *Bioresource Technology* **196,** 347–354 (2015).

109. Skinner, K. A. & Leathers, T. D. Bacterial contaminants of fuel ethanol production. *Journal of Industrial Microbiology and Biotechnology* **31,** 401–408 (2004).

110. Beckner, M., Ivey, M. L. & Phister, T. G. Microbial contamination of fuel ethanol fermentations. *Letters in Applied Microbiology* **53,** 387–394 (2011).

111. Toner, E., Adalja, A., Gronvall, G. K., Cicero, A. & Inglesby, T. V. Antimicrobial resistance is a global health emergency. *Health security* **13,** 153–155 (2015).

112. Brown, J., Conn, A., Pilcher, G., Leitao, M. & Yang, M.-Y. On the strain energy of 5-ring and 6-ring lactones. *J. Chem. Soc., Chem. Commun.,* 1817–1819 (1989).

113. Aquarone, E. Penicillin and Tetracycline as Contamination Control Agents in Alcoholic Fermentation of Sugar Cane Molasses. *Applied Microbiology* **8,** 263–268 (1960).

114. Visser, E. M., Leal, T. F., De Almeida, M. N. & Guimarães, V. M. Increased enzymatic hydrolysis of sugarcane bagasse from enzyme recycling. *Biotechnology for Biofuels* **8,** 5 (2015).

115. Roche, C., Dibble, C. J. & Stickel, J. J. Laboratory-scale method for enzymatic saccharification of lignocellulosic biomass at high-solids loadings. *Biotechnology for Biofuels* **2,** 28 (2009).

116. Du, J., Cao, Y., Liu, G., Zhao, J., Li, X. & Qu, Y. Identifying and overcoming the effect of mass transfer limitation on decreased yield in enzymatic hydrolysis of lignocellulose at high solid concentrations. *Bioresource Technology* **229,** 88–95 (2017).

117. Satari Baboukani, B., Vossoughi, M. & Alemzadeh, I. Optimisation of dilute-acid pretreatment conditions forenhancement sugar recovery and enzymatic hydrolysis ofwheat straw. *Biosystems Engineering* **111,** 166–174 (2012).

118. Brownell, H. H. & Saddler, J. N. Steam pretreatment of lignocellulosic material for enhanced enzymatic hydrolysis. *Biotechnology and Bioengineering* **29,** 228–235 (1987).

119. Barroca, M. J. M., Seco, I. M., Fernandes, P. M., Ferreira, L. M. & Castro, J. A. A. Reduction of AOX in the bleach plant of a pulp mill. *Environmental Science and Technology* **35,** 4390–4393 (2001).

120. Banerjee, G., Car, S., Scott-Craig, J. S., Hodge, D. B. & Walton, J. D. Alkaline peroxide pretreatment of corn stover: Effects of biomass, peroxide, and enzyme loading and composition on yields of glucose and xylose. *Biotechnology for Biofuels* **4,** 16 (2011).

121. Banerjee, G., Car, S., Liu, T., Williams, D. L., Meza, S. L., Walton, J. D. & Hodge, D. B. Scale-up and integration of alkaline hydrogen peroxide pretreatment, enzymatic hydrolysis, and ethanolic fermentation. *Biotechnology and Bioengineering* **109,** 922–931 (2012).

122. Acharjee, T. C., Jiang, Z., Haynes, R. D. & Lee, Y. Y. Evaluation of chlorine dioxide as a supplementary pretreatment reagent for lignocellulosic biomass. *Bioresource Technology* **244,** 1049–1054 (2017).

123. Ho, M. C., Ong, V. Z. & Wu, T. Y. Potential use of alkaline hydrogen peroxide in lignocellulosic biomass pretreatment and valorization – A review. *Renewable and Sustainable Energy Reviews* **112,** 75–86 (2019).

124. Peciulyte, A., Samuelsson, L., Olsson, L., McFarland, K. C., Frickmann, J., Østergård, L., Halvorsen, R., Scott, B. R. & Johansen, K. S. Redox processes acidify and decarboxylate steam-pretreated lignocellulosic biomass and are modulated by LPMO and catalase. *Biotechnology for Biofuels* **11,** 165 (2018).

125. Walton, P. H. & Davies, G. J. *On the catalytic mechanisms of lytic polysaccharide monooxygenases* 2016.

126. Müller, G., Várnai, A., Johansen, K. S., Eijsink, V. G. & Horn, S. J. Harnessing the potential of LPMO-containing cellulase cocktails poses new demands on processing conditions. *Biotechnology for Biofuels* **8,** 187 (2015).

127. Müller, G., Chylenski, P., Bissaro, B., Eijsink, V. G. & Horn, S. J. The impact of hydrogen peroxide supply on LPMO activity and overall saccharification efficiency of a commercial cellulase cocktail. *Biotechnology for Biofuels* **11,** 209 (2018).

128. Nitsche, C., Holloway, S., Schirmeister, T. & Klein, C. D. *Biochemistry and medicinal chemistry of the dengue virus protease* 2014.

129. Matuszak, N., Es Saadi, B., Labar, G., Marchand-Brynaert, J. & Lambert, D. M. Benzisothiazolinone as a useful template for the design of new monoacylglycerol lipase inhibitors: Investigation of the target residues and comparison with octhilinone. *Bioorganic and Medicinal Chemistry Letters* **21,** 7321–7324 (2011).

130. Schwensen, J. F., Lundov, M. D., Bossi, R., Banerjee, P., Gimenez-Arnau, E., Lepoittevin, J. P., Lidén, C., Uter, W., Yazar, K., White, I. R. & Johansen, J. D. *Methylisothiazolinone and benzisothiazolinone are widely used in paint: A multicentre study of paints from five European countries* 2015.

131. Flyvholm, M. A. Preservatives in registered chemical products. *Contact Dermatitis* **53,** 27–32 (2005).

132. Li, A., Chen, Z., Wu, Q. Y., Huang, M. H., Liu, Z. Y., Chen, P., Mei, L. C. & Hu, H. Y. Study on the removal of benzisothiazolinone biocide and its toxicity: The effectiveness of ozonation. *Chemical Engineering Journal* **300,** 376–383 (2016).

133. Liu, W. R., Yang, Y. Y., Liu, Y. S., Zhang, L. J., Zhao, J. L., Zhang, Q. Q., Zhang, M., Zhang, J. N., Jiang, Y. X. & Ying, G. G. Biocides in wastewater treatment plants: Mass balance analysis and pollution load estimation. *Journal of Hazardous Materials* **329,** 310–320 (2017).

134. Fuller, S. J., Denyer, S. P., Hugo, W. B., Pemberton, D., Woodcock, P. M. & Buckley, A. J. The mode of action of l,2-benzisothiazolin-3-one on Staphylococcus aureus. *Letters in Applied Microbiology* **1,** 13–15 (1985).

135. Resch, M. G., Baker, J. O. & Decker, S. R. Low Solids Enzymatic Saccharification of Lignocellulosic Biomass: Laboratory Analytical Procedure (LAP). *Technical Report, NREL/TP-5100-63351,* 1–9 (2015).

136. Hynes, S. H., Kjarsgaard, D. M., Thomas, K. C. & Ingledew, W. M. Use of virginiamycin to control the growth of lactic acid bacteria during alcohol fermentation. *Journal of Industrial Microbiology and Biotechnology* **18,** 284–291 (1997).

137. Schell, D. J., Dowe, N., Ibsen, K. N., Riley, C. J., Ruth, M. F. & Lumpkin, R. E. Contaminant occurrence, identification and control in a pilot-scale corn fiber to ethanol conversion process. *Bioresource Technology* **98,** 2942–2948 (2007).

138. Phibro Ethanol Performance Group. *Lactrol(R) - Product guidelines* 2016.

139. Olsen, S. N., Borch, K., Cruys-Bagger, N. & Westh, P. The role of product inhibition as a yield-determining factor in enzymatic high-solid hydrolysis of pretreated corn stover. *Applied biochemistry and biotechnology* **174,** 146–155 (2014).

140. Sumner, E., Okull, D. & Solomon, E. *Stabilized chlorine dioxide to preserve carbohydrate feedstocks* 2016.

141. Rich, J. O. J., Bischoff, K. M. K., Leathers, T. D. T., Anderson, A. M. A., Liu, S. & Skory, C. D. C. Resolving bacterial contamination of fuel ethanol fermentations with beneficial bacteria – An alternative to antibiotic treatment. *Bioresource Technology* **247,** 357–362 (2018).

142. DuPont. *DuPont ™ FermaSure ® Ethanol Fermentation additive*

143. McDonnell, G. in *PATAI'S Chemistry of Functional Groups* 1–34 (John Wiley & Sons, Ltd, Chichester, UK, 2014).

144. Chang, I. S., Kim, B. H. & Shin, P. K. Use of sulfite and hydrogen peroxide to control bacterial contamination in ethanol fermentation. *Applied and Environmental Microbiology* **63,** 1–6 (1997).

145. Kristensen, J. B., Felby, C. & Jørgensen, H. Yield-determining factors in high-solids enzymatic hydrolysis of lignocellulose. *Biotechnology for Biofuels* **2** (2009).

146. Roche, C. M., Dibble, C. J., Knutsen, J. S., Stickel, J. J. & Liberatore, M. W. Particle concentration and yield stress of biomass slurries during enzymatic hydrolysis at high-solids loadings. *Biotechnology and Bioengineering* **104,** 290–300 (2009).

147. Humbird, D., Mohagheghi, A., Dowe, N. & Schell, D. J. Economic impact of total solids loading on enzymatic hydrolysis of dilute acid pretreated corn stover. *Biotechnology progress* **26,** 1245–1251 (2010).

148. Tengborg, C., Galbe, M. & Zacchi, G. Influence of enzyme loading and physical parameters on the enzymatic hydrolysis of steam-pretreated softwood. *Biotechnology Progress* **17,** 110–117 (2001).

149. Koppram, R., Tomás-Pejó, E., Xiros, C. & Olsson, L. Lignocellulosic ethanol production at high-gravity: Challenges and perspectives. *Trends in Biotechnology* **32,** 46–53 (2014).

150. Royal Society of Chemistry. The Amazing Horwitz Function. *AMC Technical Brief* **12** (2004).

151. Caspeta, L., Caro-Bermúdez, M. M. A. M., Ponce-Noyola, T. & Martinez, A. Enzymatic hydrolysis at high-solids loadings for the conversion of agave bagasse to fuel ethanol. *Applied Energy* **113,** 277–286 (2014).

152. Ludwig, D., Michael, B., Hirth, T., Rupp, S. & Zibek, S. High solids enzymatic hydrolysis of pretreated lignocellulosic materials with a powerful stirrer concept. *Applied Biochemistry and Biotechnology* **172,** 1699–1713 (2014).

153. Sun, F. F., Hong, J., Hu, J., Saddler, J. N., Fang, X., Zhang, Z. & Shen, S. Accessory enzymes influence cellulase hydrolysis of the model substrate and the realistic lignocellulosic biomass. *Enzyme and Microbial Technology* **79-80,** 42–48 (2015).

154. Kim, J. K., Yang, J., Park, S. Y., Yu, J. H. & Kim, K. H. Cellulase recycling in high-solids enzymatic hydrolysis of pretreated empty fruit bunches. *Biotechnology for Biofuels* **12,** 138 (2019).

155. Mussatto, S. I., Dragone, G., Fernandes, M., Milagres, A. M. & Roberto, I. C. The effect of agitation speed, enzyme loading and substrate concentration on enzymatic hydrolysis of cellulose from brewer's spent grain. *Cellulose* **15,** 711–721 (2008).

156. Selig, M., Weiss, N. & Ji, Y. Enzymatic Saccharification of Lignocellulosic Biomass - NREL/TP-510-42629. *National Renewable Energy Laboratory* (2008).

157. Mamlouk, D. & Gullo, M. *Acetic Acid Bacteria: Physiology and Carbon Sources Oxidation* 2013.

158. Kandler, O. Carbohydrate metabolism in lactic acid bacteria. *Antonie van Leeuwenhoek* **49,** 209–224 (1983).

159. Lichstein, H. C. Studies of the Effect of Sodium Azide on Microbic Growth and Respiration: III. The Effect of Sodium Azide on the Gas Metabolism of B. subtilis and P. aeruginosa and the Influence of Pyocyanine on the Gas Exchange of a Pyocyanine-Free Strain of P. aerugino. *Journal of bacteriology* **47,** 239–51 (1944).

160. Yafizham & Herwibawa, B. *The effects of sodium azide on seed germination and seedling growth of chili pepper (Capsicum annum L. cv. Landung)* in *IOP Conference Series: Earth and Environmental Science* **102** (2018), 12052.

161. Cabrol, L., Quéméneur, M. & Misson, B. Inhibitory effects of sodium azide on microbial growth in experimental resuspension of marine sediment. *Journal of Microbiological Methods* **133,** 62–65 (2017).

162. Egorov, A. M., Ulyashova, M. M. & Rubtsova, M. Y. *Bacterial enzymes and antibiotic resistance* 2018.

163. Alt, E., Leipold, F., Milatovic, D., Lehmann, G., Heinz, S. & Schömig, A. Hydrogen peroxide for prevention of bacterial growth on polymer biomaterials. *Annals of Thoracic Surgery* **68,** 2123–2128 (1999).

164. Chopra, I. & Roberts, M. Tetracycline Antibiotics: Mode of Action, Applications, Molecular Biology, and Epidemiology of Bacterial Resistance. *Microbiology and Molecular Biology Reviews* **65,** 232–260 (2001).

165. Li, Z., Chen, C. H., Liu, T., Mathrubootham, V., Hegg, E. L. & Hodge, D. B. Catalysis with CuII(bpy) improves alkaline hydrogen peroxide pretreatment. *Biotechnology and Bioengineering* **110,** 1078–1086 (2013).

166. Correia, J. A. d. C., Júnior, J. E. M., Gonçalves, L. R. B. & Rocha, M. V. P. Alkaline hydrogen peroxide pretreatment of cashew apple bagasse for ethanol production: Study of parameters. *Bioresource Technology* **139,** 249–256 (2013).

167. Hemsworth, G. R., Johnston, E. M., Davies, G. J. & Walton, P. H. Lytic Polysaccharide Monooxygenases in Biomass Conversion. *Trends in Biotechnology* **33,** 747–761 (2015).

168. Cannella, D., Hsieh, C. W. C., Felby, C. & Jørgensen, H. Production and effect of aldonic acids during enzymatic hydrolysis of lignocellulose at high dry matter content. *Biotechnology for Biofuels* **5,** 26 (2012).

169. Mohd-Zaki, Z., Bastidas-Oyanedel, J., Lu, Y., Hoelzle, R., Pratt, S., Slater, F. & Batstone, D. Influence of pH Regulation Mode in Glucose Fermentation on Product Selection and Process Stability. *Microorganisms* **4,** 2 (2016).

170. Famelart, M. H., Kobilinsky, A., Bouillanne, C. & Desmazeaud, M. J. Influence of temperature, pH and dissolved oxygen on growth of Brevibacterium linens in a fermentor. *Applied Microbiology and Biotechnology* **25,** 442–448 (1987).

171. Siegell, S. D. & Gaden, E. L. Automatic control of dissolved oxygen levels in fermentations. *Biotechnology and Bioengineering* **4,** 345–356 (1962).

172. Castillo Martinez, F. A., Balciunas, E. M., Salgado, J. M., Domínguez González, J. M., Converti, A. & Oliveira, R. P. d. S. *Lactic acid properties, applications and production: A review* 2013.

173. Yoo, J. H. *Review of disinfection and sterilization - Back to the basics* 2018.

174. Russo, I., Del Mese, P., Viretto, M., Doronzo, G., Mattiello, L., Trovati, M. & Anfossi, G. Sodium azide, a bacteriostatic preservative contained in commercially available laboratory reagents, influences the responses of human platelets via the cGMP/PKG/VASP pathway. *Clinical Biochemistry* **41,** 343–349 (2008).

175. in. *The MAK-Collection for Occupational Health and Safety* 276–284 (Wiley-VCH Verlag GmbH & Co. KGaA, Weinheim, Germany, 2012).

176. Reinhard, E., Waeber, R., Niederer, M., Maurer, T., Maly, P. & Scherer, S. Preservation of products with MCI/MI in Switzerland. *Contact Dermatitis* **45,** 257–264 (2001).

177. Nguyen, V. H. T., Nguyen, V. H. T., Li, C. B. & Zhou, G. H. The degradation of oxytetracycline during thermal treatments of chicken and pig meat and the toxic effects of degradation products of oxytetracycline on rats. *Journal of Food Science and Technology* **52,** 2842–2850 (2015).

178. López-Peñalver, J. J., Sánchez-Polo, M., Gómez-Pacheco, C. V. & Rivera-Utrilla, J. Photodegradation of tetracyclines in aqueous solution by using UV and UV/H2O2 oxidation processes. *Journal of Chemical Technology and Biotechnology* **85,** 1325–1333 (2010).

179. Skelland, A. Non-Newtonian flow and heat transfer. *Journal of Polymer Science Part A-2: Polymer Physics* **5,** 1327–1328 (1967).

180. McGlashan, S., O'Brien, V., Awati, K. & Mackay, M. *Polymer Rheology. Fundamentals and Applications* 214–222 (1998).

181. Volynets, B., Ein-Mozaffari, F. & Dahman, Y. Biomass processing into ethanol: Pretreatment, enzymatic hydrolysis, fermentation, rheology, and mixing. *Green Processing and Synthesis* **6,** 1–22 (2017).

182. Knutsen, J. S. & Liberatore, M. W. Rheology of high-solids biomass slurries for biorefinery applications. *Journal of Rheology* **53,** 877–892 (2009).

183. Stickel, J., Knutsen, J., Liberatore, M., Luu, W., Bousfield, D. W., Klingenberg, D., Scott, T., Root, T., Ehrhardt, M. & Monz, T. Rheology measurements of a biomass slurry: An inter-laboratory study. *Rheologica Acta* **48,** 1005–1015 (2009).

184. Pimenova, N. V. & Hanley, T. R. Measurement of rheological properties of corn stover suspensions. *Applied Biochemistry and Biotechnology - Part A Enzyme Engineering and Biotechnology* **106,** 383–392 (2003).

185. Ehrhardt, M. R., Monz, T. O., Root, T. W., Connelly, R. K., Scott, C. T. & Klingenberg, D. J. Rheology of Dilute Acid Hydrolyzed Corn Stover at High Solids Concentration. *Applied Biochemistry and Biotechnology* **160,** 1102–1115 (2010).

186. Bennington, C. P., Kerekes, R. J. & Grace, J. R. The yield stress of fibre suspensions. *The Canadian Journal of Chemical Engineering* **68,** 748–757 (1990).

187. Viamajala, S., McMillan, J., Schell, D. & Elander, R. Rheology of corn stover slurries at high solids concentrations–effects of saccharification and particle size. *Bioresource Technology* **100,** 925–934 (2009).

188. Samaniuk, J. R., Wang, J., Root, T. W., Scott, C. T. & Klingenberg, D. J. Rheology of concentrated biomass. *Korea Australia Rheology Journal* **23,** 237–245 (2011).

189. Chen, X., Crawford, N., Wang, W., Kuhn, E., Sievers, D., Tao, L. & Tucker, M. Kinetics and Rheological Behavior of Higher Solid (Solids >20%) Enzymatic Hydrolysis Reactions Using Dilute Acid Pretreated, Deacetylation and Disk Refined, and Deacetylation and Mechanical Refined (DMR) Corn Stover Slurries. *ACS Sustainable Chemistry and Engineering* **7,** 1633–1641 (2019).

190. Nguyen, Q.-B. D., Akroyd, T., De Kee, D. C. & Zhu, L. Yield stress measurements in suspensions: An inter-laboratory study. *Korea Australia Rheology Journal* **18,** 15–24 (2006).

191. Cruz, A. G., Scullin, C., Mu, C., Cheng, G., Stavila, V., Varanasi, P., Xu, D., Mentel, J., Chuang, Y. D., Simmons, B. A. & Singh, S. Impact of high biomass loading on ionic liquid pretreatment. *Biotechnology for Biofuels* **6,** 52 (2013).

192. Berson, R. E., Dasari, R. K. & Hanley, T. R. Modeling of a continuous pretreatment reactor using computational fluid dynamics. *Applied Biochemistry and Biotechnology* **130,** 621–630 (2006).

193. He, W., Park, C. S. & Norbeck, J. M. Rheological study of comingled biomass and coal slurries with hydrothermal pretreatment. *Energy and Fuels* **23,** 4763–4767 (2009).

194. Correâ, L. J., Badino, A. & Cruz, A. Power consumption evaluation of different fed-batch strategies for enzymatic hydrolysis of sugarcane bagasse. *Bioprocess and Biosystems Engineering* **39,** 825–833 (2016).

195. Du, J., Li, Y., Zhang, H., Zheng, H. & Huang, H. Factors to decrease the cellulose conversion of enzymatic hydrolysis of lignocellulose at high solid concentrations. *Cellulose* **21,** 2409–2417 (2014).

196. Palmqvist, B., Kadić, A., Hägglund, K., Petersson, A. & Lidén, G. Scale-up of high-solid enzymatic hydrolysis of steam-pretreated softwood: the effects of reactor flow conditions. *Biomass Conversion and Biorefinery* **6,** 173–180 (2016).

197. Kadić, A. & Lidén, G. Viscosity reduction of pretreated softwood by endoglucanases. *Journal of Chemical Technology and Biotechnology* **93,** 2440–2446 (2018).

198. Coffman, P., McCaffrey, N., Gardner, J., Bhagia, S., Kumar, R., Wyman, C. E. & Tanjore, D. In Situ Rheological Method to Evaluate Feedstock Physical Properties Throughout Enzymatic Deconstruction. *Frontiers in Energy Research* **6,** 53 (2018).

199. Nguyen, T. C., Anne-Archard, D., Coma, V., Cameleyre, X., Lombard, E., Binet, C., Nouhen, A., To, K. A. & Fillaudeau, L. In situ rheometry of concentrated cellulose fibre suspensions and relationships with enzymatic hydrolysis. *Bioresource Technology* **133,** 563–572 (2013).

200. Le, T., Anne-Archard, D., Coma, V., Cameleyre, X., Lombard, E., To, K. A., Pham, T. A., Nguyen, T. C. & Fillaudeau, L. Using in-situ viscosimetry and morphogranulometry to explore hydrolysis mechanisms of filter paper and pretreated sugarcane bagasse under semi-dilute suspensions. *Biochemical Engineering Journal* **127,** 9–20 (2017).

201. Lavenson, D. M., Tozzi, E. J., Mccarthy, M. J. & Powell, R. L. Yield stress of pretreated corn stover suspensions using magnetic resonance imaging. *Biotechnology and Bioengineering* **108,** 2312–2319 (2011).

202. Cardona, M. J., Tozzi, E. J., Karuna, N., Jeoh, T., Powell, R. L. & McCarthy, M. J. A process for energy-efficient high-solids fed-batch enzymatic liquefaction of cellulosic biomass. *Bioresource Technology* **198,** 488–496 (2015).

203. Zhong, J.-J. .-J., Fujiyama, K., Seki, T. & Yoshida, T. A quantitative analysis of shear effects on cell suspension and cell culture of perilla frutescens in bioreactors. *Biotechnology and Bioengineering* **44,** 649–654 (1994).

204. Nguyen, Q. D. & Boger, D. V. Measuring The Flow Properties Of Yield Stress Fluids. *Annual Review of Fluid Mechanics* **24,** 47–88 (1992).

205. Wiman, M., Palmqvist, B., Tornberg, E. & Lidén, G. Rheological characterization of dilute acid pretreated softwood. *Biotechnology and Bioengineering* **108,** 1031–1041 (2011).

206. Kristensen, J., Felby, C. & Jørgensen, H. *Determining yields in high solids enzymatic hydrolysis of biomass* in *Applied Biochemistry and Biotechnology* **156** (2009), 127–132.

207. Bakker, A. & Benz, G. Mixing in Industrial Fermenters. *10th International Biotechnology Symposium* (1996).

208. Klingenberg, D. J., Root, T. W., Burlawar, S., Scott, C. T., Bourne, K. J., Gleisner, R., Houtman, C. & Subramaniam, V. Rheometry of coarse biomass at high temperature and pressure. *Biomass and Bioenergy* **99,** 69–78 (2017).

209. Park, S., Baker, J. O., Himmel, M. E., Parilla, P. A. & Johnson, D. K. Cellulose crystallinity index: Measurement techniques and their impact on interpreting cellulase performance. *Biotechnology for Biofuels* **3,** 10 (2010).

210. Chang, V. S. & Holtzapple, M. T. Fundamental factors affecting biomass enzymatic reactivity. *Applied Biochemistry and Biotechnology - Part A Enzyme Engineering and Biotechnology* **84-86,** 5–37 (2000).

211. Meunier-Goddik, L., Bothwell, M., Sangseethong, K., Piyachomkwan, K., Chung, Y., Thammasouk, K., Tanjo, D. & Penner, M. Physicochemical properties of pretreated poplar feedstocks during simultaneous saccharification and fermentation. *Enzyme and Microbial Technology* **24,** 667–674 (1999).

212. Pino, M., Rodríguez-Jasso, R., Michelin, M., Flores-Gallegos, A., Morales-Rodriguez, R., Teixeira, J. & Ruiz, H. Bioreactor design for enzymatic hydrolysis of biomass under the biorefinery concept. *Chemical Engineering Journal* **347,** 119–136 (2018).

213. Du, J., Zhang, F., Li, Y., Zhang, H., Liang, J., Zheng, H. & Huang, H. Enzymatic liquefaction and saccharification of pretreated corn stover at high-solids concentrations in a horizontal rotating bioreactor. *Bioprocess and Biosystems Engineering* **37,** 173–181 (2014).

214. Qin, W. High consistency enzymatic hydrolysis of lignocellulose. *Master of Applied Science Dissertation* (2010).

215. Hou, W., An, R., Zhang, J. & Bao, J. On-site measurement and modeling of rheological property of corn stover hydrolysate at high solids content. *Biochemical Engineering Journal* **107,** 61–65 (2016).

216. Thomas, C. R. & Geer, D. Effects of shear on proteins in solution. *Biotechnology Letters* **33,** 443–456 (2011).

217. Huang, R., Su, R., Qi, W. & He, Z. Bioconversion of Lignocellulose into Bioethanol: Process Intensification and Mechanism Research. *Bioenergy Research* **4,** 225–245 (2011).

218. Verardi, A., De, I., Ricca, E. & Calabr, V. in *Bioethanol* (2012).

219. Berlin, A., Maximenko, V., Gilkes, N. & Saddler, J. Optimization of enzyme complexes for lignocellulose hydrolysis. *Biotechnology and Bioengineering* **97,** 287–296 (2007).

220. Ouyang, J., Dong, Z., Song, X., Lee, X., Chen, M. & Yong, Q. Improved enzymatic hydrolysis of microcrystalline cellulose (Avicel PH101) by polyethylene glycol addition. *Bioresource Technology* **101,** 6685–6691 (2010).

221. Jenkins, T. Toward a biobased economy: examples from the UK. *Biofuels, Bioproducts and Biorefining* **2,** 133–143 (2008).

222. Thompson, N., Puri, D. & Speller, P. *Method for the hydrolysis of lignocellulosic biomass* 2020.

223. Sipos, B., Dienes, D., Schleicher, Á., Perazzini, R., Crestini, C., Siika-aho, M. & Réczey, K. Hydrolysis efficiency and enzyme adsorption on steam-pretreated spruce in the presence of poly(ethylene glycol). *Enzyme and Microbial Technology* **47,** 84–90 (2010).

224. Sipos, B., Szilágyi, M., Sebestyén, Z., Perazzini, R., Dienes, D., Jakab, E., Crestini, C. & Réczey, K. *Mechanism of the positive effect of poly(ethylene glycol) addition in enzymatic hydrolysis of steam pretreated lignocelluloses* 2011.

225. Rocha-Martín, J., Martinez-Bernal, C., Pérez-Cobas, Y., Reyes-Sosa, F. M. & García, B. D. Additives enhancing enzymatic hydrolysis of lignocellulosic biomass. *Bioresource Technology* **244,** 48–56 (2017).

226. Haven, M. Ø., Lindedam, J., Jeppesen, M. D., Elleskov, M., Rodrigues, A. C., Gama, M., Jørgensen, H. & Felby, C. Continuous recycling of enzymes during production of lignocellulosic bioethanol in demonstration scale. *Applied Energy* **159,** 188–195 (2015).

227. Haven, M. Ø. & Jørgensen, H. Adsorption of β-glucosidases in two commercial preparations onto pretreated biomass and lignin. *Biotechnology for Biofuels* **6** (2013).

228. Knutsen, J. S. & Liberatore, M. W. Rheology modification and enzyme kinetics of high solids cellulosic slurries. *Energy and Fuels* **24,** 3267–3274 (2010).

229. Walkling, D. & Shangraw, R. F. Rheology of microcrystalline cellulose carboxymethylcellulose gels. *Journal of Pharmaceutical Sciences* **57,** 1927–1933 (1968).

230. Beuguel, Q., Tavares, J. R., Carreau, P. J. & Heuzey, M.-C. Rheological behavior of cellulose nanocrystal suspensions in polyethylene glycol. *Journal of Rheology* **62,** 607–618 (2018).

231. Ching, Y. C., Ershad Ali, M., Abdullah, L. C., Choo, K. W., Kuan, Y. C., Julaihi, S. J., Chuah, C. H. & Liou, N. S. *Rheological properties of cellulose nanocrystal-embedded polymer composites: a review* 2016.

232. Moberg, T., Tang, H., Zhou, Q. & Rigdahl, M. Preparation and viscoelastic properties of composite fibres containing cellulose nanofibrils: Formation of a coherent fibrillar network. *Journal of Nanomaterials* **2016** (2016).

233. Moberg, T., Sahlin, K., Yao, K., Geng, S., Westman, G., Zhou, Q., Oksman, K. & Rigdahl, M. Rheological properties of nanocellulose suspensions: effects of fibril/particle dimensions and surface characteristics. *Cellulose* **24,** 2499–2510 (2017).

234. Russ, D. C., Thomas, J. M., Miller, Q. S. & Berson, R. E. Predicting power for a scaled-up non-newtonian biomass slurry. *Chemical Engineering and Technology* **38,** 53–60 (2015).

235. Wooley, R., Ruth, M., Sheehan, J., Majdeski, H. & Galvez, A. Lignocellulosic Biomass to Ethanol Process Design and Economics Utilizing Co-Current Dilute Acid Prehydrolysis and Enzymatic Hydrolysis Current and Futuristic Scenarios Lignocellulosic Biomass to Ethanol Process Design and Economics Utilizing Co-Current D. *Contract,* 132 (1999).

236. Xue, S., Uppugundla, N., Bowman, M., Cavalier, D., Da Costa Sousa, L., E Dale, B. & Balan, V. Sugar loss and enzyme inhibition due to oligosaccharide accumulation during high solids-loading enzymatic hydrolysis. *Biotechnology for Biofuels* (2015).

237. Pihlajaniemi, V., Sipponen, M., Kallioinen, A., Nyyssölä, A. & Laakso, S. Rate-constraining changes in surface properties, porosity and hydrolysis kinetics of lignocellulose in the course of enzymatic saccharification. *Biotechnology for Biofuels* **9** (2016).

238. Kont, R., Kurašin, M., Teugjas, H. & Väljamäe, P. Strong cellulase inhibitors from the hydrothermal pretreatment of wheat straw.

239. Liu, Y., Xu, J., Zhang, Y., Yuan, Z. & Xie, J. Optimization of high solids fed-batch saccharification of sugarcane bagasse based on system viscosity changes. *Journal of Biotechnology* **211,** 5–9 (2015).

240. Yang, B., Dai, Z., Ding, S. & Wyman, C. Enzymatic hydrolysis of cellulosic biomass. *Biofuels* **2,** 421–449 (2014).

241. Liguori, R., Ventorino, V., Pepe, O. & Faraco, V. Bioreactors for lignocellulose conversion into fermentable sugars for production of high added value products. *Applied microbiology and biotechnology* **100,** 597–611 (2016).

242. Chen, H. & Liu, Z. Enzymatic hydrolysis of lignocellulosic biomass from low to high solids loading. *Engineering in Life Sciences* **17,** 489–499 (2017).

243. De Gooijer, C., Bakker, W., Beeftink, H. & Tramper, J. *Bioreactors in series: An overview of design procedures and practical applications* 1996.

244. Karanth, N. G. Multiple continuous stirred tank reactors vs Batch reactors - some design considerations. *Biotechnology Letters* **1,** 139–144 (1979).

245. Geng, W., Jin, Y., Jameel, H. & Park, S. Strategies to achieve high-solids enzymatic hydrolysis of dilute-acid pretreated corn stover. *Bioresource Technology* **187,** 43–48 (2015).

246. Andrić, P., Meyer, A., Jensen, P. & Dam-Johansen, K. *Reactor design for minimizing product inhibition during enzymatic lignocellulose hydrolysis. II. Quantification of inhibition and suitability of membrane reactors* 2010.

247. Garcia-Ochoa, F., Santos, V. E. & Gomez, E. in *Comprehensive Biotechnology, Second Edition* Sept., 179–198 (Elsevier Inc., 2011).

248. Jiang, M., Zhao, Y., Liu, G. & Zheng, J. Enhancing mixing of particles by baffles in a rotating drum mixer. *Particuology* **9,** 270–278 (2011).

249. Rabiner, L. & Gold, B. in *Chemical Process Equipment* 0, 1308–1310 (Elsevier, 1985).

250. Wilkens, R., Henry, C. & Gates, L. How to scale-up mixing processes in non-newtonian fluids. *Chemical Engineering Progress* **99,** 44–52 (2003).

251. Palmqvist, B., Wiman, M. & Lidén, G. Effect of mixing on enzymatic hydrolysis of steam-pretreated spruce: A quantitative analysis of conversion and power consumption. *Biotechnology for Biofuels* **4,** 10 (2011).

252. Kadic, A. & Liden, G. Does sugar inhibition explain mixing effects in enzymatic hydrolysis of lignocellulose? *Journal of Chemical Technology and Biotechnology* (2016).

253. Kadic, A. *The effects of mixing on the enzymatic hydrolysis of lignocellulosic biomass* PhD thesis (2017).

254. Correâ, L. J., Badino, A. & Cruz, A. Mixing design for enzymatic hydrolysis of sugarcane bagasse: Methodology for selection of impeller configuration. *Bioprocess and Biosystems Engineering* **39,** 285–294 (2016).

255. Dynamix agitators. *Mixing 101: Baffled by Baffles ?*

256. Mcfarlane, C. & Nienow, A. W. Studies of High Solidity Ratio Hydrofoil Impellers for Aerated Bioreactors. 1. Review. *Biotechnology Progress* **11,** 601–607 (1995).

257. Mcfarlane, C. M., Zhao, X. .-M. & Nienow, A. W. Studies of High Solidity Ratio Hydrofoil Impellers for Aerated Bioreactors. 2. Air—Water Studies. *Biotechnology Progress* **11,** 608–618 (1995).

258. McFarlane, C. & Nienow, A. Studies of High Solidity Ratio Hydrofoil Impellers for Aerated Bioreactors. 3. Fluids of Enhanced Viscosity and Exhibiting Coalescence Repression. *Biotechnology Progress* **12,** 1–8 (1996).

259. McFarlane, C. & Nienow, A. Studies of high solidity ratio hydrofoil impellers for aerated bioreactors. 4. Comparison of impeller types. *Biotechnology Progress* **12,** 9–15 (1996).

260. Benz, G. T. *Hydrofoil Impellers vs. Pitched Blade Turbines in Lignocellulosic Slurries* 2017.

261. Zhang, J., Chu, D., Huang, J., Yu, Z., Dai, G. & Bao, J. Simultaneous saccharification and ethanol fermentation at high corn stover solids loading in a helical stirring bioreactor. *Biotechnology and Bioengineering* **105,** 718–728 (2010).

262. Liu, K., Zhang, J. & Bao, J. Two stage hydrolysis of corn stover at high solids content for mixing power saving and scale-up applications. *Bioresource Technology* **196,** 716–720 (2015).

263. He, Y., Zhang, L., Zhang, J. & Bao, J. Helically agitated mixing in dry dilute acid pretreatment enhances the bioconversion of corn stover into ethanol. *Biotechnology for Biofuels* **7,** 1–13 (2014).

264. Zhang, L., Zhang, J., Li, C. & Bao, J. Rheological characterization and CFD modeling of corn stover-water mixing system at high solids loading for dilute acid pretreatment. *Biochemical Engineering Journal* **90,** 324–332 (2014).

265. Hou, W., Zhang, L., Zhang, J. & Bao, J. Rheology evolution and CFD modeling of lignocellulose biomass during extremely high solids content pretreatment. *Biochemical Engineering Journal* **105,** 412–419 (2016).

266. Battista, F., Gomez Almendros, M., Rousset, R., Boivineau, S. & Bouillon, P. Enzymatic hydrolysis at high dry matter content: The influence of the substrates' physical properties and of loading strategies on mixing and energetic consumption. *Bioresource Technology* **250,** 191–196 (2018).

267. Battista, F., Gomez Almendros, M., Rousset, R. & Bouillon, P. Enzymatic hydrolysis at high lignocellulosic content: Optimization of the mixing system geometry and of a fed-batch strategy to increase glucose concentration. *Renewable Energy* **131,** 152–158 (2019).

268. Benz, G. Impeller Selection for Lignocellulosic Hydrolysis Reactors. *Biofuels digest,* 2–3 (2017).

269. Penney, W. R. Chapter 10 – Mixing and Agitation. *Chemical Process Equipment* **3,** 277–328 (2005).

270. Nguyen, Q. *Tower reactors for bioconversion of lignocellulosic material* 1997.

271. Li, C., Tanjore, D., He, W., Wong, J., Gardner, J. L., Sale, K., Simmons, B. & Singh, S. Scale-up and evaluation of high solid ionic liquid pretreatment and enzymatic hydrolysis of switchgrass. *Biotechnology for Biofuels* **6** (2013).

272. Palmqvist, B. & Lidén, G. Torque measurements reveal large process differences between materials during high solid enzymatic hydrolysis of pretreated lignocellulose. *Palmqvist and Lidén Biotechnology for Biofuels* **5** (2012).

273. Carvajal, D., Marchisio, D., Bensaid, S. & Fino, D. Enzymatic Hydrolysis of Lignocellulosic Biomasses via CFD and Experiments. *Ind. Eng. Chem. Res* **51,** 7518–7525 (2012).

274. Benz, G. T. Agitating fibrous materials. *Chemical Engineering Progress* **106,** 28–32 (2010).

275. Zhang, X., Paice, M. & Saddler, J. High consistency enzymatic hydrolysis of hardwood substrates. *Bioresource Technology* **100,** 5890–5897 (2009).

276. Bustamante, M., Cerri, M. & Badino, A. C. Comparison between average shear rates in conventional bioreactor with Rushton and Elephant ear impellers. *Chemical engineering science*, 1–10 (2013).

277. Zhang, R., Gikas, P., Zhu, B., Lord, J., Choate, C., Rapport, J., El-Mashad, H., Jenkins, B. & Brown, M. R. California Department of Resources Recycling and Recovery Integration of Rotary Drum Reactor and Anaerobic Digestion Technologies for Treatment of Municipal Solid Waste DEPARTMENT OF RESOURCES RECYCLING AND RECOVERY (2010).

278. Wang, W., Walton, J. & McCarthy, K. Flow profiles of power law fluids in scraped surface heat exchanger geometry using MRI. *Journal of Food Process Engineering* **22,** 11–27 (1999).

279. Jin, J., Liu, G. L., Shi, S. Y. & Cong, W. Studies on the performance of a rotating drum bioreactor for bioleaching processes - Oxygen transfer, solids distribution and power consumption. *Hydrometallurgy* **103,** 30–34 (2010).

280. Goswami, T. Conventional industrial ice cream freezers and its thermal design: a review. *J Food Sci Nutr* **1** (2018).

281. Alam, M., Mamun, A., Qudsieh, I., Muyibi, S., Salleh, H. & Omar, N. Solid state bioconversion of oil palm empty fruit bunches for cellulase enzyme production using a rotary drum bioreactor. *Biochemical Engineering Journal* **46,** 61–64 (2009).

282. Sigma-Aldrich. *Bench-top laboratory roller mill*

283. Larsen, J., Østergaard Petersen, M., Thirup, L., Li, H. & Iversen, F. The IBUS process - Lignocellulosic bioethanol close to a commercial reality. *Chemical Engineering and Technology* **31,** 765–772 (2008).

284. Larsen, J., Haven, M., Thirup, L., Gregg, D. & Saddler, J. N. Inbicon makes lignocellulosic ethanol a commercial reality. *Biomass and Bioenergy* **46,** 36–45 (2012).

285. Miyashita, H., Yoshida, M., Yamane, T. & Nishimura, T. Heat Transfer Correlation in High Prandtl (High Schmidt) Number Fluid in Votator Type Scraped Surface Heat Exchanger. *Journal of Chemical Engineering of Japan* **30,** 545–549 (1997).

286. Sangrame, G., Bhagavathi, D., Thakare, H. & Das, H. Performance evaluation of a thin film scraped surface evaporator for concentration of tomato pulp. *Journal of Food Engineering* **43,** 205–211 (2000).

287. Sun, K.-H., Pyle, D., Fitt, A., Please, C., Baines, M. & Hall-Taylor, N. Numerical study of 2D heat transfer in a scraped surface heat exchanger. *Computers & Fluids* **33,** 869–880 (2004).

288. Van Der Gulik, G. J., Wijers, J. G. & Keurentjes, J. T. Hydrodynamics and scale-up of horizontal stirred reactors. *Industrial and Engineering Chemistry Research* **40,** 4731–4740 (2001).

289. Henkel, K.-D. Reactor Types and Their Industrial Applications. *Ullmann's Encyclopedia of Industrial Chemistry*, 415–432 (2000).

290. Shibasaki, N., Hirose, K., Yonemoto, T. & Tadaki, T. Suspension culture of Nicotiana tabacum cells in a rotary-drum bioreactor. *Journal of Chemical Technology & Biotechnology* **53,** 359–363 (1992).

291. Alam, M. Z. M. M. Z., Muhammad, N., Mahmat, M. M. E., Alam, M. Z. M. M. Z., Muhammad, N. & Mahmat, M. M. E. Production of cellulase from oil palm biomass as substrate by solid state bioconversion. *American Journal of Applied Sciences* **2,** 569–572 (2005).

292. Lin, Y. S., Lee, W. C., Duan, K. J. & Lin, Y. H. Ethanol production by simultaneous saccharification and fermentation in rotary drum reactor using thermotolerant Kluveromyces marxianus. *Applied Energy* **105,** 389–394 (2013).

293. Lin, Y.-S. & Lee, W.-C. *SSF of cogongrass to ethanol* tech. rep. 3 (2011), 2744–2756.

294. Fung, C. J. & Mitchell, D. A. Baffles increase performance of solid-state fermentation in rotating drum bioreactors. *Biotechnology Techniques* **9,** 295–298 (1995).

295. Liu, G., Jin, J., Wen, S., Wang, Z., Zhang, Q. & Cong, W. Research on the characteristic of power consumption in a novel rotating drum bioleaching reactor of different sizes. *Minerals Engineering* **53,** 16–23 (2013).

296. Wang, E.-Q. Q., Li, S.-Z. Z., Tao, L., Geng, X. & Li, T.-C. C. Modeling of rotating drum bioreactor for anaerobic solid-state fermentation. *Applied Energy* **87,** 2839–2845 (2010).

297. Carvalho, L., da Silva, O. B., da Almeida, G., da Oliveira, J., Parachin, N. & Carmo, T. Production Processes for Monoclonal Antibodies. *Fermentation Processes* (2017).

298. Viola, E., Arcieri, G., Zimbardi, F., Valerio, V., Cerone, N. & Corato, U. D. Evaluation of a pilot-scaled paddle dryer for the production of ethanol from lignocellulose including inhibitor removal and high-solids enzymatic hydrolysis. *Biotechnology Reports* **9,** 38–45 (2016).

299. Davis, R., Bartling, A. & Tao, L. *Biochemical Conversion of Lignocellulosic Biomass to Hydrocarbon Fuels and Products: 2019 State of Technology and Future Research* tech. rep. (2018).

300. Ascanio, G., Castro, B. & Galindo, E. Measurement of Power Consumption in Stirred Vessels—A Review. *Chemical Engineering Research and Design* **82,** 1282–1290 (2004).

301. Benz, G. T. Determining torque split for multiple impellers in slurry mixing. *Chemical Engineering Progress* **108,** 45–48 (2012).

302. Norwood, K. W. & Metzner, A. B. Flow patterns and mixing rates in agitated vessels. *AIChE Journal* **6,** 432–437 (1960).

303. Ascanio, G. *Mixing time in stirred vessels: A review of experimental techniques* 2015.

304. Kraume, M. & Zehner, P. Experience with experimental standards for measurements of various parameters in stirred tanks: A comparative test. *Chemical Engineering Research and Design* **79,** 811–818 (2001).

305. Ghorbanian, M., Russ, D. C. & Berson, R. E. Mixing analysis of PCS slurries in a horizontal scraped surface bioreactor. *Bioprocess and Biosystems Engineering* **37,** 2113–2119 (2014).

306. Yang, N. & Wang, R. Sustainable technologies for the reclamation of greenhouse gas CO2. *Journal of Cleaner Production* **103,** 1–9 (2014).

307. Zhang, Q., Zhang, P., Pei, Z. J. & Wang, D. *Relationships between cellulosic biomass particle size and enzymatic hydrolysis sugar yield: Analysis of inconsistent reports in the literature* 2013.

308. Sun, S. S., Sun, S. S., Cao, X. & Sun, R. *The role of pretreatment in improving the enzymatic hydrolysis of lignocellulosic materials* 2016.

309. Fan, Z., South, C., Lyford, K., Munsie, J., Van Walsum, P. & Lynd, L. R. Conversion of paper sludge to ethanol in a semicontinuous solids-fed reactor. *Bioprocess and Biosystems Engineering* **26,** 93–101 (2003).

310. Ghorbanpour Khamseh, A. & Miccio, M. *Comparison of batch, fed-batch and continuous well-mixed reactors for enzymatic hydrolysis of orange peel wastes* in *Process Biochemistry* **47** (2012), 1588–1594.

311. Kinnarinen, T., Shakhanova, M., Hietanen, E., Salmimies, R., Häkkinen, A. & Louhi-Kultanen, M. Effect of mixing on enzymatic hydrolysis of cardboard waste: Saccharification yield and subsequent separation of the solid residue using a pressure filter. *Bioresource Technology* **110,** 405–411 (2012).

312. Singh, A., Kumar, P. K. & Schügerl, K. Adsorption and reuse of cellulases during saccharification of cellulosic materials. *Journal of Biotechnology* **18,** 205–212 (1991).

313. Büchs, J., Maier, U., Milbradt, C. & Zoels, B. Power consumption in shaking flasks on rotary shaking machines: I. Power consumption measurement in unbaffled flasks at low liquid viscosity. *Biotechnology and Bioengineering* **68,** 589–593 (2000).

314. Büchs, J., Maier, U., Milbradt, C. & Zoels, B. Power consumption in shaking flasks on rotary shaking machines: II. Nondimensional description of specific power consumption and flow regimes in unbaffled flasks at elevated liquid viscosity. *Biotechnology and Bioengineering* **68,** 594–601 (2000).

315. Y, Z., J, M., D, C., R, L., W, M., A, O. & HL, M. Life cycle emissions and cost of producing electricity from coal, natural gas, and wood pellets in Ontario, Canada. *Environmental Science and Technology* **44,** 538–544 (2010).

316. Croughan, M. S., Konstantinov, K. B. & Cooney, C. The future of industrial bioprocessing: Batch or continuous? *Biotechnology and Bioengineering* **112,** 648–651 (2015).

317. Ponton, J. Optimization of Chemical Processes. *Chemical Engineering Science* **44,** 3005 (1989).

318. Dutta, S. *Optimization in Chemical Engineering* (2016).

319. Mais, U., Esteghlalian, A. R. & Saddler, J. N. in *Biotechnology for Fuels and Chemicals* 463–472 (Humana Press, 2002).

320. Ingesson, H., Zacchi, G., Yang, B., Esteghlalian, A. R. & Saddler, J. N. The effect of shaking regime on the rate and extent of enzymatic hydrolysis of cellulose. *Journal of Biotechnology* **88,** 177–182 (2001).

321. Tavizón-Pozos, J. A., Ibarra, I. S., Guevara-Lara, A. & Galán-Vidal, C. A. in, 77–103 (2019).

322. Timung, R., Mohan, M., Chilukoti, B., Sasmal, S., Banerjee, T. & Goud, V. V. Optimization of dilute acid and hot water pretreatment of different lignocellulosic biomass: A comparative study. *Biomass and Bioenergy* **81,** 9–18 (2015).

323. Lu, X., Zhang, Y. & Angelidaki, I. Optimization of H2SO4-catalyzed hydrothermal pretreatment of rapeseed straw for bioconversion to ethanol: Focusing on pretreatment at high solids content. *Bioresource Technology* **100,** 3048–3053 (2009).

324. Flores-gómez, C., Escamilla Silva, E., Zhong, C., Dale, B., Da, L., Sousa, C. & Balan, V. Conversion of lignocellulosic agave residues into liquid biofuels using an AFEX ™ -based biorefinery. *Biotechnology for Biofuels* **11** (2018).

325. Rezende, C. A., Atta, B. W., Breitkreitz, M. C., Simister, R., Gomez, L. D. & McQueen-Mason, S. J. Optimization of biomass pretreatments using fractional factorial experimental design. *Biotechnology for Biofuels* **11,** 206 (2018).

326. Ávila-Lara, A. I., Camberos-Flores, J. N., Mendoza-Pérez, J. A., Messina-Fernández, S. R., Saldaña-Duran, C. E., Jimenez-Ruiz, E. I., Sánchez-Herrera, L. M. & Pérez-Pimienta, J. A. Optimization of alkaline and dilute acid pretreatment of agave bagasse by response surface methodology. *Frontiers in Bioengineering and Biotechnology* **3,** 146 (2015).

327. Li, K., Qin, J. C., Liu, C. G. & Bai, F. W. Optimization of pretreatment, enzymatic hydrolysis and fermentation for more efficient ethanol production by Jerusalem artichoke stalk. *Bioresource Technology* **221,** 188–194 (2016).

328. Zhou, J., Wang, Y. H., Chu, J., Luo, L. Z., Zhuang, Y. P. & Zhang, S. L. Optimization of cellulase mixture for efficient hydrolysis of steam-exploded corn stover by statistically designed experiments. *Bioresource Technology* **100,** 819–825 (2009).

329. Zambare, V. P., Zambare, A. V., Barh, D. & Christopher, L. P. Optimization of enzymatic hydrolysis of prairie cordgrass for improved ethanol production. *Journal of Renewable and Sustainable Energy* **4,** 193–205 (2012).

330. Sotaniemi, V. H., Taskila, S., Ojamo, H. & Tanskanen, J. Controlled feeding of lignocellulosic substrate enhances the performance of fed-batch enzymatic hydrolysis in a stirred tank reactor. *Biomass and Bioenergy* **91,** 271–277 (2016).

331. Gusakov, A. V. *Alternatives to Trichoderma reesei in biofuel production* 2011.

332. Jeoh, T., Cardona, M. J., Karuna, N., Mudinoor, A. R. & Nill, J. *Mechanistic kinetic models of enzymatic cellulose hydrolysis—A review* 2017.

333. Gnansounou, E. & Dauriat, A. Techno-economic analysis of lignocellulosic ethanol: A review. *Bioresource Technology* **101,** 4980–4991 (2010).

334. Nguyen, Q. A., Dickow, J. H., Duff, B. W., Farmer, J. D., Glassner, D. A., Ibsen, K. N., Ruth, M. F., Schell, D. J., Thompson, I. B. & Tucker, M. P. NREL/DOE ethanol pilot-plant: Current status and capabilities. *Bioresource Technology* **58,** 189–196 (1996).

335. Tao, L., Tan, E. C., Mccormick, R., Zhang, M., Aden, A., He, X. & Zigler, B. T. Techno-economic analysis and life-cycle assessment of cellulosic isobutanol and comparison with cellulosic ethanol and n-butanol. *Biofuels, Bioproducts and Biorefining* **8,** 30–48 (2014).

336. Kazi, F. K., Fortman, J. A., Anex, R. P., Hsu, D. D., Aden, A., Dutta, A. & Kothandaraman, G. Techno-economic comparison of process technologies for biochemical ethanol production from corn stover. *Fuel* **89,** S20–S28 (2010).

337. Kazi, F. K., Fortman, J. & Anex, R. Techno-Economic Analysis of Biochemical Scenarios for Production of Cellulosic Ethanol Techno-Economic Analysis of Biochemical Scenarios for Production of Cellulosic Ethanol (2010).

338. Humbird, D., Davis, R., Tao, L., Kinchin, C., Hsu, D., Aden, A., Schoen, P., Lukas, J., Olthof, B., Worley, M., Sexton, D. & Dudgeon, D. Process Design and Economics for Biochemical Conversion of Lignocellulosic Biomass to Ethanol. *Renewable Energy* **303,** 147 (2011).

339. Davis, R., Grundl, N., Tao, L., Biddy, M. J., Tan, E. C. D., Beckham, G. T., Humbird, D., Thompson, D. N. & Roni, M. S. *Process Design and Economics for the Conversion of Lignocellulosic Biomass to Hydrocarbon Fuels and Coproducts: 2018 Biochemical Design Case Update* tech. rep. November (2018).

340. Aden, A., Ruth, M., Ibsen, K., Jechura, J., Neeves, K., Sheehan, J. & Wallace, B. *Lignocellulosic Biomass to Ethanol Process Design and Economics Utilizing Co-Current Dilute Acid Prehydrolysis and Enzymatic Hydrolysis for Corn Stover* tech. rep. (2002).

341. Mandegari, M. A., Farzad, S. & Görgens, J. F. *Recent trends on techno-economic assessment (TEA) of sugarcane biorefineries* 2017.

342. Vasconcelos, M. H., Mendes, F. M., Ramos, L., Dias, M. O. S., Bonomi, A., Jesus, C. D. F., Watanabe, M. D. B., Junqueira, T. L., Milagres, A. M. F., Ferraz, A. & Santos, J. C. d. Techno-economic assessment of bioenergy and biofuel production in integrated sugarcane biorefinery: Identification of technological bottlenecks and economic feasibility of dilute acid pretreatment. *Energy* **199,** 117422 (2020).

343. MacRelli, S., Mogensen, J. & Zacchi, G. Techno-economic evaluation of 2 nd generation bioethanol production from sugar cane bagasse and leaves integrated with the sugar-based ethanol process. *Biotechnology for Biofuels* **5,** 22 (2012).

344. Seabra, J. E., Tao, L., Chum, H. L. & Macedo, I. C. A techno-economic evaluation of the effects of centralized cellulosic ethanol and co-products refinery options with sugarcane mill clustering. *Biomass and Bioenergy* **34,** 1065–1078 (2010).

345. Wingren, A., Galbe, M. & Zacchi, G. Energy considerations for a SSF-based softwood ethanol plant. *Bioresource Technology* **99,** 2121–2131 (2008).

346. Frankó, B., Galbe, M. & Wallberg, O. Bioethanol production from forestry residues: A comparative techno-economic analysis. *Applied Energy* **184,** 727–736 (2016).

347. Sassner, P., Galbe, M. & Zacchi, G. Techno-economic evaluation of bioethanol production from three different lignocellulosic materials. *Biomass and Bioenergy* **32,** 422–430 (2008).

348. Wingren, A., Galbe, M. & Zacchi, G. Techno-economic evaluation of producing ethanol from softwood: Comparison of SSF and SHF and identification of bottlenecks. *Biotechnology Progress* **19,** 1109–1117 (2003).

349. Joelsson, E., Wallberg, O. & Börjesson, P. Integration potential, resource efficiency and cost of forest-fuel-based biorefineries. *Computers and Chemical Engineering* **82,** 240–258 (2015).

350. Lindberg, T. *An application of DOE in the evaluation of optimization functions in a statistical software* PhD thesis (2010), 25.

351. Ahmed, M. H. OEE can be your key. *Industrial Engineer* **45,** 43–48 (2013).

352. Walker, A. The Independent Review of Charging for Household Water and Sewerage Services. *UK Government Reports,* 1–204 (2009).

353. GOV.UK. *Prices of fuels purchased by manufacturing industry - Statistical data sets* 2014.

354. Ghadge, R. S., Patwardhan, A. W., Sawant, S. B. & Joshi, J. B. Effect of flow pattern on cellulase deactivation in stirred tank bioreactors. *Chemical Engineering Science* **60,** 1067–1083 (2005).

355. Sartorius Stedim Data Analytics. User Guide to Modde 9. **12,** 316 (2009).

356. Savitz, A. W. & Weber, K. *The sustainability sweet spot* 2007.

357. Osterman, K. *Ethanol Producer Magazine – The Latest News and Data About Ethanol Production* 2012.

358. IBioC. *From concept to commercialisation, enabling bio-based growth* tech. rep. ().

359. Hsu, T. A., Himmel, M., Schell, D., Farmer, J. & Berggren, M. Design and initial operation of a high-solids, pilot-scale reactor for dilute-acid pretreatment of lignocellulosic biomass. *Applied Biochemistry and Biotechnology - Part A Enzyme Engineering and Biotechnology* **57-58,** 3–18 (1996).

360. Liang, L., Li, C., Xu, F., He, Q., Yan, J., Luong, T., Simmons, B. A., Pray, T. R., Singh, S., Thompson, V. S. & Sun, N. Conversion of cellulose rich municipal solid waste blends using ionic liquids: Feedstock convertibility and process scale-up. *RSC Advances* **7,** 36585–36593 (2017).

361. Li, C., Liang, L., Sun, N., Thompson, V. S., Xu, F., Narani, A., He, Q., Tanjore, D., Pray, T. R., Simmons, B. A. & Singh, S. Scale-up and process integration of sugar production by acidolysis of municipal solid waste/corn stover blends in ionic liquids. *Biotechnology for Biofuels* **10** (2017).

362. Noorman, H. J., Van Winden, W., Heijnen, J. J. & Van Der Lans, R. G. in *RSC Green Chemistry* 55, 1–41 (Royal Society of Chemistry, 2018).

363. Mathias, P. M. & Corp, F. Reactions and Separations, 30–37 (2009).

364. Rajendran, K. & Murthy, G. S. How does technology pathway choice influence economic viability and environmental impacts of lignocellulosic biorefineries? *Biotechnology for Biofuels* **10,** 268 (2017).

365. Piccolo, C. & Bezzo, F. A techno-economic comparison between two technologies for bioethanol production from lignocellulose. *Biomass and Bioenergy* **33,** 478–491 (2009).

366. Frank, E., Han, J., Palou-Rivera, I., Elgowainy, A. & Wang, M. User Manual for Algae Life-Cycle Analysis with GREET. ANL/ESD/11-7, 1–46 (2011).

367. Blacker, A., Bourne, R. & Reynolds, W. *MSW Process Control Systems (WO2019220092)* 2019.

Appendix A

Rheology of MSW-derived slurries

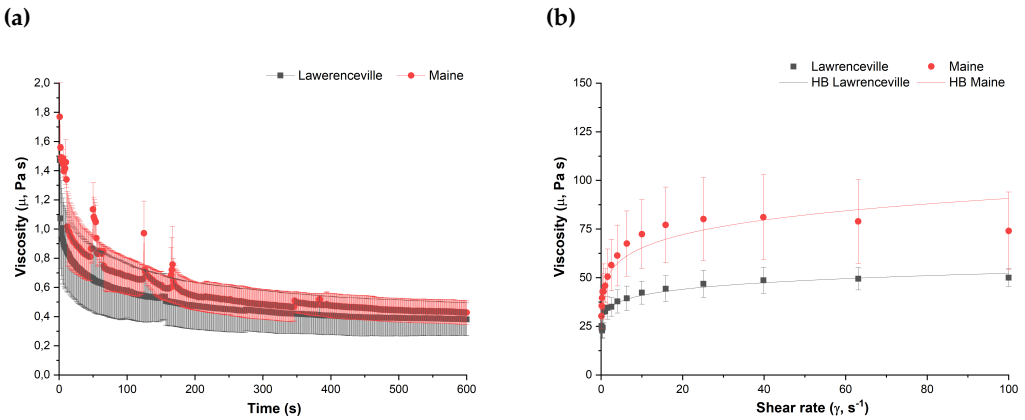

Figure A.1. Preconditioning (a) and flow sweep (b) steps for Lawrenceville and Maine pulps
Experiments were carried out from triplicate samples, previously selected by the quartering-cornering method to acquire a representative sample

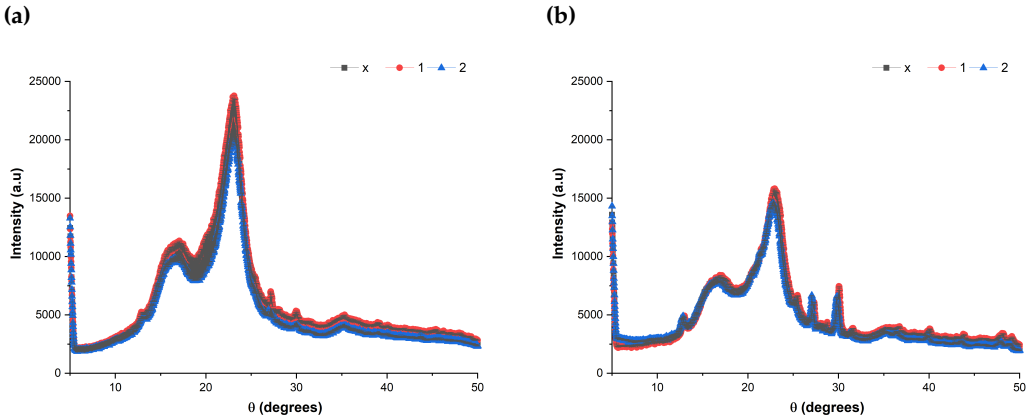

Figure A.2. XRD intensity scan of cryomilled MSW pulps for crystallinity index calculations: Lawrenceville (a) and Maine (b) pulps
Experiments were carried out from duplicate samples, previously dried at 105 ° C and milled down to 4000 μm

Table A.1. Power-law properties of parallel bottle roller (PBR) hydrolysates of duplicate hydrolysis (PBR_1 and PBR_2)

Time (hr)	**K (Pa s^2), x $\pm$ σ**	**n (dimensionless), x $\pm$ σ**	**r^2, x $\pm$ σ**
PBR_1			
0.5	423,71 $\pm$ 8,6691	0.0541 $\pm$ 0,0075	0,9929 $\pm$ 0,0003
1	163,98 $\pm$2,5898	0,1114 $\pm$ 0,0063	0,9962 $\pm$ 0,0002
2	226,47 $\pm$ 5,3115	0,0824 $\pm$ 0,0090	0,9918 $\pm$ 0,0003
4	286,56 $\pm$ 3,6384	0,0970 $\pm$ 0,0051	0,9969$\pm$ 0,0012
8	92,567 $\pm$ 1,1418	0,0917 $\pm$ 0,0051	0,9976$\pm$ 0,0001
24	66,296 $\pm$ 0,5450	0,1344 $\pm$ 0,0069	0,999$\pm$ 0,0004
PBR_2			
0.5	327,36 $\pm$ 5,4993	0,0671 $\pm$ 0,0087	0,9957 $\pm$ 0,0009
1	349,54 $\pm$ 9,5141	0,0727 $\pm$ 0,0101	0,9891 $\pm$ 0,0002
2	371,73 $\pm$ 7,8765	0,0523 $\pm$ 0,0079	0,9933 $\pm$ 0,0002
4	382,40 $\pm$ 8,0977	0,0593 $\pm$ 0,0076	0,9933 $\pm$ 0.0008
8	55,167 $\pm$ 0,3386	0,1101 $\pm$ 0,0020	0,9994 $\pm$ 0.0004
24	46,755 $\pm$ 0,4793	0,0979 $\pm$ 0,0038	0,9984 $\pm$ 0,0001

Table A.2. Power-law properties of B79 and B80 hydrolysate runs

Hydrolysis time (hr)	**K (Pa s^n), x $\pm$ σ**	**n (dimensionless), x $\pm$ σ**	**r^2, x $\pm$ σ**
0	1589.0 $\pm$ 28.583	0.0741 $\pm$ 0.0070	0.9991 $\pm$ 0.0002
5	299.12 $\pm$ 3.1270	0.0969 $\pm$ 0.0109	0.9984 $\pm$ 0.0020
24	773.63 $\pm$ 13.123	0.0712 $\pm$ 0.0049	0.9989 $\pm$ 0.0005
32	276.86 $\pm$ 9.5062	0.0885 $\pm$ 0.0248	0.9997 $\pm$ 0.0002
48	220.06 $\pm$ 3.4903	0.1060 $\pm$ 0.0290	0.9989 $\pm$ 0.0004
56	39.510 $\pm$ 1.0978	0.1096 $\pm$ 0.0336	0.9966 $\pm$ 0.0033
72	20.366 $\pm$ 0.8846	0.1165 $\pm$ 0.0388	0.9979 $\pm$ 0.0013
0	1589.0 $\pm$ 28.583	0.0741 $\pm$ 0.0063	0.9991 $\pm$ 0.0002
5	167.08 $\pm$ 1.8747	0.1475 $\pm$ 0.0292	0.9990 $\pm$ 0.0008
24	816.83 $\pm$ 22.733	0.0990 $\pm$ 0.0139	0.9957 $\pm$ 0.0029
32	593.29 $\pm$ 4.8911	0.0807 $\pm$ 0.0106	0.9998 $\pm$ 0.0001
48	72.940 $\pm$ 1.3102	0.1450 $\pm$ 0.0274	0.9995 $\pm$ 0.0002
56	261.51 $\pm$ 5.5993	0.1428 $\pm$ 0.0152	0.9981 $\pm$ 0.0003
72	110.75 $\pm$ 1.2306	0.1332 $\pm$ 0.0243	0.9993 $\pm$ 0.0001

Averages and standard deviations are calculated from a two-step ascending (0.1-100 s^{-1}) and descending (100 - 0.01 s^{-1}) flow sweep with pre-conditioning (170 s^{-1} for 10 min) in duplicate

(a)

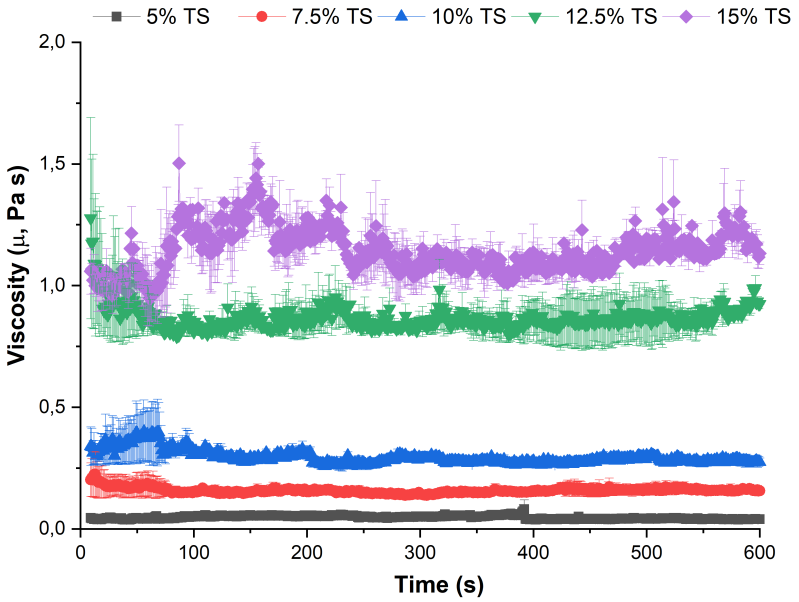

(b)

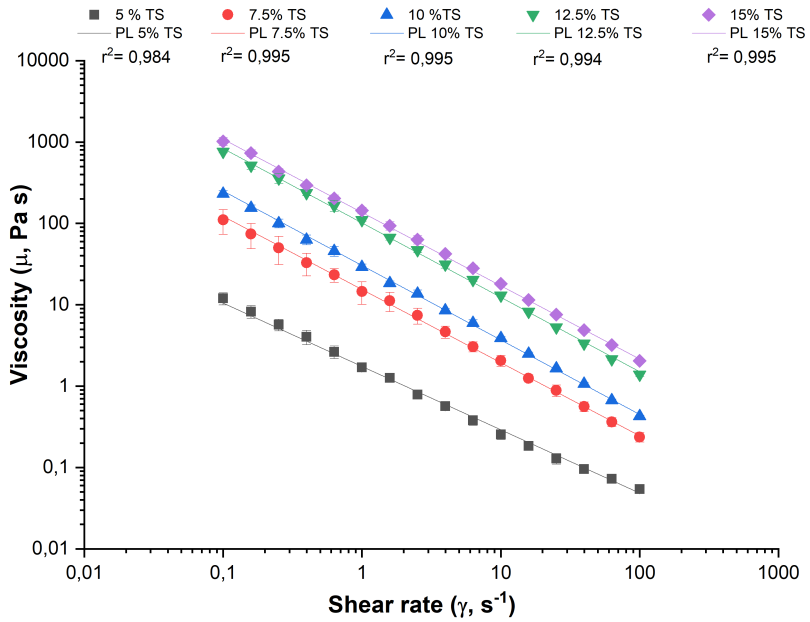

Figure A.3. Preconditioning (a) and flow sweep (b) steps of milled MSW slurries (5 to 15 %TS)

Experiments were performed in two sets of ascending and descending flow sweep with pre-conditioning (170 s^{-1}) Flow sweeps were carried out with a 20000 μm gap length, in contrast to manufacturer's requirements (4000 μm)

(a)

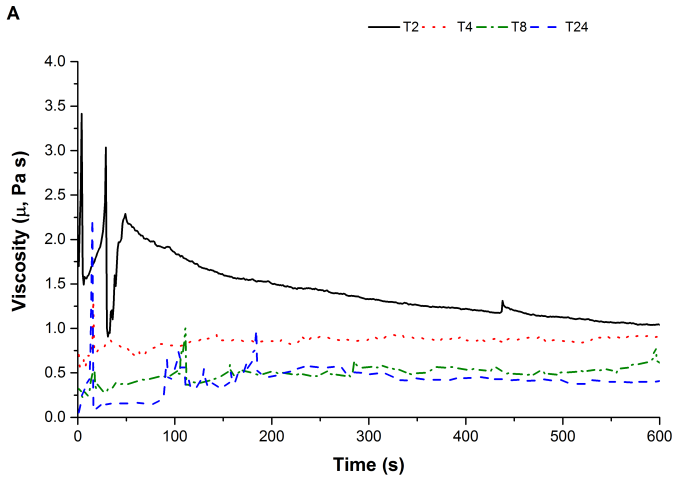

(b)

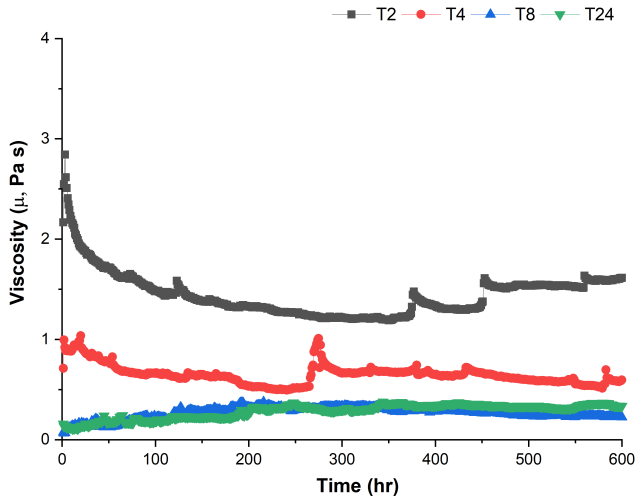

(c)

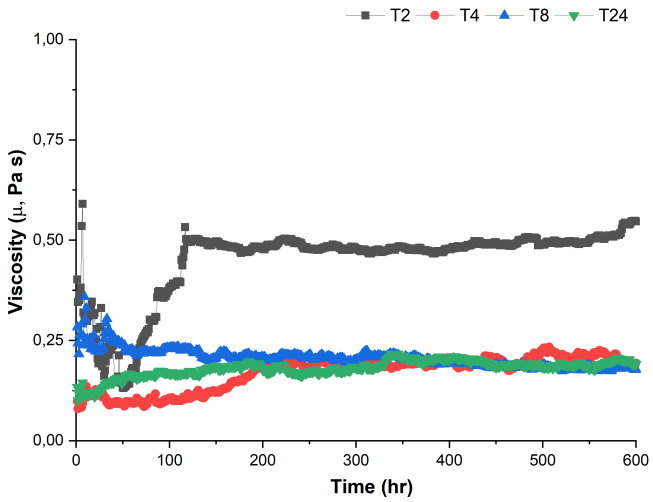

Figure A.4. Pre-conditioning step of hydrolysates processed in 1.5 L STRs: 5 % TS (a), 6 % TS (b) and 7 % TS (c)

(a)

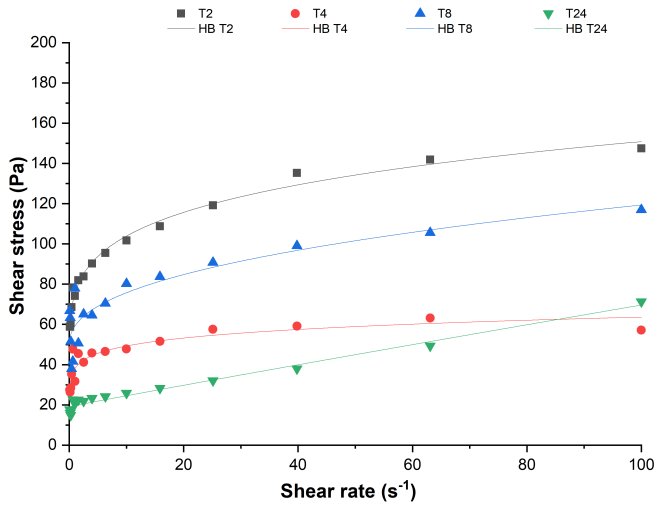

(b)

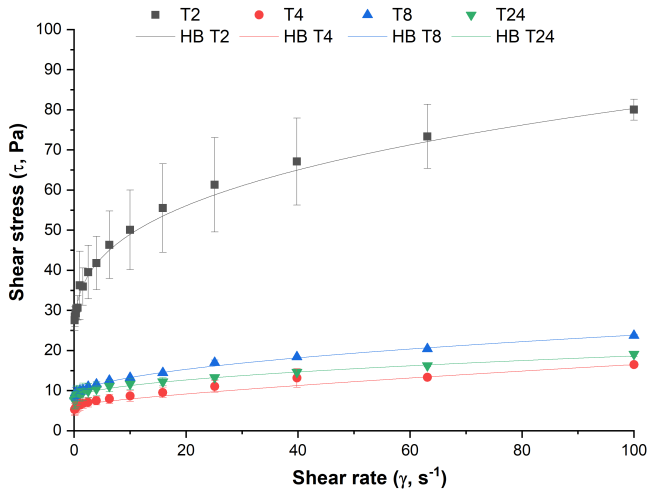

(c)

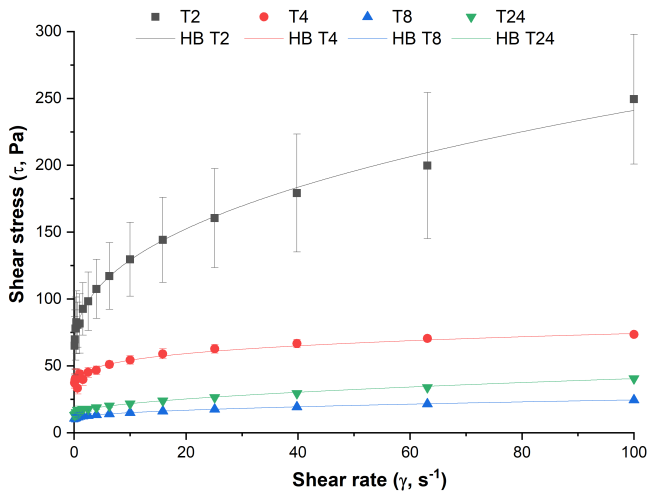

Figure A.5. Flow-sweep with Herschel-Bulkley model fitting of hydrolysates processed in 1.5 L STRs: 5 % TS (a), 6 % TS (b) and 7 % TS (c)

(a)

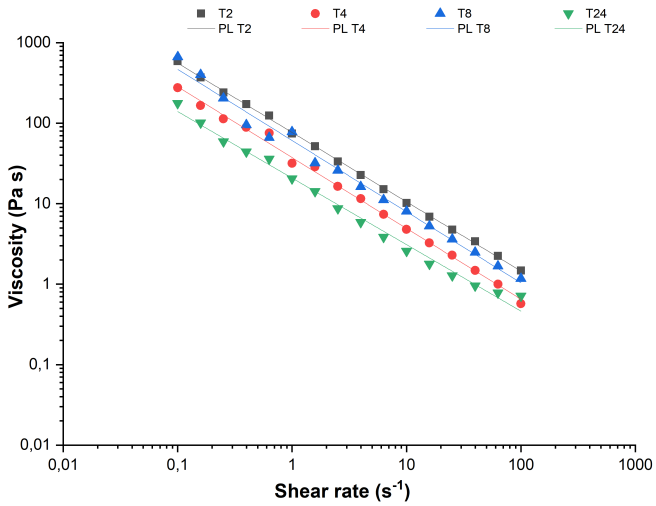

(b)

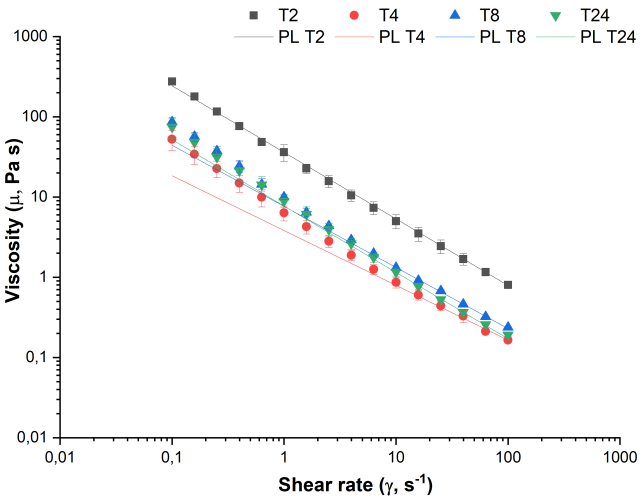

(c)

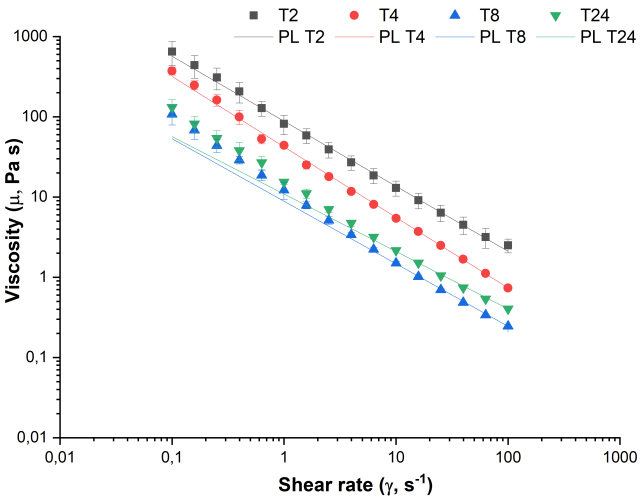

Figure A.6. Flow-sweep with Power-law model fitting of hydrolysates processed in 1.5 L STRs: 5 % TS (a), 6 % TS (b) and 7 % TS (c)

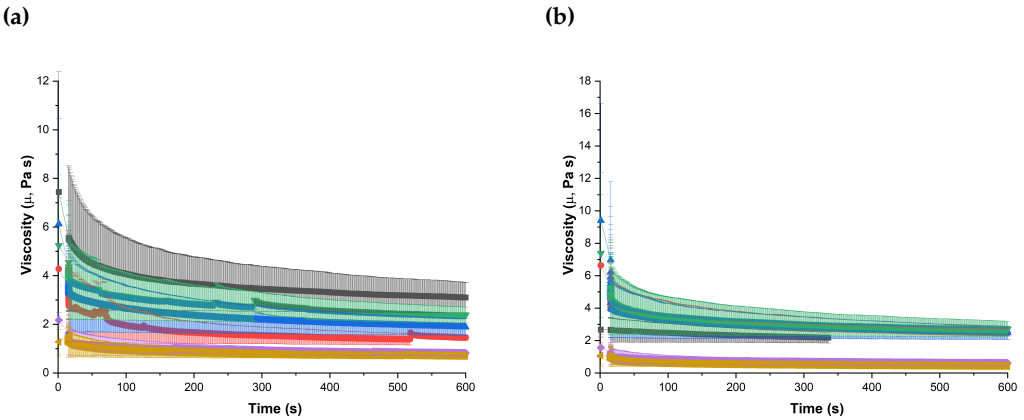

Figure A.7. Pre-conditioning of parallel bottle rollers hydrolysates at 170 s^{-1} for 10 min
Error bars represent standard deviation of duplicated pre-conditioning steps per sample

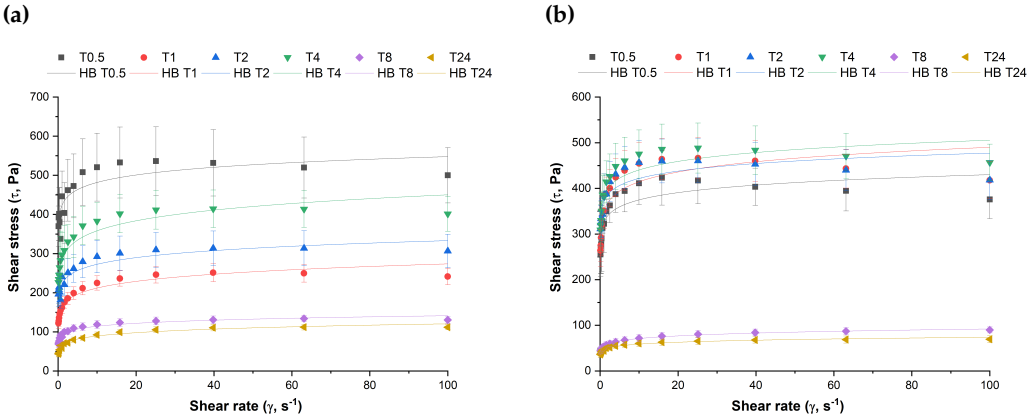

Figure A.8. Shear sweep of PBRs hydrolysates, with Herschel-Bulkley model fitting
Error bars represent standard deviation of duplicated two-step (ascending and descending) sweep per sample

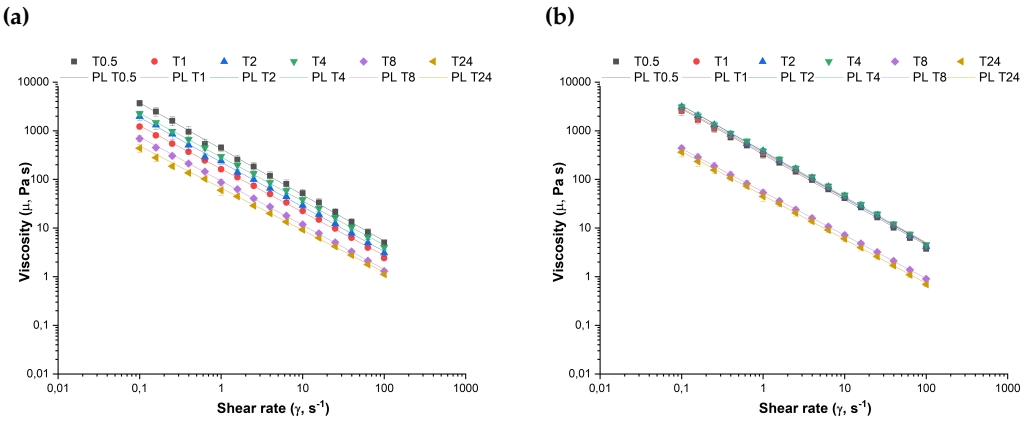

Figure A.9. Flow sweep of PBRs hydrolysates, with Power-law model fitting
Error bars represent standard deviation of duplicated two-step (ascending and descending) sweep per sample

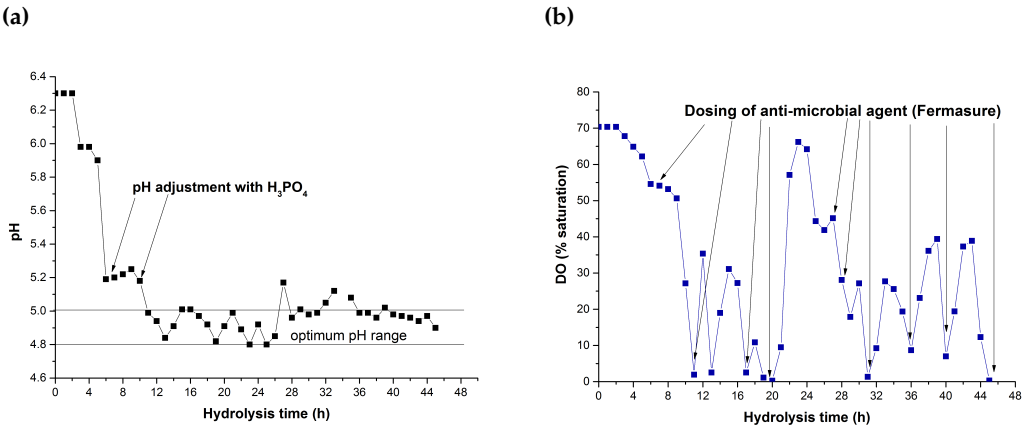

Figure A.10. pH/DO monitoring during the demonstration-scale run
Straight lines represent the optimum pH range of 4.75-5.25, recommended by Novozymes [100]

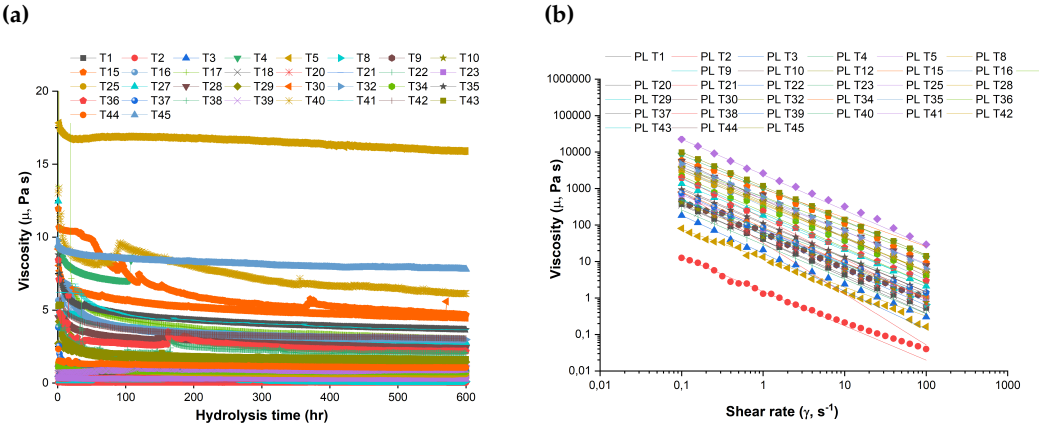

Figure A.11. Pre-conditioning (a) and flow sweep (b) test of demonstration-scale hydrolysates

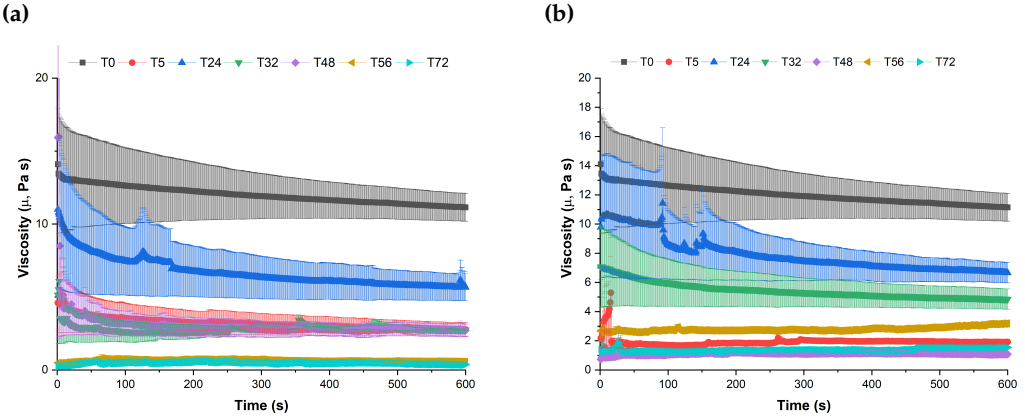

Figure A.12. Pre-conditioning of B79 and B80 hydrolysates runs
Error bars represent standard deviation of duplicated pre-conditioning steps per sample

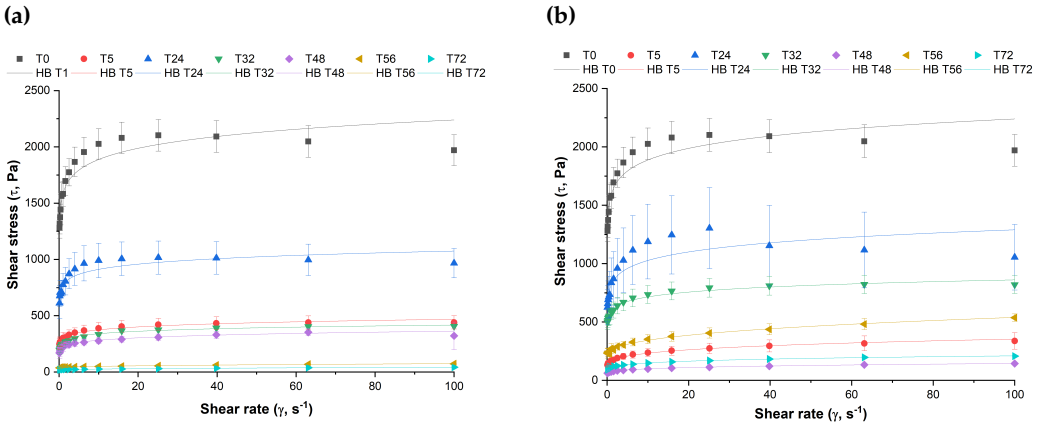

Figure A.13. Flow sweep of B79 and B80 hydrolysates runs with Herschel-Bulkley model fitting

Error bars represent standard deviation of duplicated two-step (ascending and descending) sweep per sample

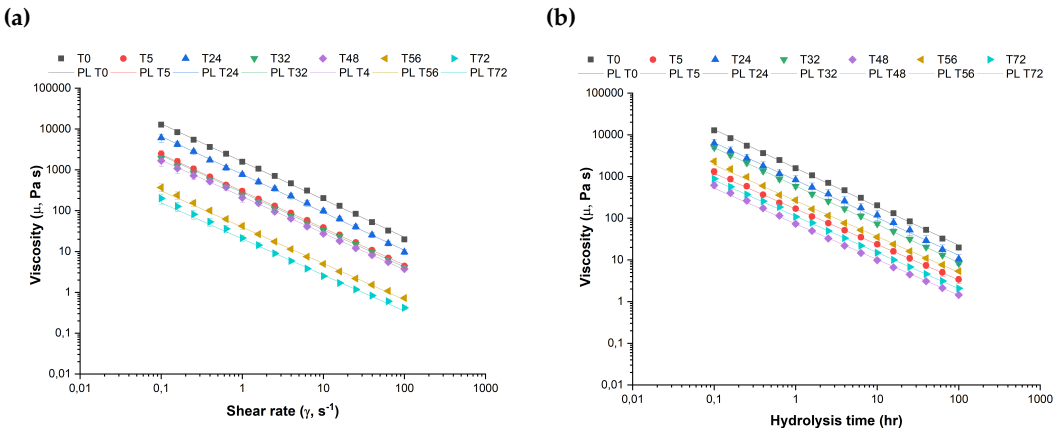

Figure A.14. Flow sweep of B79 and B80 hydrolysates runs with Power-law model fitting

Error bars represent standard deviation of duplicated two-step (ascending and descending) sweep per sample

Appendix B

Reactor design for enzymatic saccharification of MSW-derived pulp

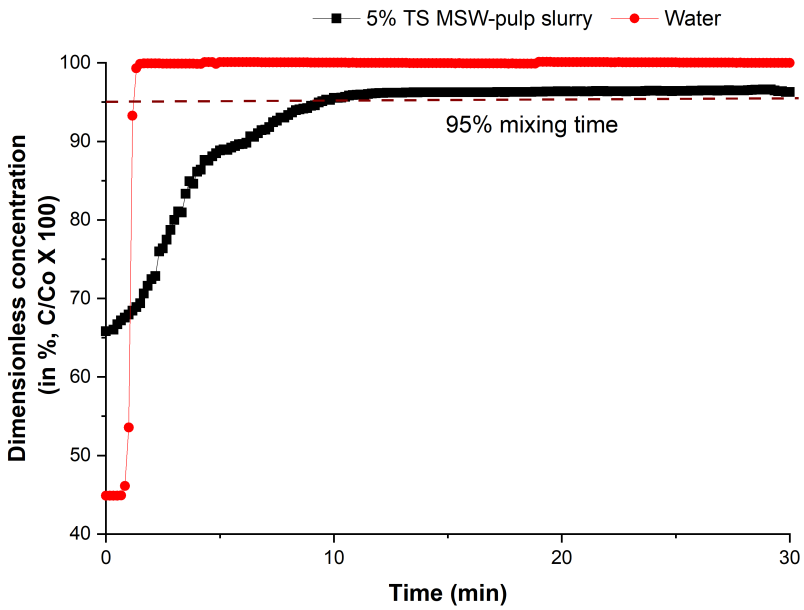

Figure B.1. Percentage of dimensionless conductivity concentration over time after trace injection for water and MSW-pulp dilutions

Reaction conditions: water (200 rpm) and MSW-pulp (600 rpm) on a single pitched-blade turbine (40 mm diameter)

Table B.1. Summary of rotary drum reactor power characteristics, survey by the US Davis study [277]

	Pinetop-Lakeside	**Nantucket**	**Delaware County**	**Rapid City**	**Cobb Country**
Rotational speed, rpm	1	1	5	0,83	1
Drum diameter, m	3,1	3,8	4,3	3,6	4
Drum length, m	38,1	56,4	24,4	56,4	48,8
Drum volume, m^3	1150	2558	3184	2296	2452
Power input, HP/drum	75	200	120	125	450
Specific power input, kW [3]	0,04	0,05	0,06	0,04	0,13

1 HP equal to 745.7 watts and 1 kW equal to 10^3 and kW/m^3 = W/L

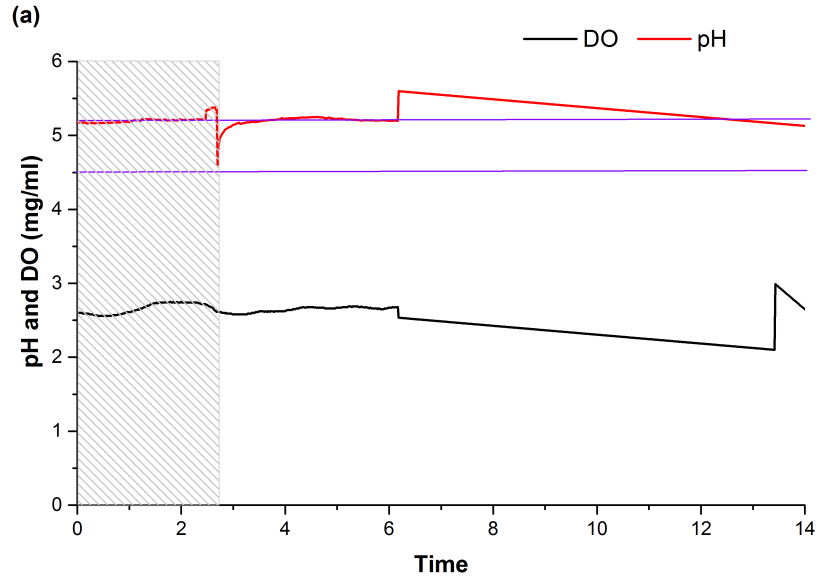

(a)

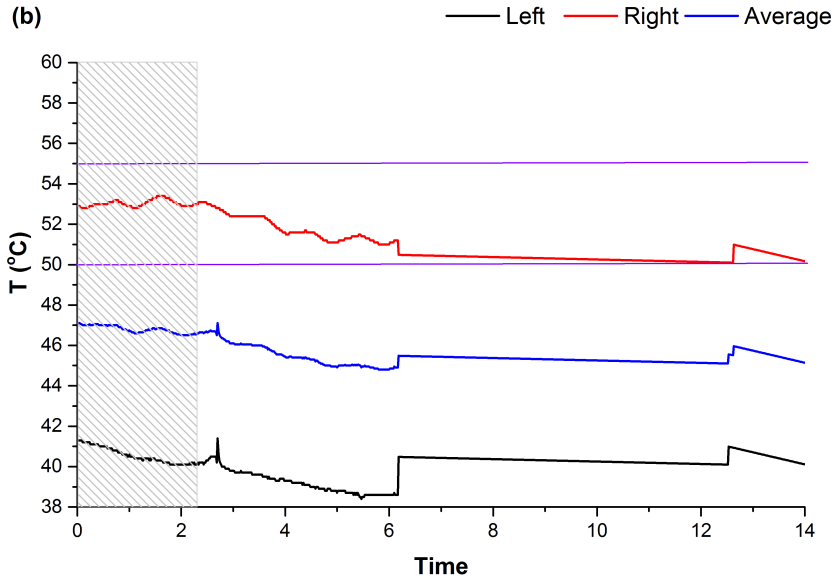

(b)

Figure B.2. Process monitoring during the SSBR batch hydrolysis (no.1): pH/DO (a) and temperature (b) measurements

Reaction conditions:8%TS, 2%E:S, 0.1%BIT, 30% V, 50 rpm, 50° and pH 4.75-5.25 Dotted lines on each graph represent the optimum conditions for Cellic CTec3 enzymes: 4.75-5.25 and 50-55 °C for pH and temperature, respectively, as recommended [100]

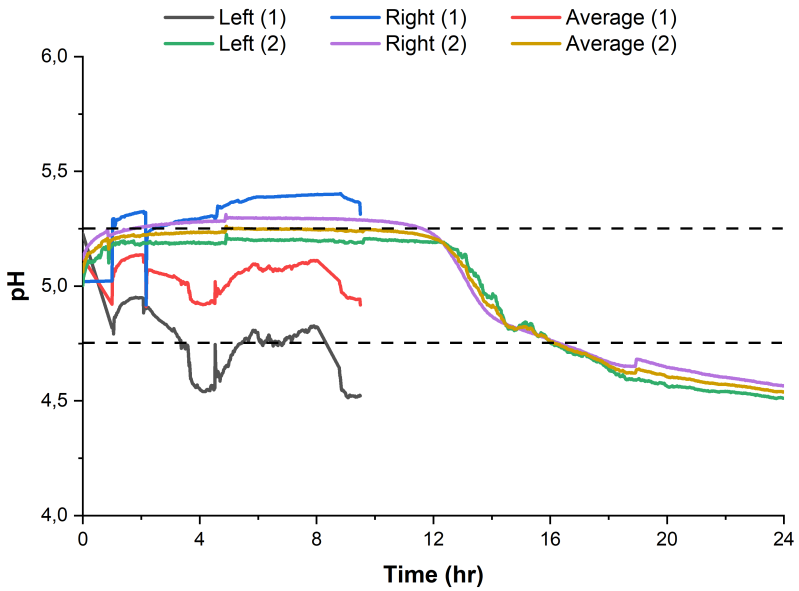

(a)

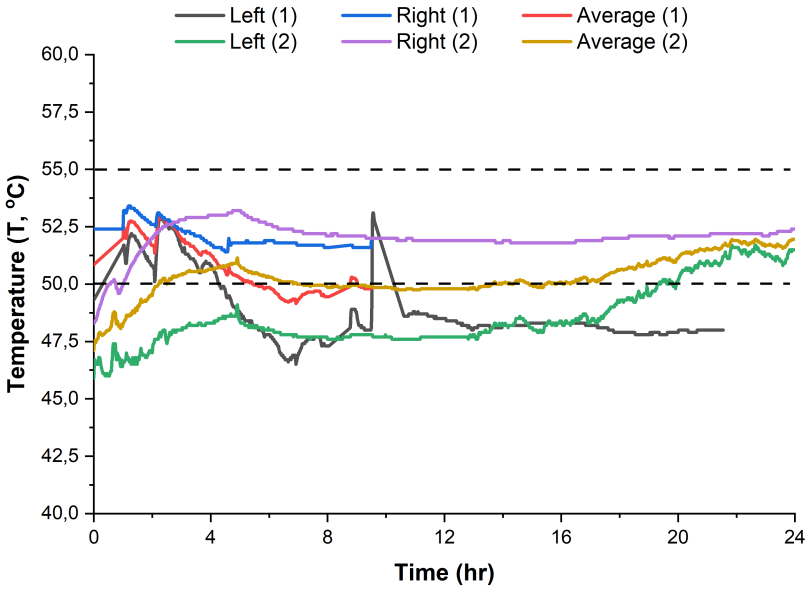

(b)

Figure B.3. Process monitoring during one-time purge SSBR two-stage hydrolysis: pH/DO (a) and temperature (b) measurements

Dotted lines on each graph represent the optimum conditions for Cellic CTec3 enzymes: 4.75-5.25 and 50-55 °C for pH and temperature, respectively, as recommended [100]

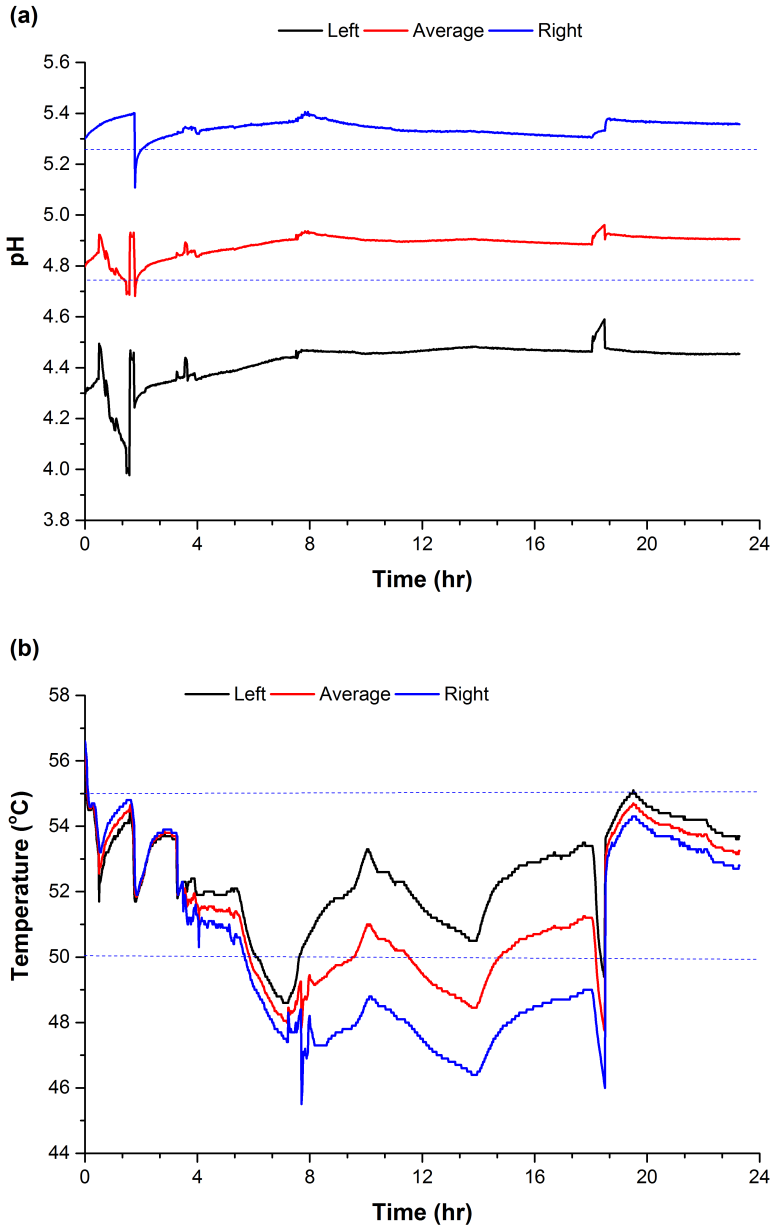

Figure B.4. Process monitoring during semi-continuous SSBR (2 aliquots) hydrolysis (no. 1): pH/DO (a) and temperature (b) measurements

Dotted lines on each graph represent the optimum conditions for Cellic CTec3 enzymes: 4.75-5.25 and 50-55 °C for pH and temperature, respectively, as recommended [100]

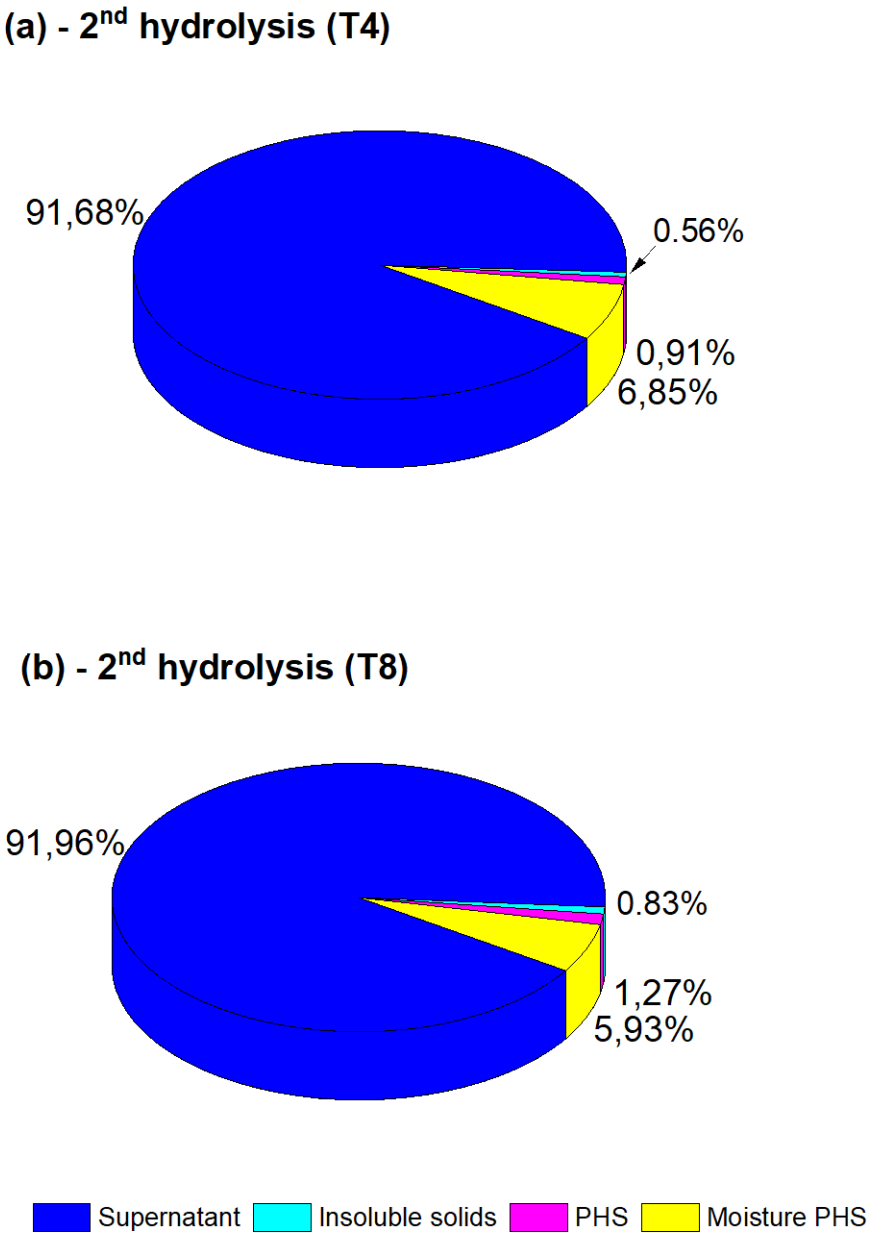

Figure B.5. Compositional analysis of aliquot transferred to secondary hydrolysis at T4 (a) and T8 (b) from the SSBR hydrolysis

Legend: supernatant is liquid fraction after filtration, insoluble soluble are particles in supernatant and PHS is solid filtrate fraction of slurry

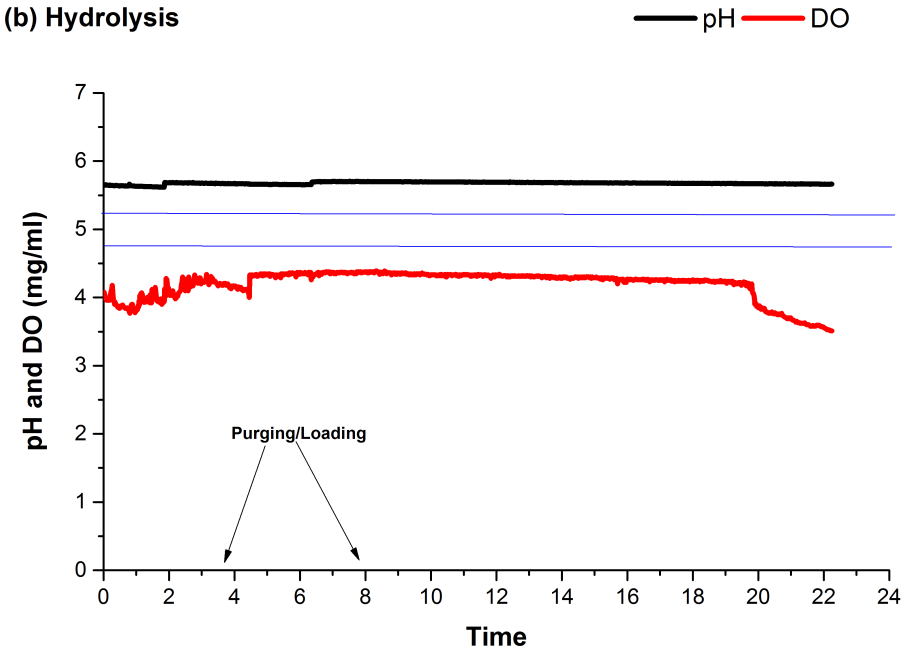

(a)

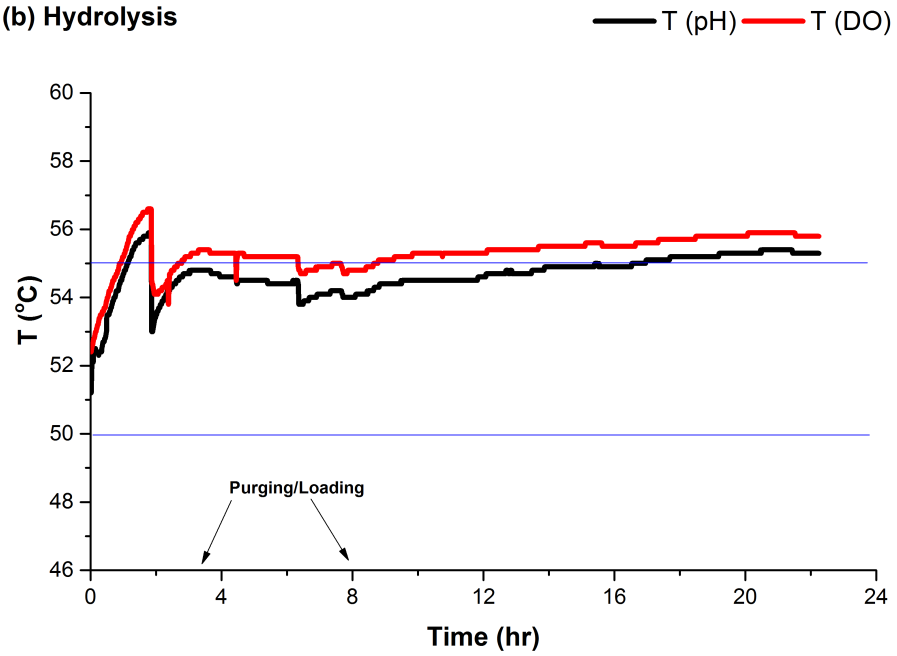

(b)

Figure B.6. Process monitoring during semi-continuous SSBR (2 aliquots) hydrolysis (no. 2): pH/DO (a) and temperature (b) measurements

Dotted lines on each graph represent the optimum conditions for Cellic CTec3 enzymes: 4.75-5.25 and 50-55 °C for pH and temperature, respectively, as recommended [100]

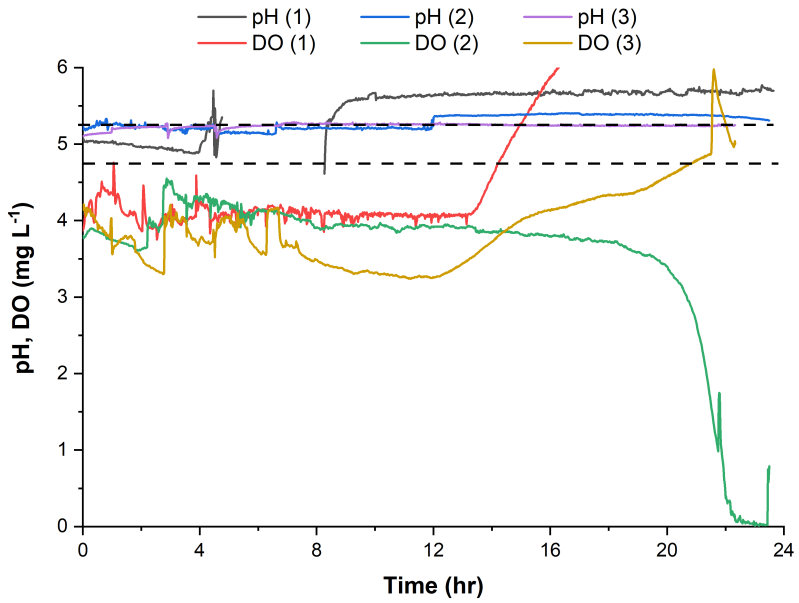

(a)

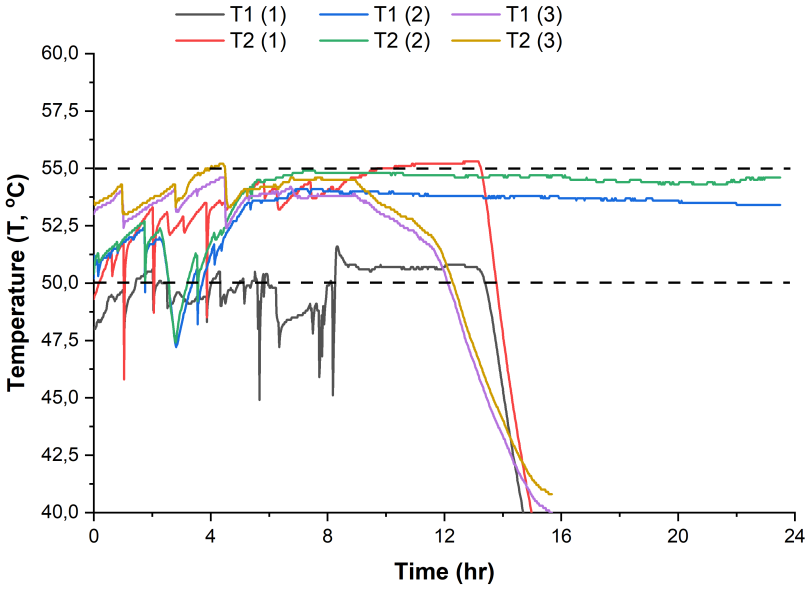

(b)

Figure B.7. Process monitoring during semi-continuous SSBR (3 aliquots) hydrolysis: pH/DO (a) and temperature (b) measurements

Dotted lines on each graph represent the optimum conditions for Cellic CTec3 enzymes: 4.75-5.25 and 50-55 °C for pH and temperature, respectively, as recommended [100]

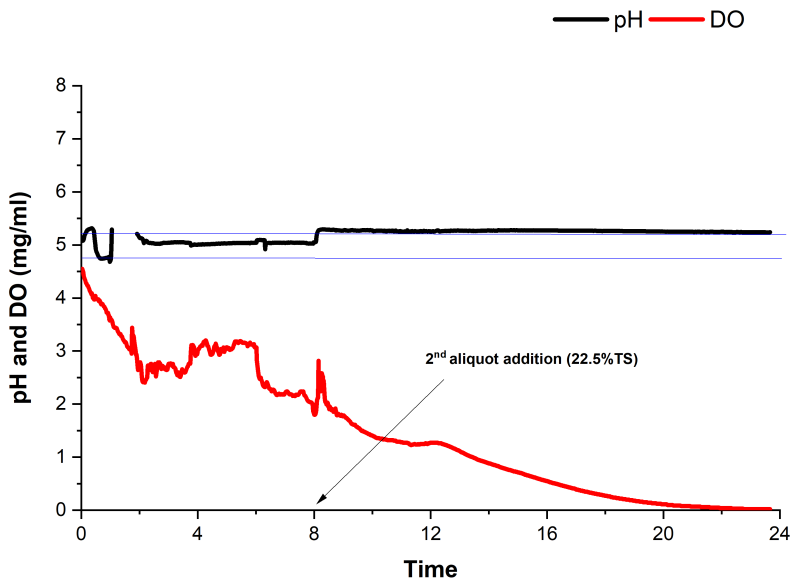

(a)

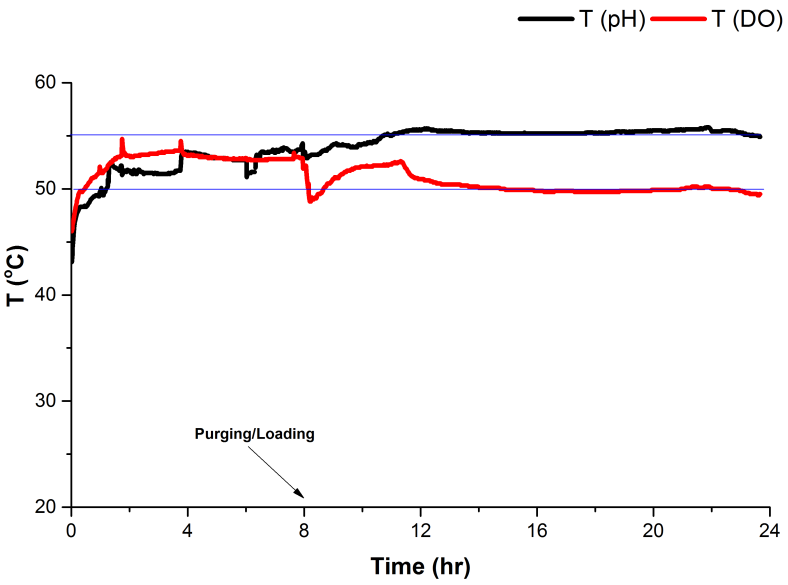

(b)

Figure B.8. Process monitoring during the fed-batch hydrolysis: (a) pH/DO and (b) temperatures measurements

Legend: blue on each graph represent the optimum conditions for Cellic CTec3 enzymes: 4.75-5.25 and 50-55 °C for pH and temperature, respectively, as recommended [100].And, the arrows represent the time of second aliquot addition.

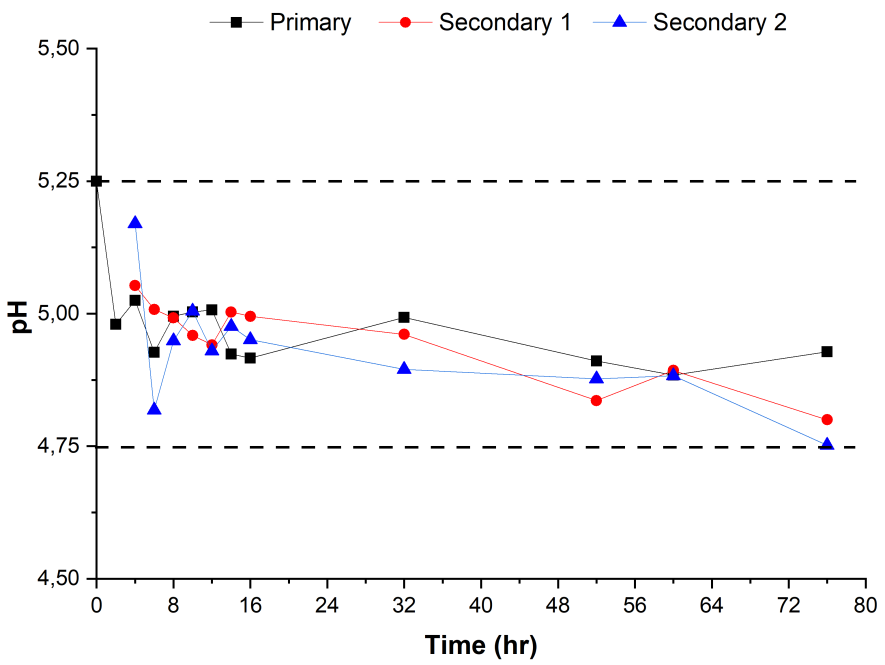

(a)

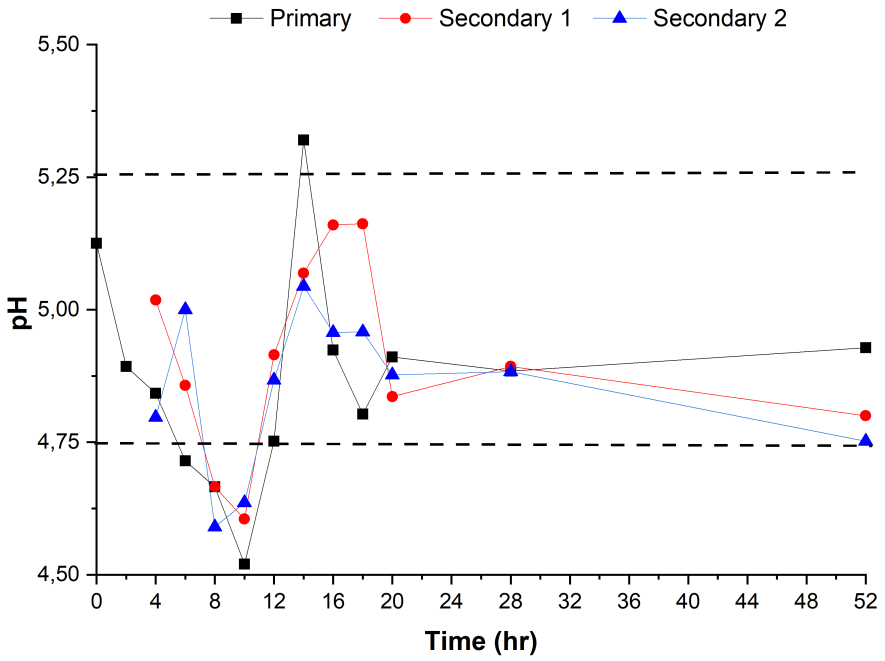

(b)

Figure B.9. Off-line pH monitoring of primary and secondary reactors during the pseudo-flow hydrolysis run: (a) batch 1 and (b) batch 2

Dotted lines on each graph represent the optimum conditions for Cellic CTec3 enzymes: 4.75-5.25 and 50-55 °C for pH and temperature, respectively, as recommended

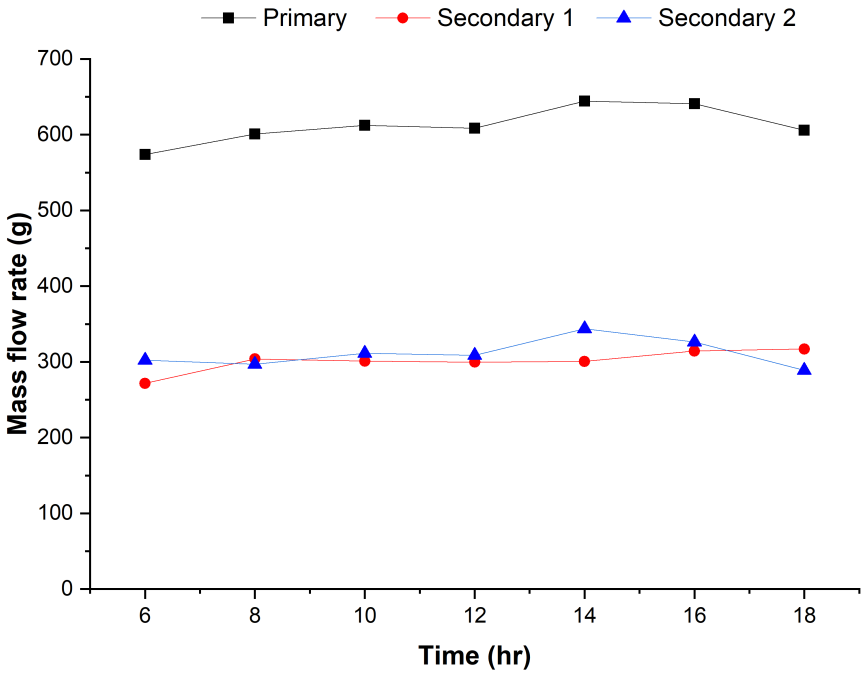

(a)

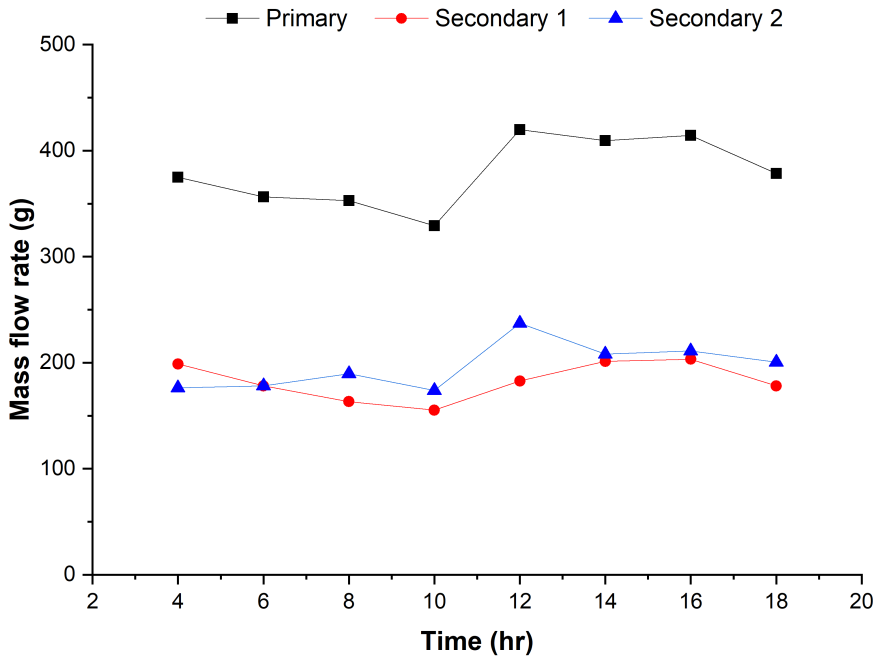

(b)

Figure B.10. Off-line monitoring of mass flow rates for primary and secondary reactors aliquots during the pseudo-flow period: (a) batch 1 and (b) batch 2

Note: An approximate 500-ml was withdrawn from the primary hydrolysis reactor, split between secondary reactor 1 and 2

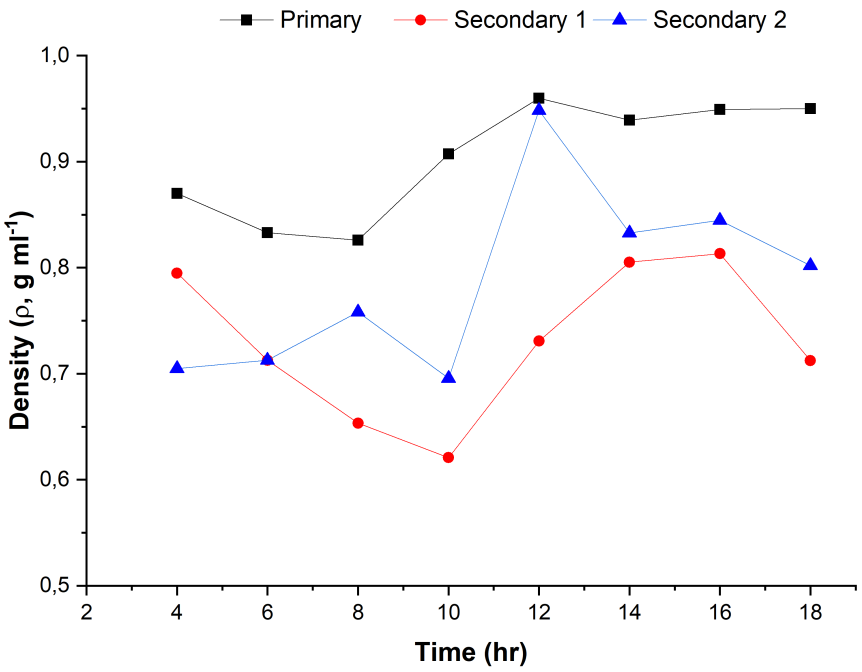

(a)

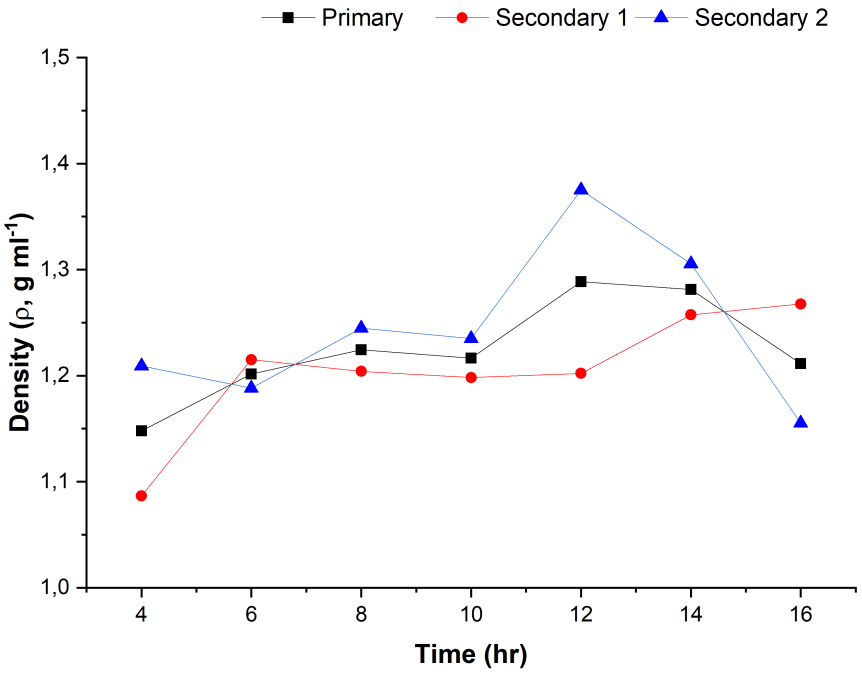

(b)

Figure B.11. Off-line monitoring of bulk density for primary and secondary reactors aliquots during the pseudo-flow hydrolysis: (a) batch 1 and (b) batch 2

Note: An approximate 500-ml was withdrawn from the primary hydrolysis reactor, split between secondary reactor 1 and 2

Appendix C

Optimisation, modelling and techno-economic assessment for scaling-up

Table C.1. Summary of MLR fit for the three factors of the minimum mixing requirements study

Parameter (units)	r^2	Q^2	Model validity	Reproducibility
Initial glucose (T1, g L^{-1})	0.99	0.94	0.51	0.99
Final glucose (T24, g L^{-1})	0.93	0.32	0.48	0.99
Total energy consumption (E, W min)	0.99	0.99	NA	1

Table C.2. Individual power inputs per reactor configuration at pilot-scale

	Liquefaction reactor (kW)			Saccharification reactor (kW)		
Reactor configuration	**RDB**	**RDB Heating**	**Pumps**	**STR**	**STR Heating**	**Pump**
Two-stage (6/48)	0,55	1,5	0,15	0,4	6,0	0,15
Two-stage (12/42)	1,11	3,0	0,30	0,2	4,5	0,30
Two-stage (18/36)	1,65	4,5	0,45	0,10	3,0	0,45
Two-stage (24/30)	2,22	6,0	0,60	0,05	1,5	0,60
Batch	NA	NA	NA	0,4	6,0	0,15
Two-stage (Fed-batch)	0,55	1,5	0,15	0,4	6,0	0,15
Modified Two-stage (6/48)	0,55	1,5	0,15	0,2	4,5	0,15

Table C.3. Individual power inputs per reactor configuration at demonstration-scale

	Liquefaction reactor (kW)			Saccharification reactor (kW)		
Reactor configuration	**RDB**	**RDB Heating**	**Pumps**	**STR**	**STR Heating**	**Pump**
Two-stage (6/48)	30	28	4	400	36	4
Two-stage (12/42)	60	56	2	175	15,7	2
Two-stage (18/36)	90	84	1,5	100	9,00	1,5
Two-stage (24/30)	120	112	1	62,5	5,62	1
Batch	NA	NA	NA	36	6,0	4
Two-stage (Fed-batch)	30	28	4	400	36	4
Modified Two-stage (6/48)	30	28	4	400	36	4

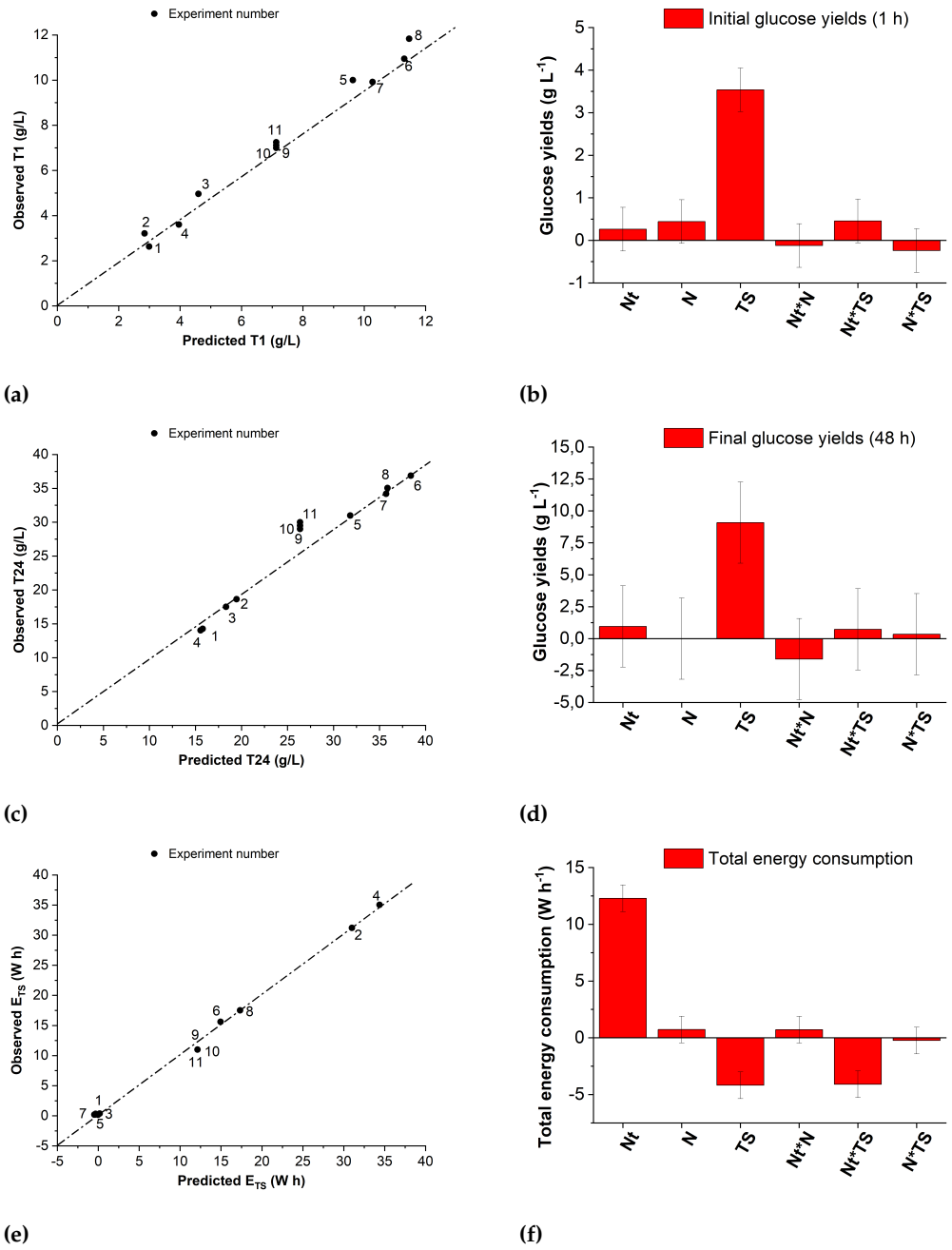

Figure C.1. Observed vs predicted plots for the responses: (a) T1, (c) T24 and (e) E_{TS}

Figure C.2. Coefficient plots of investigated factors and their interaction to the responses: (b) initial glucose yields, (d) final glucose yields and (f) total energy consumption

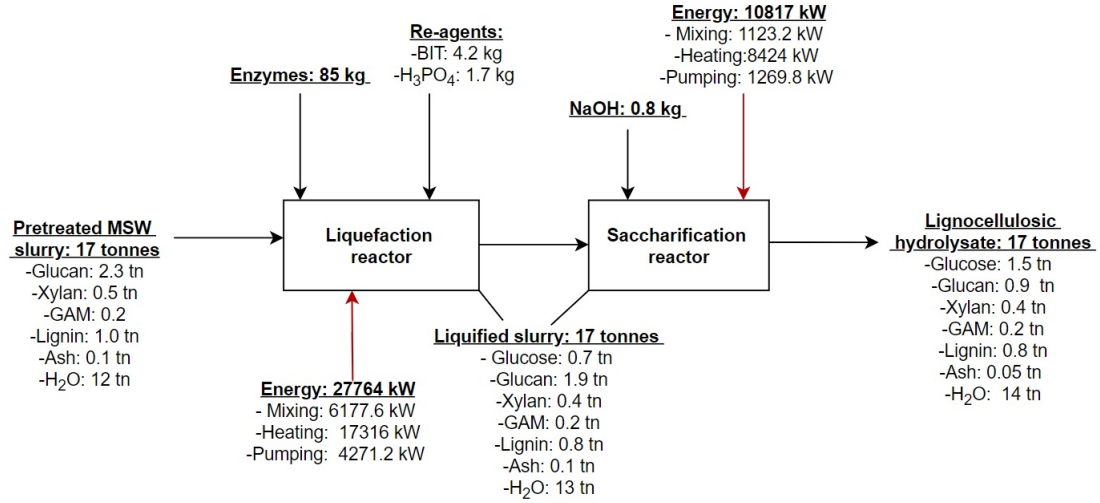

Figure C.3. Mass/energy balances of the 12/42 two-stage hydrolysis configurations at pilot-scale

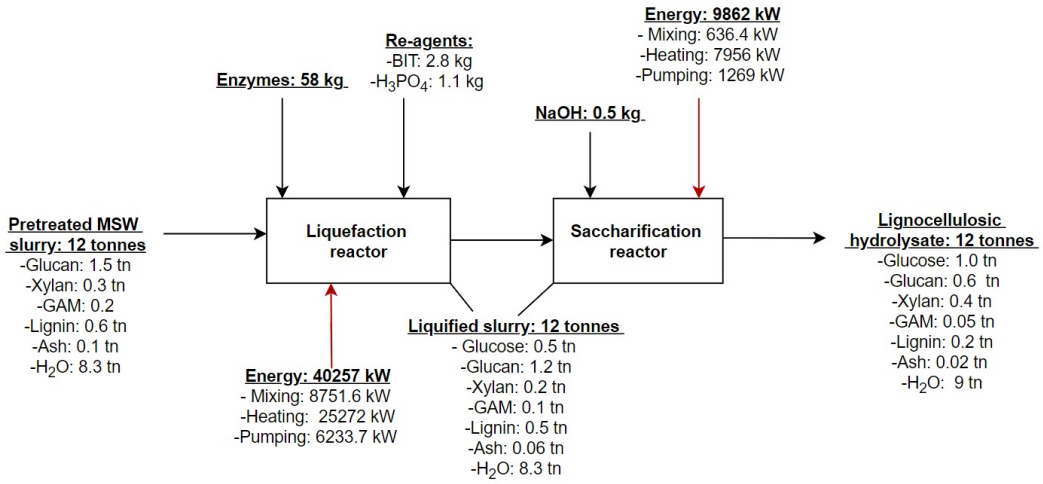

Figure C.4. Mass/energy balances of the 18/36 two-stage hydrolysis configurations at pilot-scale

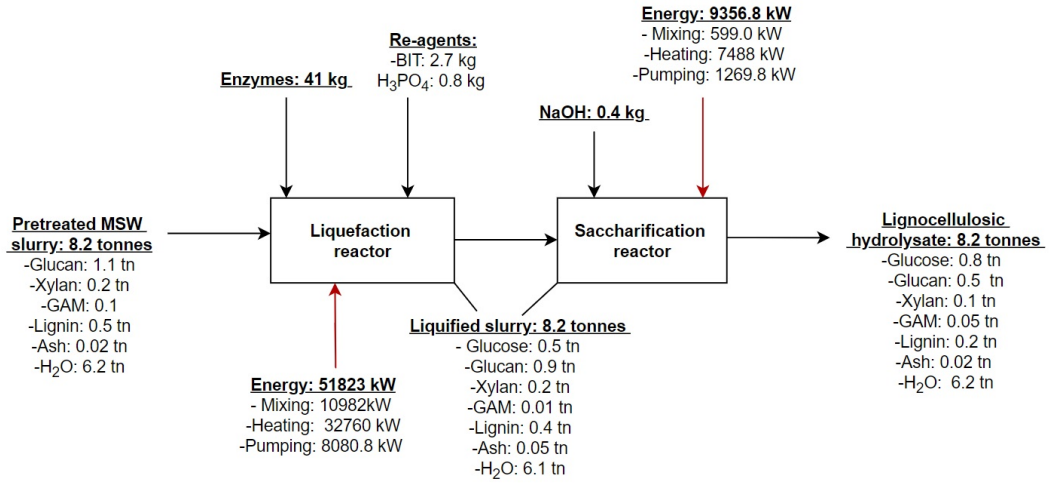

Figure C.5. Mass/energy balances of the 24/30 two-stage hydrolysis configurations at pilot-scale

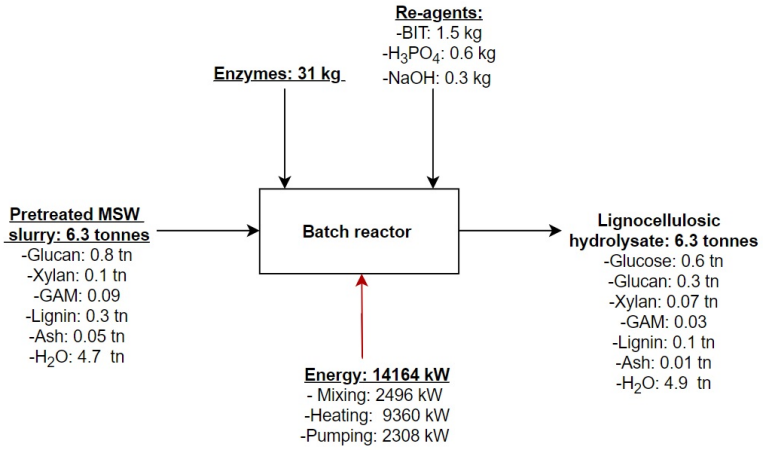

Figure C.6. Mass/energy balances of the batch hydrolysis configurations at pilot-scale

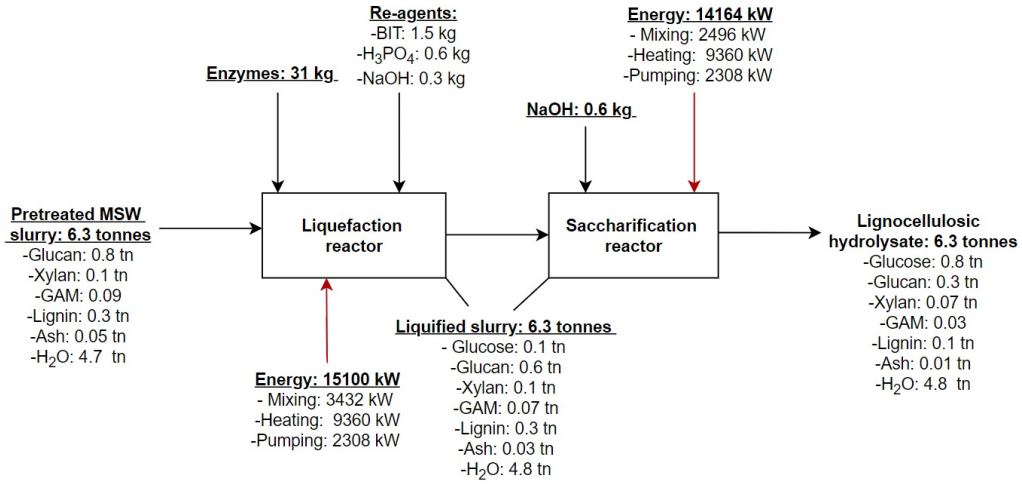

Figure C.7. Mass/energy balances of the two-stage fed-batch hydrolysis configuration at pilot-scale

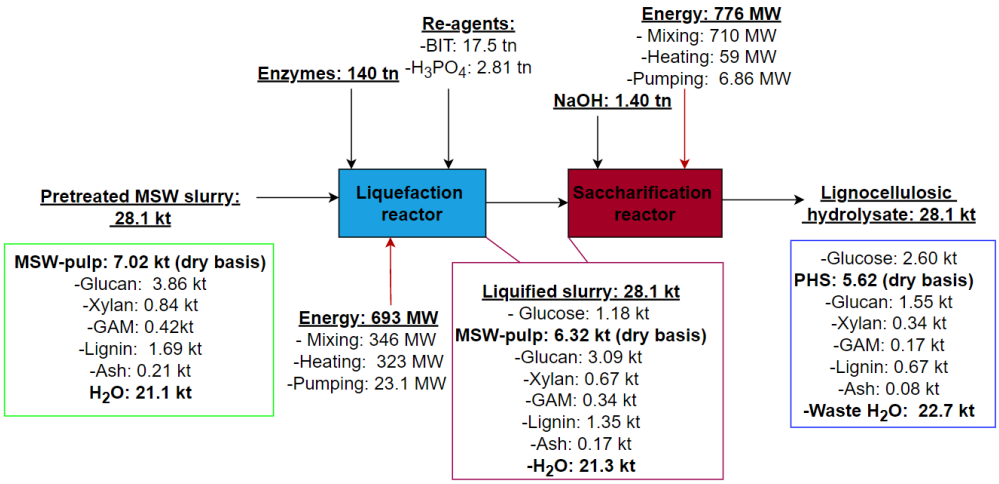

Figure C.8. Mass/energy balances of the 12/42 two-stage hydrolysis configurations at demonstration-scale

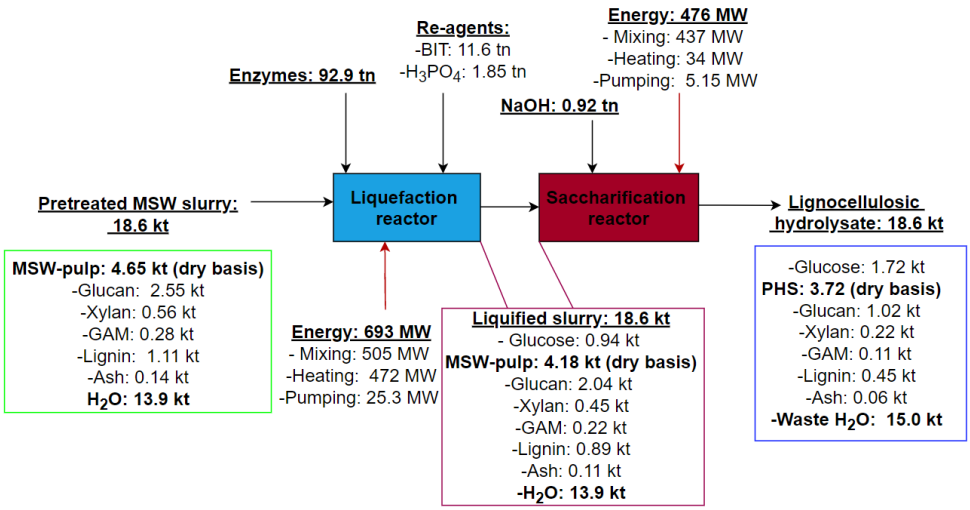

Figure C.9. Mass/energy balances of the 18/36 two-stage hydrolysis configuration at demonstration-scale

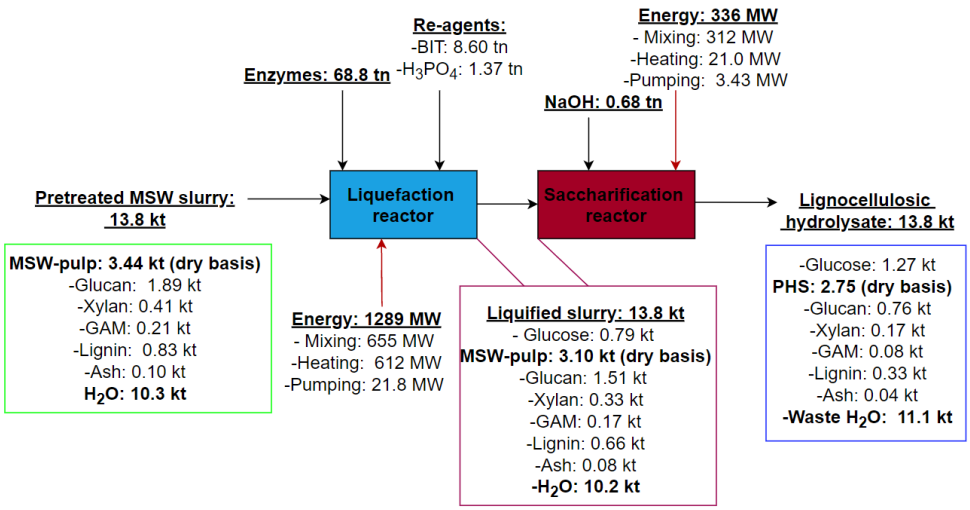

Figure C.10. Mass/energy balances of the 24/30 two-stage hydrolysis configuration at demonstration-scale

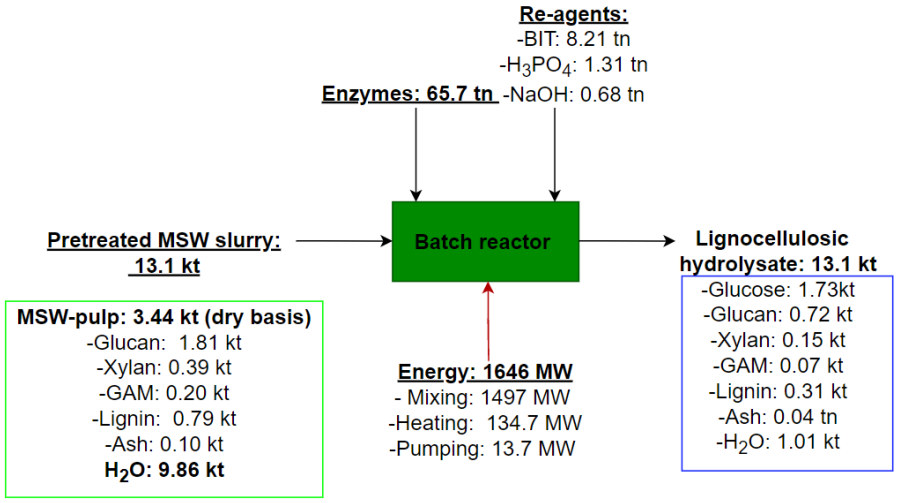

Figure C.11. Mass/energy balances of the batch configuration at demonstration-scale

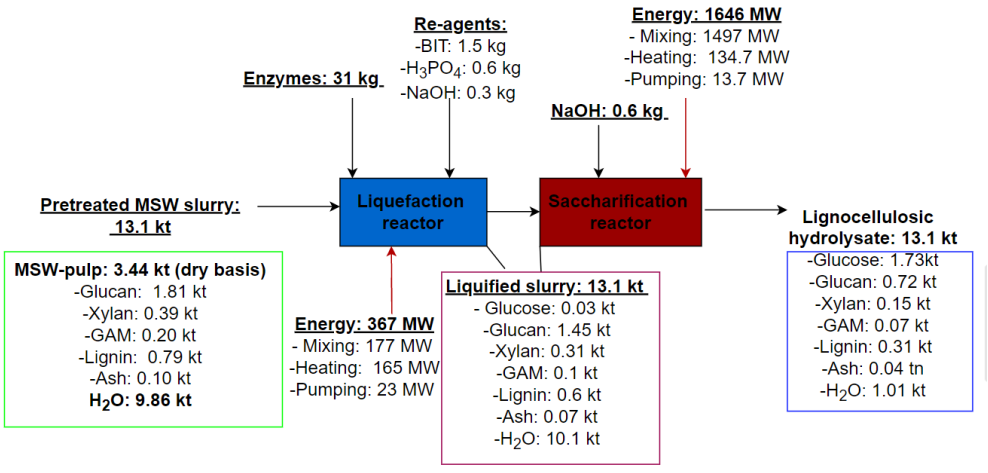

Figure C.12. Mass/energy balances of the fed-batch configuration at demonstration-scale